UNIVERSITÉ DE STRASBOURG

ÉCOLE DOCTORALE Physique – Chimie Physique

ICPEES - UMR 7515

THÈSE présentée par :

Pierre Furtwengler

Soutenue le : **6 avril 2018**

pour obtenir le grade de : **Docteur de l'Université de Strasbourg**

Discipline/ Spécialité : Chimie des Polymères

Synthèse et caractérisation de nouveaux synthons et mousses biosourcés, à partir de sorbitol

THÈSE dirigée par :

M. AVEROUS Luc	Professeur, Université de Strasbourg

RAPPORTEURS :

M. PIZZI Antonio	Professeur, Université de Lorraine
Mme LANGLOIS Valérie	Professeur, Université de Paris-Est (UPEC)

AUTRES MEMBRES DU JURY :

Mme BAHLOULI Nadia	Professeur, Université de Strasbourg

MEMBRES INVITES :

M.PERRIN Rémi	Directeur R&D, SOPREMA
M.REDL Andreas	Chef de projet, TEREOS

ICPEES, Institut de Chimie et Procédés pour l'Energie, l'Environnement et la Santé – UMR 7515

25 rue Becquerel – 67087 Strasbourg Cedex 2

CONFIDENTIEL

COMMUNICATIONS LIEES AUX TRAVAUX DE THESE

Publications

Les résultats présentés dans cette thèse font l'objet de quatre articles et d'une revue bibliographique.

Articles publiés :

- Furtwengler P., Perrin R., Redl A., Avérous L. - "Synthesis and characterization of polyurethane foams derived of fully renewable polyester polyols from sorbitol", European Polymer Journal, 2017, 97, 319-327, doi: 10.1016/j.eurpolymj.2017.10.020
- Furtwengler P., Matadi Boumbimba R., Avérous L. - "Elaboration and characterization of advanced biobased polyurethane foams presenting anisotropic behavior", Macromolecular: Material and Engineering, 2018, doi: 10.1002/mame.201700501

Articles soumis :

- Furtwengler P., Matadi Boumbimba R., Sarbu A., Avérous L. - « Novel rigid polyisocyanurate foams from synthetized biobased polyester polyol with enhanced properties » soumis dans ACS Sustainable Chemistry & Engineering
- Furtwengler P., Avérous L. - "From D-sorbitol to five-membered bis(cyclo-carbonate) as platform for the synthesis of different original biobased chemicals and polymers soumis dans ACS Sustainable Chemistry & Engineering

Articles qui seront soumis ultérieurement :

- Furtwengler P., Avérous L. - "From renewable polyols to polyurethanes and polyisocyanurate foams": A review

Brevets

Les résultats présentés dans cette thèse ont fait l'objet de trois brevets déposés à l'international et de deux dépôts de brevet national.

Brevets déposés à l'international :

- Bindschedler P.E., Sarbu A., Laurichesse S., Perrin R., Furtwengler P., Avérous L., Redl A. - Méthode de production de polyol polyesters et leur utilisation dans le polyuréthane, PCT/IB2017/055107, déposé le 24.08.2017
- Bindschedler P.E., Sarbu A., Laurichesse S., Perrin R., Furtwengler P., Avérous L., Redl A. - Mousse rigide comprenant un polyol polyester, PCT/IB2017/055110, déposé le 24.08.2017
- Bindschedler P.E., Sarbu A., Laurichesse S., Perrin R., Furtwengler P., Avérous L., Redl A. - Mousse souple ou semi flexible comprenant un polyol polyester, PCT/IB2017/055116, déposé le 24.08.2017

Brevet déposé en France :

- Bindschedler P.E., Sarbu A., Laurichesse S., Perrin R., Furtwengler P., Avérous L., Redl A. - Process for producing a five-membered polycycloaliphatic carbonate, FR 17/00351, déposé le 31.03.2017
- Bindschedler P.E., Sarbu A., Perrin R., Furtwengler P., Avérous L., Redl A. – Mousse rigide avec un pouvoir isolant amélioré, FR 18/00072 déposé le 22/01/2018

Conférences

Les résultats présentés dans cette thèse ont fait l'objet d'une communication dans une conférence internationale :

- P. Furtwengler, L. Avérous - "Sorbitol modification towards novel polyurethanes foams with anisotropic mechanical behavior", *poster*, 16th European Polymer Federation (EPF) congress, Lyon (France, 2 au 7 juillet 2017)

LISTE DES ABRÉVIATIONS

1,2 ETH / EG	1,2-ethanediol / Ethylene glycol
1,3 PROP	1,3-propanediol
1,4 BDO	1,4-butanediol
1,6-HEX	1,6-hexanediol
1,8 OCT	1,8-octanediol
1,10 DCO	1,10-decanediol
1,5 MD	1,5-diamino-2-methylpentane
1,4 B	1,4-diaminobutane
1,6 H	1,6-hexamethylene diamine
Å	Angström
AA	Adipic acid (ou acide adipique)
ASTM	American society for testing and material
ATR	Attenuated total reflexion
AV	Acid value
BTPP	Tert-butylimino-tri(pyrrolidino)phosphorarane
GLY	Glycerol
4,4' MDI	4,4'-diphenylmethylene diisocyanate
$CDCl_3$	Deuterated chloroform
CES	Chromatographie d'exclusion stérique
CFC	chlorofluorocarbon
Cl-TDP	2-chloro-4,4,5,5-tetramethyl-1,3,2-dioxaphospholane
CO_2	Carbon dioxide
Đ	Dispersity
D-BisCC	D-sorbitol based bis(cyclo-carbonate)
DBTL	Dibutyl tin (II) dilaurate
DBU	1.8-diazabicyclo[5.4.0]undec7-ene
DDA	Diamine based on dimer fatty acid
DDI	Dimer fatty acid-based diisocyanate
DEC	Diethyl carbonate
DEG	Diethylene glycol
DMA	Dynamic mechanical analysis
DMC	Diméthyle carbonate (ou dimethyl carbonate)
DMCHA	N,N-dimethylcyclohexylamine
DMSO-d_6	Deuterated dimethyl sulfoxide
DP_n	Number-average degree of polymerization
DSC	Differential scanning calorimetry
DTG	Derivative thermogravimetric analysis
EC	Ethylene carbonate
EELDI	Ethyl ester L-lysine diisocyanate
EG	Ethylene glycol
eq.	Molar equivalent (ou equivalent molaire)
EPS	Molded expanded polystyrene
EtOH	Ethanol
FTIR	Fourrier transform infrared
HDI	1,6-hexamethyl diisocyanate
HS	Hard segment
IC	Indice caractéristique
IOH / I_{OH}	Indice hydroxyle (ou hydroxyl index)
ISO	International organization of standardization
IUPAC	International Union of Pure and Applied Chemistry
K_2CO_3	Potassium carbonate
KE	Potassium 2-ethylhexanoate
KOH	Potassium hydroxide (ou hydroxide de potassium)
KP	Potassium propionate
L	Longitudinal direction according to the foam rising direction
MeOH	Methanol
M_n	Number-average molar mass (ou masse molaire moyenne en nombre)
mol.%	Mol percent
M_w	Weight-average molar mass (ou masse molaire moyenne en poids)

NaOH	Sodium hydroxide
NCO	Isocyanate function
NIPU	Non-isocyanate polyurethane
NMR	Nuclear magnetic resonance
OH	Hydroxyl function
OH-value / OHV	Hydroxyl index
pbw	part by weight
PDI	Pentamethylene diisocyanate
PDMS	Polyether polysiloxane
pMDI	polymeric 4,4'-diphenylmethylene diisocyanate
PEG	Polyethylene glycol
PET	Polyethylene terephthalate
PF	Phenolic foam
PHU	Poly(hydroxyurethane)
PIT	Poly(isosorbide)terephthalate
PIR	Mousse polyisocyanurate rigide (ou rigid polyisocyanurate foam)
pK_{BH+}	Basicity constant
PU(s)	Polyurethane(s)
PUF	Polyurethane foam
PUIR	Polyisocyanurate-polyurethane
PUR	Mousse polyurethane rigide (ou rigid polyurethane foam)
PVDF	Polyvinylidene fluoride
TCPP	Tris(1-chloro-2-propyl) phosphate
R	Anisotropic coefficient
REF	Reference
ROP	Ring opening polymerization
SA	Succinic acid
SEC	Size exclusion chromatography
SEM	Scanning electron microscopy
Sn(oct)	Stannous octoate
T	Transversal direction according to the foam rising direction
T_b	Boiling temperature
T_c	Crystallization temperature
$T_{d,2\%}$	2 wt.% degradation temperature
$T_{d,50\%}$	50 wt.% degradation temperature
$T_{deg,max}$	Maximal degradation rate temperature
$T_{ébu}$	Température d'ébulittion
T_f	Température de fusion
T_g	Glass transition temperature
Tanδ	Loss factor
TBD	1.3.5-triazabicyclo[4.4.0]dec-5-ene
TDI	2,4-toluene diisocyanate
TGA	Thermogravimetric analysis
T_m	Melting temperature
TNBT	titanium (IV) butoxide
TTIP	Titanium (IV) isopropoxide
wt%	Weight percentage
XPS	extruded expanded polystyrene
%pds	Pourcentage massique
λ	Coefficients de conductivité thermique (ou thermal conductivity coefficient)
γ	Surface tension
δ_d	Hansen dispersion parameters
δ_p	Hansen polar parameters
δ_h	Hansen hydrogen bonding parameters

SOMMAIRE

Communications liées aux travaux de thèse *III*

Liste des abréviations *VII*

Sommaire *XI*

Liste des illustrations *XV*

Introduction générale *1*

Chapitre 1 : Mousses polyuréthanes et polyols biosourcés – Etat de l'art *11*

Introduction du Chapitre 1 12
Abstract 14
Introduction 14
Polyurethane history and isocyanate chemistry 15
Elaboration of Polyurethane foams 17
Classification of the Polyurethane foams 17
Formulation of Polyurethane foams 18
Polyisocyanates 18
Blowing agents 20
Catalysts 21
Surfactants 21
Polyols for the elaboration of biobased PU Foams 22
Introduction 22
Aliphatic polyols 22
Neat Polyols 22
Modified Polyols 25
Neat Polysaccharides and derivate 25
Polyether polyols 26
Polyester polyols 31
Polyol obtained from thiol-ene coupling chemistry 33
Polyols from triglycerides. 33
Aromatic polyols 39
Aromatic polyols from liquefied lignocellulosic biomass 39
Aromatic polyether polyol based on alkoxylation of biomass 41
Mannich polyols 42
Aromatic polyester polyol from glycolysis 44
Biobased Non-Isocyanate Polyurethane 45
NIPU generalities 45
NIPU foams 46
PU foams recyclability 48
Conclusions 50
References 51
Conclusion et perspectives du premier Chapitre 58

Chapitre 2 : Synthese de polyols biosourcés pour l'elaboration de mousses polyurethanes *59*

Introduction du Chapitre 2 60
Chapitre 2.1: Synthesis and characterization of polyurethane foams derived of fully renewable polyester polyols from sorbitol 62
Abstract 63

Introduction 63
Experimental part 65
Materials 65
Methods 66
Polyester polyol synthesis 67
Detailed foam processing 68
Results and discussion 69
Synthesis and characterization of polyester polyols 69
Study of the polyurethanes foams 73
Foams morphology: 73
Study of the PUF kinetic 74
Comparison of different blowing systems 74
Effect of the addition of biobased polyester polyol: 75
Biobased contents of the polyesters and foams: 76
Conclusion 76
Acknowledgements 77
References 77
Chapitre2.2: Elaboration and characterization of advanced biobased polyurethane foams presenting anisotropic behavior
79
Abstract: 80
Introduction 80
Experimental Section 82
Chemical 82
Synthesis of the sorbitol-based polyol 82
PU foams synthesis 83
Characterizations 83
Results and discussion 84
Conclusion 93
References 93
Conclusion et perspectives du Chapitre 95
Chapitre 3 : Elaboration de mousses polyisocyanurates à partir de polyols biosourcés
97
Introduction du Chapitre 3 98
Abstract: 100
Introduction 100
Materials and methods 102
Preparation of PUIR foams 102
Characterizations 103
Results and discussions 105
Study of the compatibility between the polyols 105
PUIR foam reaction times and kinetics 105
Closed cell content and Foams morphologies (SEM) 109
Foams properties and performances 111
Conclusion 115
Acknowledgements 116
Références 116
Conclusion et perspectives du Chapitre 118

Chapitre 4 : Développement d'une nouvelle molécule plateforme biosourcée à partir du sorbitol *119*

Introduction du Chapitre 4 120
Abstract 122
Introduction 122
Experimental part 125
Materials: 125
Synthesis with catalyst of D-sorbitol-based Bis(cyclo-carbonate): 125
Synthesis without catalyst of D-sorbitol-based Bis(cyclo-carbonate): 126
Synthesis of cyclopentanediol by trans-esterification: 127
NIPU synthesis: 127
Synthesis of polyether polyols 127
Acetylation of samples 128
General methods and analysis: 128
Results and discussion 129
Synthesis of D-BisCC 129
Catalyst screening and D-BisCC kinetic study 132
D-BisCC yield optimization based on continuous flow rate system 134
Synthesis of polyether/polycarbonate by ROP of D-BisCC 135
Synthesis of polyhydroxyurethanes 137
Conclusion 141
Acknowledgements 141
References 141
Conclusion et perspectives du Chapitre 144

Conclusion générale et perspectives *145*

Bibliographie générale *151*

Annexes *165*

Annexe 1 : Définitions et exemples relatifs à la formulation de mousses polyuréthane ou polyisocyanurate 166
Annexe 2 : Supporting information du sous-Chapitre 2.1 169
Annexe 3: Supporting information de sous-Chapitre 2.2 187
Annexe 4: Supporting information de Chapitre 3 192
Annexe 5 : Supporting information de Chapitre 4 199
Annexe 6: Synthèse du BASAB et de mousses PUIR à l'échelle pilote 217

LISTE DES ILLUSTRATIONS

Figures

Introduction générale

Figure. 1: Structure chimique du sorbitol 4

Figure 2: vision schématique du projet PURBio 5

Figure 3: Isomères du sorbitol 5

Figure 4: Principales molécules d'intérêt résultantes du sorbitol 6

Figure 5: Procédé industriel d'obtention du sorbitol par hydrogénation du D-glucose 7

Chapitre 1

Figure 1.1: Irreversible reaction involving isocyanate groups with the synthesis of isocyanurate, urea, imide, carbodiimide, amine, amide or oxazolidone groups. 16

Figure 1.2: Reversible reactions involving the isocyanate group with the synthesis of urethane, uretidinedione, thioruthane, allophanate and biuret 17

Figure 1.3: Chemical structures of the main biobased and fossil-based polyisocyanate 19

Figure 1.4: Alkoxylation reaction on (a) an alcohol or (b) water 26

Figure 1.5: Different routes to obtain polyester polyols: (a) polycondensation of diols and diacids, (b) ROP of ethylene oxide and carboxylic acid, (c) ROP of cyclic carbonate and carboxylic acid, (d) ROP of ε-caprolactone and alcohol, (e) ROP of lactic acid and alcohol (f) Polyesters transesterification. 31

Figure 1.6: Photo-initiated thiol-ene coupling reaction 33

Figure 1.7: Triglyceride chemical modification by (I) epoxydation follow by oxirane opening by DEG, (II) hydroformylation and hydrogenation, (III) ozonolysis and hydrogenation, (IV) transamidation, (V) self-metathesis, (VI) transesterification.... 34

Figure 1.8: Mannich-based polyols synthesis: (a) Synthesis of N-(2-hydroxyethyl)-1,3-oxazolidine, (b) Mannich based formation, (c) Mannich polyol polymerization 43

Figure 1.9: PET glycolysis (a) general mechanism with a diol and (b) specific case of the EG as glycol 44

Figure 1.10: Main chemical routes to synthetized NIPU by (a) with acyl azide, (b) transurethanization, or (c) aminolysis 46

Figure 1.11: Chemical blowing agent based on polydimethylsiloxane reactional pathway 47

Figure 1.12: PU at end of life recycling patways. 48

Figure 1.13: Glycolysis reactional pathway of urethane groups with (a) glycols or (b) water and (c) urea groups with glycols 49

Figure 1.14: Schematic of the chem-biotechnology strategy 49

Chapitre 2

Figure 2.1: Exemples de voies d'obtentions de polyols et diacides courants à partir de la biomasse. 60

Figure 2.2:Reaction of Isocyanate with a. hydroxyl function to form urethane group, b. water to obtain urea and carbon dioxide released 64

Figure 2.3: Structures of the sorbitol- based polyesters at the end of the first synthesis step (on the top) and at the end of the two-step reactions (on the bottom) with R_1 from C5 to C6, and R_2 from C2 to C12 69

Figure 2.4 : FTIR spectra of the reactional intermediate and the final polyester polyol (Table 1, entry 3 at the end of the first synthesis step and final product 70

Figure 2.5: Polyester polyols dynamic viscosity in function of temperature 72

Figure 2.6: SEM images of PUF in the rise direction, a: close cell from the reference foam (REF). b: open cells from biobased PUF (PUF 2) 74

Figure 2.7: Isocyanate reactivity with alcohol (a), water (b), urethane (c), urea or isocyanate trimerization (e). 81

Figure 2.8: Foaming reaction profiles: evolution of the temperature (a), maximum height (b), and foaming rate (c) vs. time during the foaming step 86

Figure 2.9: a. FTIR spectra of formulated foams, b. FTIR spectra zoom on isocyanurate absorption band area 88

Figure 2.10 : TGA (a) and DTG (b) curves for PU-based foams under dry air 88

Figure 2.11: SEM images of PU foam samples in T (top) and L direction (bottom) 89

Figure 2.12: -a) storage, loss modulus and Tan δ evolution of REF, and -b) polyester-based PU foam B100-2 90

Figure 2.13: Stress strain curves of both REF and polyester-based PU foam (B100-2) , in –a) L direction (top), -b) T direction (bottom) 91

Figure 2.14: Stress-strain curves of different polyester-based PU foam, in –a) L direction (top), -b) T direction (bottom) 92

Chapitre 3

Figure 3.1: Diisocyanate trimerization in presence of potassium carboxylate catalyst 101

Figure 3.2: PUIR foaming. Evolution of (a) temperature, (b) foaming rate, and (c) normalized height (H/Hmax) vs. time. . 107

Figure 3.3: Evolution of the foam temperature vs. time for REF, PU-0/85/15-KE and PU-0/85/15-KP 108

Figure 3.4: Images of the PUIR foams (a) REF, (b) PU-0/85/15-KE and (c) PU-0/85/15-KP (from left to right) 109

Figure 3.5: REF PUIR foam SEM images, magnify x40 (see scale bars). a. in transversal direction to the foam rise, b. in the foam rise direction (from bottom to top). 109

Figure 3.6: Cells diameters distribution in transversal direction to the foam rise of diffrent PUIR foams 110

Figure 3.7: Stress-strain curves in (a) longitudinal and (b) transversal direction to the foam rise, for foam systems from the reference to 65% of substitution 114

Chapitre 4

Figure 4.1: D-BisCC from D-sorbitol 130

Figure 4.2: D-sorbitol and D-mannitol structures 131

Figure 4.3: Proposed reaction path-way of D-sorbitol with DMC, from Mazurek-Budzynsky et al.(Mazurek-Budzyńska et al., 2016) 131

Figure 4.4: Influence of the number of equivalent of DMC on the kinetic profile with a distillation bridge device 133

Figure 4.5: Influence of the number of equivalent of DMC on the kinetic profile with vigreux distillation column 134

Figure 4.6: General mechanism to obtain ether linkage from five-membered BisC, with CO_2 formation 135

Figure 4.7: NMR spectra: (a) ^{1}H-NMR of the D-BisCC and 1-octanol mixture (b) ^{1}H-NMR and (c) ^{13}C-NMR of the synthesized product. 136

Figure 4.8: FT-IR spectra of BisCC, PHU-P, PHU-B, PHU-D, PHU-D and PUH-H 138

Figure 4.9: aminolysis reactional pathway between a five-membered BisCC and a primary amine 138

Figure 4.10: a) TGA and b) DTG curves of PHU-P, PHU-B, PHU-D and PHU-H 140

Annexes

Figure SI 1: 1H-NMR of the reactional intermediate 169

Figure SI 2: 1H-NMR spectra of EASAE 170

Figure SI 4: ^{1}H-NMR spectra of BASAB 171

Figure SI 5: ^{1}H-NMR spectra of HASAH 171

Figure SI 6: ^{1}H-NMR spectra of OASAO 172

Figure SI 7: ^{1}H-NMR spectra of DASAD 172

Figure SI 8: ^{1}H-NMR spectra of DoASADo 173

Figure SI 9: ^{13}C-NMR spectra of EASAE 174
Figure SI 10: ^{13}C-NMR spectra of PASAP 175
Figure SI 11: ^{13}C-NMR spectra of BASAB 175
Figure SI 12: ^{13}C-NMR spectra of HASAH 176
Figure SI 13: ^{13}C-NMR spectra of OASAO 176
Figure SI 14: ^{13}C-NMR spectra of DASAD 177
Figure SI 15: ^{13}C-NMR spectra of DoASADo 177
Figure SI 16: ^{13}C-NMR spectra of neat sorbitol 178
Figure SI 17: ^{13}C-NMR spectra of adipic acid 178
Figure SI 18: ^{13}C-NMR spectra of succinic acid 179
Figure SI 19: ^{13}C-NMR spectra of the reactional intermediate 179
Figure SI 20 : ^{31}P-NMR spectra of EASAE 180
Figure SI 21: ^{31}P-NMR spectra of PASAP 180
Figure SI 22: ^{31}P-NMR spectra of BASAB 181
Figure SI 23: ^{31}P-NMR spectra of HASAH 181
Figure SI 24: ^{31}P-NMR spectra of OASAO 181
Figure SI 25: ^{31}P-NMR spectra of DASAD 182
Figure SI 26: ^{31}P-NMR spectra of DoASADo 182
Figure SI 27: polyester polyols viscosity vs. the shear rate at 20°C and 25°C 183
Figure SI 28: TGA and DTG of BASAB 184
Figure SI 29: DSC of BASAB 185
Figure SI 30: Polyester α-and β-scission mechanisms 185
Figure SI 31: FT-IR spectra of the BASAB reactional intermediate and the BASAB polyester polyol 187
Figure SI 32: ^{1}H-NMR of the BASAB reactional intermediate 188
Figure SI 33 : ^{13}C-NMR spectra of the BASAB reactional intermediate 189
Figure SI 34: ^{1}H-NMR spectra of BASAB 189
Figure SI 35: ^{13}C-NMR spectra of BASAB 190
Figure SI 36: Foams tomography images in T direction of B85-4, REF, B100-4 and B100-2 190
Figure SI 37 : HSPiP modeled solubility spheres of fossil-based (green wire frame sphere) and BASAB (grey wire frame sphere) polyol based on Hansen solubility parameters 193
Figure SI 38: foams evolution of the cream, gel and tack free times vs. the biobased polyester polyol content 193
Figure SI 39: PUIR foams SEM images, magnify x40 (scales are given) of all formulations 194
Figure SI 40: All PUIR foams cells diameters, a. minimal diameter distribution in the transversal direction, b. maximal diameter distribution in the transversal direction, c. minimal diameter distribution in the longitudinal direction, d. maximal diameter distribution in the longitudinal direction 195
Figure SI 41: FTIR spectra of: a. REF, PU-90/10/0-KE, PU-75/25/0-KE,PU-65/35/0-KE, PU-55/45/0-KE; b. Reference, PU-45/55/0-KE,PU-65/35/0-KE, PU-0/85/15-KE , PU-0/85/15-KP foams 196
Figure SI 42: PIR foams a. TGA curves, under dry air; b. DTGA curves, under dry air 196
Figure SI 43: All formulated PUIR foams flammability results 196
Figure SI 44: Longitudinal and transversal Young's modulus evolution as function of biobased polyol concentration 197

Figure SI 45: DSC analysis of the D-sorbitol-based BisCC 199

Figure SI 46: FT-IR analysis of the D-sorbitol-based BisCC 199

Figure SI 47 (a) ^{1}H-NMR spectrum and (b) ^{13}C-NMR spectrum of sorbitol-based BisCC 200

Figure SI 48: ^{1}H-NMR cis-1,2-cyclopentanediol before the reaction with dimethyl carbonate 201

Figure SI 49: ^{1}H-NMR trans-1,2-cyclopentanediol before the reaction with DMC 201

Figure SI 50: ^{1}H-NMR cis-1,2-cyclopentanediol after the reaction with DMC 202

Figure SI 51: ^{1}H-NMR trans-1,2-cyclopentanediol after the reaction with DMC 202

Figure SI 52: ^{1}H-NMR of distillated subsidiary products of the catalyzed reaction between D-sorbitol and DMC 203

Figure SI 53: Theoretical reactional product one mole of BisCC with two moles of 1-octanol. 204

Figure SI 54: SEC curves of macromolecules products Entries 5 to 9 (Table 6) 204

Figure SI 55: ^{31}P-NMR spectra and hydroxyl content of macromolecules 5 to 9 from Table 8 206

Figure SI 56: FTIR spectra of ROP products presented in Table 8, Entries 2-4 207

Figure SI 57: FTIR analysis of PHUs 208

Figure SI 58 : : SEC curves a) PHU-P and b) PHU-H 209

Figure SI 59: SEC curves of a) PHU-0.2B, b) PHU-0.4B, c) PHU-0.6B, d) PHU-0.8B, e) PHU-B, f) PHU-0.2D, g) PHU-0.4D, h) PHU-0.6D, i) PHU-0.8D, j) PHU-D 210

Figure SI 60: ^{1}H-NMR of PHU-P sample 211

Figure SI 61: ^{1}H-NMR of PHU-B sample 211

Figure SI 62: ^{1}H-NMR of PHU-D sample 212

Figure SI 63: ^{1}H-NMR of PHU-H sample 212

Figure SI 64: ^{13}C-NMR of PHU-P sample 213

Figure SI 65: ^{13}C-NMR of PHU-B sample 213

Figure SI 66: ^{13}C-NMR of PHU-D sample 214

Figure SI 67: ^{13}C-NMR of PHU-H sample 214

Figure SI 68: a) TGA and b) DTG curves of PHU-0.2B, PHU-0.4B, PHU-0.6B, PHU-0.8B samples; b) TGA and c) DTG curves of PHU-0.2D, PHU-0.4D, PHU-0.6D, PHU-0.8D samples 215

Figure SI 69: a) DSC curves of PHU-0.2B, PHU-0.4B, PHU-0.6B, PHU-0.8B, PHU-B samples and b) PHU-0.2D, PHU-0.4D, PHU-0.6D, PHU-0.8D, PHU-D samples, c) Tg evolution in function of the 1.4 B content compared to predicted Tg obtained by Fox Law, d) Tg evolution in function of the 1.5 MD content compared to predicted Tg obtained by Fox Law. 215

Figure SI 70: enchaînement des étapes de synthèse du BASAB à l'échelle pilote (900kg) 218

Figure SI 71: principe de fonctionnement d'une ligne de production de mousse polyuréthane 219

Figure SI 72: exemple de panneaux de mousses PUIR issus de l'essai à l'échelle du pilote industriel 220

Tableaux

Chapitre 1

Table 1.1: General PU foams classification 18

Table 1.2:Thermal conductivity coefficient of common blowing agents. 21

Table 1.3: Relationships between the main polyols properties and PU foams behavior 22

Table 1.4: Structures and main properties of short polyols 24

Table 1.5: Alkoxylated polyethers average conditions and resulting polyol and foams mains properties 29

Table 1.6: Lipid profiles of different vegetable oils 35

Table 1.7: Polyols and PU foams properties obtained from vegetal oil derivates 38

Table 1.8:Conditions of lignocellulosic biomass liquefaction and some corresponding polyols and PU foams properties 40

Table 1.9: Mannich polyol properties in function of the building block botanic origin and corresponding PU foams properties 43

Table 1.10: PET glycolysis and esterifications conditions and resulting PU foams properties 45

Table 1.11: NIPU foams properties 48

Chapitre 2

Table 2.1: Synthesis of polyester polyols with the corresponding designations and the formulations 68

Table 2.2: PUF formulations in wt. % and in parts to the total polyol content, with the final estimated biobased contents, the kinetic results, the Foamat data the and closed cell content 69

Table 2.3 : IOH and AV data from the biobased polyester polyols 71

Table 2.4 : Thermal behavior of the polyester polyols 73

Table 2.5 : Foam characteristic time comparison between a reference and with un-neutralized and neutralized BASAB (Formulations are similar than the reference, see Table 2) 74

Table 2.6 : Main properties of the polyether and biobased BASAB polyester polyols. 83

Table 2.7: PU foams formulations and the main corresponding characteristic times linked to the foaming process 84

Table 2.8: PU foam cell morphology 89

Table 2.9 : Main foams parameters 90

Table 2.10 : Main mechanical properties and glass transition temperatures. 92

Chapitre 3

Table 3.1: Comparison of the fossil-based and BASAB polyols properties 102

Table 3.2: Detailed formulations for the elaboration of the PUIR foams. 103

Table 3.3: Characteristic time of REF, PU-0/85/15-KE and PU-0/85/15-KP foams 108

Table 3.4: Feret diameters and anisotropic coefficients R in longitudinal and transversal directions, for PUIR foams. 111

Table 3.5: All formulated PUIR foams apparent density and close cells content 111

Table 3.6: PUIR foams degradation temperature at 50% and 100% of weight loss and DTG results 113

Table 3.7: Mechanical and thermal conductivity parameters of the different PUIR Foams 114

Chapitre 4

Table 4.1: Chemical structures and properties of building blocks. D-sorbitol and different polycyclic sorbitol derivatives. 123

Table 4.2: DDA main properties 125

Table 4.3: BisCC synthesis from D-sorbitol and DMC or EC, under different conditions and catalyst systems 126

Table 4.4: Synthesis of BisCC from D-sorbitol using a continuous feed of DMC 126

Table 4.6: Conditions of synthesis to obtain polyether / polycarbonate from D-BisCC. 128

Table 4.7: ESI and elementary analysis of D-BisCC. Theoretical and experimental results. 130

Table 4.8: Properties of main synthetized macromolecular architectures 137

Table 4.9: Main properties of the synthetized PHUs 141

Annexes

Table SI 1: Exemple de calcul de formulation d'une mousse PUR destiné à l'isolation du bâtiment 167

Table SI 2: Exemple de calcul d'une mousse PUR avec un mélange d'agents gonflants chimiques et physiques 167

Table SI 3 : Exemple de calcul d'une mousse PUR avec un mélange d'agents gonflants chimiques et physiques 168

Table SI 4 : Main properties and cost of glycerol and sorbitol 169

Table SI 5: Global yields of the polyol polyesters from 1H-NMR integration 173

Table SI 6: Polyester polyol hydroxyl and carboxyl acid quantifications from ^{31}P-NMR integration 182

Table SI 7: detailed used solvents for solubility sphere modeling and their Hansen parameters associated with BASAB and PS 2412 solubility score 192

Table SI 8: PUIR foams Shore 00 Hardness results 195

Table SI 9 : quantité de matière nécessaire à la synthèse du BASAB à l'échelle pilote 217

Table SI 10 : comparaison des propriétés du BASAB produit à l'échelle du laboratoire et pilote 219

Table SI 11 : comparaison des propriétés des mousses produite à l'échelle du laboratoire et pilote 220

INTRODUCTION GÉNÉRALE

Les polymères sont aujourd'hui des matériaux incontournables dans notre quotidien. Ils sont utilisés pour un grand nombre d'applications en raison de leur faible coût, leurs grandes fonctionalités et facilités de mise en œuvre. Il existe deux grandes sources de matières premières pour l'élaboration des polymères : les ressources fossiles et la biomasse. Les polymères issus de la biomasse sont appelés « polyméres biosourcés ». Le terme biopolymére concerne specifiquement les polymères directement élaborés par des organismes vivants (polysaccharides, proteines). Les polymères de synthèse entièrement issus de ressources fossiles sont apparus au début du XX^{e} siècle avec le développement de la Bakélite, synthétisée par le chimiste belge Léo Baekeland. Depuis, le développement des polymères synthétiques, communément appelés plastiques, n'a jamais cessé de croître passant de 2 millions de tonnes en 1950 à 322 millions de tonnes en 2015. L'homme aurait ainsi produit plus de 8,3 milliards de tonnes de plastiques. Ce qui place les plastiques en troisième position des matériaux les plus fabriqués derrière le ciment et l'acier.

Les polymères satisfont à l'heure actuelle un grand nombre d'applications allant de la simple bouteille aux applications médicales. Néanmoins, l'inconvénient majeur pour les polymères majoritairement issus de ressources fossiles est leur impact environnemental. Leur empreinte carbone ne peut plus être négligée. De plus, comme tout produit issu de l'industrie pétrolière, certains polymères issus de ressources fossiles font face à la raréfaction de certaines fractions du pétrole et encore plus à la fluctuation des prix de ce dernier. À cela viennent s'ajouter de nouvelles directives et contraintes législatives territoriales ou mondiales. Ces pressions à l'encontre des matières fossiles et le contexte actuel de transition énergétique encouragent grandement la recherche scientifique et industrielle à développer de nouveaux polymères et plus largement de nouveaux matériaux plus respectueux de l'environnement. Ainsi, l'essor de la production de bioplastiques biodégradables ou durables ne cesse de croître. Elle était de 1,7 million de tonnes en 2014 et est estimée à 7.8 millions de tonnes pour 2019.

Une famille importante de polymère est la famille des polyuréthanes (PUs). La production de PUs était de l'ordre de 18 millions de tonnes en 2016, plaçant les PUs à la 6^{e} place des polymères les plus produits à l'échelle mondiale. Les PUs sont des matériaux polyvalents puisqu'ils peuvent être utilisés dans un grand nombre d'applications tel que l'ameublement, la literie, le transport, la construction et l'électroménager. La part la plus importante de la production des PUs est consacrée à l'élaboration de mousses polyuréthanes souples ou rigides. Les mousses polyuréthanes souples sont par exemple utilisées pour des applications dans l'ameublement, la literie et l'isolation acoustique. Les mousses polyuréthanes rigides sont principalement employées pour des applications d'isolation thermique. Les deux principaux piliers de l'industrie des PUs sont liés à la production de polyisocyanates et les polyols. Historiquement, polyisocyanates et polyols sont issus de matières pétrosourcées parfois dangereuses pour la santé telles que les dérivés du phosgène, l'oxyde d'éthylène et l'oxyde de propylène. Néanmoins, la production de polyols biosourcés est en pleine croissance. Un grand nombre de synthons issus de la biomasse présentent une fonctionnalité adéquate pour la synthése de nouveaux polyols qui peuvent entrer dans la composition des mousses polyuréthanes.

Les mousses polyuréthanes souples occupent la première place du marché des PUs. Elles peuvent également inclure les mousses dites semi-rigides / semi-flexibles. Les mousses semi-rigides se distinguent par une reversibilité partielle après une grande déformation alors que les mousses flexibles (ou souples) sont totalement réversible. Les mousses PU semi-flexible sont principalement élaborées en bloc ou par moulage (moule chaud ou froid). Les mousses semi-flexibles à cellules ouvertes sont utilisées par exemple dans l'automobile alors que les mousses souples moulées seront destinés à la confection de sièges (Ashida, 2006).

Les mousses polyuréthanes rigides occupent la deuxième place du marché des PUs et sont extrêmement importantes. Elles représentent actuellement une des solutions les plus performantes pour l'isolation des bâtiments collectifs ou individuels. L'idée d'utiliser des matériaux spécifiquement pour l'isolation du bâtiment est apparue en 1940 en ayant pour objectif de réduire les consommations énergétiques des pays lors

des hivers rigoureux. Néanmoins la réelle prise de conscience sur le besoin de tels matériaux est arrivée après la seconde guerre mondiale lorsque les chocs pétroliers successifs de 1973, 1979 et 2008 ont entraîné une envolée des prix de l'énergie. Suite à cela un grand nombre de produits pour l'isolation des toitures et des bâtiments est apparu (Tibério Cardoso et al., 2012). On citera à titre d'exemple la laine de roche, la ouate de cellulose, le polystyrène expansé et extrudé, les mousses phénoliques, les mousses polyuréthanes, et les mousses polyisocyanurates. La densité, la capacité thermique massique et les coefficients de conductivités thermiques (λ) de quelques matériaux communs de construction sont donnés dans le Tableau 1. Par opposition, le Tableau 2 donne les coefficients de conductivité thermique des principaux matériaux d'isolations. Plus les coefficients de conductivité thermique sont bas, plus le matériau étudié est isolant. Ces valeurs de coefficient de conductivité thermique montrent bien la supériorité des matériaux d'isolations par rapport aux matériaux de construction en termes de pouvoir isolant. Leur utilité en termes d'efficience énergétique du bâtiment n'est donc pas négligeable. Ainsi, la recherche de matériaux d'isolations toujours plus performants ne cesse de croître afin de répondre aux exigences de demain.

Tableau 1 : Principaux matériaux de constructions ainsi que leur capacité thermique massique et coefficient de conductivité thermique ("NF EN ISO 10456 - Juin 2008,")

Matériaux	Masse volumique ρ (kg/m^3)	Capacité thermique massique Cp (J/(kg.K)	Coefficient de conductivité thermique λ (W/(m.K)
Acier	7800	450	50
Béton armé (avec 2% d'acier)	2400	1000	2,5
Béton de densité moyenne	1800-2200	1000	1,15-1,65
Tuiles (argile et béton)	2000-2100	800-1000	1,0-1,5
Verre sodo-calcique	2500	750	1,00
Enduit la chaux	1600	1000	0,8
Coupure thermique en résine phénolique	1300	1200	0,30
Enduit au plâtre	600-1300	1000	0,18-0,57
Coupure thermique en polyuréthane	1200	1800	0,25
Panneaux de bois contreplaqué	300-1000	1600	0,09-0,24

Tableau 2 :Principaux matériaux d'isolation alvéolaire et leur coefficient de conductivité thermique("NF EN ISO 10456 - Juin 2008,")

Matériaux d'isolation	Type de produit	Coefficient de conductivité thermique λ W/(m.K)
Laine minéral	Vrac	0,035-0,050
	Panneaux	0,032-0,038
	Panneaux rigides	0,030-0,035
Laine de bois	Tout type	0,070-0,090
Polystyrène extrudé	Sans peau	0,025-0,040
	Avec peau	0,025-0,035
	Avec revêtement imperméable	0,025-0,040
Mousse phénolique	Mousses à cellules fermés	~ 0,025
	Mousses à cellules ouvertes	~ 0,032
Mousse de polyuréthane	Produits sans parement	0,025-0,030
	Produits avec parements imperméables	0,022-0,025

Dans ce contexte de recherche dynamique de matériaux d'isolation plus performants et de développement de nouvelles architectures moléculaires plus respectueuses de l'environnement, un partenariat tripartite a vu le jour, comprenant deux entreprises : Tereos (France) et SOPREMA (France) ainsi que la BioTeam, équipe du

Pr. Luc Avérous au sein de l'Institut de Chimie et Procédés pour l'Énergie, l'Environnement et la Santé (ICPEES – UMR 7515 – Université de Strasbourg). Ce travail de doctorat fait partie intégrante du projet collaboratif « *PURBio* » consacré au développement de nouveaux polyuréthanes biosourcés destinés à l'isolation du bâtiment**. Ce projet est financé par les deux entreprises mentionnées, la région Alsace, et l'Eurométropole de Strasbourg.**

L'objectif pour la société Tereos est de trouver de nouvelles perspectives / applications pour diversifier la valorisation de produits issus de matières premières agricoles, notamment le sorbitol (Figure. 1). Le sorbitol est un dérivé du glucose présentant une grande stabilité chimique et une fonctionnalité élevée. Idéalement, la transformation du sorbitol devra s'appuyer autant que possible sur les grands principes de la chimie verte.

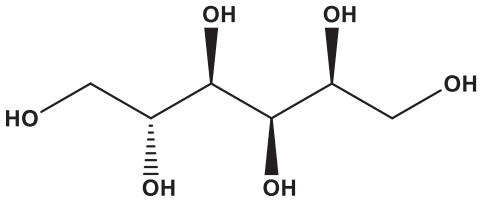

Figure. 1: Structure chimique du sorbitol

L'entreprise SOPREMA est aussi à la recherche de nouveaux polyols biosourcés destinés à l'élaboration de mousses polyuréthanes rigides (PUR) pour l'isolation du bâtiment. Plus précisément, l'entreprise recherche des polyols permettant l'élaboration de mousses tels que les polyisocyanurates rigides (PIR). Une nouvelle génération de matériaux biosourcés avec des performances améliorées.

Enfin les deux entreprises, établies en Alsace, souhaitent développer une collaboration de proximité pour acquérir de nouvelles connaissances sur leurs produits et optimiser leur gain ou coût financier respectif. De nouvelles architectures moléculaires doivent être elaborés en valorisant le sorbitol pour les besoins actuels et futurs des entreprises. Le projet de transformation du sorbitol en polyol ou en nouvelles molécules plateformes (Figure 2), est basé sur le cahier des charges simplifiés suivants :

- ✓ Les différentes opérations de transformation chimique n'impliquent pas ou peu de composés toxiques ;
- ✓ Les monomères utilisés sont préférentiellement biosourcés ou biosourçables ;
- ✓ les réactions seront autant que possible sans solvant et ne généreront pas de sous-produits toxiques ;
- ✓ Les procédés de transformation / synthése doivent pouvoir être transferable (changement d'échelle) par les entreprises Tereos et SOPREMA sur la base de leur expertise actuelle ;
- ✓ Les polyols obtenus doivent permettre l'élaboration de mousses PUR et PIR ;
- ✓ Les mousses PUR et PIR obtenues doivent présenter un taux élevé de cellules fermées, passer des tests normés d'inflammabilité, être rigides, et présenter une bonne résistance à la compression. Elles doivent présenter de faible coefficient de conductivité thermique ($\lambda \leq 25$ mW/mK).

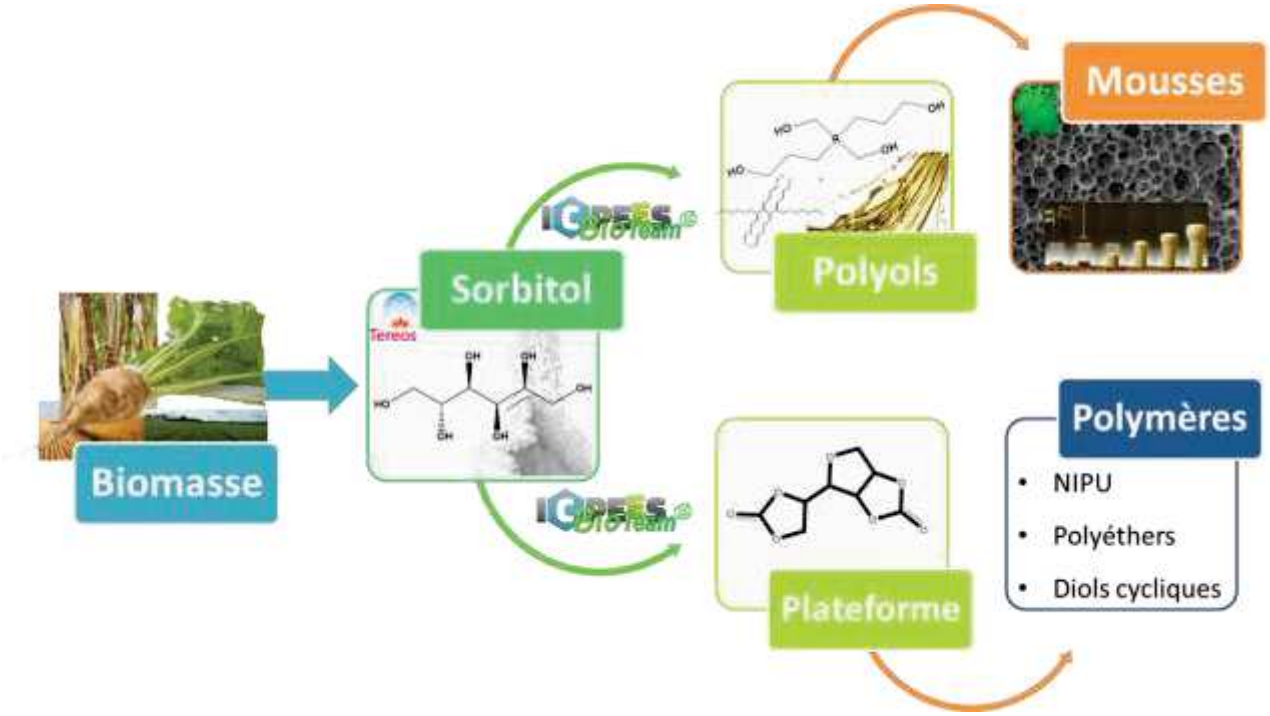

Figure 2: vision schématique du projet PURBio

Le sorbitol ou ((2S, 3R, 4R, 5R)-hexane-1,2,3,4,5,6-hexol ou D-(-)-glucitol) est un polyol linéaire à six carbone (C6) issu de la biomasse. Le sorbitol (Figure. 1) est l'isomère de trois autres polyols : le dulcitol, le mannitol et l'iditol (Figure 3) et se présente sous la forme d'un solide blanc.

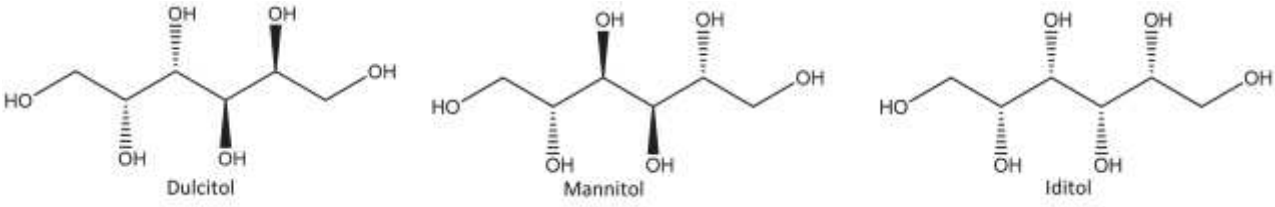

Figure 3: Isomères du sorbitol

Le sorbitol est une molécule d'intérêt qui est citée comme une des 12 molécules plateformes stratégique par le département de l'efficience énergétique et de l'énergie renouvelable (DoE-Etats-Unis) en 2004 (Holladay et al., 2007). Le sorbitol présente une fonctionnalité de 6 : 2 groupements hydroxyles primaires et 4 secondaires dont les principales propriétés sont résumées dans le Tableau 3.

Tableau 3 : Propriétés du sorbitol

Propriétés	Valeurs
Poids moléculaire (g/mol)	182,2
Prix moyen (€/kg)	0,80
Température de fusion (Tf)	98
Température d'ébullition (Téb)	296
Densité (kg/m^3)	1489
Indice hydroxyle (mg KOH/g)	1848
Solubilité dans l'eau (g/L)	2,75

Les voies de modification proposées pour le sorbitol sont principalment basées sur l'hydrogénation et la déshydratation. Les principales molécules résultantes sont présentées dans la Figure 4. Un avantage du sorbitol est son prix de 800 €/Tonnes qui est relativement stable et bas par rapport à d'autres dérivés issus de matière agricole. Par exemple le xylitol est vendu entre 1000 et 3000 $/Tonne ou le furfural à 2500 - 3000 $/Tonne.

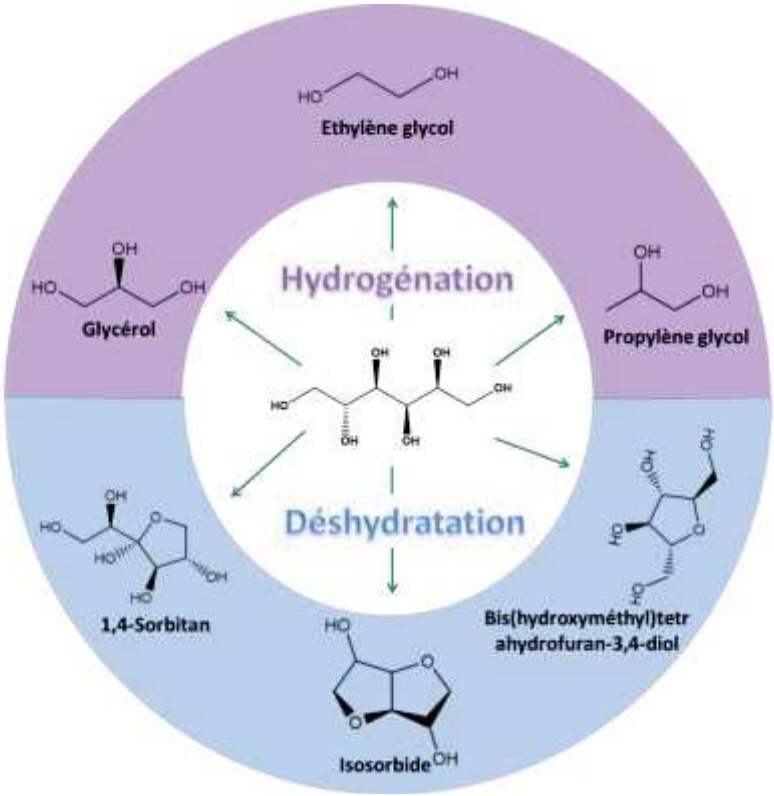

Figure 4: Principales molécules d'intérêt résultantes du sorbitol

Le sorbitol est en Europe essentiellement obtenu à partir de monosaccharides issus de la culture de la betterave sucrière. Les monosaccharides sont divisés en deux grandes familles : (i) les monosaccharides contenant une fonction aldéhyde, appelés aldoses et (ii) les monosaccharides contenant une fonction cétone, appelés cétoses. Il existe deux principales cétoses, trouvées dans la nature: le xylulose (C5) et le fructose (C6). La famille des aldoses compte quatre sucres en C5 : le xylose, l'arabinose, le ribose, et le lyxose. Par contre on recense huit sucres en C6 : le glucose, le mannose, le galactose, l'allose, le gulose, l'idose et le talose. Les plus courants sont le glucose, le fructose, le mannose et le galactose. L'idose et le talose n'existent pas à l'état naturel (Bhaumik and Dhepe, 2015). L'aldose le plus utilisé pour la production de sorbitol est le glucose. Historiquement, le sorbitol était obtenu par réduction électrochimique du D-glucose. Désormais, le sorbitol est principalement obtenu par hydrogénation de la forme linéaire du D-glucose en solution aqueuse (Fang et al., 2017). Le procédé industriel typique d'obtention du sorbitol est présenté en Figure 5. Lorsque le nickel de Raney est utilisé comme catalyseur, le pH est généralement maintenu autour de 7 pour éviter l'isomérisation du D-glucose en mannose permettant une conversion de 100 % du D-glucose en sorbitol avec une sélectivité supérieure à 99 %. D'autres voies d'obtention du sorbitol existent, notamment à partir d'amidon ou de cellulose. Historiquement, l'amidon est hydrogéné en sorbitol depuis la seconde moitié du XX^{ième} siècle (Hartstra and Van, 1950; Jacobs and Hinnekens, 1989). Parallèlement, le développement de procédés à partir de cellulose constitue une approche intéressante puisque la cellulose ne rentre pas en compétition avec l'alimentaire. Il existe d'autres procédés d'obtention du sorbitol, notamment par voie bactérienne, mais les temps de production restent relativement longs (Ochoa-Gómez and Roncal, 2017).

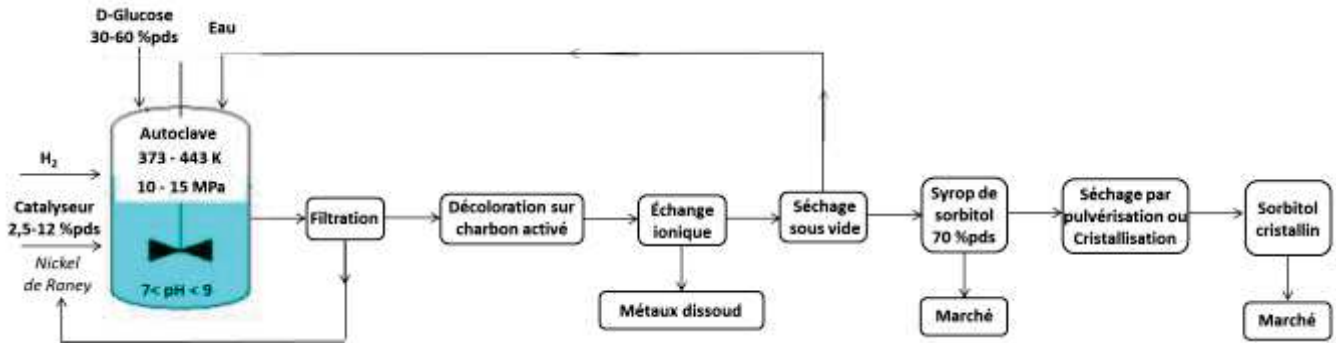

Figure 5: Procédé industriel d'obtention du sorbitol par hydrogénation du D-glucose

Par ailleurs, la production mondiale de sorbitol est croissante puisqu'elle est passée de $5x10^5$ tonnes en 2010 à $6,5x10^5$ tonnes en 2013. Le sorbitol est principalement utilisé dans les domaines de l'alimentaire, la pharmacie, la cosmétique, la chimie, la biomédecine, et des détergents (Ugarte et al., 2015). On notera que 15% de la production mondiale de sorbitol est utilisée pour la synthèse de l'acide ascorbique (vitamine C) (Gallezot et al., 1994). La stabilité thermique du sorbitol est un point non négligeable pour mettre en place les procédés chimiques de transformation et éviter, par exemple, la déshydratation du sorbitol lorsque sa cyclisation n'est pas souhaitée. La déshydratation du sorbitol en milieu acide peut commencer à 20°C lorsqu'elle est catalysée par de l'acide fluorhydrique (Defaye et al., 1990) et plus généralement entre 105 et 135°C si elle est catalysée par de l'acide sulfurique (Flèche and Huchette, 1986). En solution aqueuse, la déshydratation du sorbitol a été réalisée à 250°C sur 35h pour une conversion de 100% du sorbitol (Yamaguchi et al., 2011). Cela démontre la bonne stabilité thermique du sorbitol, spécialement en l'absence de catalyseur acide.

Le sorbitol est utilisé comme initiateur dans les réactions d'alkoxylation, cependant moins communément que le glycérol (Ionescu, 2005). Les polyols polyéthers résultants sont utilisés dans la formulation de mousses polyuréthanes depuis un demi-siécle. Néanmoins cette chimie se base sur l'utilisation de monomères extrêmement toxiques tel que l'oxyde de propylène ou d'éthylène, tous deux pétrosourcés. Le Tableau 4 compare les propriétés et la toxicité de l'oxyde d'éthylène et de l'oxyde de propylène, tous deux sont classés cancérogènes, mutagènes ou toxiques pour la reproduction (CMR). À l'inverse, les sucres tels que le sorbitol présentent une toxicité moindre poussant la recherche à les valoriser pour faire des polyols avec des approches plus respectueuses de l'environment et de la santé.

Tableau 4: Comparatif de monomères classiques utilisés pour des réactions d'alkoxylation en comparaison avec la molécule de sorbitol

	Oxyde d'éthylène	Oxyde de propylène	Sorbitol
Structure		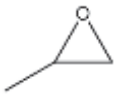	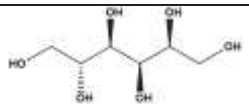
T° de fusion (°C)	-111	-112	98
T° d'ébullition (°C)	11	34	>295
Symbol SGH			aucun

Ce travail de thèse est axé sur une approche d'ingénierie macromoléculaire afin d'accéder à de nouvelles molécules et macromolécules à base de sorbitol pour des applications ciblées dans le domaine de l'isolation du bâtiment, dans un contexte d'attentes industrielles. Les sucres et leurs dérivés représentent de bons candidats pour le développement de nouvelles architectures moléculaires et macromoléculaires biosourcées en s'appuyant sur des réactions d'estérification ou transestérification en raison de leur haute fonctionnalité en groupements hydroxyles. Trois phases ont été abordés. Premièrement le sorbitol, un sucre cristallin présentant une température de fusion élevée de l'ordre de 98 °C, a été transformé en polyols linéaires de différentes tailles. Puis une étude de formulation de mousses PUs à partir de polyols biosourcés a été réalisée. Enfin, une nouvelle molécule plateforme a été obtenue à partir de sorbitol, un bis(cyclocarbonate), adapté notament mais pas uniquement au développement de polyuréthanes sans isocyanate (poly(hydroxyuréthane)).

Organisation du manuscrit :

Le manuscrit est organisé sur quatre Chapitres reposant sur une base d'articles scientifiques parues ou à paraitre dans des revues à comité de lecture anglophone. Chaque article scientifique sera encadré d'une introduction et conclusion en français. C'est pourquoi l'indulgence du lecteur est sollicitée pour les répétitions inhérentes à la forme de rédaction choisie.

Après cette introduction générale, le prochain Chapitre (Chapitre 1) sera consacré à un état de l'art sur les polyols biosourcés spécifiquement développés pour la synthèse de mousses polyuréthanes. L'historique et le developpement des polyuréthanes y seront exposés ainsi que les constituants minimums nécessaires à l'élaboration d'une mousse polyuréthane. Enfin, une partie plus développée concernera l'élaboration de nouveaux polyols à partir de biomasse.

Par la suite, les parties expérimentales et discussions sont divisées en divers Chapitres et sous Chapitres.

Le premier Chapitre expérimental (Chapitre 2) est divisé en deux sous-Chapitres. Le premier sous-Chapitre présente l'élaboration de polyols polyesters à partir du sorbitol selon un procédé d'estérification contrôlé en deux étapes. Les polyols polyesters ont été synthétisés sur la base d'une réaction en masse commençant à l'état solide entre le sorbitol et l'acide adipique ou succinique. Huit polyols polyesters sont ainsi obtenus. Ils présentent tous des propriétés compatibles avec l'élaboration de mousses polyuréthanes. L'objectif de cette première partie est aussi d'identifier le ou les polyols présentant les meilleures propriétés pour l'élaboration de mousses polyuréthanes ou polyisocyanurates. Ce premier sous-Chapitre comporte également une étude préliminaire sur les effets de l'acidité résiduelle des polyols polyesters sur les temps caractéristiques d'obtention des mousses polyuréthanes. Enfin une première série de neuf mousses polyuréthanes sera présentée afin d'approcher l'impact de différents constituants de la formulation (systèmes d'agent gonflant et nature des polyols) des mousses sur les temps caractéristiques de moussage et les profils cinétiques.

Le second sous-Chapitre est axé sur l'étude des relations existantes entre la formulation initiale d'une mousse polyuréthane et ses propriétés mécaniques résultantes. Dans un objectif de remplacement des polyéthers pétrosourcés obtenus par réaction d'alkoxylation actuellement utilisée dans l'industrie, les mousses polyuréthanes étudiées dans ce sous-Chapitre sont formulées à base d'un polyol selectioné lors de l'etude presenté dans le premier sous-Chapitre, éventuellement associé à d'autres polyols courts biosourcés. Deux familles de mousses polyuréthanes biosourcées ont été formulées pour cette étude. Une famille est formulée à partir d'un seul polyol alors que la seconde est formulée avec un mélange de polyols. Ensuite l'objectif a été d'étudier l'impact du système d'agent gonflant mixte (chimique vs. physique). Les mousses

polyuréthanes biosourcées ainsi obtenues présentent des propriétés mécaniques spécifiques et ont fait l'objet d'une étude des relations « structure / morphologie-propriétés » approfondis.

Le deuxieme Chapitre expérimental (Chapitre 3) est consacré à l'approche des systèmes de mousses PIR. Ces mousses répondent à une demande de plus en plus forte du marché de l'isolation du bâtiment de par leurs propriétés d'isolation supérieures et surtout de par leur résistance au feu amélioré par rapport aux mousses PUR conventionnelles. La chimie liée à l'élaboration de ces mousses est plus complexe que celle des mousses PUR, rendant la substitution des polyols polyesters pétrosourcés par des polyols biosourcés plus délicates. Ainsi une première approche basée sur la substitution progressive de polyols polyester pétrosourcés par un polyol polyester biosourcé dans la formulation des mousses PIR a été mise en place. Face à la diminution des propriétés des mousses PIR à fort taux de subsitution en polyols polyester pétrosourcés, le système catalytique des formulations PIR a été adapté aux polyols polyester biosourcés. Cela a permis l'obtention de mousses PIR contenant 100% de polyol biosourcé.

Le troisieme et dernier Chapitre expérimental (Chapitre 4) est dédié aux modifications chimiques du sorbitol afin d'obtenir une nouvelle molécule plateforme du type cyclo-carbonate. Sur la base d'une réaction solide / liquide catalysée entre le sorbitol et un solvant réactif non toxique, une molécule bis-cyclocarbonate (D-BisCC) a été obtenue. Le solvant réactif choisi est le diméthyle carbonate (DMC) pour une réaction de transestérification entre les groupements hydroxyles du sorbitol et du DMC. L'obtention du D-BisCC fait l'objet d'une étude complète de l'impact du système réactionnel utilisé sur la conversion du sorbitol en D-BisCC. Une étude cinétique de la réaction de transestérification a été faite sur les meilleurs systèmes réactionnels. Enfin, le D-BisCC obtenu a été etudié comme une molécule plateforme pour l'obtention de diols, et macromolécules telles que des polyéthers ou des polyhydroxyuréthanes (PHUs).

Pour finir, ce memoire sera complété par une conclusion générale qui sera suivie d'une partie bibliographique et d'annexes.

Références :

Ashida, K., 2006. Polyurethane and related foams: chemistry and technology. CRC press.

Bhaumik, P., Dhepe, P.L., 2015. Chapter 1. Conversion of Biomass into Sugars, in: Murzin, D., Simakova, O. (Eds.), Green Chemistry Series. Royal Society of Chemistry, Cambridge, pp. 1–53.

Defaye, J., Gadelle, A., Pedersen, C., 1990. Carbohydr. Res. 205, 191–202.

Fang, Z., Smith, R.L., Qi, X. (Eds.), 2017. Production of Platform Chemicals from Sustainable Resources, Biofuels and Biorefineries. Springer Singapore, Singapore.

Flèche, G., Huchette, M., 1986. Starch - Stärke 38, 26–30.

Gallezot, P., Cerino, P., Blanc, B., Fleche, G., Fuertes, P., 1994. J. Catal. 146, 93–102.

Hartstra, L., Van, W.H.A., 1950. Hydrogenation of carbohydrates. 2518235.

Holladay, J.E., Bozell, J.J., White, J.F., Johnson, D., 2007. DOE Rep. PNNL 16983.

Ionescu, M., 2005. Chemistry and technology of polyols for polyurethanes. Rapra Technology, Shawbury, Shrewsbury, Shropshire, U.K.

Jacobs, P., Hinnekens, H., 1989. Single-step catalytic process for the direct conversion of polysaccharides to polyhydric alcohols. 0329923.

NF EN ISO 10456 - Juin 2008.

Ochoa-Gómez, J.R., Roncal, T., 2017. Production of Sorbitol from Biomass, in: Fang, Z., Smith, R.L., Qi, X. (Eds.), Production of Platform Chemicals from Sustainable Resources. Springer Singapore, Singapore, pp. 265–309.

Tibério Cardoso, G., Claro Neto, S., Vecchia, F., 2012. Front. Archit. Res. 1, 348–356.

Ugarte, L., Gómez-Fernández, S., Peña-Rodríuez, C., Prociak, A., Corcuera, M.A., Eceiza, A., 2015. ACS Sustain. Chem. Eng. 3, 3382–3387.

Yamaguchi, A., Hiyoshi, N., Sato, O., Shirai, M., 2011 Green Chem. 13, 873.

CHAPITRE 1 : MOUSSES POLYURETHANES ET POLYOLS BIOSOURCES – ETAT DE L'ART

Introduction du Chapitre 1

La synthèse bibliographique présentée dans ce Chapitre est consacrée aux polyols biosourcés pouvant servir dans l'élaboration de mousses polyuréthanes. Elle se présente au format d'une revue scientifique intitulée « From renewable polyols to polyurethane and polyisocyanurate foams »

La synthèse bibliographique retrace rapidement l'histoire des polyuréthanes et la chimie des isocyanates. L'élaboration de mousses polyuréthanes necessite au moins cinq constituants : (i) un polyisocyanate (ii) un agent gonflant (iii) un catalyseur (iv) un surfactant et (v) un polyol. Le rôle et la nature des quatre premiers sont succinctement présentés pour une meilleure compréhension des systèmes moussant à base de polyuréthanes. Ensuite, un ensemble de polyols biosourcés est présenté en fonction de leur appartenance à trois grandes familles : (i) les polyols courts (ii), les polyols aliphatiques et (iii), les polyols aromatiques. Un grand nombre de polyols d'origine renouvelable sont présentés, ils constituent les grandes directions de la recherche actuelle pour de nouveaux polyols verts. Ainsi, les polyols obtenus par liquéfaction de la biomasse lignocellulosique, modification d'huiles végétales, utilisation du glycérol pur ou non raffiné, et les polyols obtenus par réaction d'estérification / transestérification, couplage thiol-ène, base de Mannich sont décrit. Enfin la synthèse des mousses sans isocyanates sera introduite, car, à l'image des polyols pour mousses polyuréthanes, les monomères mis en jeu dans leur élaboration, principalement des poly(cyclo-carbonates) et des diamines, sont généralement issus de ressources renouvelables.

From renewable polyol to polyurethane and polyisocyanurate foams

Pierre Furtwengler[a], Luc Avérous[a,*]

[a]*BioTeam/ICPEES-ECPM, UMR CNRS 7515,*

Université de Strasbourg, 25 rue Becquerel, 67087 Strasbourg, Cedex 2, France

* Corresponding author: Prof. Luc Avérous, Phone: + 333 68852784, Fax: + 333 68852716, E-mail: luc.averous@unistra.fr

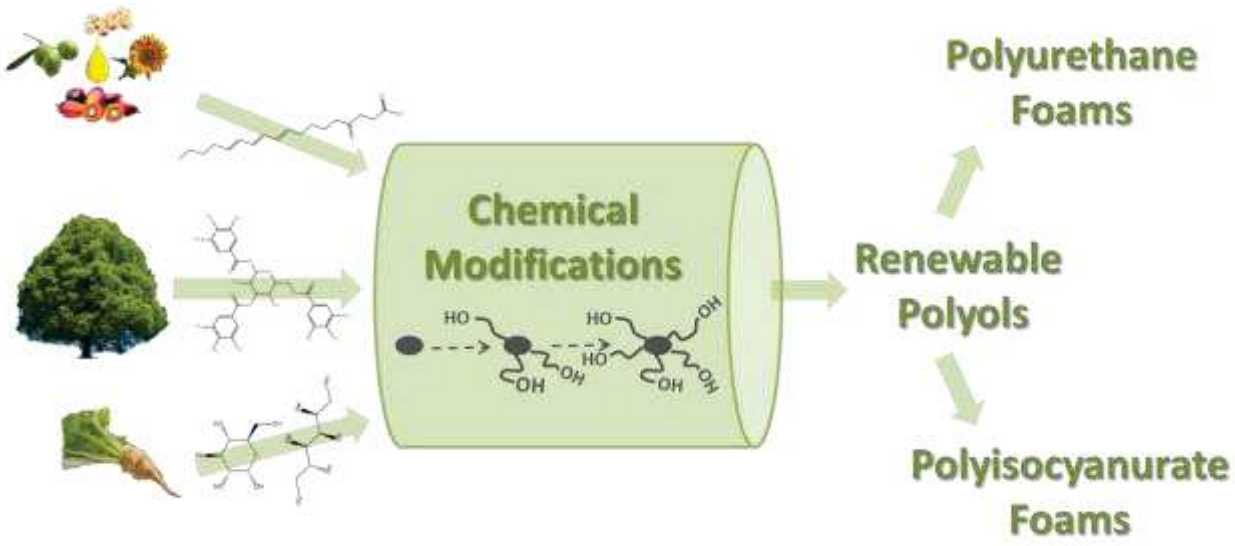

Abstract

Polyols for polyurethane (PU) and polyisocyanurate foams are a topic of interest since foams are the biggest part of the polyurethanes market. Then, these polyols constitute the highest part of polyols consumption. The large availability of chemicals and compounds from biomass has open a vast domain of chemical modifications opportunities to develop partially or fully biobased polyols, which can enter in foams formulation. This review is focused on the recent advances on the synthesis of renewable polyol dedicated to PU foams synthesis. Aliphatic and aromatic polyols have been classified as a function of their chemical structures. The different chemical pathways have been connected with the properties of the final PU-based foams. For example, correlations have been established between the polyol origin, the chemical modifications and the properties and morphologies of the corresponding foams. Recent advances in non-isocyanate polyurethane foams have been also taken into consideration.

Introduction

Bioplastics can be generally defined as biobased and/or biodegradable polymers. Biobased polymers are polymers with at least a part produced from biomass (i.e.: plants, animals, fungi, bacteria,), and generally with a renewable content superior to 20 wt%. The renewable content is often determined through the biobased carbon analysis using ASTM 6866 standard, with C^{14} measurement method. Biopolymers is a sub-class of the biobased polymers and are defined, according to IUPAC (Vert et al., 2012) as polymers formed by living organisms, such as different polysaccharides (cellulose, amylose, amylopectin, chitin, alginate,), lignins, proteins or natural rubbers.

The strong development of the biobased polymers during the last decades is generally due to (i) the need of new macromolecular architectures with new properties, (ii) the lack of some specific fractions of petrol (e.g., bitumen,), and (iii) the global context with the evolutions of the society's sensitivity, the political visions and the legal obligations concerning the sourcing of the materials (Bennett, 2012; Deutschmann and Dekker, 2012; Gandini and Belgacem, 2008). European Union has implemented a decarbonation agenda to decrease the greenhouse gases emission from the production to the end use, especially from the Kyoto protocol. The fossil resources (petrol, gas,) have been particularly targeted in this protocol (Langeveld et al., 2010).

The worldwide plastic production was higher than 330 MTons in 2016 (http://www.plasticseurope.org). But in 2017, only around 2 MTons of bioplastics were worldwide produced (http://www.european-bioplastics.org). However, the bioplastics represent after fuels the second-largest market for bioproducts and biorefineries development (Posen et al., 2016). According to the different market analysis, the current market for bioplastics is characterized by a strong dynamic growth rate with a global market value of several billions per year. According to the last results of the annual market data of the association of European Bioplastics (http://www.european-bioplastics.org), the global market is predicted to grow by 20% per year, from 2017 to 2022. There is a multitude of applications for bioplastics ranging from bottles for food in the packaging segment to keyboards in electronics, or interior parts in the automotive sector.

The most important plastics families are polyolefins (PE and PP), polyvinyl chloride (PVC), polystyrene (PS), polyethylene terephthalate (PET), and polyurethanes (PU). All of them are subject to

strong research to develop their renewable equivalents (Jiang and Zhang, 2017). Generally obtained by polyaddition between polyols and polyisocianates, PU, 6th rank among polymer worldwide production, are an attracting and interesting family of synthetic polymer as they are used in a large range of applications, presenting a wide variety of macromolecular architectures from thermoplastics to thermosets. PU chemical structure is specific to each application. PU main markets are foams (65%), coating (13%), adhesives sealant (7%), and elastomer (12%) for a global production of 14 MTons in 2010, which is expected to increase to 18 MTons in 2018 (Gandini, 2008; "Polyurethane," 2011). Polyurethane foams represent the main productions and are divided in two main categories such as (i) the flexible (or semi-flexible) foams (PUF) and (ii) the rigid polyurethane foams (PUR). PUF presents applications mainly on furniture, seats, beddings while PUR are widely used as insulating and structural materials for construction, transportation, furniture, pipe and refrigerator insulation.

A great number of biobased polyols are nowadays developed. A large part of them can fulfill the requirements to be employed in PU foams synthesis. Then, the object of the present work is focused on these polyols obtained from renewable resources which can be dedicated to the elaboration of PU foams. This study will cover the latest developments regarding the synthesis of polyols from biomass and then the elaboration of biobased PU foams. An effort will be made to link the chemical structures and origins of the polyols to the final foams structures, and their corresponding properties.

Polyurethane history and isocyanate chemistry

Isocyanates were discovered by Wurtz in 1848. Their chemistry was deeply investigated by Curtis and Hoffmann in the 19th century. PUs were firstly described by Bayer and his co-worker in 1937, from the reaction of a diisocyanate with a polyester diol (Delebecq et al., 2013) as a response to DuPont's patents on Nylon 6.6 developed in the 1930s. In 1947, Bayer at I.G. Farben Industry has obtained PU from a step-growth polymerization reaction between polyisocyanates and polyols for industrial applications, to try to replace natural rubber during World War II. The first commercial applications of PU were developed between 1945 and 1947 comprising soft elastomers, coatings and adhesives. Then its chemistry was diversified with the appearance of PUF and PUR in 1953 and 1957, respectively (Bayer, 1947; Randall and Lee, 2002). Nowadays, PU are produced by the exothermic reaction of polyisocyanate and polyol with a functionality higher or equivalent to 2, for each compound. Polyols present a large variety of chemical structures. Polyols market is mainly ruled by polyether and polyester polyols. The variability of the polyols architecture and molar mass is much more largely diverse compared to the polyisocyanate architecture. 90% of the polyisocyanate market is 4,4-diphenylmethane diisocyanate (MDI), the polymeric 4,4-diphenylmethane diisocyanate (pMDI) or the toluene diisocyanate (TDI) (Robles, 2014). These three polyisocyanates are aromatic compound, which enhance their reactivity and fire resistance of the final materials. However, MDI and TDI reactivities are different, as discussed in the dedicated chapter.

Polyurethane chemistry is mainly based on the high reactivity of the isocyanate function. Basically the isocyanate function due to the strain bonding of the –N=C=O group led to several reactions with active hydrogen-containing reactants including alcohols, amines, water, carboxylic acids, carboxylic anhydrides, ureas, thiols, urethanes and self-reaction on other isocyanate functions and derivatives (Arnold et al., 1957). Inherently to the isocyanate chemistry, several reactions including a gaseous release or a cyclization are irreversible reactions. However, the others are reversible with the exception

of the reaction of isocyanate functions with amine functions involve in the formation of the disubstituted urea linkage (Figure 1.1, Figure 1.2) (Delebecq et al., 2013). The urethane and amine formation, respectively obtained by isocyanate reaction with an alcohol and water, are two highly exothermic reactions with a release of enthalpy of 100.3 kJ/mol and 196.5 kJ/mol, respectively. This exothermicity is a key parameter in reactive process such as PU foaming process, starting at room temperature. The reaction with water undergoes the formation of one mole of carbon dioxide per mole of created amine function. Amine reacts rapidly with isocyanate to lead to urea formation. Urethanes are obtained from the reaction of isocyanate with an alcohol. But the isocyanate can also react (i) on the urethane group to form allophanate, or (ii) on the disubstituted urea to obtain biuret. Allophanate are obtained in a temperature range comprise between 120 and 150°C, whereas biuret synthesis can starts bellow 120°C (Ionescu, 2005; Lapprand et al., 2005; Petrovic and Ferguson, 1991). These reactions are summarized in Figure 1.2. Isocyanates functions have the possibility of reacting on themselves to be dimerized or trimerized. Two dimerization products are possible with (i) uretidinedione and (ii) carbodiimide, through reversible and irreversible reaction, respectively presented in Figure 1.1 and Figure 1.2. The last reaction involving isocyanate is the reaction with epoxide compound to form (poly)oxazolidone, which can be performed, for example in bulk under catalyst condition in a temperature range of 50-60°C (Senger et al., 1989).

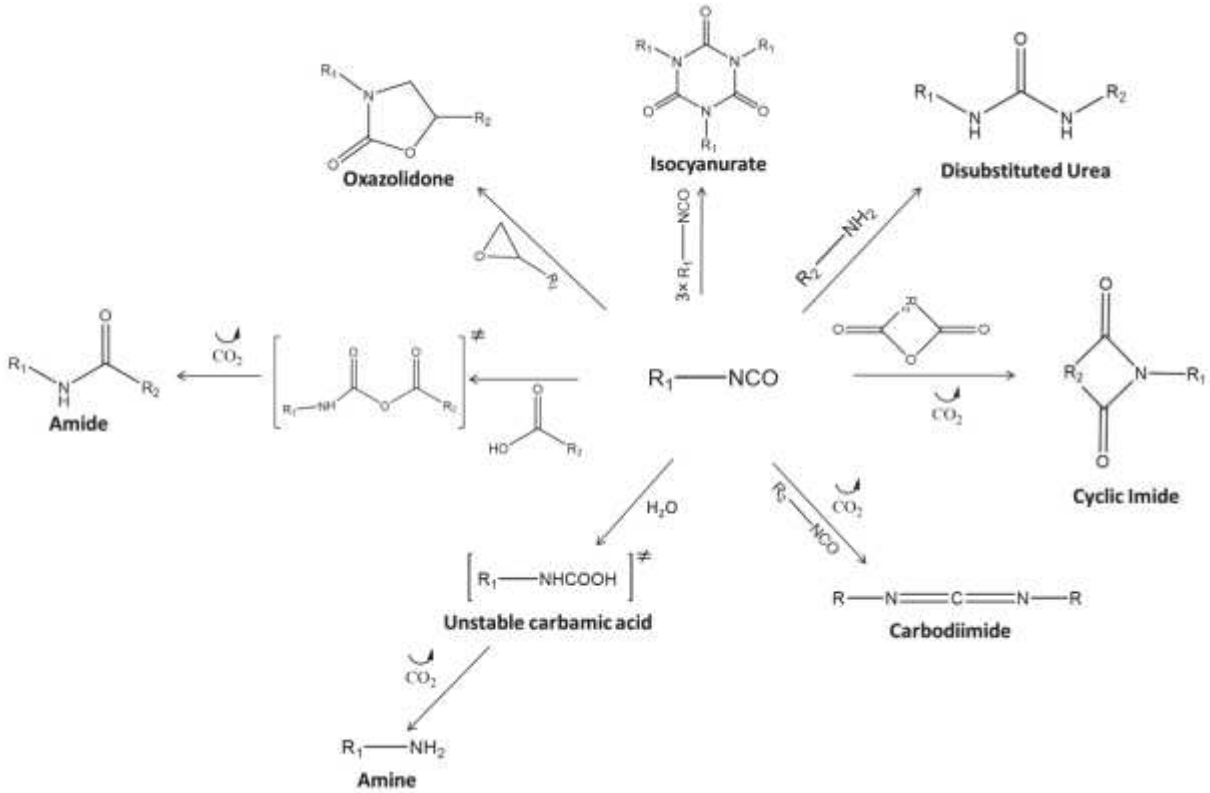

Figure 1.1: Irreversible reaction involving isocyanate groups with the synthesis of isocyanurate, urea, imide, carbodiimide, amine, amide or oxazolidone groups.

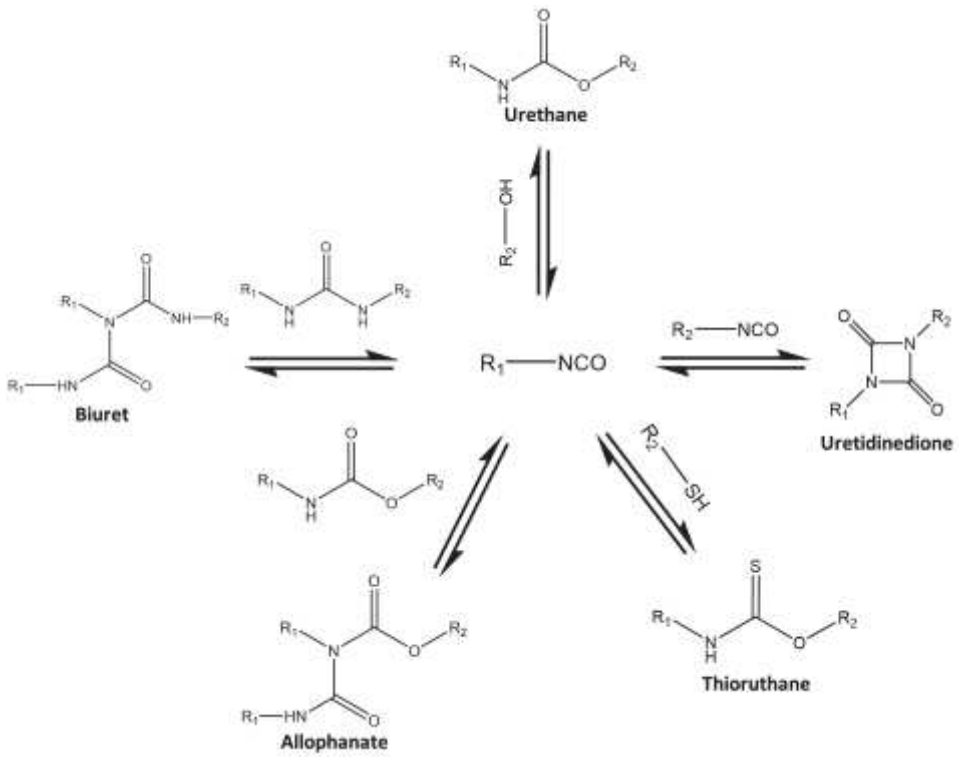

Figure 1.2: Reversible reactions involving the isocyanate group with the synthesis of urethane, uretidinedione, thioruthane, allophanate and biuret

Generally the dimerization reactions are limited to aromatic isocyanates which present a higher reactivity (Raiford and Freyermuth, 1943). Carbodiimides are promoted by heating isocyanate at high temperature or in presence of phosphorous catalyst (Figure 1.1) (Campbell and Smeltz, 1963). It is key reaction since it is widely used to polymerize MDI into pMDI, which is largely used in PU industries as it is liquid at room temperature (Silva and Bordado, 2004). Isocyanates functions can be trimerized into isocyanurate ring in presence of specific catalyst (especially potassium carboxylate), starting at 80 °C (Figure 1.1) (Slotta and Dressler, 1930a).

Elaboration of Polyurethane foams

Classification of the Polyurethane foams

Table 1.1 presents a kind of PU foam classification in connection with the density, the structure of the foam (open or close cells) and some applications. PU-based materials are ranked in function of their behaviors with rigid, semi-rigid or soft foams. Sub-categories can be determined through the foam density (Table 1.1), from low to high density (25 to higher than 1000 kg/m^3). Table 1.1 shows that PUF are divided in three categories, the conventional PUF represent 80% of the production whereas viscoelastic and high resilient foams represent 15 and 5 % of the production, respectively. In a same category of foam, a relationship exists between the foam density and the applications, some examples are given in Table 1.1.

Table 1.1: General PU foams classification

PU Foam Nature	PU foam behavior	Density range (kg/m^3)	Cellular nature	Applications	References
Rigid	Low density	25 - 50	Closed-cells	Insulation	(Avar et al., 2012)
	High density	80 to sup.1000	Closed-cells	Cryogenic insulation	(Ashida, 2006; Jeong and Shim, 2017)
Semi Rigid	Low density	40 - 80	Various	Leather, adhesives, architectural coatings	(Gao et al., 2010; Rehkopf et al., 1994; Yao et al., 2017)
Flexible	Low density	40 - 80	Open-cells	Cushioning	(Szycher, 2013)
	Viscoelactic	60 - 80	Open-cells	Specific cushioning / memory foams	(Ain et al., 2017; Aou et al., 2017; Zieleniewska et al., 2017)
	High resilient (above 50% of resilience)	10 - 90	Open-cells	Cushioning	(Adnan et al., 2017; Avar et al., 2012)
Foamed urethane	Elastomer	320 - 960	n.c	Shock-absorption, joint, shoe soles	(Ashida, 2006)

Formulation of Polyurethane foams

Five reactants are mandatory to obtain polyurethane foamed materials. We usually find (i) a polyisocyanate, (ii) a polyol), (iii) a catalyst system, (iv) a surfactant, and (v) a blowing agent. With the exception of the polyols, each of these components are described below

Polyisocyanates

Polyisocyanates are mostly used in polyurethane synthesis. Isocyanates can be synthesized according to four principal reactions which are (i) Curtius, (ii) Hoffman or (iii) Lossen rearrangements, and (iv) the phosgenation of primary amines. Reactions (i) (ii) and (iii) involve nitrenes as intermediary reactional product, which are not desirable for large-scale production. Instead, the phosgenation is well handle at industrial scale, despite the phosgene toxicity. In PU chemistry, main and major diisocanates are the 2,4-toluene diisocyanate (TDI), 2,6-toluene diisocyanate, 4,4'-diphenylmethane diisocyanate (MDI), 1,6-hexamethyl diisocyanate (HDI), 4,6'-xylylene diisocyanate (XDI) and the isophorone diisocyanate (Çaylı and Küsefoğlu, 2008). The uses of HDI are focused on adhesive and coating as HDI does not turn yellow under sun exposure. But HDI is less reactive than TDI and MDI (Woods, 1982). Conventional polyisocyanates in PU foams formulation are TDI and pMDI with an average functionality of 2 and 2.7, respectively. TDI and pMDI are petroleum-based isocyanates and are conventionally obtained from phosgene or diphosgene chemistry (Ozaki and others, 1972; Saunders and Slocombe, 1948; Sigurdsson et al., 1996). pMDI and TDI isocyanate groups have different reactivity with hydroxyl groups (Nagy et al., 2015). The isocyanate functions of pMDI present small differences of reactivity, whereas the reactivity of the para-isocyanate and the ortho-isocyanate group of TDI are incomparable. For pMDI, the first isocyanate group reacts 1.5 times faster than the second one with a hydroxyl group. For TDI, the para-isocyanate group reacts between 3 to 6 times faster than the ortho one in regard to hydroxyl groups. pMDI is generally preferred to formulate PUR as it offers a more homogeneous reaction kinetic. It also has a lowest vapor pressure than conventional polyisocyanates and thus pMDI is the least hazardous polyisocyanate to handle. Whereas, TDI is

preferred for PUF with open cells. However, it is clearly not suited for PUR due to the inhomogeneous polymerization rate limiting a synergy between cells wall formation and gas expansion (Ashida, 2006; Engels et al., 2013).

In order to obtain PU with high biobased content, different polyisocyanates have emerged during the two decades. Cayli and al. (Çaylı and Küsefoğlu, 2008) have been pioneer on this type of approach through a two-step reaction. Soybean oil-based isocyanate (70 % yield) has been developed. The process implies a bromination followed by a conversion of the brome into isocyanate with an excess of AgNCO. More recently, a linear saturated terminal aliphatic diisocyanate based on fatty acid as Curtius rearrangement precursors, was synthetized (Hojabri et al., 2009). Through the literature, the most largely developed biobased diisocyanates are (i) dimer fatty acid-based diisocyanate (DDI), (ii) ethyl ester L-lysine diisocyanate (EELDI) derived from the lysine and (iii) pentamethylene diisocyanate (PDI) (Figure 1.3) with renewable contents of 91, 75 and 71%, respectively (Charlon et al., 2014; Storey et al., 1994).

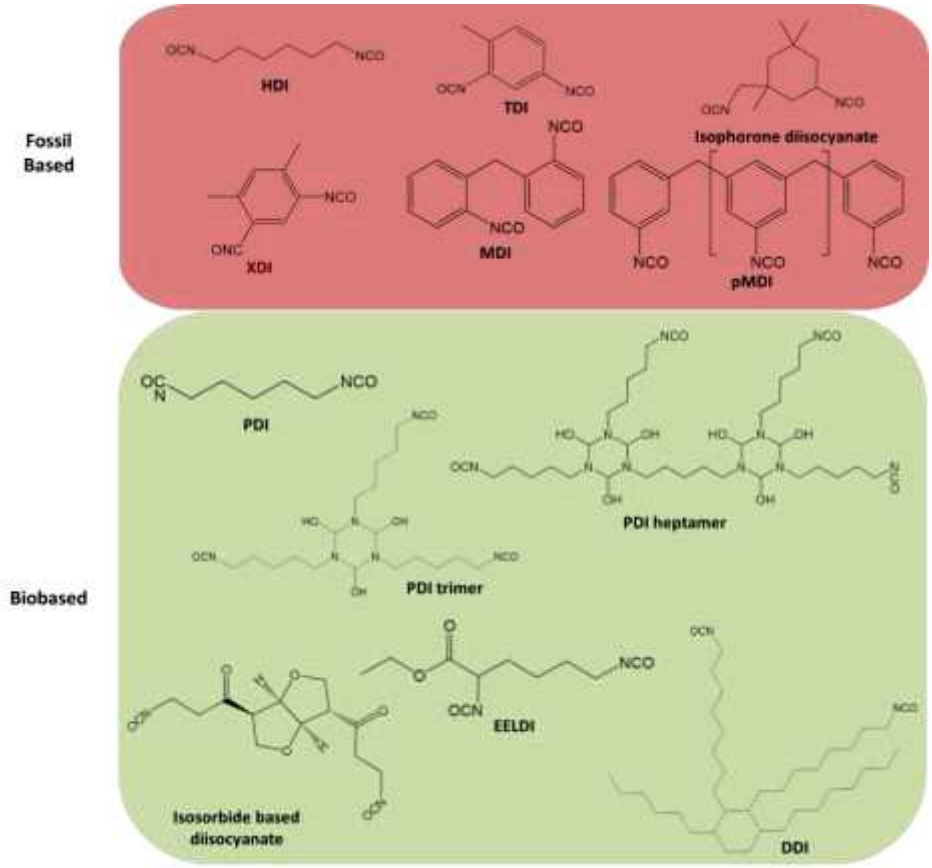

Figure 1.3: Chemical structures of the main biobased and fossil-based polyisocyanate.

Recently, a biobased diisocyanate was derived from isomannide or isosorbide (Figure 1.3) (Zenner et al., 2013). The isosorbide based diisocyanate was obtained from an esterification reaction in solvent-free condition with succinic diacid, followed by a Curtius rearrangement. Because of the isosorbide steric configuration, the resulting PU are stereo-irregular. Whereas isomannide diisocyanate-based PU are stereo-regular.

Commercials versions of biobased polyisocyanate are now largely available. For example, PDI derived from glucose is commercialized by Covestro and DDI derived from fatty diacid is supplied by Cognis-BASF (Charlon et al., 2014).

Blowing agents

Blowing agents are commonly used to obtain PU foams. They are divided into two main families with (i) chemical and (ii) physical blowing agents as a function of their mechanisms.

The chemical blowing agent is a compound that reacts during the foaming process and liberated a gas to origin the foam expansion. Commonly water is used as a chemical blowing agent. CO_2 is produced by reaction of water with isocyanate functions as the generated unstable carbamic acid spontaneously decomposes into an amine and CO_2 (Figure 1.1). Carboxylic acids can also act as a chemical blowing agent when reacted with isocyanate function with the synthesis of an unstable anhydride, which is decomposed into an amide and CO_2. In the specific case of formic acid, two moles of gas are liberated, one mole of CO_2 and one mole of carbon monoxide (Arnold et al., 1957; Blagbrough et al., 1986; Sorenson, 1959).

Physical blowing agents are low boiling point compounds. They expand the foam by vaporization during an exothermic process. Historically, common physical blowing agent where chlorofluorocarbon (CFC), but they were banned in 1987 by Montreal Protocol due to their high ozone depletion potential (Layer, 1988). Nowadays, most of the physical blowing agents are normal-pentane (n-pentane), cyclopentane, halogen-fee azeotropes and liquid carbon dioxide (Ashida et al., 1995; Jefferson and Salyer, 1971). Although largely used nowadays, the main drawback of the alkanes is their flammability (Fleurent and Thijs, 1995).

Due to the eco-friendly aspect of the CO_2, new blowing agent systems were developed. For example, a new blowing agent for PU foams based on palmitic acid to release entrapped CO_2 has been recently reported (Long et al., 2016). The direct introduction of fluidic CO_2 or N_2 into the mix has also been investigated (Hopmann and Latz, 2015; Kharbas et al., 2017).

In PU foams formulation, the blowing agent is chosen in function of the expected final material properties. For example, water is mainly used as blowing agent for PUF in continuous fabrications e.g., for mattresses, or discontinuous productions for acoustic absorbers or automotive parts. Water presents some strong advantages such as its low cost. It is also a non-harmful and easily available compound. Instead, PUR (e.g., for building insulation) is physically blown with low thermal conductivity gas such as n-pentane (Engels et al., 2013; Hopmann and Latz, 2015) since the expansion gas is responsible of 60 to 65% of the thermal conductivity value of low-density foams (Fleurent and Thijs, 1995). Main blowing agents and their thermal conductivity coefficient are presented in Table 1.2. To complement the effect of the expansion gas, the PU solid part and the radiative component of the thermal conductivity linked to the foam accounts for 20-35 % of the thermal properties (Septevani et al., 2015).

Table 1.2:Thermal conductivity coefficient of common blowing agents. (Hejna et al., 2017b; Randall and Lee, 2002)

Blowing agent	Chemical family	Thermal conductivity coefficient at 10°C (mW/(m×K))
Air		24.9
Carbon dioxide (CO_2)		15.3
CCl_2F (CFC-11)	Chlorofluorocarbon	7.4
$CHClF_2$ (HCFC-22)	Hydrochlorofluorocarbons	9.9
CH_3CClF_2 (HCFC-142b)		8.4
CH_3CCl_2F (HCFC-141b)		8.8
CH_2FCF_3 (HFC-134a)	Hydrofluorocarbons	12.4
CHF_2CH_3 (HFC-152a)		14.7 (at 25°C)
$CH_3CH_2CHF_2$ (HFC-245fa)		12.5
$CH_3CH_2CF_2CH_3$ (HFC-365mfc)		10.6
Iso-butane	Hydrocarbons	14.8
Iso-pentane		12.8
n-pentane		13.7
Cyclo-pentane		11.4

Catalysts

PU foams catalysts and the corresponding catalytic mechanisms has been recently reviewed (Silva and Bordado, 2004). Four main families of catalyst are involved in PU foams formulation. They are (i) tertiary amines, (ii) organometallic catalysts, (iii) quaternary ammonium salts and (iv) alkali metal carboxylates. The tertiary amine activity is not significantly correlated to the amine pKa value. However, amine catalyst activity is strongly enhanced by the number of tertiary amine group with an increase of the activity from the mono to the tetra-amine (Van Maris et al., 2005). Concerning the organometallic catalysts, one of the most used is a organo-tin catalyst with the dibutyltin dilaureate (DBTL) (Majumdar et al., 2000). It presents a strong catalytic activity towards isocyanates and hydroxyl functions. Whereas another widely used catalyst is 1,4-diazobicyclo[2.2.2]-octane (DABCO), a tertiary amine, to catalyzed the isocyanate / water reaction (Schuster et al., 2017). It is also well know that the trimerization reaction of di-isocyanates happens at high temperature (Slotta and Dressler, 1930a) in presence of specific catalyst (Silva and Bordado, 2004). The main catalyst family for these reactions are the carboxylate derivate and quaternary ammonium salts (Britain and Gemeinhardt, 1960; Schwetlick and Noack, 1995).

Surfactants

Surfactants are essential ingredients since they stabilize and control the size and the dispersity of the air bubbles into the initial reactive foaming mix. These bubbles act as nucleation points of the blowing agent (Rossmy et al., 1977). The diverse functions of the surfactants include (i) the emulsification of the reactants presenting low compatibility, (ii) the generation of air bubbles during mixing, (iii) the nucleation and stabilization of the developing foam up to the gelation time (Grimminger and Muha, 1995; Zhang et al., 1999). Surfactants do not impact on the foam kinetic. They prevent the coalescence which can eventually cause cells and foam collapse (Yasunaga et al., 1996; Zhang et al., 1999). Common PU foams surfactants are grafted polysiloxane with polyether pendant side chains (Han et al., 2009). These surfactants are often named “silicone” in foam formulation. It has been showed that the surfactant content greatly decreases the surface tension of foam mix (Zhang et al., 1999). In the

case of n-pentane-based foams, the surfactant must ensure a fine, quick, and stable distribution of the alkane in the emulsion. Its role is also to maintain the alkane in the emulsion (Grimminger et al., 1995). In PUF obtained with water, we can found that the surfactant concentration impacts on the phase separation and more particularly on hard domains ordering (Kaushiva et al., 2000).

Polyols for the elaboration of biobased PU Foams

Introduction

This review is mainly focused on renewable polyols which are specifically designed for biobased PU foams. Table 1.3 shows that there is a strong connection between the polyol properties and structures, and the behavior or type of the corresponding foams. Three main properties are highlighted such as the hydroxyl value (OH value), the functionality and the number-average molar mass (Mn).

Table 1.3: Relationships between the main polyols properties and PU foams behavior

PU Foams behavior	Polyol properties			
	OH value (mg KOH/g)	Functionality	Mn (g/mol)	References
Rigid	350 - 800	3 - 8	300 - 1000	(Ionescu, 2005)
Semi rigid	100 – 200	3 – 3.5	500 - 2000	(Adnan et al., 2017; Ain et al., 2017; Ashida, 2006)
Flexible	5 - 100	2 - 3	3000 - 6000	(Oliviero et al., 2017; Pawlik and Prociak, 2012; Zlatanić et al., 2015)

Polyols can be classified into three main types with (i) short (less than 12C) (ii) aliphatic or (iii) aromatic polyols.

Aliphatic polyols

Neat Polyols

To reach specific PU foams properties, short polyols can be added to enhance foams properties with for example, fatty biobased polyols. Short polyols are generally more reactive than longer and fatty polyols since they present higher hydroxyl group's accessibility and mobility during the foaming process. As a support for these explanations, short polyol structures, functionalities, and OH values are presented in the Table 1.4.

Obviously, one of the most abundant short polyol is the glycerol due to its low price, low toxicity, and high availability (He et al., 2017). Neat glycerol was associated with tung oil in flexible PU foams synthesis (Soto et al., 2016). The high reactivity and OH value of the glycerol were responsible for significant changes in the characteristic times associated to the foams elaboration. It shortened the gel and tack-free time, at the origin of foams densification (Calvo-Correas et al., 2015; Soto et al., 2016). In the elaboration of PUR, neat glycerol is often incorporated to increase the OH value in blends with low OH value polyol, such as castor oil (Carriço et al., 2017, 2016). High glycerol content increase density (Calvo-Correas et al., 2015), friability and eventually the yields of the corresponding foams (Carriço et al., 2017).

Since it is a more and more available byproduct of biodiesel production, crude glycerol (CG) is on the rise. CG is composed of glycerol (23-63 %wt), methanol, water, soap, fatty acid methyl ester, fatty acid, monoglycerides and diglycerides (Hu et al., 2012). In contrast with the previously exposed highly

rigid foams obtained from pure glycerol, CG is an efficient option to decreased foam rigidity (Carriço et al., 2016) thanks to the presence of short size chains to decrease the cross-link density and increase polymer-free volume. For instance, flexible PU foams with small cell size (100 µm) for sound absorption, only based on CG or blended with coffee ground polyol, show an enhanced mechanical properties with an increase of sound absorption (Gama et al., 2017). CG can be an opportunity to obtain low density foams with low thermal conductivity (from 36 to 49 mW/(m×K)) (Gama et al., 2016). Instead, CG composition is suitable for chemical self-reaction transformation into polyols. Two main reactional patterns were identified: (i) catalyzed reaction at high temperature (150-200°C) under atmospheric pressure or (ii) uncatalyzed reaction at lower temperature (110°C) under vacuum. The resulting polyols present high OH values, comprised between 350 to 550 mg KOH/g (Cong Li et al., 2014; Luo et al., 2013). CG derivative polyols were successfully used in PU foaming process. Whereas, in similar conditions the modification of neat glycerol conducts to solid materials not suitable for foaming process (Luo et al., 2013). Interestingly, from CG lower OH value polyols were obtained through microbial and chemical transformation (Uprety et al., 2017). As discussed below, CG is used in biomass liquefaction or vegetable oil transesterification.

Ethylene glycol (EG) and diethylene glycol (DEG) were employed as highly reactive diols in association with polyols presenting higher functionality (Ribeiro da Silva et al., 2013). These short diols generally improved foams morphology with increased density. However, in contrast with observations made with glycerol, these smaller diols have a strong impact on all foaming characteristic time, starting with the cream time. For instance, previous studies (Calvo-Correas et al., 2015) report a 33% time faster cream time in foam formulation with 20 wt% of DEG.

Biobased 1,3-propanediol (PDO), 2,3-propanediol and 1,4-butanediol (BDO) are obtained by fermentation from different biomass such as corn syrup or glycerol (Debuissy et al., 2017c, 2017). They are conventional chain extenders in PU chemistry, more particularly on the synthesis of thermoplastic polyurethane (TPU). The incorporation of PDO to foam TPU has been investigated (Rashmi et al., 2013). The two highly reactive primary hydroxyls of the PDO were an advantage as the foaming reaction exothermicity was improved resulting in a decrease of the rising time. The PDO incorporation to the PU network consequently increases the density and hard segment content, resulting in material with higher compressive strength and modulus.

To increase foams crosslink density, trimethylolpropane has also been previously mentioned (Ge et al., 2000a). Some research associated palm oil with highly branched sugar polyol such as sorbitol and pentaerythritol (Badri et al., 2001; Chuayjuljit et al., 2007, 2010). All pentaerythritol hydroxyl are primary whereas sorbitol is bearing two primary and four secondary hydroxyls (Table 1.4). The sugar alcohols were added to palm oil to obtain a homogeneous and higher OH value polyol blend to increase the final crosslink density of the foams network. The addition of sorbitol to modified palm kernel oil increases the compressive strength by 10%, the closed cell content by 6% and decrease the thermal conductivity by 19% of resulting foam panel (Badri et al., 2001). However, the hygroscopic nature of the sorbitol increased the foam water absorption. Likewise, pentaerythritol has been employed as a transesterification agent in excess with palm oil to increase the OH value (Chuayjuljit et al., 2007, 2010). Neat saccharides such as sorbitol, mannitol or xylose are often incorporated to PU foams to increase the properties of the PUR (Barber, 2004).

Table 1.4: Structures and main properties of short polyols

Chemical Name	Chemical structure	Precursor	Biobased	Molar mass (g/mol)	OH functionality	OH value (mg KOH/g)
Ethylene glycol	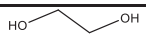	Glycerol	Yes	62	2	1809
1,3-Propanediol	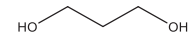	Glycerol	Yes	76	2	1476
Diethylene glycol	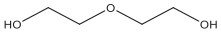	Glycerol	Yes	106	2	1058
Glycerol	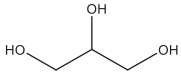	Triglyceride	Yes	92	3	1829
3-hydroxy-N,N-bis(2-hydroxyethyl)butanamide	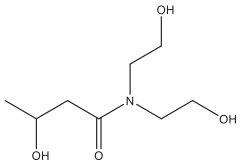	n.c	no	191	3	881
Trimethylolpropane	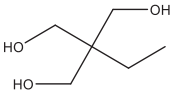	Formaldehyde and butanal	Potentially	134	3	1256
Pentaerythritol	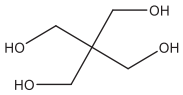	Acetaldehyde and formaldehyde	No	136	4	1650
Xylose	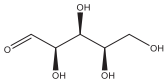	Polysaccharide	Yes	150	5	1870
Xylitol	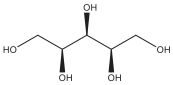	Polysaccharide (Xylan)	Yes	152	5	1845
D-Fructose	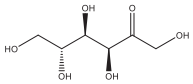	Extracted from biomass (annual plant)	Yes	180	5	1558
D-Glucose	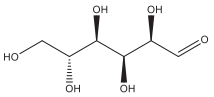	starch	Yes	180	6	1870
D-Sorbitol	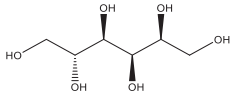	Glucose	Yes	182	6	1849
D-Mannitol	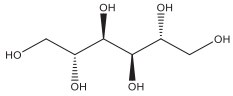	Glucose	Yes	182	6	1849
Sucrose	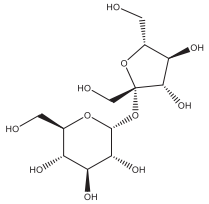	Extracted biomass (sugar cane, sugar beet)	Yes	342	11	1804

Diethanolamine (DEOA) is known to consequently accelerate foaming and the cross-linking rate of the PU network as it is composed of hydroxyls and highly reactive amine functions. It is thus often associated to the elaboration of molded PU foams to reach dimensional stability in lower time and to decrease the demolding cycle time. Nevertheless, it tends to be incorporated into the hard domain, altering the chemical structure and foam morphology (Kaushiva and Wilkes, 2000). A biobased alternative to the fossil based DEOA has been found with the 3-hydroxy-N,N-bis(2-hydroxyethyl)butanamide (HBHBA) industrially produced by Metabolix Inc (Lan et al., 2014).

HBHBA is less reactive than DEOA but leads to foams with higher mechanical properties and open cells content. HBHBA produced a better ordering of hard domains and increased hydrogen bonding within the hard domains (Lan et al., 2014).

Short polyols have not been deeply investigated in the past. They constitute a chemical family of interest, especially to enhance the reactivity and the functionality of some biobased or fatty polyols to improve the mechanical properties of the resulting foams.

Modified Polyols

In the previous section, short polyols clearly appear to tune foams characteristic times and properties. Most of the aliphatic polyols used in PU foams elaboration are longer polyols. Many of them are partially or fully biobased.

Neat Polysaccharides and derivate

Neat polysaccharides and derivate are also used for the elaboration of PU foams. For instance, some abstruse studies look at the incorporation of starch as specific filler to try to promote a biodegradation of the foams (Czupryński et al., 2012; Ge et al., 2000a). Starch and sucrose may also act as foam density managers (Nikje and Garmarudi, 2006). A purpose of the addition of starch into PU foams is to tune the degradation of foams. This strategy presents interesting perspectives for instance in the case of (bio)degradation in soil. Same observations were made with foams based on molasses-polyol (Kobashigawa et al., 2001). Starch has been modified with PEG, catalyzed by sulfuric acid to obtain polyols with OH value from 270 to 369 mg KOH/g (Yao et al., 1996). The starch content of the polyol was up to 70 wt%. But above 60 wt%, the resulting polyol was too viscous to be mixed with MDI and foamed. Water-absorbing foams with a density of 30-50 kg/m^3 were obtained. The foams could absorb water up to 2000 wt% in few minutes and reveal proper water-retention capacity. Starch has been investigated as chain extender and compared to neat glycerol (Kang et al., 2014). Regardless the chain extender type foams reactivity and density increase because of the cross-linking density increase. Starch can be considered as an efficient chain extender regarding mechanical properties.

Molasses is a byproduct of the sugar cane industry and it mainly composed of different saccharides such a: sucrose (eight hydroxyl groups), glucose (five hydroxyl groups) or fructose (five hydroxyl groups). Molasses is a very viscous product that can be dissolved in other polyol e.g. polyethylene glycol (PEG) to form molasses-polyol. Molasses act as strong cross-linking agents as foams obtained with 50/50 (wt%/wt%) of molasses/PEG present a density of 45 kg/m^3 and a strength of 90 kPa. When the molasses contents increase to 90/10, the density increased to 60 kg/m^3 and the strength at 400 kPa (Kobashigawa et al., 2001).

Chitosan is obtained by controlled deacetylation of chitin, one of the main component of the exoskeleton of insects, crustaceans and fungi. Hydroxyls and amines groups are available along the backbone and then this macromere can be integrated into the macromolecular architectures of PU. PU foams containing up to 14 wt% of chitosan in respect to the total polyol amount presented improved thermal stability (Dong et al., 2012). Chitosan incorporation as polyol in PU foams promotes the use of foams for example, for dye decolorization.

Polyether polyols

Polyether polyols generally present a lower viscosity and higher dispersity compared to polyester polyols. They provide a better mechanical properties especially for PUF foams (Ionescu, 2005). Besides, polyether polyols provide a better hydrolytic and ageing stability compared to polyester polyols. Then, polyether polyols are ruling the polyol market and represent around 69% of the polyol production for PU foams in 2016. Most of the polyether polyols are obtained from ring-opening anionic polymerization of oxirane. Such a reaction commonly called alkoxylation, is widely performed under basis catalytic conditions at high temperature (110-200°C), and in a close pressure reactor (Claire Pavier and Gandini, 2000; C. Pavier and Gandini, 2000). They are in a gaseous state at the reactional temperatures. The reactor pressure is driven by the oxiranes content in most of the case. The reactor pressure decreased with the consumption of the oxiranes at the end of the reaction. Base type catalyst such as trimethylamine (TEA), 1,4-diazobicyclo[2.2.2]octane (DABCO) potassium *tert*-butoxide (*t*-BuOK), NaOH, KOH or potassium methoxide (CH_3OK) have been reported in the literature (Ionescu and Petrović, 2010; C. Pavier and Gandini, 2000; Wilson et al., 1996). According to the type of catalysts, strong variations in the activities has been observed. It has been found that KOH is the best catalyst then catalysts activities decreased in the following order NaOH > DABCO > TEA and *t*-BuOK (Claire Pavier and Gandini, 2000; Wilson et al., 1996). The optimum seems to be 10 wt% of KOH(Claire Pavier and Gandini, 2000). Higher content increases side reactions, such as the homopolymerization. KOH can be easily removed at the end of the reaction by different approaches (Galanis and Dasgupta, 2001; Hu et al., 1997; Yu et al., 2015).

Different oxiranes can be used such as propylene oxide (PO), ethylene oxide (EO) or butylene oxide (BO) (Herzberger et al., 2016). In order to increase the final biobased content, oxiranes can be biobased. Ethylene oxide can be obtained from ethanol from e.g. sugar cane. PO can be biobased through a multistep process from glucose (Table 1.4) (Gandini and Lacerda, 2015). And finally, BO can be more or less easily biobased from butanol biosynthesized by fermentation (Arbenz and Avérous, 2014)

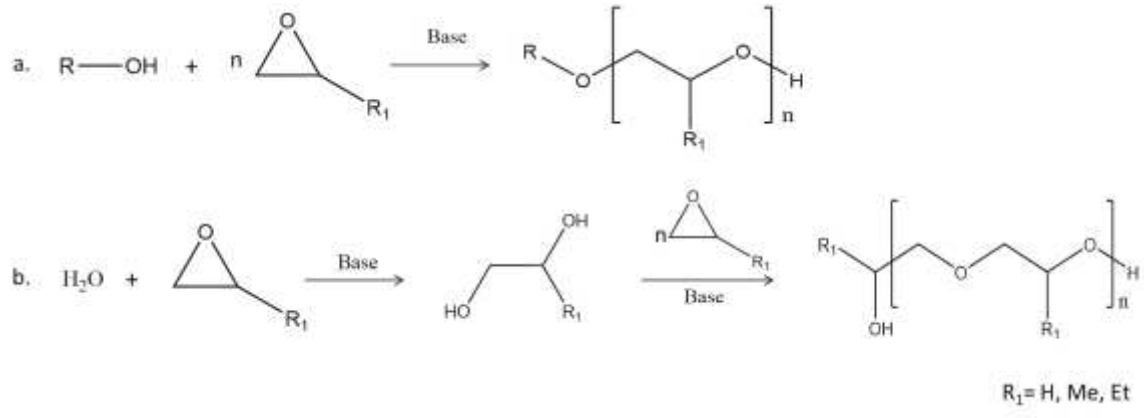

.

Figure 1.4: Alkoxylation reaction on (a) an alcohol or (b) water

To polymerize the oxiranes into polyether polyols, the reaction has to be initiated by a short polyol called starter or chain initiator. It is possible to have more than one starter involved in the polymerization. In this case these starters are called co-initiator. The functionality of the starter or starters blend drive the polyether polyol functionality as oxypropylation essentially ward hydroxyl

functions of the starter by grafting e.g., poly(propylene oxide) chains with secondary hydroxyl at the end. To increase the reactivity of the hydroxyl groups, such polyether polyol can be end-capped with EO (Worley et al., 2008) (Figure 1.4). Aliphatic biobased starters involved in alkoxylation are presented in Table 1.5. Starters for aliphatic polyether polyols are very often biobased and selected among glycerol, sorbitol, sucrose, trimethylolpropane, pentaerythritol (Table 1.4), saccharide or polysaccharide (Carr et al., 1994; Ionescu, 2005; Rieger and Amann, 2012). Wu and Glasser were the first to introduce lignins as starter to obtain aromatic-aliphatic polyethers (Wu and Glasser, 1984). Glycerol, ethylene diamine, propylene glycol, diethylene glycol and water (considered as a diol) have been reported has co-initiator to tune the polyol final functionality and viscosity(Hu et al., 1997; Ionescu and Petrović, 2010). Ionescu et al. (Ionescu and Petrović, 2010) reported that the polyol viscosity is affected by its OH value, functionality and the chemical structure. Polyols with low functionality and OH value present a lower viscosity than their homologues with higher OH value. Then, the use co-initiator is a powerful approach to decrease the viscosity of the final polyol. Water is really effective in this role (Hu et al., 1997). To control the polyol viscosity, another parameter is the oxirane structure. For instance, polyols obtained from ethoxylation were 10-40 times less viscous than oxypropylated polyol.

Polyether polyols from alkoxylated (poly)saccharides are often brown (Hu et al., 1997; Viswanathan et al., 2008; Wilson et al., 1996), resulting from a caramelization reaction. The color of the polyols can be decreased by specific decolorization steps (Wilson et al., 1996) or working with non-reducing sugars (Hu et al., 1997; Viswanathan et al., 2008). (Poly)saccharide are excellent starters to obtain aliphatic polyether polyols with high functionality, designed for PUR. As presented in Table 1.5, most of the elaborated foams were low density PUR, suitable for insulation applications. Soft foams were reported from ethoxylated inulin, a high functionality polysaccharide starter (Rogge et al., 2005). The authors successfully reported a high molar mass, low OH value polyols, perfectly designed for PUF by ethoxylated inulin with EO.

Some carbohydrate polymers such as amylose and amylopectin can be also modified by alkoxylation. But a pre-treatment before alkoxylation is often required because of their solid nature. For instance, glucoside has been pretreated by twin screw extrusion of cornstarch, ethylene glycol and sulfuric acid (Carr, 1992). Some authors used a stable emulsion of water, cornstarch and soybean oil in association with propylene glycol into foams formulation (Cunningham et al., 1998). In both case low density PUR are obtained (Table 1.5). More recently, glycerol was modified with an oxirane blend of byglycidyl propargyl ether and PO, to obtained alkynyl-polyether polyols (Velencoso et al., 2013). Then, the alkynyl part of the polyol was used to be "*clicked*" with 4-azidomethyl-7-methoxycoumarin. The functionalized polyol had fluorescent properties that can be introduced into the PU foam. PO and EO can be used together to design polyols for foams (Zarzyka, 2016). The hydroxyalkyaltion of N,N'-tetrakis(2-hydroxyethyl)oxamide by ethylene carbonate catalyzed by potassium carbonate at 160°C was performed. The resulting polyether polyols, despite a high viscosity (20 000 - 25 000 mPa.s at 25°C), were successfully used to obtain water blown PU foams.

Most of these polyols present suitable properties for rigid or semi flexible foams due to their high functionality. For instance, alkoxylation process can be adapted to design polyol for PUF by increasing the graft poly(propylene oxide) chain length or by homopolymerization of the EO or PO. Water and triol (e.g., glycerol) are the preferred starters for PUF (Takeyasu et al., 1992; Yukuta et al.,

1981). Nevertheless, the biobased content of such polyol is very low because only the starter can be biobased. A vast majority of polyether polyols for PU foams are synthesized by alkoxylation. However, other chemical routes are developed such as the polycondensation and ring opening polymerization of different non-epoxy chemicals as e.g., thermo-catalytic polycondensation of waste glycerol to obtain low density PUR (Ionescu and Petrović, 2010; Piszczyk et al., 2014, p.). Melamine-based polyether polyols (HMM-PG) were obtained from the reaction of propylene glycol (PG) with hexamethoxy-methylene melamine (HMMM), under acidic conditions (Y. Liu et al., 2017). HMM-PG based PU foams present interesting self-extinguishing and low flammability properties. However, alkoxylation process keeps two major advantages. Reaction products (i.e. polyols) can be directly used without solvent removal or separation steps. Moreover, a blend of starters can be prepared to tune the OH value and the viscosity of the polyol.

Table 1.5: Alkoxylated polyethers average conditions and resulting polyol and foams mains properties

	Building block	Chemical modification				Polyols caractersitics			Foams properties and morphology					
		Nature	Catalyst	T (°C)	Reaction time (h)	Functionality	OH value (mg KOH/g)	Visocsity (mPa.s, at 25°C)	Nature	Blowing agent	Density (kg/m^3)	Compression at 10 % strain (mPa)	Closed cells content (%)	Ref.
Polyethers Aliphatics	Sucrose	oxypropylation	KOH, TEO, *t*-BuOK	110	4-35	8	275-490	100-165000	rigid	HCFC	31	0.55	n.c	(Wilson et al., 1996)
	Sorbitol	oxypropylation	KOH, Al_2O_3	100-150	4-30	6	500 (average)	n.c	rigid	n.c	n.c	n.c	n.c	(Austin et al., 1978, 1979; T and F, 1965)
	Pentaerythritol	oxypropylation	KOH	120-150	2-17	4	350-600	7000	rigid	n.c	n.c	n.c	n.c	(De and Pettingill, 1963; Hayden and Foucht, 1978; Ionescu, 2005)
	Glycerol	oxypropylation	KOH			3	150-600	270-750	n.c	n.c	n.c	n.c	n.c	(Ionescu, 2005)
	Lactitol	oxypropylation	KOH, TEO, *t*-BuOK	110	4-35	9	275-490	100-150000	rigid	HCFC	29	0.42	n.c	(Wilson et al., 1996)
	Lactose	oxypropylation	KOH	120	16	8	410	2000	rigid	Freon	56-59	0.42-0.49	90	(Viswanathan et al., 2008)
	Inulin	ethoxylation	Et_3N	n.c	n.c	>11	78-1011	n.c	flexible	Water	32-51	n.c	n.c	(Rogge et al., 2005)
	Reduced sweet wey (lactose+ sorbitol+ ducitol)	oxypropylation	KOH	110	n.c	6-9	500-700	1-170000	rigid	HCFC	28-32	0.12-0.16	73-93	(Hu et al., 1997)
	6-aminouracil	oxypropylation	TEA	50-70	12.5-38	4	n.c	n.c	rigid	Water	229-47	0.22-0.34	n.c	(Chmiel-Szukiewicz, 2013)
	Sugar beet pulp	oxypropylation	KOH	100-160	4h	n.c	200-600	7000-49000	No foams	n.c	n.c	n.c	n.c	(Claire Pavier and Gandini, 2000; C. Pavier and Gandini, 2000)
	Limonene	thiol-ene	None	RT	8	4	450-490	11500-19000	rigid	HCFC	31-33	0.17-0.19	87-92	(Gupta et al., 2014)
	α-Phellandrene	thiol-ene	none	RT	8	3-4	500-550	150-620	rigid	Water	28-39	0.15-0.22	90	(Elbers et al., 2017)
	Cornstarch	blended	none	n.c	n.c	n.c	870	n.c	rigid	Water	50-64	n.c	n.c	(Cunningham et al., 1998)
	Corn sugar	commercial	n.c	n.c	n.c	n.c	80	n.c	flexible	Water	38-42	n.c	n.c	(Ugarte et al., 2014a, 2014b)

	Glycerin	carbon michael additioln	*t*-butyl AcAc	115	5	6	0	919-11600	rigid	HFC	30-60	n.c	90-95	(Sonnenschein et al., 2016)
	Crude glycerol	self – condensation	n.c	n.c	n.c	12-16	190-290	2800-19000	rigid	n-pentane	34-36	0.14-0.18	65-82	(Piszczyk et al., 2014)
Polyethers Aromatics	Kraft, soda, organosolv Lignin	oxypropylation	KOH	160	0.5-2	n.c	280-430	2700-7000	rigid	n-pentane	18-31	n.c	n.c	(Cateto et al., 2009, 2014)
	Kraft, soda, organosolv Lignin	oxypropylation	KOH	140-195	0.3-15	n.c	80-305	2500-345000	rigid	HFC	17-28	n.c	n.c	(Nadji et al., 2005)
	Tannin	oxypropylation	KOH	150	n.c	6.5	256	7000	rigid	Isopentane	32-35	0.21-0.26	90-97	(Arbenz et al., 2016a)

n.c: not communicated

Polyester polyols

Polyester synthesis was firstly studied by Carothers in 1929 when the step-growth mechanism was established following up on the reaction between aliphatic dicarboxylic acids and diols (Carothers, 1929, 1931; Carothers et al., 1932; Carothers, 1936). Nowadays, several synthesis routes were developed to obtain polyester polyols including the conventional polycondensation reaction, transesterification and ring opening polymerization (ROP) (Bednarek, 2016; Christopher L. WIlson and L, 1958) (Figure 1.5). As described below, the modification of vegetal oil into polyols may imply transesterification process or formation of ester bonds. Polyester polyols for PU foams were often based on adipic acid (AA), phthalic anhydride and glycol such as the trimethylolpropane (Ionescu, 2005; Smith, 1963). Polyester polyols are less extensively developed than polyether polyols because of the higher cost, lower hydrolysis resistance, higher rigidity and lower functionality (McAdams and Farmer, 2003). The strong polyester polyols development is nowadays linked to the fast development of polyisocyanurate (PIR) foams, which present a lower flammability and higher mechanical behaviors (Dominguez-Rosado et al., 2002; Reichmann and Phillips, 1988).

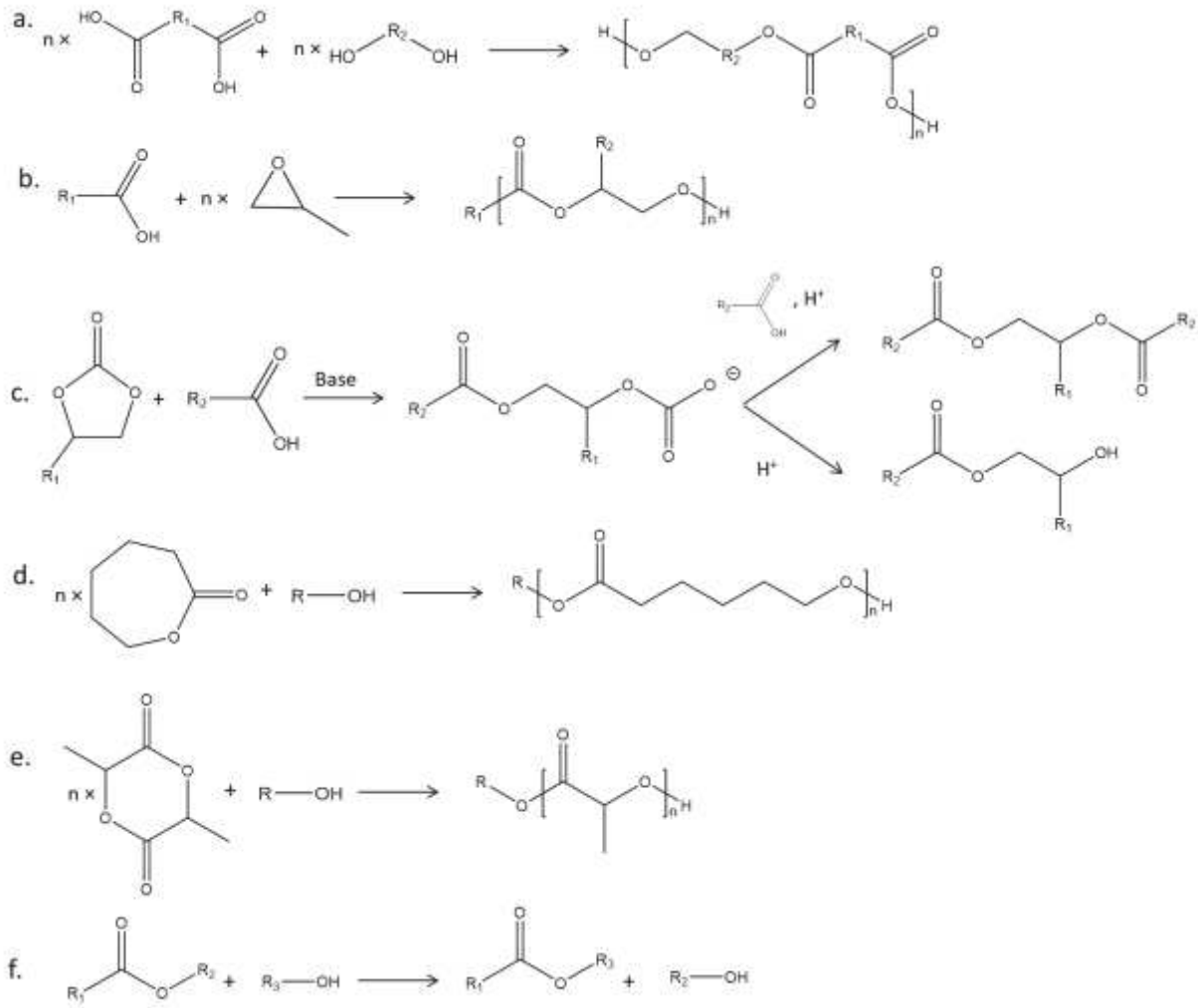

Figure 1.5: Different routes to obtain polyester polyols: (a) polycondensation of diols and diacids, (b) ROP of ethylene oxide and carboxylic acid, (c) ROP of cyclic carbonate and carboxylic acid, (d) ROP of ε-caprolactone and alcohol, (e) ROP of lactic acid and alcohol (f) Polyesters transesterification.

The most developed cyclic monomers for polyester polyols synthesis by ROP are lactones as ε-caprolactone and lactides (Fritz and Young, 1965; Hostettler, 1965). The ROP of five-membered alkylene carbonates or

propylene oxide by carboxylic acid or cyclic acid anhydrides (Figure 1.5-b,c) is used to obtain a mixture of hydroxyalkyl esters (Clements, 2003; Ionescu, 2005; Suh et al., 2010). ROP of lactones or related cyclic monomers, which are presented in Figure 1.5-d, is an attractive way to obtain aliphatic polyesters. Several parameters influence the lactone polymerization such as (i) the monomer ring size (ii) the position and number of substituent on the ring, (iii) the reaction parameters (solvent, monomer, initiator, catalyst, temperature,), and (iv) the potential side reactions due to transesterification (Figure 1.5-f) (Olivier Coulembier Philippe Dubois and Jean-Marie Raquez, 2009). For PU foams, several biodegradable polyesters were prepared from ROP of lactides or/and ε-caprolactone. They were started with different biobased initiators such as glucose, methyl-α-glucoside, pentaerythritol, ethylene glycol, castor oil and glycerol (Cook et al., 1974; P. Madden et al., 1972; Smith, 1963; Yoshioka et al., 2004a, 2004b; Young and Fritz). Typical, ROP reactions times were 0.5-24 h at 90-200°C, in presence of metal catalyst. However, these conditions are not suitable for ROP initiated on crude saccharide. Glucose can be easily oxidized into gluconic acid and then dehydrate into hydroxymethylfurfural under typical ROP conditions (Yoshioka et al., 2004a, 2004b). Thus, the resulting polyol was colored and presented an acidic pH which was unsuitable for PU foams elaboration. The replacement of glucose by methyl-α-glucoside solved the issue by stabilizing the acetal with the cyclic pyranose structure.

After ROP, the resulting OH value were 20 to 1400 mg KOH/g, driven by the initiator/cyclic monomer ratio. Polyols functionalities were comprised between 2 to 4. The wide range of initiators/cyclic monomers combinations gave the opportunity to elaborate flexible, semi-flexible and rigid PU foams, with a density panel starting from 24 to 560 kg/m^3.

Nevertheless, polyols derived from ROP have a tendency to crystallize with PCL chains. The crystallization can be avoided by the introduction of lactide as a ROP co-monomer. This introduction decreased the polyol viscosity and increased the OH value by grafting smaller polymer chains on the initiator, compared to PCL. Based on similar chemistry, it is possible to tune semi-flexible foams to rigid foams by enhancing the polyol functionality from 3 (trimethylolpropane) to 4 (pentaerythritol) (Smith, 1963). Foams elaborated from polyester polyols obtained from ε-caprolactone ROP were more thermally stable than foams obtained with comparable polyether polyols (P. Madden et al., 1972). Obviously, ROP is a very usefully polymerization technic to obtain a wide range of polyol with suitable properties for PU foams. The ROP has demonstrated to be an adapted polymerization technic for both, the synthesis of polyether and polyester polyols.

Polyester polyol have been obtained by the polycondensation of rosin with maleic anhydride, DEG and EG (Jin et al., 2002). The reaction was conducted in a temperature range of 215-240 °C, under an inert atmosphere. After the reaction completion, the polyester polyols presented an acid and OH value of 0.5 and 392 mg KOH/g, respectively. Such polyols present appropriate properties to elaborate low density PUR with a low thermal conductivity (23.0 mW/(m×K)) (Gao et al., 2013). Rosin-based polyester polyol is industrially developed by Jiangsu Qianglin Bioenergy with such properties. Polyester polyols from citric acid and propane-1,2-diol or pentane-1,5-diol were synthetized in xylene with or without catalyst (Liszkowska, 2017). The final polyester polyols presented an acid value range between 23 to 52 mg KOH/g and a viscosity evolving from 4000 mPa.s to solid at 25 °C in function of the monomers length. Additionally, foams containing uncatalyzed polyester polyols presented better foaming characteristic times and higher closed cell content. Recently, biobased linear aliphatic polyester polyol from sorbitol, diacid and several diols obtained without catalyst has been reported (Furtwengler et al., 2017). To avoid undesirable crosslinking reaction from the sorbitol high functionality a bulky two-steps esterification process at 150°C in absence of catalysts was developed. Resulting OH values were above 400 mg KOH/g. A strong dependence of the polyester

polyol viscosity as a function of diol length has been shown. The residual acidity of such polyols consequently impacts the kinetic profile of the resulting foams, which was greatly improved by the incrementing a polyol neutralization steps.

Polyol obtained from thiol-ene coupling chemistry

The thiol-ene coupling chemistry is versatile and has been firstly reported by Posner (Posner, 1905) for the addition of mercaptans to olefins. Thiol-ene reactions are based on classical free radical addition composed by an initiation stage, a propagation and a termination step. Additionally, transfer steps can occur. Then, the photochemistry of thiols has been developed during the last century, according to Machado *et al*. (Machado et al., 2017). The main advantages of the photo-induced reaction are the fast kinetic, mild reaction conditions and the reduced influence of the oxygen or humidity as inhibitors on the free radical reaction. According to these advantages, the thiol-ene coupling chemistry (Figure 1.6) has been recognized as being a part of the "click" chemistry (Lowe, 2014) with many applications such as surface functionalization, molecule conjugation, crosslinking, grafting and polymerization of renewable building blocks (Machado et al., 2017).

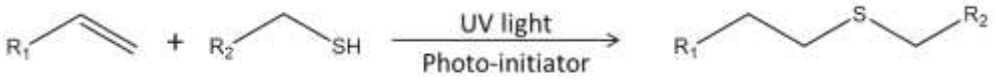

Figure 1.6: Photo-initiated thiol-ene coupling reaction

Thiol-ene "click" chemistry is a suitable alternative to conventional method to obtain polyols with new architectures. To the best of our knowledge, only few papers are dedicated to the synthesis of polyols for PU foams from thiol-ene "click" chemistry. For instance, Gupta et al. (Gupta et al., 2014) reported the synthesis of a polyol from renewable limonene. More recently, Elbers *et al*. (Elbers et al., 2017) also reported the synthesis of polyol from thiol-ene click chemistry on α-phellandrene, a mono-terpene. In both case, 2-hydroxy-2-methylpropiophenone was used as reaction photoinitiator. Reactions took place at room temperature under ultraviolet radiation (365 µm) for 8 h to obtain high OH value polyols, which are used in partial or total substitution of commercial polyol for low density polyurethane foams with high-closed cell (>90%) (Table 1.5).

Polyols from triglycerides.

Vegetable oils are mainly composed of triglycerides, which are an important feedstock for PU foams production due the ability and variability of the resources. In term of price, rapeseed oil, palm oil and soybean oil are the most affordable for large scale productions (Stirna et al., 2013). Vegetal oils are used for polyol production in consideration of the location, rapeseed and sunflower oils for Europe:, palm and coconuts oils for Asia, and soybean oils for US (Zieleniewska et al., 2015). Vegetable oils for PU-based materials is a vast domain based on a rich oleo-chemistry (Desroches et al., 2012; Noreen et al., 2016; Petrovic, 2008; Pfister et al., 2011).

At the exception of castor and lesquerella oil, vegetable oils are not bearing hydroxyl groups (Soto et al., 2017). Thus, before being used as polyols in PU foams elaboration hydroxyl groups must be generated by chemical reactions. Depending on their origins, vegetable oils present a large range of composition based on different fatty acids. The most widely study and available vegetable oils compositions are presented in Table 1.6. Chemical modifications of vegetable oils are essentially focused on the unsaturation of the fatty acids. Then, different reactions such as epoxidation followed by ring opening, transamidation, transesterification,

hydroformylation, methathesis and ozonolyze (Narine et al., 2007a; Petrović et al., 2005; Septevani et al., 2015; Stirna et al., 2013; Zieleniewska et al., 2015), as presented in Figure 1.7, can be involved.

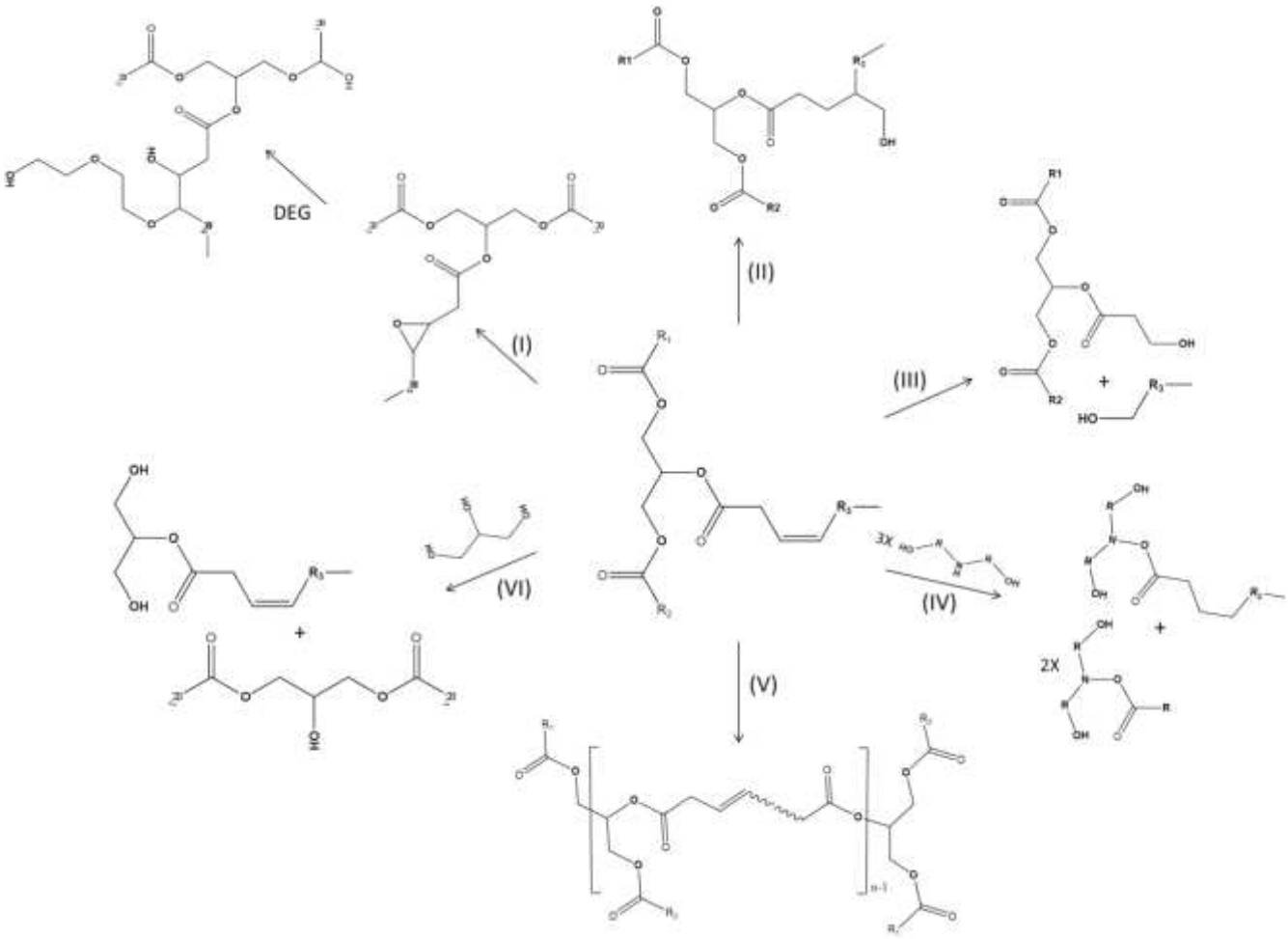

Figure 1.7: Triglyceride chemical modification by (I) epoxydation follow by oxirane opening by DEG, (II) hydroformylation and hydrogenation, (III) ozonolysis and hydrogenation, (IV) transamidation, (V) self-metathesis, (VI) transesterification

Unsaturated vegetable oils are modified by epoxidation and ring opening reactions with haloacids or alcohols, hydration and ozonolyisis (Yeganeh and Hojati-Talemi, 2007). The resulting polyols bring hydroxyl functions with a pending chain, which act as a plasticizer reducing the material rigidity and glass transition temperature (Tg) (Ji et al., 2015).

Table 1.6: Lipid profiles of different vegetable oils (Mosiewicki et al., 2015; Petrovic, 2008; Petrović et al., 2005; Pfister et al., 2011).

	Lauric acid (C12:0)	Palmitic acid (C16:0)	Stearic acid (C18:0)	Oleic acid (C18:1)	Linoleic acid (C18:2)	Linolenic acid (C18:3)	Other
Rapeseed oil	n.c	n.c	n.c	61	21	8	10
Castor oil	0	4	2	61	21	9	3
Palm oil	0	44	4	39	10	0.5	2.5
Palm kernel oil	48	8	2.5	15	2	0	24.5
Soybean oil	0	11	4	25	53	6	n.c
Low-saturated canola oil	n.c	4	2	65	19	8	n.c
Cottonseed oil	0.1	21.5	2.5	18.5	54.5	1	1.9
Coconut oil	47	9	3	7	2	0.1	31.9
Linseed oil	0	6	4	22	16	52	0
Corn oil	0	11	2	25.4	59.6	1.2	0.8
Olive oil	0	13.7	2.5	71.1	10	0.6	2.1
Peanut oil	0	11.4	2.4	48.3	31.9	0	6
Sesame oil	0	9	6	41	43	1	0
Sunflower oil	0	5.2	2.7	37.2	53.8	1.0	0.1

Rapeseed oil based polyols present a medium OH values comprise between 70 to 390 mgKOH/g, suitable for the synthesis of PUR and PIR foams (see Table 1.7) (Kairytė and Vėjelis, 2015; Kurańska et al., 2015; Mosiewicki et al., 2015; Stirna et al., 2013; Zieleniewska et al., 2015). Molded PUR-PIR foams with a density range comprise between 42 to 45 kg/m^3 with a high-closed cells content (sup. to 85%) were successfully obtained from rapeseed oil-based polyols (Kurańska et al., 2015). They were particularly suitable for building insulation with a thermal conductivity below 24.5 mW/(m×K). The highest content of secondary hydroxyl in epoxyded rapeseed oils increase the foaming characteristic time and the open cell content, with a corresponding mechanical properties decrease (Kurańska and Prociak, 2016). To improve the compressive strength and increase the Tg of such foams, the addition of fillers such as cellulose micro/nanocristals is efficient (Mosiewicki et al., 2015).

Due to the huge soybean production in the world and more particularly in the Americas, soybean oil is widely used for PU foams elaboration. Most of the resulting polyols present secondary hydroxyl groups from the conversion of unsaturation into epoxy, followed by the oxirane opening (Ji et al., 2013, 2015; Zhang et al., 2007). For instance, Petrovic's research group developed two families of polyols based on secondary (Guo et al., 2000, 2006; Zlatanić et al., 2004) and primary hydroxyl groups, by ozonolysis or hydroformylation of the unsaturations of the soybean oil, respectively (Guo et al., 2006; Petrović et al., 2005). Polyol based on primary hydroxyl groups gave PU foams with properties comparable to conventional PU fossil-based foams (Guo et al., 2006). Nevertheless, these polyols require several chemical transformation steps leading to an expensive material. Generally, soybean based polyols present suitable low OH value (Table 1.7) for flexible PU foam formulation (Campanella et al., 2009; Ji et al., 2015; S. Li et al., 2017; Sonnenschein and Wendt, 2013; Tan et al., 2011a; Zlatanić et al., 2015). The addition of soybean polyol into flexible foams formulation generally decrease the mechanical properties (Sonnenschein and Wendt, 2013), except if the polyol contains primary hydroxyl and high OH value from the glycolysis of the soybean oil, for example. A recent work (S. Li et al., 2017, p.) based on self-metathesis of soybean oil shows the obtaining of various polyols with OH value range between 83 to 263 mg KOH/g. Resulting PUF foams present excellent recovery properties particularly suitable for applications requiring resiliency. Because of

the general low OH value of the soybean-based polyol, PUR were less investigated (Ji et al., 2013, 2015; Tan et al., 2011b). When the soybean polyol content is increased in PUR, the thermal properties decrease while foams density, Tg and aging increase (Ji et al., 2015; Tan et al., 2011b). Only Ji *et al.* (Ji et al., 2013) obtained soybean polyol with an OH value above 300 mgKOH/g with rigid properties. Soybean derivates are already used at industrial scale by Ford for exemple in car seat foam conception (Mielewski et al., 2005). Many industrial polyols based on epoxidized soybean for PU foams industry are commercially available from BIOBASED TECHNOLOGIES, CARGILL, COGNIS-BASF, OLEOCHEMICALS, OLEON, BAYER, DOW CHEMICAL, for example (Desroches et al., 2012).

Castor oil (CO) has a basic OH value of 160-168 mg KOH/g, from the secondary hydroxyl groups. CO is non-edible and does not compete with food. CO has been considered for the synthesis of PU foams (Ogunniyi, 2006) without chemical modification. Such foams present interesting mechanical and thermal properties. Nevertheless, the low OH value leads to some weaknesses such as a low reactivity, a slow curing rates and a strong shrinkage of the resulting foams (M. Zhang et al., 2014a). Chemical modifications of the CO lead to higher OH value (400 mg KOH/g) polyol, more adapted for PUR (building insulation,) (Ionescu et al., 2016; Q. F. Li et al., 2016; C. Liu et al., 2017; Tibério Cardoso et al., 2012; Yeganeh and Hojati-Talemi, 2007; L. Zhang et al., 2014; M. Zhang et al., 2014b). To reach such a OH value, CO is mainly transesterified with glycerol, followed by an epoxidation step and oxirane opening (Q. F. Li et al., 2016; L. Zhang et al., 2014; M. Zhang et al., 2014b).It was generally observed that the used of CO based polyol increases the compressive strength of the foams. Zhang *et al.* (L. Zhang et al., 2014) modified their polyols by partially grafting diethyl phosphate on the OH groups. They obtained interesting flame retardant properties. Whereas by a similar technic, benzene ring were grafted onto CO based polyols. They observed an increase of reactivity, and the thermal and physical properties of the PU foams (M. Zhang et al., 2014b). Especially these foams present a low thermal conductivity range between 21-23 mW/(m×K) which correspond to commercial fossil-based foams e.g., for building applications. Finally, Ionescu *et al*. (Ionescu et al., 2016) reported CO based polyol with a functionality of 6 by modifying the CO oil by Michael thiol-ene reaction. Resulting PU foams present short characteristic times, high-closed cell content (sup. 90%) and density range of 35-38 kg/m^3.

Palm oil is one of the most widely used oils in the world due to its low price with a high production capacity (Marcovich et al., 2017, p.). Several chemical modifications such as epoxidation of the unsaturations followed by oxirane opening (Marcovich et al., 2017; Pawlik and Prociak, 2012), glycolysis (Pawlik and Prociak, 2012; Tanaka et al., 2008), cross-metathesis (Pillai et al., 2016) or transesterification (Chuayjuljit, 2007; Badri et al., 2000; Chuayjuljit et al., 2007) have been reported to convert palm oil into polyols. In most of the case, glycolysis and epoxidation result in low OH value polyols (Table 1.7). The resulting materials are flexible open cells foams or semi-rigid foams (Marcovich et al., 2017; Ng et al., 2017; Pawlik and Prociak, 2012; Pillai et al., 2016; Tanaka et al., 2008; Zhou et al., 2016). To further increased the OH value beyond 300 mg KOH/g and to elaborate closed cells PUR, specific cross-metathesis (Pillai et al., 2016) or transesterification involving highly functional sugar alcohol such as pentaerythritol (Chuayjuljit et al., 2007, 2010) or sorbitol (Badri et al.,2001; Badri et al., 2000) have been reported. The addition of palm oil-based polyol to PU foam can lead to more uniform cell size with the dangling fatty chain of such polyols acting as plasticizers, decreasing PU foam Tg and increasing the tensile strength. Additionally, the incorporation of palm kernel oil based polyol to polyols blend facilitate the addition of blowing agent with a corresponding cells size decrease in the final PU foams (Septevani et al., 2015). However, the obtained polyols are highly viscous (Table 1.7) and then most of the resulting foams cannot be elaborated at room temperature.

Triglycerides such as tung oil (Ribeiro da Silva et al., 2013; Soto et al., 2016), cotton-seed oil (Pawar et al., 2016b), linseed oil (Calvo-Correas et al., 2015) coconut oil (Paruzel et al., 2017), karanja oil (Himabindu et al., 2017; Palanisamy et al., 2011) or baru oil (Almeida et al., 2016), have been modified and used in PU foams, but less extensively than others. Canola oil has to be mentioned as a potential candidate since Narine *et al.*(Narine et al., 2007b) developed polyols from canola oil by ozonolysis. These polyols present primary terminal hydroxyl groups with an OH value of 150-170 mg KOH/g. Same OH value from karana oil, from modified tung oil, ranged between 163-223 mg KOH/g for the elaboration of flexible and semi flexible PU foams. Polyols with OH value ranging between 220 to 560 mg KOH/g for PUR, were obtained from cotton seed (Pawar et al., 2016b), linseed (Calvo-Correas et al., 2015) and coconut oil (Paruzel et al., 2017). Paruzel *et al.* (Paruzel et al., 2017) study novel perspective of coconut oil used. The transesterification of the coconut oil gave OH value of 560 mg KOH/g. The resulting polyols were successfully used in PU foams with a suitable thermal conductivity of 23 mW/(m×K).

Microalgae are also another interesting source of triglycerides which does not compete with food or mobilize arable lands surface for growth. Microalgae oils from different species (Arbenz et al., 2017a; Kosmela et al., 2017; Pawar et al., 2016a; Petrović et al., 2013) were transformed in polyol by epoxidation and oxirane opening (Arbenz et al., 2017a; Pawar et al., 2016a; Petrović et al., 2013), ozonolysis and reduction (Petrović et al., 2013), hydroformylation (Petrović et al., 2013), or liquefaction in purified CG (Kosmela et al., 2017), to obtain rigid PU foams. Except on a specific study, OH value of the resulting polyols were above 300 mg KOH/g leading to PU foams with comparable properties to conventional fossil-based foams .(Petrović et al., 2013) with OH value range between 50 and 150 mg KOH/g. Nevertheless, they obtained rigid PU foams by addition of glycerol to their polyols. Arbenz *et al*. (Arbenz et al., 2017a) were the first to report the elaboration of PUR-PIR foams with a substitution of 25 wt% of the fossil-based polyol by epoxide microalgae oil without prior oxirane opening.

Table 1.7: Polyols and PU foams properties obtained from vegetal oil derivates

		Polyols				**Foams properties**			
Feedstock	Chemical modification	OH value range (mg KOH/g)	Viscosity range (mPa.s, 25°C)	Behavior	Blowing agent	Density range (kg/m^3)	Compressive strength at 10% of deformation (MPa)	Closed-cell content (%)	**Ref.**
Rapeseed oil	epoxidation, transamidation, transesterification	77-390	150-650	rigid	Water, acetone	34-90	0.56-0.87	55-96	(Kairytė and Vėjelis, 2015; Kurańska et al., 2015; Kurańska and Prociak, 2016; Mosiewicki et al., 2015; Stirna et al., 2013)
Soybean oil	epoxidation	150-333	550-8900	Rigid	Water, HCFC-141b	38-50	n.c	90	(Ji et al., 2013, 2015; Karadeniz et al., 2017; Tan et al., 2011b)
	Epoxidation, glycolysis, ethoxylated	71-260	6000 – 16 000	flexible	Water	15-167	n.c	Open cells	(Campanella et al., 2009; S. Li et al., 2017, p.; Petrović et al., 2005; Zlatanić et al., 2015)
Castor oil	Transesterification, michael thiol-ene	220-465	480 – 19 000	rigid	Water, cyclopentane, HCFC-141b	37-60	0.12-0.22		(Ionescu et al., 2016; Tibério Cardoso et al., 2012; Yeganeh and Hojati-Talemi, 2007; L. Zhang et al., 2014; M. Zhang et al., 2014b)
Palm oil	Cross-metathesis, transesterification	136-460	260 – 35 000	Rigid	Water, HCF	39-250	0.14-0.27	85-95	(Chuayjuljit et al., 2007, 2010, Pillai et al., 2016)
	Epoxidation, polycondensation	98-116	320 - 5000	Semi rigid	Water	29-135	n.c	30-40	(Marcovich et al., 2017; Ng et al., 2017)
	epoxidation	110	1470	flexible	water	40-193	n.c	Open cells	(Pawlik and Prociak, 2012)
Tung oil	Tung oil bled with short diol	223	n.c	Semi rigid	Water	53-77	n.c	n.c	(Ribeiro da Silva et al., 2013)
Tung oil	Alkaline transesterification	163	n.c	Flexible	water	31-65	n.c	Open cells	(Soto et al., 2016)
Cottonseed oil	Epoxidation	365-370	200-210	Rigid	Water or cyclopentane	55	n.c	n.c	(Pawar et al., 2016b)
Linseed oil	Hydroxylation	216	n.c	Rigid	Water	40-55	0.19-0.47	n.c	(Calvo-Correas et al., 2015)
Coconut oil	Transesterification	270-333	3500-9500	Rigid	n-pentane	40-44	0.35	91	(Paruzel et al., 2017)

Aromatic polyols

Aromatic polyols from liquefied lignocellulosic biomass

The lignocellulosic biomass, also referred as plant dry matter, has an average composition of 30-35% of cellulose, 15-35% of hemicellulose and 20-35% of lignins (Yue et al., 2017; Zheng et al., 2017). Solvolysis liquefaction of lignocellulosic biomass which results on a blend of aromatic and aliphatic polyols, has been largely reviewed (D'Souza et al., 2017; Hu et al., 2014). The two main types of biomass solvolysis liquefaction are performed in presence of phenol or with polyhydric alcohols. In presence of phenol, liquefaction process results in phenols-rich products which can be used for instance in phenolic resins (Alma et al., 1996; Lee et al., 2002; Lin et al., 1994). Solvolysis liquefaction with polyhydric alcohols gives polyols, with a low concentration in phenols, suitable for polyurethane synthesis (Kurimoto et al., 1999; Maldas and Shiraishi, 1996). The most studied biomass dedicated to polyol for PU foams are bark (D'Souza et al., 2014; Ge et al., 2000b), wood (Maldas and Shiraishi, 1996; Xu et al., 2014; Yue et al., 2017), sugar beet pulp (Zheng et al., 2017), corn bran (Lee et al., 2000), bagasse (Abdel Hakim et al., 2011; Huang and Wang, 2017), bamboo (Gao et al., 2010), peanut shells [219,220], waste paper (Lee et al., 2002), wheat straw (Chen and Lu, 2009; H. Li et al., 2017a), tannin (M. Basso et al., 2014; M. C. Basso et al., 2014; Ge et al., 2003; Tondi and Pizzi, 2009), or neat lignin (Jin et al., 2011; H.-Q. Li et al., 2016a; Li and Ragauskas, 2012; Mahmood et al., 2016; Xue et al., 2017). The liquefaction of the lignocellulosic biomass results in a mixture with the cleavage of β-1,4-glycosidic bonds of cellulose and lignins fractions (Bernardini et al., 2015a; Hu et al., 2014; Maldas and Shiraishi, 1996; Zou et al., 2009). Liquefaction can be performed with acid or alkaline catalysts. Acid catalyzed reactions temperatures are comprise between 90 to 220°C and preferably between 130 to 180°C, whereas reactions temperature are higher, around 250°C, under basis conditions. (Abdel Hakim et al., 2011; D'Souza et al., 2014). Undeniably, sulfuric acid (H_2SO_4) and sodium hydroxide (NaOH) are the preferred catalysts (Zhang et al., 2016). Liquefaction products are commonly neutralized since they present an average acidity of 40 mg KOH/g due to by-products and eventual catalyst residues (Chen and Lu, 2009; Ge et al., 2000b; Kurimoto et al., 1999). Liquefaction reaction times are short and comprised between 15-45 minutes (Hu et al., 2014). Reaction rate constant is greatly influenced by the catalyst content, instead a temperature increase does not significantly affect the reaction rate constant (Lee et al., 2000). One of the reasons for reaction rate decrease is the recondensation of lignin fragments in acid media, increasing the residues content (Chen and Lu, 2009). Liquefaction solvents are polyhydric alcohols such as methanol, n-octanol, ethylene glycol, glycerol, poly(ethylene glycol) (PEG), poly(propylene glycol) and glycerol. Solvents can be used solely but they are often used in duo, typically PEG with glycerol (Lee et al., 2000; H.-Q. Li et al., 2016a; Zheng et al., 2017). They are generally used in excess to overcome the biomass viscosity with a ratio of around 4/1 (solvent/biomass, wt/wt). In the case of PU foams elaboration, these polyhydric alcohols are involved in the PU network formation. For instance, solvents mixture of PEG 400 and glycerol was used for semi-rigid and rigid PU foams elaboration (Gao et al., 2010; Lee et al., 2000, 2002), whereas for PUF, higher molar mass solvent (e.g., PEG 4000) are preferred (Ge et al.2003),. Indeed, the polyhydric solvent molar mass greatly influence the final OH value of the liquefied polyol (Jin et al., 2011). For instance, the increase PEG molar mass from 400 to 1000 g/mol decreases the OH value of the corresponding polyol from 410 to 190 mg KOH/g. The incorporation of biobased polyol from liquefied lignocellulosic biomass affects foams morphology, close cell content, compressive strength and the flammability. These polyols acted as cross-linking agents, increasing foam density and compressive strength. The cross-linking is particularly visible with liquefied-polyol presenting OH value higher than 1000 mg KOH/g.(Xu et al., 2014) resulting in friable

foams with irregular morphology. D'Souza *et al*. (D'Souza et al., 2014) also reported a drastic change of morphology in foams prepared with 100 wt% of liquefied polyol with a close cell content dropping until 1-3%, with also a compressive strengths decrease. Additionally to the aromaticity, the inorganic components from the lignocellulosic biomass can decrease foams flammability (Ge et al., 2000b). In certain case, the compressive strength of such foams was directly linked to the density (H.-Q. Li et al., 2016a). Polyols and foams derived from liquefied biomass are dependent on the liquefaction process and the biomass. Main polyols and resulting foams properties are summarized in Table 1.8 as a function of the resource.

Another liquefaction (H. Li et al., 2017b) is based on the fast pyrolysis, of wheat straw for example. The main advantage is the process rapidity. This liquefied polyol presents an OH value of 78 mg KOH/g after drying and impurities extraction, perfectly suitable to obtain PUF for cushioning applications. For example, the optimal foam was less resilient of 40% than the highly resilient foam develop by Ge *et al*. (Ge et al., 2000b) from liquefied bark. The tensile strength of such foam was comparable to the tensile of flexible foam developed by Zlatanic *et al*. (Zlatanić et al., 2015) from ethoxylated soybean oil.

Table 1.8:Conditions of lignocellulosic biomass liquefaction and some corresponding polyols and PU foams properties

Lignocel-lulosic biomass nature	Liquefaction condition				Polyol		Foam				
	Main solvent	Solvent ratio	Catalyst	Temperatu-re (°C)	OH value (mg KOH/g)	Viscosity (25°C, mPa.s)	Nature	Density (kg/m^3)	Blowing agent	σ_{10} (kPa)	Ref.
Wood	PEG, Methanol	1/4 to 1/6	H_2SO_4	120-180	280-1323	1000-1600	Rigid	39-116	Water	0.15	(Xu et al., 2014; Yue et al., 2017)
Wood	PEG	5/5 to /3	NaOH	150-250	193-629	n.c	Rigid	26-57	Water	0.07-0.1	(Maldas and Shiraishi, 1996)
Bark	PEG, PPG, glycerol	1/3	H_2SO_4	90-150	300-450	700-1000	Rigid & Flexible	29-75	Water	0.01-0.1	(D'Souza et al., 2014; Ge et al., 2000b)
Neat lignin	PEG, Glycerol, Ethanol	1/1 to 4/1	H_2SO_4	140-170	210-460	2500 to not measurable at 25°C	Rigid & Flexible	20-100	Acetone or water	0.0135-1.15	(Bernardini et al., 2015a; H.-Q. Li et al., 2016a; Mahmood et al., 2016)
Bagasse	n.c	n.c	n.c	n.c	430	2600	Rigid	44-61	Water	0.09-0.27	(Huang and Wang, 2017)
Waste paper	PEG, glycerol	1/3	H_2SO_4	150	330-400	2600-3900	n.c	35-51	Water	0.068-0.195	(Lee et al., 2002)
Corn bran	PEG, Glycerol	1/2 to 1/5	H_2SO_4	170	350-450	2000-14 000	n.c	35-45	Water	0.038-0.107	(Lee et al., 2000)
bamboo	PEG, glycerol	1/2 to 1/5	H_2SO_4	160	178-200	500-2200	Semi-rigid	23-45	Water	0.03-0.07	(Gao et al., 2010)
Peanut Shell	PEG, glycerol	1/10	H_2SO_4	150	452	47	rigid	47-77	Water and auxiliary	0.13-0.19	(Zhang et al., 2017, 2016)
Wheat straw	PEG, glycerin	4/1 to 3/2	H_2SO_4	130-160	250-430	1000-2000	Rigid	30-40	HCFC-141b	0.1-0.2	(Chen and Lu, 2009)
Wheat straw	Fast pyrolysis	500	78	87	Flexible	96-111	Water	n.c	n.c	n.c	(H. Li et al., 2017b)

A slightly different approach consists of lignin liquefaction through hydrolysis reaction followed by lignin oxypropylation (Mahmood et al., 2016). As also seen below, lignin is one of the most oxypropylated biomass. Liquefied biomass-based foams present very high mechanical properties whereas the foam density is around 64 kg/m^3.

Tannins are aromatic resource extracted from ligno-based biomass. Tannins have been liquefied for the elaboration of antimicrobial PU foams in presence of PEG at 120°C for 1h (Ge et al., 2003) with a preservation of the bacteriostatic activity of the tannins when incorporate to PU foams. Tannins based PU foams were also developed with ethoxylated fatty amine and pMDI (M. C. Basso et al., 2014). Condensed flavonoid tannins were added as reticulated agent in proportion of 30 to 50 wt% in respect to the ethoxylated fatty amine. Obtained foams were highly flexible. Additionally, the addition of tannins generally enhances fire properties by slowing down PU foams burning. Otherwise, tannins were mixed with furfuryl alcohol and other additives prior to foaming process (M. Basso et al., 2014). Such foams were phenolic-polyurethanes foams and demonstrated that urethane linkages were preferentially formed with two flavonoid group.

The lignocellulosic biomass liquefaction is a promising process to developed novel biobased polyols and especially from biomass waste. A wide range of polyols can be obtained through this process with suitable properties to PU foams formulation. These properties seem suitable for PU foams elaboration and illustrated by its wide potential of applications.

Aromatic polyether polyol based on alkoxylation of biomass

A myriad of aromatic polyether polyols is obtained from alkoxylation of lignocellulosic biomass. Beyond the previously exposed reaction parameters (catalyst, temperature, reactant), solid lignocellulosic biomass has to be ground before chemical modification as it has been proved that granulometry greatly influence the alkoxylation products since fibrous materials mainly react at the surface (Pavier et al., 2000). Many lignocellulosic biomass have been studied in alkoxylation reaction (rapeseed cake (Serrano et al., 2010), olive stone (Matos et al., 2010)) and reviewed (Aniceto et al., 2012), but few researches have been conducted up to the PU foams. Only these will be mentioned in the present study. Lignin and tannin alkoxylated polyether polyols represent the largest part of new aromatic polyols for PU foams.

Lignin oxypropylation (LOP) was firstly described by Glasser *et al*. (Wu and Glasser, 1984) and has been largely investigated during the last decades. Oxypropylation are generally performed in a thermoregulated closed reactor at a temperature comprise between 150 and 180°C with lignin (10-40 wt%) and propylene oxide (OP). The most common catalyst is potassium hydroxide (KOH) between 1 to 5 %wt (Arshanitsa et al., 2015; Cateto et al., 2009; Wu and Glasser, 1984). LOP with alkaline catalyst has been found to be much more efficient than with acidic condition (Ahvazi et al., 2011). Some authors have focused their works on polyether polyols using oxypropylated lignins for rigid and flexible PU foams. Different lignins (L) from softwoods, hardwood and from non-wood lignins were studied and compared .(Cateto et al., 2009). L/OP ratios were comprised between 10/90 and 40/60(w/v) to target polyether polyols with OH value comprise between 300 and 800 mg KOH/g with viscosity below 300 Pa.s. It stand out that lignin from softwood requires a longer reaction time, then most of the LOP were successfully used for PU foams elaboration.

PUR foams were formulated from oxypopylated lignins with a partial or total substitution of commercial and conventional polyols (Cateto et al., 2014; Nadji et al., 2005). The botanic origin of the lignin influence the final foams (Nadji et al., 2005). It seems that oxypropylated organosolv lignins and oxidized organosolv lignins (from softwood) were not suitable for PUR formulations. Whereas, L from hardwood and from non-wood (organosolv and soda) gave suitable PUR with interesting (i) insulating properties, (ii) dimensional

stabilities and (iii) resistance against climatic and accelerated ageing (Cateto et al., 2014). Li *et al*.(H.-Q. Li et al., 2016b) liquefied alkaline lignin with polyethylene glycol 400 at 140 °C under acidic condition to obtain a lignin based polyether polyol (LPP). They observed an increase of the heat resistance of the foam at high content of LPP due to the rigid and aromatic lignin structure. Bernardini *et al*.(Bernardini et al., 2015b) used an environmentally friendly microwave irradiation process to liquefy oxypropylated lignin at room temperature. Liquefied lignin influences the cell shape as they observed anisotropic cellular structure in formulated foams (Jeong et al., 2013). Most of the polyols obtained from lignin oxypropylation are suitable for PU foams elaboration. Nevertheless, LOP is influenced by the lignin nature. Organosolv and soda lignins were faster oxypropylated than kraft or oxidized organosolv lignins. The reactivity differences are mainly dependent on the lignin molar mass and the accessibility of the OH groups.

Recently, tannins were subject to oxypropylation (Arbenz et al., 2016) and oxybutylation (Arbenz and Avérous, 2014), both under catalyzed by alkaline catalyst at 150°C. Resulting polyols OH value were range between 140 to 370 mg KOH/g in function of the botanic origin of the tannin. Likewise, polyol viscosity evolved from 1 to 253 Pa.s. Oxypropylated tannin based polyol was used up to fully replace conventional polyol in polyisocyanurate foams preparation. Such foams, thanks to the tannin aromaticity presented a better flame resistance behavior due to the formation of coke at foams surfaces.

Mannich polyols

Mannich polyols are a class of aromatic polyols obtained by at least a two step-pathway with (i) the synthesis of the Mannich base, and (ii) the formation of Mannich polyol. As reported, renewable Mannich polyols for PU foams are derived from cardanol (thermal decarboxylation of anacardic acid extract from cashew nut shell) (Gandhi et al., 2015; Ionescu et al., 2012; Rotaru et al., 2008) and from modified limonene (Gupta et al., 2015). The oxazolidine route is the privileged synthetic route to obtain Mannich polyols for PU foams instead of the classical techniques based on an aqueous solution of formaldehyde (Gandhi et al., 2015). All the authors have worked with cardanol followed by a chemical modification. Firstly, the N-(2-hydroxyethyl)-1,3-oxazolidine is synthesized from diethanolamine reaction with paraformaldehyde at equimolar ratio, at 50-65°C (Figure 1.8-a). The Mannich base is generally obtained in mild conditions with reaction temperature range from 70 to 95°C, reacting the N-(2-hydroxyethyl)-1,3-oxazolidine on the cardanol (Figure 1.8-b). Finally, the Mannich base is subject to oxypropylation (Ionescu et al., 2012), ethoxylation (Gandhi et al., 2015) or specific ring opening reactions (Figure 1.8-c) (Gandhi et al., 2015).

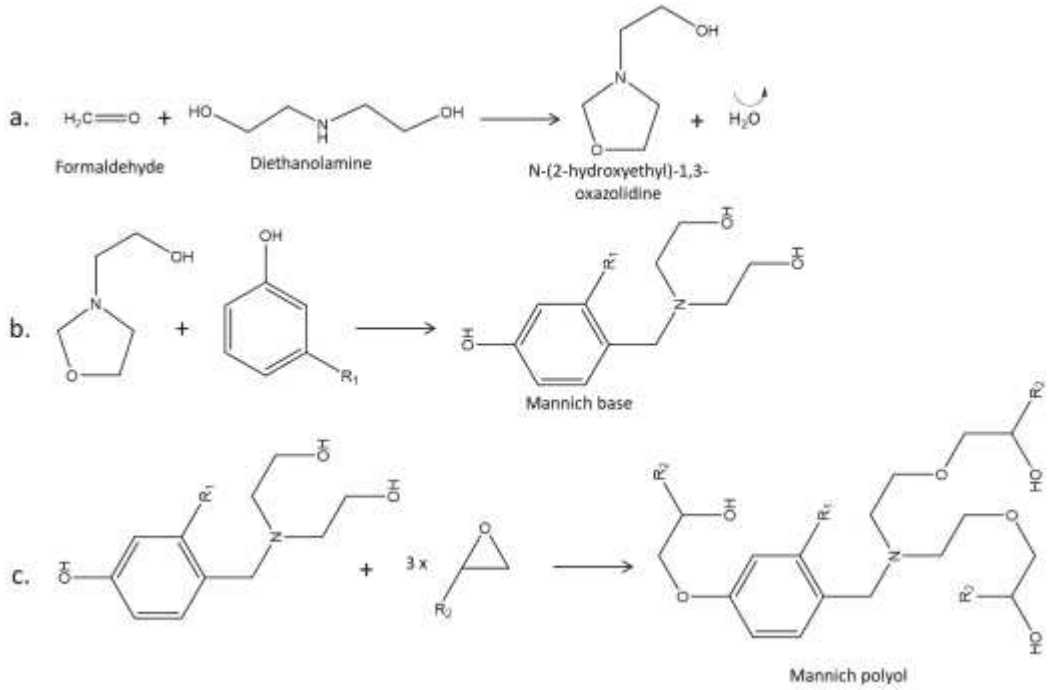

Figure 1.8: Mannich-based polyols synthesis: (a) Synthesis of N-(2-hydroxyethyl)-1,3-oxazolidine, (b) Mannich based formation, (c) Mannich polyol polymerization

In the case of limonene, the procedure is slightly different. A Friedel-Craft alkylation between the limonene and a phenol is performed. Then the Mannich base and the polyol were generated (Gupta et al., 2015). Such Mannich polyol and foams properties are presented in Table 1.9. According to Table 1.9, it is obvious that Mannich polyol are really suitable for the elaboration of PUR foams.

Table 1.9: Mannich polyol properties in function of the building block botanic origin and corresponding PU foams properties

Biomass	Mannich polyol properties			PU foams properties					Ref.
	Functionality	OH value (mg KOH/g)	Viscosity (mPa.s, 25°C)	Blowing agent	Density (Kg/m^3)	Compressive strength at 10% of strain (MPa)	Closed cells content (%)	Themal conductivity (mW/(m×K))	
Cashew nut shell	3-5	370-440	3200-5090	HFC	28-32	0.175-0.190	82-90	22.3-22.4	(Ionescu et al., 2012)
Cashew nut shell	3	331-346	n.c.	Water	120-150	n.c.	n.c.	n.c.	(Gandhi et al., 2015)
Limonene	3-6	452	22 000	HFC	33-38	0.235-0.267	92-93	n.c.	(Gupta et al., 2015)

Mannich polyols present very interesting properties for spray foaming since they are very reactive polyols thanks to their tertiary amine, which is a strong catalyst of the hydroxyl - isocyanate reaction. Mannich polyol can even be too reactive preventing its used as sole polyol in PU foams preparation (Gupta et al., 2015). It means that biobased Mannich polyol can be blended with less reactive biobased polyols if needed.

Aromatic polyester polyol from glycolysis

In general, renewable aromatic polyester polyols are less studied than the polyether polyol for foams elaboration. More and more often polyols come from the recycling of conventional polymers, for instance from poly(ethylene terephthalate) (PET) or PU glycolysis or glycosylate (Datta and Kopczyńska, 2016). PU and PET glycolysis products are carbamate and oligoester, respectively (Beneš et al., 2012). Besides and worldwide, more and more often PET (or polyethylene furanoate (PEF) in a close future), and PU are partially or fully biobased. Then the corresponding products of degradation can be biobased. The glycolysis is a sustainable route as it preserves biobased or fossil feedstock. The PET glycolysis depolymerized PET into oligoester, ethylene glycol (Figure 1.9-a) and bis(hydroxylethylene) terephthalate (BHET) (Figure 1.9-b) (George and Kurian, 2014; Nikles and Farahat, 2005).The PU glycolysis will be developed below.

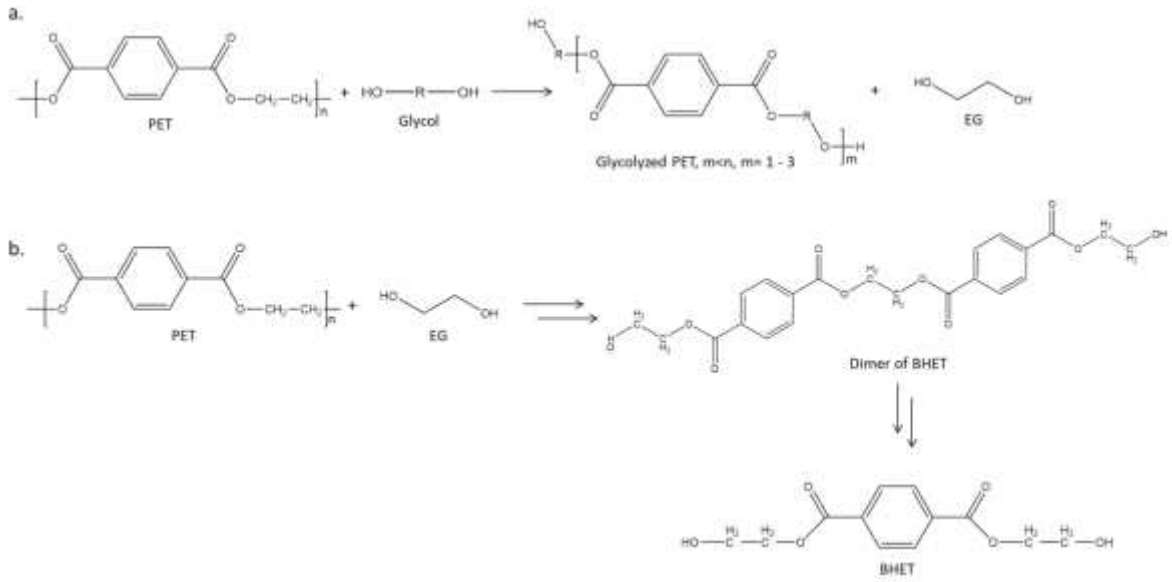

Figure 1.9: PET glycolysis (a) general mechanism with a diol and (b) specific case of the EG as glycol

Various glycols, introduce in large excess, such as EG, diethylene glycol (DEG), low molar mass polyethylene glycol (PEG), propylene glycol (PPG), neopentyl glycol 1,4 butanediol (BDO), glycerol, triethanolamine (TEA) were investigated in PET glycolysis with a temperature range of 150-250°C (Kacperski and Spychaj, 1999; Karayannidis and Achilias, 2007; Luo and Li, 2014; Vaidya and Nadkarni, 1987; Vitkauskiene et al., 2011), in presence of various transesterification catalysts (Luo and Li, 2014; Roy et al., 2013; Vitkauskiene et al., 2011) (Table 1.10). OH values of the oligoesters are dependent on the glycol involved in the process and are presented in Table 1.10. When, the glycolyzed polyol is designated to the PU industry it is often subject to an esterification reaction with biobased diacids such as succinic acid, adipic acid (AA) or sebacic acid (SA) and other polyols (Nikles and Farahat, 2005; Roy et al., 2013; Vaidya and Nadkarni, 1988). The glycols and esterification agents significantly affect the final polyester polyol viscosities (Vaidya and Nadkarni, 1987, 1988), and the compatibility with the foams blowing agents (Vitkauskiene et al., 2011), to manage the foam compressive strength.(Roy et al., 2013). Recently, the elaboration of low density PU foams from the reaction of glycolyzed PET in DEG by CG has been reported (Luo and Li, 2014). The main drawback of the glycolysis is the energy cost due to the high temperature linked to the reaction times. This is at the origin of the development of microwave irradiation as alternative energy source for glycolysis. However, a decrease of reactivity is observed with high molecular mass glycol (Chaudhary et al., 2013; Roy et al., 2013).

Table 1.10: PET glycolysis and esterifications conditions and resulting PU foams properties

Glycolysis conditions						esterification conditions				Resulting PU foams		Reference
Glycol (G)	Ratio PET/G	Tempe - rature (°C)	Temps (h)	Catalyst	OH-value (mg KOH/g)	Chemi -cal	Tempe-rature (°C)	Time (h)	Catalyz er	OH value (mg KOH /g	Densit y (kg / m^3)	Compres sive strength (MPa)	
TEA	1/2	240	n.c	Absence	240						27-35	0.075-0.165	(Kacperski and Spychaj, 1999)
DEG	8/1	240	5	DBTL	313						52	0.49	(Vitkauskiene et al., 2011)
DEG+ AA+G LY	8-3/1	240	5	DBTL	300-233		One step process				37-70	0.24-0.6	
DEG or PEG	1/2-6	MW	1	ZnA	32-410						82-185	0.005-0.89	(Chaudhary et al., 2013)
EG	7/3-2/6	200	8	ZnA	374-440		No foamed material presented						(Vaidya and Nadkarni, 1987, 1988)
DEG	1/2	230	4	Ti(IV)	n.c	CG	200	3	Ti(IV)	280-440	25-29	0.09-0.18	(Luo and Li, 2014)
EG	1/2-6	MW	1	ZnA	n.c		Similar to first step				n.c	n.c	(Chaudhary et al., 2013)
DEG	1/2-6	MW	1	ZnA	430	AA+S A	200	3	PTSA	20-28	187-376	0.02-0.16	(Roy et al., 2013)
PEG	1/4	215	2,5	DBTO	n.c	AA	215	1,5	DBO	102	40-50	0.32-0.4	(Čuk et al., 2015)

MW: microwave

After PET glycolysis, low OH value (102 mg KOH/g) of the aromatic polyester polyols were obtained (Čuk et al., 2015). Such polyols were blended with polyester polyols obtained from liquefied wood. The resulting polyol was esterified with AA to obtain polyester polyols with high OH values. Foams elaborate from this polyester polyol blend presented low densities (41-50 kg/m^3), and a thermal conductivity at 29 mW/(m×K).

The PET glycolysis is a route of increasing interest to obtain a wide range of aromatic and potentially biobased polyester polyols for PU foams. The possibility of a second esterification after the glycolysis is very strong leverage to tuned polyols architectures and properties. Untill now, most of the studied systems are orientated on PUF, certainly because they ruled the market of PU foams. Glycols or diacids involved in the polyester polyols are biobased or can be potentially biobased. Polyol from glycolysis can be seen as halfway polyols between sustainable and renewable material for PU foams elaboration.

Biobased Non-Isocyanate Polyurethane

NIPU generalities

Non-Isocyanate Polyurethane (NIPU) is a promising way to develop "green" polyurethanes based on 100 % of renewable resources, on agreement with several principles of the green chemistry. Isocyanate and polyisocyanate compounds are toxic and harmful to the human body and are at the origin of respiratory disease as severe asthma. For instance, MDI and TDI are classified as CMR (Carcinogen, Mutagen and Reprotoxyc) and are facing increasing regulatory scrutiny from the United States Environmental Protection Agency and the European Union REACH regulation (Baur et al., 1994; Nakashima et al., 2002). NIPU is a nice alternative to avoid the toxic polyisocyanate for the elaboration of PU-based materials. To synthetized

NIPU, three main routes have been investigated such as the A-B type azide condensation, the transurethane reaction and the aminolysis (Maisonneuve et al., 2015).

The A-B type azide condensation is a reaction involving an A-B type monomer containing two functions, an acyl azide and hydroxyl group. Before polymerization, the acyl azide group has to undergo a Curtis rearrangement to promote the conversion into isocyanate group (Figure 1.10-a). The Curtis rearrangement is generally performed in a temperature range of 80-100 °C prior to the polyaddition between isocyanate and hydroxyl groups. The main advantage of this strategy is the promotion an A-B monomer bearing both reactive functions. The polyaddition is performed with a perfect control of the stoichiometry as it is required to obtain high molar mass polymers. However, the main drawback of this strategy is the formation of isocyanate function as reactional intermediate (Calle et al., 2016; More et al., 2012; Palaskar et al., 2010).

The transurethanization is a two-step process. The first step is the synthesis of the diurethane (or carbamate) then the polycondensation of the diurethane with diol at high temperature (Figure 1.10-b). Continuous removal of reaction subsidiary product is achieved to increase the yield up to 89% (Deepa and Jayakannan, 2008a) of obtain NIPU via the transurethane process (Chenguo Li et al., 2014; S. Li et al., 2014).

The most studied route is the aminolysis reaction. This reaction involves the cyclic carbonate ring opening by an amine function to form urethane bonds. Due to ecological and economic reason; five members cyclic-carbonate are the most investigated system as they can be obtained through a process implying CO_2 consumption (Rokicki and Piotrowska, 2002). To obtain these polymers, a molar ratio close to 1:1 of bis-cyclic carbonate and diamine are used. NIPU obtained via aminolysis are polyhudroxyurethanes (PHU or PHUs) as the reaction involved the formation of the primary and secondary hydroxyl groups per synthesized urethane function (Figure 1.10-c). Generally the primary/secondary hydroxyl group ratio is 30/70. Urethanes bearing secondary hydroxyl groups are more stable (Carré et al., 2014, 2015; Kihara and Endo, 1993a; Maisonneuve et al., 2015). The main drawback of the aminolysis reaction is the slow kinetic, and the PHUs low molar masses mainly due to side reactions, which are promoted by heat or catalysts (Besse et al., 2015). To increase the molar mass, an answer is the elaboration of cross-linked PHUs to form foams.

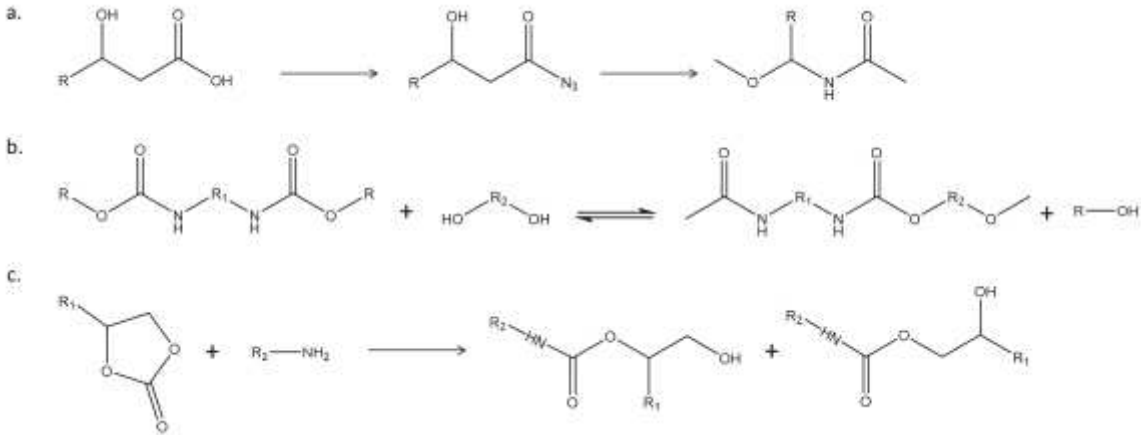

Figure 1.10: Main chemical routes to synthetized NIPU by (a) with acyl azide, (b) transurethanization, or (c) aminolysis

NIPU foams

NIPU foams has been rarely described in the literature and to the best of our knowledge only three foaming system have been described. They are based on aminolysis reaction. The main problem to foamed NIPU system is the absence of formation of gas during the chemical process, as conventional PUs. The first NIPU

foams system described in the literature was recently published by Cornille *et al*.(Cornille et al., 2015). These authors proposed a foam comprising bifunctional and trifunctional five-membered carbonate and diamine. The aminolysis reaction between amines and cyclic-carbonate was catalyzed by 1,5,7-triazabicyclo[4.4.0]dec-5-ene (TBD). The chemical blowing agent was polydimethylsiloxane. Gaseous H_2 is released by reaction of SiH with amines (Figure 1.11). All compound where mixed together and pour into a silicone mold for 12 h at 80°C, and 4 h at 120°C. Flexible foams with open cells foam with a density range of 194-295 $kg.m^{-3}$ according to the trifunctional reactant content (cyclic carbonate and/or amine) were obtained. Nevertheless, compared to traditional PU foaming there are two main drawbacks. The foaming time is very long and the foaming temperature very high compared to classical PU foaming systems. Cornille *et al.* (Cornille et al., 2016a) were the first to reported room temperature to elaborate flexible NIPU foam. They used thiourea as catalyst. Flexible foams where obtained after three days of reaction at room temperature.

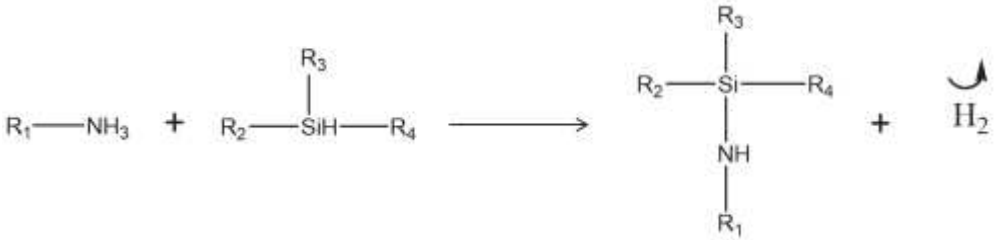

Figure 1.11: Chemical blowing agent based on polydimethylsiloxane reactional pathway

Blattmann *et al*. (Blattmann et al., 2016, p.) obtained NIPU foams using a mixture of tricyclic five membered-carbonate (carbonated polyglycidylethers of trimethylopropane or TMPGC) and ethoxylated trimethylopropane (EO-TMPGC), and hexamethylene diamine (HMDA) catalyzed by 1,4-diazabicyclo[2.2.2]octane (DABCO). This initial blend was mixed and cooled down to 20-25 °C before adding the physical blowing agent, a liquid blend of fluorocarbons. Then the foaming process attempted in a tempered mold a 50°C. They claimed a foam formation in 20 min followed with a long cure, 14h at 80 °C. The open cell flexible foams densities were from 142 to 219 $kg.m^{-3}$.

Finally, the latest NIPU foam system was developed by Grignard et al.(Grignard et al., 2016) with CO_2 blown NIPU under supercritical conditions at a temperature closed to the melting temperature of the NIPU matrix i.e. a temperature range of 80-100 °C with 100 - 300 bars of CO_2. Samples were foamed in few seconds with a fast depressurization. They also used a two-step process where the reactor is cooled down to 0 °C before depressurization to prevent foaming starts before depressurization. Final foams densities were in range of 110 to 176 $kg.m^{-3}$. They present an interesting pore size comprises between 2.6 to 10.8 µm. However, foam samples thermal conductivity was comprised between 50.1 to 64.7 mW/(m×K), which is rather high compared to conventional insulating PUR foams.

An alternative to the neat NIPU foam system has been developed by Figosvsky et al. (WO03028644A2). They developed a hybrid system called HNIPU, based on four different monomers: star epoxy monomers, acrylic monomers, cyclic carbonates monomers and primary diamines monomers. A physical blowing agent (i.e. pentane) was used.

Despite the obvious interest of developing original NIPU foams, only few works have been performed on the subject. In general, the current developed systems are suffering of the inherent low reactivity of the NIPU synthesis. Foams kinetic were rather long or required long curing times compared to traditional PUR foams system which took place at room temperature in few minutes. Thus, efforts are provided to develop blowing

systems with a kinetic similar to the NIPU polymerization'one. NIPU foams properties are summarized in Table 1.11 as a brief overview.

Table 1.11: NIPU foams properties

Blowing agent nature	Foaming temperature (°C)	Foams density (kg/m^3)	Foams cell size (µm)	Foams thermal conductivity (mW/(m×K))	References
Chemical	80 – 120	197 – 295	n.c[a]	n.c[a]	(Cornille et al., 2015)
Chemical	Room temperature	271 – 303	140 – 1300	100.4 – 115.5	(Cornille et al., 2016a)
Physical	50 -80	142 – 219	135 – 171	n.c[a]	(Blattmann et al., 2016)
Physical	80 – 100	110 - 176	2.6 – 10.8	50.1 – 64.7	(Grignard et al., 2016)

PU foams recyclability

The end life of biobased or fossil-based PU foams must be taken into account in a global sustainable approach. It is a challenging question due to the chemically crosslinked structures of the samples. PU material recycling is a worldwide concern linked to regulations evolutions. Actually, four main strategies exist (i) mechanical, (ii) chemical recycling, (iii) biochemical recycling, (iv) thermo-mechanical recycling or (v) energy production, and (vi) biochemical. The different technics are presented in Figure 1.12. The PU recycling subject has already been largely reviewed (Grause et al., 2011; Nikje et al., 2011; Zia et al., 2007).

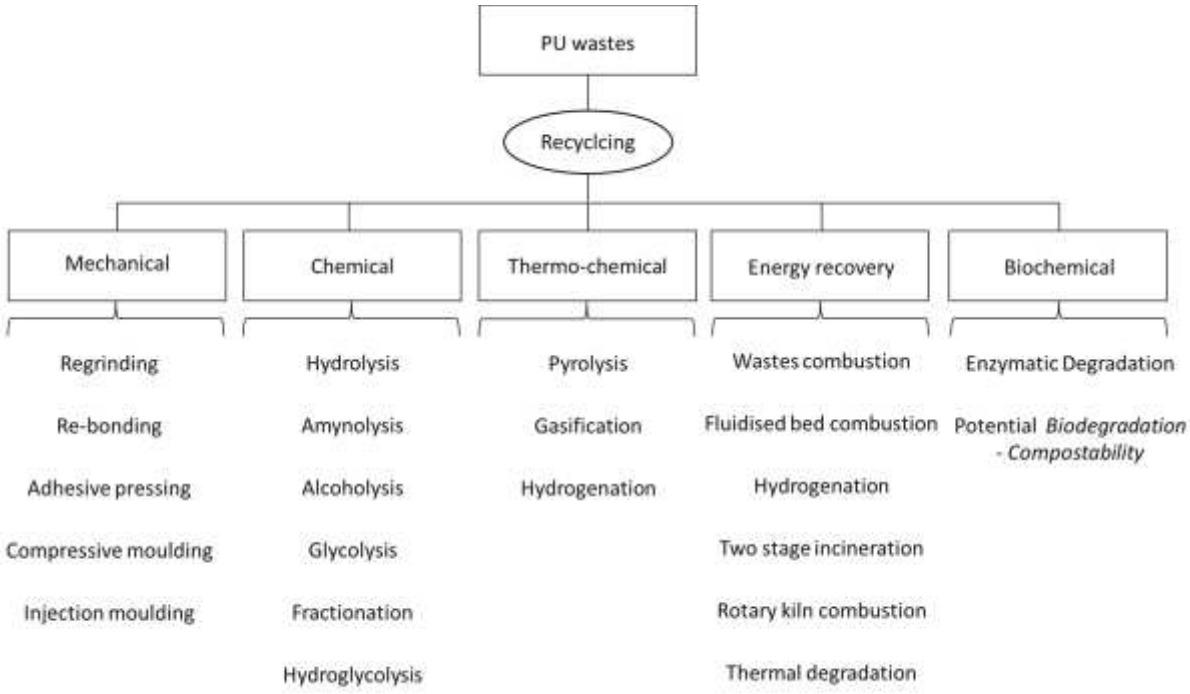

Figure 1.12: PU at end of life recycling patways.

The glycolysis and the grinding technology are the most developed and advanced route for PU-based materials recycling (Quadrini et al., 2013). As PET glycolysis (see before), byproducts from glycolyzed PU foams can be reintroduced into novel PU foams formulations. The PU foams glycolysis chemical mechanism involved several transesterification of the carbamate linkage by hydroxyl groups (Figure 1.13) from glycols

(Ulrich et al., 1978). The PU foam glycolysis is often characterized of "split-phase" glycolysis because of the phase separation in glycolysis reactor. The upper phase contains lighter reaction products such as polyols. Whereas the lowest phase contains heavier products such as glycol excess, carbamates, aromatic amines, solids residues (Molero et al., 2006; Carolina Molero et al., 2008; Nikje et al., 2007). PU foams glycolysis is generally performed at a temperature of 180-220°C, to avoid side reactions (F et al., 1987). The glycolysis process is sluggish in absence of catalyst. The most common side product is the diphenylmethanediamine, formed in presence of water (Figure 1.13) (Wu et al., 2003).

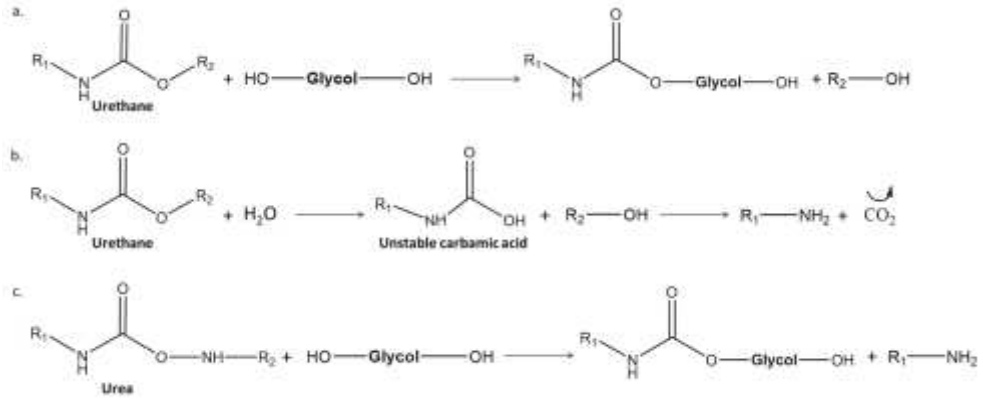

Figure 1.13: Glycolysis reactional pathway of urethane groups with (a) glycols or (b) water and (c) urea groups with glycols

Prefered glycols for the reaction are low cost and low viscosity diols, typically DEG (Molero et al., 2006; Simón et al., 2015a; Yu and Lee, 2014). The glycol size influences the glycolysis conditions (Molero et al., 2006; Carolina Molero et al., 2008; C. Molero et al., 2008). Glycolysis of flexible or rigid PU foams wastes results in high OH value polyols (Wu et al., 2002, 2003). Glycolyzed polyols from the upper phase present similar functionality in regard to virgin polyols used in the initial foams elaboration and thus, are efficiently incorporated in new foams (Nikje et al., 2011, Nikje and Mohammadi, 2010). Such foams densities were 44-52 kg/m^3, whereas pentaerythritol/glycerol mixture was used as glycols, foams densities were range between 52-171 kg/m^3. Simon et *al*. (Simón et al., 2013, 2014, 2015b, 2015a, 2016) deeply investigates the glycolysis of flexible PU foams. Recovered polyols from upper phase and bottom phase presented an average OH value 40-60 and 600 mg KOH/g, respectively. Recovered polyol were successfully integrated up to 75 wt% into novel PU foams. In several cases, the upper phase was incorporated to flexible PU foams formulation whereas the bottom phase was converting in rigid PU foams.

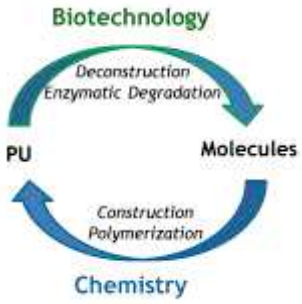

Figure 1.14: Schematic of the chem-biotechnology strategy

A growing interest to PU foams degradation by microorganisms such as fungi has been noticed. Currently, efficient foam (bio)degradation with filamentous fungi is described but there is a lack of information on the

associated enzymatic mechanisms. Such degradation is really efficient on polyester polyols based PU foams (Álvarez-Barragán et al., 2016). However, degradation results on polyether polyols based foams are less convincing (Matsumiya et al., 2009). Fungi degrade the material in simple molecule such as CO_2, H_2O, N_2 and CH_4 which are difficult to recovered and valorized, this is called the mineralization (Lucas et al., 2008). That is why the most promising alternative is to limit the (bio)degradation at the depolymerization, without mineralization, by the use of isolated enzyme. Enzymatic degradation products could be recovered such as DEG, AA or trimethylolpropane(Cregut et al., 2013). These products can be reused for new polymerization as presented in Figure 1.14, at the origin of the rising research on enzymatic degradation mechanism.

Conclusions

Polyols are a chemical family which can be widely derived from the biomass. The variety of the biomass can provide a great number of highly functional monomers, oligomers or polymers. Depending of the chemicals modifications of such derivates, numerous polyols with large portfolio of OH value and molecular mass can be obtained. These polyols can fit to diverse types of PU foams elaborations. This development is made possible by the versatility of the biomass functionality given a theoretical access to almost all main chemical reactions. Polyols for PU foams are obtained by different pathways such as ROP (including alkoxylation reaction), esterification, transesterification process and epoxidation followed by oxirane opening. The research on polyols is largely open to renewable building-blocks from diverse resources, such as from ligno-cellulose biomass (wood and annual cultures), from oleo-chemistry or from mono/oligo/poly-sugars.

Lignocellulosic feedstocks provide a substituent amount of aromatic chemicals for alkoxylation or liquefaction modification into polyether polyols with high OH values. Monosaccharide alkoxylation or polycondensation provide high OH value polyesters polyols. By opposition to high OH-value polyols, vegetal oils are a relevant feedstock to obtain low OH value polyol. Additionally, the economic status of the CG is unmatched and placed its high OH value derived polyols on the rise.

Microalgae production is starting and need some strong improvement to be cost competitive. However, this field constitutes a promising route to develop novel biobased polyols. Microalgae are well-known to entrapped CO_2, no competing with food industry and not mobilized arable land for production. Efforts to enhance polyols for PU foams based on microalgae should be maintained. In the same direction, research on NIPU foams is at its early stage and should be pursue to avoid toxic isocyanates from the PU foams production.

One of the most challenging points of using biomass derivatives is their variabilities, sometimes their lacks of reactivity and also very often their solid natures (e.g. lignin, tannin, saccharide,) or their high viscosity preventing a direct incorporation into foams formulation without chemical modifications. The alkoxylation is the conventional response to obtain low viscosity polyethers polyols. However, the process reactants and conditions are not very eco-friendly. Improvement on alkoxylation conditions can be achieved with a cyclic carbonate approach, also called green alkoxylation and already develop on tannin, but not used in PU foams (Duval and Avérous, 2016). On another side, liquefaction processes are essentially based on harmless solvent, used in large excess.

Obviously, the main obstacle in the increase of the renewable content of polyols is not the biomass but the development of chemical process based on the main green chemistry principles.

All the efforts to develop biobased polyol for PU foams strongly support the possibility of a future with cost-competitive fully biobased polyol for a more sustainable foams production, in parallel to the growing

development of biobased polyisocyanates, associated with the need to take into account a chemical or biochemical recycling of the foams, at the end of life.

References

Abdel Hakim, A.A., Nassar, M., Emam, A., Sultan, M., 2011. Mater. Chem. Phys. 129, 301–307.

Adnan, S., Tuan Noor, M.T.I., 'Ain, N.H., Devi, K.P.P., Mohd, N.S., Shoot Kian, Y., Idris, Z.B., Campara, I., Schiffman, C.M., Pietrzyk, K., Sendijarevic, V., Sendijarevic, I., 2017. J. Appl. Polym. Sci. 134, 45440.

Ahvazi, B., Wojciechowicz, O., Ton-That, T.-M., Hawari, J., 2011. J. Agric. Food Chem. 59, 10505–10516.

Ain, N.H., Tuan Noor, M.T., Mohd Noor, M.A., Srihanum, A., Devi, K.P., Mohd, N.S., Mohdnoor, N., Kian, Y.S., Hassan, H.A., Campara, I., Schiffman, C.M., Pietrzyk, K., Sendijarevic, V., Sendijarevic, I., 2017. J. Cell. Plast. 53, 65–81.

Alma, M.H., Yoshioka, M., Yao, Y., Shiraishi, N., 1996. Holzforschung 50, 85–90.

Almeida, E.L. de, Goulart, G.A.S., Claro Neto, S., Chierice, G.O., Siqueira, A.B. de, 2016. Polímeros 26, 176–184.

Álvarez-Barragán, J., Domínguez-Malfavón, L., Vargas-Suárez, M., González-Hernández, R., Aguilar-Osorio, G., Loza-Tavera, H., 2016. Appl. Environ. Microbiol. 82, 5225–5235.

Aniceto, J.P.S., Portugal, I., Silva, C.M., 2012. ChemSusChem 5, 1358–1368.

Aou, K., Schrock, A.K., Baugh, D., Gamboa, R.R., Ulmer, L.C., 2017. Polymer 117, 183–197.

Arbenz, A., Avérous, L., 2014. RSC Adv 4, 61564–61572.

Arbenz, A., Frache, A., Cuttica, F., Avérous, L., 2016. Polym. Degrad. Stab. 132, 62–68.

Arbenz, A., Perrin, R., Avérous, L., 2017. J. Polym. Environ.

Arnold, R.G., Nelson, J.A., Verbanc, J.J., 1957. Chem. Rev. 57, 47–76.

Arshanitsa, A., Vevere, L., Telysheva, G., Dizhbite, T., Gosselink, R.J.A., Bikovens, O., Jablonski, A., 2015. Holzforschung 69.

Ashida, K., 2006. Polyurethane and related foams: chemistry and technology. CRC press.

Ashida, K., Morimoto, K., Yufu, A., 1995. J. Cell. Plast. 31, 330–355.

Austin, A.L., Levis, W.W., Pizzini, L.C., Hartman, R.J., 1978. Polyurethane foam from an oxyalkylated product. US 4105597.

Austin, A.L., Levis, W.W., Pizzini, L.C., Hartman, R.J., 1979. Process for preparing a polyurethane foam from an oxyalkylated product. US 4177335.

Avar, G., Meier-Westhues, U., Casselmann, H., Achten, D., 2012. Polyurethanes, in: Polymer Science: A Comprehensive Reference. Elsevier, pp. 411–441.

Badri, K.H., Ahmad, S.H., Zakaria, S., 2000. J. Mater. Sci. Lett. 19, 1355–1356.

Badri, K.H., Ahmad, S.H., Zakaria, S., 2001. J. Appl. Polym. Sci. 82, 827–832.

Badri2001-The production of a high-functionality RBD palm kernel-based polyester polyol.

Barber, T.A., 2004. Rigid urethane foams using saccharides as reactive components. WO2004060948A2.

Badri2001-The production of a high-functionality RBD palm kernel-based polyester polyol.

Basso, M., Pizzi, A., Lacoste, C., Delmotte, L., Al-Marzouki, F., Abdalla, S., Celzard, A., 2014. Polymers 6, 2985–3004.

Basso, M.C., Giovando, S., Pizzi, A., Pasch, H., Pretorius, N., Delmotte, L., Celzard, A., 2014. J. Appl. Polym. Sci. 131, n/a-n/a.

Baur, X., Marek, W., Ammon, J., Czuppon, A.B., Marczynski, B., Raulf-Heimsoth, M., Roemmelt, H., Fruhmann, G., 1994. Int. Arch. Occup. Environ. Health 66, 141–152.

Bayer, O., 1947. Angew. Chem. 59, 257–272.

Bednarek, M., 2016. Prog. Polym. Sci. 58, 27–58.

Beneš, H., Vlček, T., Černá, R., Hromádková, J., Walterová, Z., Svitáková, R., 2012. Eur. J. Lipid Sci. Technol. 114, 71–83.

Bennett, S.J., 2012. Energy Policy 50, 95–108.

Bernardini, J., Anguillesi, I., Coltelli, M.-B., Cinelli, P., Lazzeri, A., 2015a. Polym. Int. 64, 1235–1244.

Bernardini, J., Cinelli, P., Anguillesi, I., Coltelli, M.-B., Lazzeri, A., 2015b. Eur. Polym. J. 64, 147–156.

Besse, V., Camara, F., Méchin, F., Fleury, E., Caillol, S., Pascault, J.-P., Boutevin, B., 2015. Eur. Polym. J. 71, 1–11.

Blagbrough, I.S., Mackenzie, N.E., Ortiz, C., Scott, A.I., 1986. Tetrahedron Lett. 27, 1251–1254.

Blattmann, H., Lauth, M., Mülhaupt, R., 2016. Macromol. Mater. Eng. 301, 944–952.

Britain, J.W., Gemeinhardt, P.G., 1960. J. Appl. Polym. Sci. 4, 207–211.

Calle, M., Lligadas, G., Ronda, J.C., Galià, M., Cádiz, V., 2016. Eur. Polym. J. 84, 837–848.

Calvo-Correas, T., Mosiewicki, M.A., Corcuera, M.A., Eceiza, A., Aranguren, M.I., 2015. J. Renew. Mater. 3, 3–13.

Campanella, A., Bonnaillie, L.M., Wool, R.P., 2009. J. Appl. Polym. Sci. 112, 2567–2578.

Campbell, T.W., Smeltz, K.C., 1963. J. Org. Chem. 28, 2069–2075.

Carothers, W.H., 1929. J. Am. Chem. Soc. 51, 2548–2559.

Carothers, W.H., 1931. Chem. Rev. 8, 353–426.

Carothers, W.H., 1936. Trans. Faraday Soc. 32, 39.

Carothers, W.H., Dorough, G.L., Natta, F.J. van, 1932. J. Am. Chem. Soc. 54, 761–772.

Carr, C., 1992. Starch-Stärke 44, 183–187.

Carr, R.H., Hernalsteen, J., Devos, J., 1994. J. Appl. Polym. Sci. 52, 1015–1022.

Carré, C., Bonnet, L., Avérous, L., 2014. RSC Adv 4, 54018–54025.

Carré, C., Bonnet, L., Avérous, L., 2015. RSC Adv 5, 100390–100400.

Carriço, C., Fraga, T., Carvalho, V., Pasa, V., 2017. Molecules 22, 1091.

Carriço, C.S., Fraga, T., Pasa, V.M.D., 2016. Eur. Polym. J. 85, 53–61.

Cateto, C.A., Barreiro, M.F., Ottati, C., Lopretti, M., Rodrigues, A.E., Belgacem, M.N., 2014. J. Cell. Plast. 50, 81–95.

Cateto, C.A., Barreiro, M.F., Rodrigues, A.E., Belgacem, M.N., 2009. Ind. Eng. Chem. Res. 48, 2583–2589.

Çaylı, G., Küsefoğlu, S., 2008. J. Appl. Polym. Sci. 109, 2948–2955.

Charlon, M., Heinrich, B., Matter, Y., Couzigné, E., Donnio, B., Avérous, L., 2014. Eur. Polym. J. 61, 197–205.

Chaudhary, S., Surekha, P., Kumar, D., Rajagopal, C., Roy, P.K., 2013. J. Appl. Polym. Sci. 129, 2779–2788.

Chen, F., Lu, Z., 2009. J. Appl. Polym. Sci. 111, 508–516.

Chmiel-Szukiewicz, E., 2013. J. Appl. Polym. Sci. 127, 1595–1600.

Christopher L. WIlson, C.L., L, C.J.B., 1958. Method of making polyester composition. 2863855A.

Chuayjuljit, S., Maungchareon, A., Saravari, O., 2010. J. Reinf. Plast. Compos. 29, 218–225.

Chuayjuljit, S., Sangpakdee, T., Saravari, O., 2007. J. Met. Mater. Miner. 17.

Chuayjuljit2007-Processing and Properties of Palm Oil-Based Rigid Polyurethane Foam.

Clements, J.H., 2003. Ind. Eng. Chem. Res. 42, 663–674.

Cook, W., Hostettler, F., Lombardi, F., 1974. Polyurethane foams based on liquid poly (e-caprolactone) polyester polyols. 3806473.

Cornille, A., Dworakowska, S., Bogdal, D., Boutevin, B., Caillol, S., 2015. Eur. Polym. J. 66, 129–138.

Cornille, A., Guillet, C., Benyahya, S., Negrell, C., Boutevin, B., Caillol, S., 2016. Eur. Polym. J. 84, 873–888.

Cregut, M., Bedas, M., Durand, M.-J., Thouand, G., 2013. Biotechnol. Adv. 31, 1634–1647.

Čuk, N., Fabjan, E., Grželj, P., Kunaver, M., 2015. J. Appl. Polym. Sci. 132, 41522.

Cunningham, R.L., Gordon, S.H., Felker, F.C., Eskins, K., 1998. J. Appl. Polym. Sci. 69, 957–964.

Czupryński, B., Liszkowska, J., Paciorek-Sadowska, J., 2012. J. Appl. Polym. Sci. 126, E44–E53.

Datta, J., Kopczyńska, P., 2016. Crit. Rev. Environ. Sci. Technol. 46, 905–946.

De, G.M., Pettingill, O.H., 1963. Certain oxyalkylated polyols. US 3110737.

Debuissy, T., Pollet, E., Avérous, L., 2017a. Eur. Polym. J. 97, 328–337.

Debuissy, T., Sangwan, P., Pollet, E., Avérous, L., 2017b. Polymer 122, 105–116.

Deepa, P., Jayakannan, M., 2008. J. Polym. Sci. Part Polym. Chem. 46, 2445–2458.

Delebecq, E., Pascault, J.-P., Boutevin, B., Ganachaud, F., 2013. Chem. Rev. 113, 80–118.

Desroches, M., Escouvois, M., Auvergne, R., Caillol, S., Boutevin, B., 2012. Polym. Rev. 52, 38–79.

Deutschmann, R., Dekker, R.F.H., 2012. Biotechnol. Adv. 30, 1627–1640.

Dominguez-Rosado, E., Liggat, J.J., Snape, C.E., Eling, B., Pichtel, J., 2002. Polym. Degrad. Stab. 78, 1–5.

Dong, K., Guo, X., Xu, J., Yang, D., Qiu, F., 2012. Polym.-Plast. Technol. Eng. 51, 754–759.

D'Souza, J., Camargo, R., Yan, N., 2014. J. Appl. Polym. Sci. 131, 40599.

D'Souza, J., Camargo, R., Yan, N., 2017. Polym. Rev. 57, 668–694.

Duval, A., Avérous, L., 2016. ACS Sustain. Chem. Eng. 4, 3103–3112.

Elbers, N., Ranaweera, C.K., Ionescu, M., Wan, X., Kahol, P.K., Gupta, R.K., 2017. J. Renew. Mater. 5, 74–83.

Engels, H.-W., Pirkl, H.-G., Albers, R., Albach, R.W., Krause, J., Hoffmann, A., Casselmann, H., Dormish, J., 2013. Angew. Chem. Int. Ed. 52, 9422–9441.

F, S., M, M., A, R.S., 1987. Cell. Polym. 6, 27–41.

Fleurent, H., Thijs, S., 1995. J. Cell. Plast. 31, 580–599.

Fritz, H., Young, D.M., 1965. Polyurethane polymers from lactone polyesters. 3186971.

Furtwengler, P., Perrin, R., Redl, A., Avérous, L., 2017. Eur. Polym. J. 97, 319–327.

Galanis, S., Dasgupta, P.K., 2001. Anal. Chim. Acta 429, 101–110.

Gama, N., Silva, R., Carvalho, A.P.O., Ferreira, A., Barros-Timmons, A., 2017. Polym. Test. 62, 13–22.

Gama, N.V., Silva, R., Costa, M., Barros-Timmons, A., Ferreira, A., 2016. Polym. Test. 56, 200–206.

Gandhi, T.S., Patel, M.R., Dholakiya, B.Z., 2015a. J. Polym. Eng. 35.

Gandhi, T.S., Patel, M.R., Dholakiya, B.Z., 2015b. Int. J. Plast. Technol. 19, 30–46.

Gandini, A., 2008. Macromolecules 41, 9491–9504.

Gandini, A., Belgacem, M.N., 2008. The State of the Art, in: Monomers, Polymers and Composites from Renewable Resources. Elsevier, pp. 1–16.

Gandini, A., Lacerda, T.M., 2015. Prog. Polym. Sci. 48, 1–39.

Gao, L., Zheng, G., Zhou, Y., Hu, L., Feng, G., Xie, Y., 2013. Ind. Crops Prod. 50, 638–647.

Gao, L.-L., Liu, Y.-H., Lei, H., Peng, H., Ruan, R., 2010. J. Appl. Polym. Sci. NA-NA.

Ge, J., Shi, X., Cai, M., Wu, R., Wang, M., 2003. J. Appl. Polym. Sci. 90, 2756–2763.

Ge, J., Zhong, W., Guo, Z., Li, W., Sakai, K., 2000a. J. Appl. Polym. Sci. 77, 2575–2580.

Ge, J., Zhong, W., Guo, Z., Li, W., Sakai, K., 2000b. J. Appl. Polym. Sci. 77, 2575–2580.

George, N., Kurian, T., 2014. Ind. Eng. Chem. Res. 53, 14185–14198.

Grause, G., Buekens, A., Sakata, Y., Okuwaki, A., Yoshioka, T., 2011. J. Mater. Cycles Waste Manag. 13, 265–282.

Grignard, B., Thomassin, J.-M., Gennen, S., Poussard, L., Bonnaud, L., Raquez, J.-M., Dubois, P., Tran, M.-P., Park, C.B., Jerome, C., Detrembleur, C., 2016. Green Chem 18, 2206–2215.

Grimminger, J., Muha, K., 1995. J. Cell. Plast. 31, 48–72.

Guo, A., Cho, Y., Petrović, Z.S., 2000. J. Polym. Sci. Part Polym. Chem. 38, 3900–3910.

Guo, A., Zhang, W., Petrovic, Z.S., 2006. J. Mater. Sci. 41, 4914–4920.

Gupta, R.K., Ionescu, M., Radojcic, D., Wan, X., Petrovic, Z.S., 2014. J. Polym. Environ. 22, 304–309.

Gupta, R.K., Ionescu, M., Wan, X., Radojcic, D., Petrovic, Z.S., 2015. J. Polym. Environ. 23, 261–268.

Han, M.S., Choi, S.J., Kim, J.M., Kim, Y.H., Kim, W.N., Lee, H.S., Sung, J.Y., 2009. Macromol. Res. 17, 44–50.

Hayden, D.E., Foucht, M.E., 1978. Polyurethane foam system. US 4072623.

He, Q. (Sophia), McNutt, J., Yang, J., 2017. Renew. Sustain. Energy Rev. 71, 63–76.

Hejna, A., Kosmela, P., Kirpluks, M., Cabulis, U., Klein, M., Haponiuk, J., Piszczyk, Ł., 2017. J. Polym. Environ.

Herzberger, J., Niederer, K., Pohlit, H., Seiwert, J., Worm, M., Wurm, F.R., Frey, H., 2016. Chem. Rev. 116, 2170–2243.

Himabindu, M., Kamalakar, K., Karuna, M., Palanisamy, A., 2017. J. Renew. Mater. 5, 124–131.

Hojabri, L., Kong, X., Narine, S.S., 2009. Biomacromolecules 10, 884–891.

Hopmann, C., Latz, S., 2015. Polymer 56, 29–36.

Hostettler, F., 1965. Lactone polyesters. 3169945.

Hu, M., Hwang, J.-Y., Kurth, M.J., Hsieh, Y.-L., Shoemaker, C.F., Krochta, J.M., 1997. J. Agric. Food Chem. 45, 4156–4161.

Hu, S., Luo, X., Li, Y., 2014. ChemSusChem 7, 66–72.

Hu, S., Luo, X., Wan, C., Li, Y., 2012. J. Agric. Food Chem. 60, 5915–5921.

Huang, G., Wang, P., 2017. Polym. Test. 60, 266–273.

Ionescu, M., 2005. Chemistry and technology of polyols for polyurethanes. Rapra Technology, Shawbury, Shrewsbury, Shropshire, U.K.

Ionescu, M., Petrović, Z.S., 2010. J. Cell. Plast. 46, 223–237.

Ionescu, M., Radojčić, D., Wan, X., Shrestha, M.L., Petrović, Z.S., Upshaw, T.A., 2016. Eur. Polym. J. 84, 736–749.

Ionescu, M., Wan, X., Bilić, N., Petrović, Z.S., 2012. J. Polym. Environ. 20, 647–658.

Jefferson, R.T., Salyer, I.O., 1971. Process for closed-cell rigid polyurethane foams. 355,85,31.

Jeong, H., Park, J., Kim, S., Lee, J., Ahn, N., 2013. Fibers Polym. 14, 1301–1310.

Jeong, H., Shim, W.J., 2017. Pol. Marit. Res. 24.

Ji, D., Fang, Z., He, W., Luo, Z., Jiang, X., Wang, T., Guo, K., 2015a. Ind. Crops Prod. 74, 76–82.

Ji, D., Fang, Z., He, W., Luo, Z., Jiang, X., Wang, T., Guo, K., 2015b. Ind. Crops Prod. 74, 76–82.

Ji, D., Fang, Z., Wan, Z.D., Chen, H.C., He, W., Li, X.L., Guo, K., 2013. Adv. Mater. Res. 724–725, 1681–1684.

Jiang, L., Zhang, J., 2017. Biodegradable and Biobased Polymers, in: Applied Plastics Engineering Handbook. Elsevier, pp. 127–143.

Jin, J.F., Chen, Y.L., Wang, D.N., Hu, C.P., Zhu, S., Vanoverloop, L., Randall, D., 2002. J. Appl. Polym. Sci. 84, 598–604.

Jin, Y., Ruan, X., Cheng, X., Lü, Q., 2011. Bioresour. Technol. 102, 3581–3583.

Kacperski, M., Spychaj, T., 1999. Polym. Adv. Technol. 10, 620–624.

Kairytė, A., Vėjelis, S., 2015. Ind. Crops Prod. 66, 210–215.

Kang, S.M., Kang, M.S., Kwon, S.H., Park, H., Kim, B.K., 2014. J. Polym. Eng. 34.

Karadeniz, K., Çalıkoğlu, Y., Sen, M.Y., 2017. Polym. Bull. 74, 2819–2839.

Karayannidis, G.P., Achilias, D.S., 2007. Macromol. Mater. Eng. 292, 128–146.

Kaushiva, B.D., McCartney, S.R., Rossmy, G.R., Wilkes, G.L., 2000. Polymer 41, 285–310.

Kaushiva, B.D., Wilkes, G.L., 2000. J. Appl. Polym. Sci. 77, 202–216.

Kharbas, H.A., McNulty, J.D., Ellingham, T., Thompson, C., Manitiu, M., Scholz, G., Turng, L.-S., 2017. J. Cell. Plast. 53, 373–388.

Kihara, N., Endo, T., 1993. J. Polym. Sci. Part Polym. Chem. 31, 2765–2773.

Kobashigawa, K., Tokashiki, T., Naka, H., Hirose, S., Hatakeyama, H., 2001. Recent Adv. Environ. Compat. Polym. Camb. Woodhead Publ. 229–34.

Kosmela, P., Kazimierski, P., Formela, K., Haponiuk, J., Piszczyk, Ł., 2017. J. Ind. Eng. Chem.

Kurańska, M., Prociak, A., 2016. Ind. Crops Prod. 89, 182–187.

Kurańska, M., Prociak, A., Kirpluks, M., Cabulis, U., 2015. Ind. Crops Prod. 74, 849–857.

Kurimoto, Y., Doi, S., Tamura, Y., 1999. Holzforschung 53.

Lan, Z., Daga, R., Whitehouse, R., McCarthy, S., Schmidt, D., 2014. Polymer 55, 2635–2644.

Langeveld, J.W.A., Dixon, J., Jaworski, J.F., 2010. Crop Sci. 50, S-142.

Lapprand, A., Boisson, F., Delolme, F., Mechin, F., Pascault, J.-P., 2005. Polym. Degrad. Stab. 90, 363–373.

Layer, O., 1988.

Lee, S.-H., Teramoto, Y., Shiraishi, N., 2002. J. Appl. Polym. Sci. 83, 1482–1489.

Lee, S.-H., Yoshioka, M., Shiraishi, N., 2000. J. Appl. Polym. Sci. 78, 319–325.

Li, Chenguo, Li, S., Zhao, J., Zhang, Z., Zhang, J., Yang, W., 2014. J. Polym. Res. 21.

Li, Cong, Luo, X., Li, T., Tong, X., Li, Y., 2014. Polymer 55, 6529–6538.

Li, H., Mahmood, N., Ma, Z., Zhu, M., Wang, J., Zheng, J., Yuan, Z., Wei, Q., Xu, C. (Chunbao), 2017a. Ind. Crops Prod. 103, 64–72.

Li, H., Mahmood, N., Ma, Z., Zhu, M., Wang, J., Zheng, J., Yuan, Z., Wei, Q., Xu, C. (Chunbao), 2017b. Ind. Crops Prod. 103, 64–72.

Li, H.-Q., Shao, Q., Luo, H., Xu, J., 2016a. J. Appl. Polym. Sci. 133, 43261

Li, Q.F., Feng, Y.L., Wang, J.W., Yin, N., Zhao, Y.H., Kang, M.Q., Wang, X.W., 2016. Plast. Rubber Compos. 45, 16–21.

Li, S., Bouzidi, L., Narine, S.S., 2017. Eur. Polym. J. 93, 232–245.

Li, S., Zhao, J., Zhang, Z., Zhang, J., Yang, W., 2014. RSC Adv. 4, 23720.

Li, Y., Ragauskas, A.J., 2012. J. Wood Chem. Technol. 32, 210–224.

Lin, L., Yoshioka, M., Yao, Y., Shiraishi, N., 1994. J. Appl. Polym. Sci. 52, 1629–1636.

Liszkowska, J., 2017. Polym. Bull. 74, 283–305.

Liu, C., Long, Y., Xie, J., Xie, X., 2017. Polymer 116, 240–250.

Liu, Y., He, J., Yang, R., 2017. J. Mater. Sci. 52, 4700–4712.

Long, Y., Sun, F., Liu, C., Huang, D., Xie, X., 2016. J. Appl. Polym. Sci. 133.

Lowe, A.B., 2014. Polymer 55, 5517–5549.

Lucas, N., Bienaime, C., Belloy, C., Queneudec, M., Silvestre, F., Nava-Saucedo, J.-E., 2008. Chemosphere 73, 429–442.

Luo, X., Hu, S., Zhang, X., Li, Y., 2013. Bioresour. Technol. 139, 323–329.

Luo, X., Li, Y., 2014. J. Polym. Environ. 22, 318–328.

Machado, T.O., Sayer, C., Araujo, P.H.H., 2017. Eur. Polym. J. 86, 200–215.

Mahmood, N., Yuan, Z., Schmidt, J., Tymchyshyn, M., Xu, C. (Charles), 2016. Green Chem 18, 2385–2398.

Maisonneuve, L., Lamarzelle, O., Rix, E., Grau, E., Cramail, H., 2015. Chem. Rev. 115, 12407–12439.

Majumdar, K.K., Kundu, A., Das, I., Roy, S., 2000. Appl. Organomet. Chem. 14, 79–85.

Maldas, D., Shiraishi, N., 1996. Int. J. Polym. Mater. 33, 61–71.

Marcovich, N.E., Kurańska, M., Prociak, A., Malewska, E., Kulpa, K., 2017. Ind. Crops Prod. 102, 88–96.

Matos, M., Barreiro, M.F., Gandini, A., 2010. Ind. Crops Prod. 32, 7–12.

Matsumiya, Y., Murata, N., Tanabe, E., Kubota, K., Kubo, M., 2009. J. Appl. Microbiol.

McAdams, C.A., Farmer, S., 2003. J. Cell. Plast. 39, 369–386.

Mielewski, D.F., Flanigan, C.M., Perry, C., Zaluzec, M.J., Killgoar, P.C., 2005. Ind. Biotechnol. 1, 32–34.

Molero, C., de Lucas, A., Rodríguez, J.F., 2006. Polym. Degrad. Stab. 91, 221–228.

Molero, Carolina, de Lucas, A., Rodríguez, J.F., 2008. Polym. Degrad. Stab. 93, 353–361.

Molero, C., de Lucas, A., Romero, F., Rodríguez, J.F., 2008. J. Appl. Polym. Sci. 109, 617–626.

More, A.S., Gadenne, B., Alfos, C., Cramail, H., 2012. Polym. Chem. 3, 1594.

Mosiewicki, M.A., Rojek, P., Michałowski, S., Aranguren, M.I., Prociak, A., 2015. J. Appl. Polym. Sci. 132, 41602.

Nadji, H., Bruzzèse, C., Belgacem, M.N., Benaboura, A., Gandini, A., 2005. Macromol. Mater. Eng. 290, 1009–1016.

Nagy, T., Antal, B., Czifrák, K., Papp, I., Karger-Kocsis, J., Zsuga, M., Kéki, S., 2015. J. Appl. Polym. Sci. 132, 42127.

Nakashima, K., Takeshita, T., Morimoto, K., 2002. Environ. Health Prev. Med. 7, 1–6.

Narine, S.S., Kong, X., Bouzidi, L., Sporns, P., 2007a. J. Am. Oil Chem. Soc. 84, 65–72.

Narine, S.S., Yue, J., Kong, X., 2007b. J. Am. Oil Chem. Soc. 84, 173–179.

Ng, W.S., Lee, C.S., Chuah, C.H., Cheng, S.-F., 2017. Ind. Crops Prod. 97, 65–78.

Nikje, A., Mohammad, M., Haghshenas, M., Garmarudi, A.B., 2007. Polym.-Plast. Technol. Eng. 46, 265–271.

Nikje, M.M.A., Garmarudi, A.B., 2006. Polym.-Plast. Technol. Eng. 45, 1101–1107.

Nikje, M.M.A., Garmarudi, A.B., Idris, A.B., 2011. Des. Monomers Polym. 14, 395–421.

Nikje, M.M.A., Mohammadi, F.H.A., 2010. Polym.-Plast. Technol. Eng. 49, 818–821.

Nikles, D.E., Farahat, M.S., 2005. Macromol. Mater. Eng. 290, 13–30.

Noreen, A., Zia, K.M., Zuber, M., Tabasum, S., Zahoor, A.F., 2016. Prog. Org. Coat. 91, 25–32.

Ogunniyi, D., 2006. Bioresour. Technol. 97, 1086–1091.

Olivier Coulembier Philippe Dubois, Jean-Marie Raquez, 2009. Handbook of Ring-Opening Polymerization. Wiley-VCH, Weinheim.

Oliviero, M., Verdolotti, L., Stanzione, M., Lavorgna, M., Iannace, S., Tarello, M., Sorrentino, A., 2017. J. Appl. Polym. Sci. 134, 45113.

Ozaki, S., others, 1972. Chem Rev 72, 457–496.

P. Madden, J., Baker, G.K., H. Smith, C., 1972. J. Cell. Plast. 8, 201–207.

Palanisamy, A., Karuna, M.S.L., Satyavani, T., Rohini Kumar, D.B., 2011. J. Am. Oil Chem. Soc. 88, 541–549.

Palaskar, D.V., Boyer, A., Cloutet, E., Alfos, C., Cramail, H., 2010. Biomacromolecules 11, 1202–1211.

Paruzel, A., Michałowski, S., Hodan, J., Horák, P., Prociak, A., Beneš, H., 2017. ACS Sustain. Chem. Eng. 5, 6237–6246.

Pavier, Claire, Gandini, A., 2000. Ind. Crops Prod. 12, 1–8.

Pavier, C., Gandini, A., 2000. Carbohydr. Polym. 42, 13–17.

Pawar, M.S., Kadam, A.S., Dawane, B.S., Yemul, O.S., 2016a. Polym. Bull. 73, 727–741.

Pawar, M.S., Kadam, A.S., Singh, P.C., Kusumkar, V.V., Yemul, O.S., 2016b. Iran. Polym. J. 25, 59–68.

Pawlik, H., Prociak, A., 2012. J. Polym. Environ. 20, 438–445.

Petrovic, Z.S., Ferguson, J., 1991. Prog. Polym. Sci. 16, 695–836.

Petrovic, Z., 2008. Polym. Rev. 48, 109–155.

Petrović, Z.S., Wan, X., Bilić, O., Zlatanić, A., Hong, J., Javni, I., Ionescu, M., Milić, J., Degruson, D., 2013. J. Am. Oil Chem. Soc. 90, 1073–1078.

Petrović, Z.S., Zhang, W., Javni, I., 2005. Biomacromolecules 6, 713–719.

Pfister, D.P., Xia, Y., Larock, R.C., 2011. ChemSusChem 4, 703–717.

Pillai, P.K.S., Li, S., Bouzidi, L., Narine, S.S., 2016. Ind. Crops Prod. 84, 273–283.

Piszczyk, Ł., Strankowski, M., Danowska, M., Hejna, A., Haponiuk, J.T., 2014. Eur. Polym. J. 57, 143–150.

Posen, I.D., Jaramillo, P., Griffin, W.M., 2016. Environ. Sci. Technol. 50, 2846–2858.

Posner, T., 1905. Berichte Dtsch. Chem. Ges. 38, 646–657.

Quadrini, F., Bellisario, D., Santo, L., 2013. Polym. Eng. Sci. 53, 1357–1363.

Raiford, L.C., Freyermuth, H.B., 1943. J. Org. Chem. 08, 230–238.

Randall, D., Lee, S. (Eds.), 2002. The polyurethanes book. Huntsman Polyurethanes] ; New York : Distributed by John Wiley & Sons, [Everberg, Belgium.

Rashmi, B.J., Rusu, D., Prashantha, K., Lacrampe, M.F., Krawczak, P., 2013. J. Appl. Polym. Sci. 128, 292–303.

Rehkopf, J.D., Mcneice, G.M., Rudin, A., 1994. J. Cell. Plast. 30, 34–43.

Reichmann, W.W., Phillips, B.A., 1988. J. Cell. Plast. 24, 601–610.

Ribeiro da Silva, V., Mosiewicki, M.A., Yoshida, M.I., Coelho da Silva, M., Stefani, P.M., Marcovich, N.E., 2013. Polym. Test. 32, 665–672.

Rieger, B., Amann, M. (Eds.), 2012. Synthetic biodegradable polymers, Advances in polymer science. Springer, Heidelberg ; New York.

Robles, H., 2014. Urethane, in: Encyclopedia of Toxicology. Elsevier, pp. 889–891.

Rogge, T.M., Stevens, C.V., Vandamme, A., Booten, K., Levecke, B., D'hooge, C., Haelterman, B., Corthouts, J., 2005. Biomacromolecules 6, 1992–1997.

Rokicki, G., Piotrowska, A., 2002. Polymer 43, 2927–2935.

Rossmy, G.R., Kollmeier, H.J., Lidy, W., Schator, H., Wiemann, M., 1977. J. Cell. Plast. 13, 26–35.

Rotaru, I., Ionescu, M., Donescu, D., Vuluga, M., 2008. Mater. Plast. 45, 23–28.

Roy, P.K., Mathur, R., Kumar, D., Rajagopal, C., 2013. J. Environ. Chem. Eng. 1, 1062–1069.

Saunders, J.H., Slocombe, R.J., 1948. Chem. Rev. 43, 203–218.

Schuster, F., Ngako Ngamgoue, F., Goetz, T., Hirth, T., Weber, A., Bach, M., 2017. J Mater Chem C 5, 6738–6744.

Schwetlick, K., Noack, R., 1995. J. Chem. Soc. Perkin Trans. 2 395.

Senger, J.S., Yilgor, I., McGrath, J.E., Patsiga, R.A., 1989. J. Appl. Polym. Sci. 38, 373–382.

Septevani, A.A., Evans, D.A.C., Chaleat, C., Martin, D.J., Annamalai, P.K., 2015. Ind. Crops Prod. 66, 16–26.

Serrano, L., Alriols, M.G., Briones, R., Mondragón, I., Labidi, J., 2010. Ind. Eng. Chem. Res. 49, 1526–1529.

Sigurdsson, S.T., Seeger, B., Kutzke, U., Eckstein, F., 1996. J. Org. Chem. 61, 3883–3884.

Silva, A.L., Bordado, J.C., 2004. Catal. Rev. 46, 31–51.

Simón, D., Borreguero, A.M., de Lucas, A., Molero, C., Rodríguez, J.F., 2013. J. Mater. Cycles Waste Manag.

Simón, D., Borreguero, A.M., de Lucas, A., Rodríguez, J.F., 2014. Polym. Degrad. Stab. 109, 115–121.

Simón, D., Borreguero, A.M., de Lucas, A., Rodríguez, J.F., 2015a. Polym. Degrad. Stab. 121, 126–136.

Simón, D., Borreguero, A.M., de Lucas, A., Rodríguez, J.F., 2015b. Polym. Degrad. Stab. 116, 23–35.

Simón, D., de Lucas, A., Rodríguez, J.F., Borreguero, A.M., 2016. Polym. Degrad. Stab. 133, 119–130.

Slotta, K.H., Dressler, H., 1930. Berichte Dtsch. Chem. Ges. B Ser. 63, 888–898.

Smith, C.H., 1963. Ind. Eng. Chem. Prod. Res. Dev. 2, 27–31.

Sonnenschein, M.F., Wendt, B.L., 2013. Polymer 54, 2511–2520.

Sonnenschein, M.F., Werness, J.B., Patankar, K.A., Jin, X., Larive, M.Z., 2016. Polymer 106, 128–139.

Sorenson, W.R., 1959. J. Org. Chem. 24, 978–980.

Soto, G., Castro, A., Vechiatti, N., Iasi, F., Armas, A., Marcovich, N.E., Mosiewicki, M.A., 2017. Polym. Test. 57, 42–51.

Soto, G.D., Marcovich, N.E., Mosiewicki, M.A., 2016. J. Appl. Polym. Sci. 133.

Stirna, U., Fridrihsone, A., Lazdiņa, B., Misāne, M., Vilsone, D., 2013. J. Polym. Environ. 21, 952–962.

Storey, R.F., Wiggins, J.S., Puckett, A.D., 1994. J. Polym. Sci. Part Polym. Chem. 32, 2345–2363.

Suh, H.S., Ha, J.Y., Yoon, J.H., Ha, C.-S., Suh, H., Kim, I., 2010. React. Funct. Polym. 70, 288–293.

Szycher, M., 2013. Szycher's handbook of polyurethanes. CRC Press, Boca Raton, Fla.

T, P.J.J., F, S.W., 1965. Process for oxyalkylating solid polyols. US 3190927.

Takeyasu, H., Sonobe, T., Yamaguchi, Y., Doi, T., 1992. Polyurethane flexible foam and method for its production. Google Patents.

Tan, S., Abraham, T., Ference, D., Macosko, C.W., 2011. Polymer 52, 2840–2846.

Tanaka, R., Hirose, S., Hatakeyama, H., 2008. Bioresour. Technol. 99, 3810–3816.

Tibério Cardoso, G., Claro Neto, S., Vecchia, F., 2012. Front. Archit. Res. 1, 348–356.

Tondi, G., Pizzi, A., 2009. Ind. Crops Prod. 29, 356–363.

Ugarte, L., Fernández-d'Arlas, B., Valea, A., González, M.L., Corcuera, M.A., Eceiza, A., 2014a. Polym. Eng. Sci. 54, 2282–2291.

Ugarte, L., Saralegi, A., Fernández, R., Martín, L., Corcuera, M.A., Eceiza, A., 2014b. Ind. Crops Prod. 62, 545–551.

Ulrich, H., Odinak, A., Tucker, B., Sayigh, A.A.R., 1978. Polym. Eng. Sci. 18, 844–848.

Uprety, B.K., Reddy, J.V., Dalli, S.S., Rakshit, S.K., 2017. Bioresour. Technol. 235, 309–315.

Vaidya, U.R., Nadkarni, V.M., 1987. J. Appl. Polym. Sci. 34, 235–245.

Vaidya, U.R., Nadkarni, V.M., 1988. J. Appl. Polym. Sci. 35, 775–785.

Van Maris, R., Tamano, Y., Yoshimura, H., Gay, K.M., 2005. J. Cell. Plast. 41, 305–322.

Velencoso, M.M., Gonzalez, A.S., García-Martínez, J.C., Ramos, M.J., De Lucas, A., Rodriguez, J.F., 2013. Polym. Int. 62, 783–790.

Vert, M., Doi, Y., Hellwich, K.-H., Hess, M., Hodge, P., Kubisa, P., Rinaudo, M., Schué, F., 2012. Pure Appl. Chem. 84.

Viswanathan, T., Burrington, D., Richardson, T., 2008. J. Chem. Technol. Biotechnol. Biotechnol. 34, 52–56.

Vitkauskiene, I., Makuska, R., Stirna, U., Cabulis, U., 2011. J. Cell. Plast. 47, 467–482.

Wilson, M.E., Hu, M., Kurth, M.J., Hsieh, Y.-L., Krochta, J.M., 1996. J. Appl. Polym. Sci. 59, 1759–1768.

Figovsky, Shapovalov, Preparation of oligomeric cyclocarbonates and their use in ionisocyanate or hybrid nonisocyanate polyurethanes, WO03028644A2.

Woods, G., 1982. Flexible polyurethane foams: chemistry and technology. Applied Science Publishers, London ; Englewood, N.J.

Worley, W.G., Shah, H.M., Athey, P.S., Bruchertseifer, C., Mueller, G., 2008. Polyurethane polymer systems. 20110098417.

Wu, C.-H., Chang, C.-Y., Cheng, C.-M., Huang, H.-C., 2003. Polym. Degrad. Stab. 80, 103–111.

Wu, C.-H., Chang, C.-Y., Li, J.-K., 2002. Polym. Degrad. Stab. 75, 413–421.

Wu, L.C.-F., Glasser, W.G., 1984. J. Appl. Polym. Sci. 29, 1111–1123.

Xu, J., Jiang, J., Hse, C.-Y., Shupe, T.F., 2014. J. Appl. Polym. Sci. 131, 40096.

Xue, B.-L., Huang, P.-L., Sun, Y.-C., Li, X.-P., Sun, R.-C., 2017. RSC Adv 7, 6123–6130.

Yao, W., Wang, H., Guan, D., Fu, T., Zhang, T., Dou, Y., 2017. Adv. Mater. Sci. Eng. 2017, 1–7.

Yao, Y., Yoshioka, M., Shiraishi, N., 1996. J. Appl. Polym. Sci. 60, 1939–1949.

Yasunaga, K., Neff, R.A., Zhang, X.D., Macosko, C.W., 1996. J. Cell. Plast. 32, 427–448.

Yeganeh, H., Hojati-Talemi, P., 2007. Polym. Degrad. Stab. 92, 480–489.

Yoshioka, M., Miyata, A., Nishio, Y., 2004a. J. Wood Sci. 50, 504–510.

Yoshioka, M., Miyata, A., Yagi, T., Nishio, Y., 2004b. J. Wood Sci. 50, 511–518.

Young, D.M., Fritz, H.,. Foamed polymer of isocyanate modified lactone polyesters and method of preparing same. 2990379.

Yu, C.-Y., Lee, W.-J., 2014. Polym. Degrad. Stab. 101, 60–64.

Yu, F., Saha, P., Suh, P.W., Kim, J.K., 2015. J. Appl. Polym. Sci. 132, 41410.

Yue, D., Oribayo, O., Rempel, G.L., Pan, Q., 2017. RSC Adv 7, 30334–30344.

Yukuta, T., Yagura, K., Fuchigami, N., 1981. Method of producing flexible reticulated polyether polyurethane foams.

Zarzyka, I., 2016. J. Cell. Plast. 52, 545–561.

Zenner, M.D., Xia, Y., Chen, J.S., Kessler, M.R., 2013. ChemSusChem 6, 1182–1185.

Zhang, G., Zhang, Q., Wu, Y., Zhang, H., Cao, J., Han, D., 2017. J. Appl. Polym. Sci. 134, 45582.

Zhang, L., Jeon, H.K., Malsam, J., Herrington, R., Macosko, C.W., 2007. Polymer 48, 6656–6667.

Zhang, L., Zhang, M., Hu, L., Zhou, Y., 2014. Ind. Crops Prod. 52, 380–388.

Zhang, M., Pan, H., Zhang, L., Hu, L., Zhou, Y., 2014. Ind. Crops Prod. 59, 135–143.

Zhang, Q., Zhang, G., Han, D., Wu, Y., 2016. J. Appl. Polym. Sci. 133.

Zhang, X.., Macosko, C.., Davis, H.., Nikolov, A.., Wasan, D.., 1999. J. Colloid Interface Sci. 215, 270–279.

Zheng, Z.-Q., Liu, Y., Li, D., Wang, L., Adhikari, B., Chen, X.D., 2017. Int. J. Food Eng. 13.

Zhou, X., Sain, M.M., Oksman, K., 2016. Compos. Part Appl. Sci. Manuf. 83, 56–62.

Zia, K.M., Bhatti, H.N., Ahmad Bhatti, I., 2007. React. Funct. Polym. 67, 675–692.

Zieleniewska, M., Leszczyński, M.K., Kurańska, M., Prociak, A., Szczepkowski, L., Krzyżowska, M., Ryszkowska, J., 2015. Ind. Crops Prod. 74, 887–897.

Zieleniewska, M., Ryszkowska, J., Bryskiewicz, A., Auguscik, M., Szczepkowski, L., Swiderski, A., Wrzesniewska-Tosik, K., 2017. Polimery 62, 127–135.

Zlatanić, A., Javni, I., Ionescu, M., Bilić, N., Petrović, Z.S., 2015. J. Cell. Plast. 51, 289–306.

Zlatanić, A., Lava, C., Zhang, W., Petrović, Z.S., 2004. J. Polym. Sci. Part B Polym. Phys. 42, 809–819.

Zou, X., Qin, T., Huang, L., Zhang, X., Yang, Z., Wang, Y., 2009. Energy Fuels 23, 5213–5218.

2011. Focus Powder Coat. 2011, 7–8.

Conclusion et perspectives du premier Chapitre

L'état de l'art exposé dans ce premier Chapitre montre clairement l'étendue et la capacité de la biomasse à satisfaire la demande en polyols destinés à l'élaboration de systèmes polyuréthanes expansés. Au-delà du caractère aliphatique ou aromatique des polyols obtenus, on a pu distinguer trois grandes voies d'obtention de polyol à partir de la biomasse (i) par polymérisations de synthons (ii), par modification chimique d'acides / d'huiles grasses et (iii) les procédés de liquéfactions de la biomasse. Les différentes approches développées permettent de synthétiser des polyols aux architectures moléculaires variées satisfaisant un ensemble de critères pour l'élaboration de matériaux polyuréthanes alvéolaires flexibles, semi-flexibles et rigides avec une large gamme de densité.

Les polyols les plus développés sont les polyols notamment obtenus par réaction d'alkoxylation et donc partiellement biosourcés. Cette voie présente le grand avantage d'être applicable à n'importe quel synthon contenant des fonctions hydroxyles et peut être aussi initiée sur des synthons de nature solide. Cela en fait la voie de transformation la plus developpée pour les modifications chimiques de la lignine et des tannins. Les conditions d'alkoxylation présentes quelques limites, mais le caractère biosourçable de l'oxyde d'éthylène, de l'oxyde de propylène et de l'oxyde de butylène à partir du « bio-éthylène », du propylène glycol et du butanol ouvre quelques perspectives d'avenir pour ce type de réactions pour l'elaboration de composés largement biosourcés. De manière générale, la biomasse ligno-cellulosique brute devrait être préférentiellement transformée par des voies de liquéfaction plutôt que d'alkoxylation afin de promouvoir l'utilisation de solvants de moins toxiques. De manière assez récurrente, le solvant de liquéfaction préférable est un mélange de glycérol et de poly(éthylène glycol), qui donne des polyols complètement biosourçables.

La biomasse qui est abondamment décrite dans la littérature est l'huile végétale. Elle est classiquement modifiée pour obtenir des polyols à base de longues chaînes faiblement fonctionnalisées. Ils sont principalement destinés à l'élaboration de mousses polyuréthane flexibles ou semi-rigides. Les avantages majeurs liés à l'utilisation de polyols issus d'huiles végétales sont leur faible coût et grande disponibilité. Il existe aussi des alternatives telles que les polyols obtenus par couplage thiol-ène, les polyols de Mannich….

De manière très surprenante, la littérature scientifique décrit très peu le développement de polyols polyesters biosourcés pour des applications de mousses polyuréthane. La synthése et la valorsiation de polyols polyesters biosourcés va faire l'objet d'une large partie des Chapitres expremimentaux de ce mémoire. En effet, la suite de ce travail consiste dans un premier temps à synthétiser une gamme de polyols polyesters à base d'un sucre, le sorbitol.

CHAPITRE 2 : SYNTHESE DE POLYOLS BIOSOURCES POUR L'ELABORATION DE MOUSSES POLYURETHANES

Introduction du Chapitre 2

Le Chapitre 2 est orienté sur la synthèse de polyols polyester à partir du sorbitol et de molécules bifonctionelles d'origine biosourcées ou potentiellement biosourçables. La synthèse de tels polyols est contrôlée de façon à obtenir des structures pour l'élaboration de mousses PUR et PIR. Dans le cadre de cette étude, une gamme de huit polyols a été développée et caractérisée (détermination de la structure des polyols, propriétés thermiques, rhéologiques, valeur d'indice hydroxyles et d'acidité) afin de formuler et caractériser des mousses PUR.

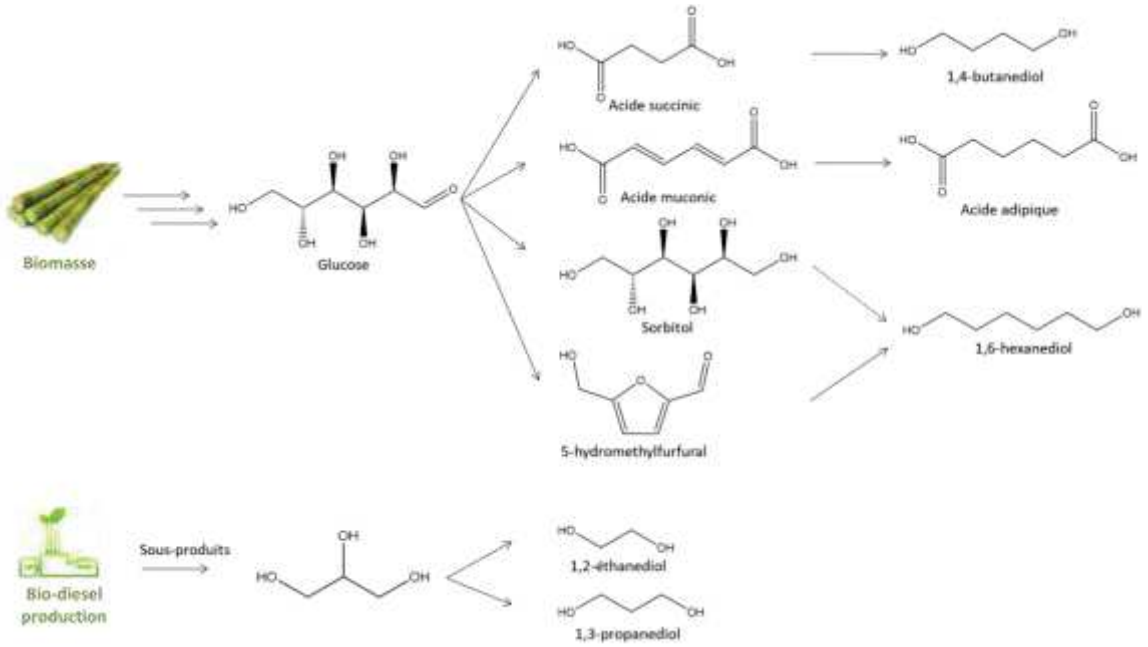

Figure 2.1: Exemples de voies d'obtentions de polyols et diacides courants à partir de la biomasse.

Les principaux monomères ou synthons, impliqués dans ces synthèses sont l'acide succinique et adipique et des diols de C2 à C12. L'acide adipique et l'acide succinique peuvent tous deux être biosynthétisé à partir du glucose tout comme le sorbitol (C6). L'acide succinique peut ensuite être réduit en 1,4-butanediol (C4). Le 1,2-ethylène glycol (C2) et 1,3-propanediol peuvent quant à eux être obtenus par hydrogénolyse du glycérol. Le 1,6-hexanediol peut être obtenu à partir du sorbitol, de l'acide adipique ou encore du 5-hydroxymethylfurfural. Par contre l'hydrogénolyse sélective des quatre liaisons C-O du sorbitol en 1,6-hexanediol reste complexe (Fang et al., 2017; Gandini and Lacerda, 2015). La Figure 2.1 présente des exemples de voie d'obtention de ces monomères à partir de la biomasse. Les diols de plus grandes tailles (à partir de C8) sont classés comme étant potentiellement biosourçables, mais ne le sont pas à l'heure actuelle (Jiang and Loos, 2016).

Dans l'ensemble de ce Chapitre plusieurs mousses polyuréthanes avec leurs formulations sont présentés. La méthodologie et les calculs sous-jacents à l'élaboration des formulations de mousses polyuréthanes partent tous d'un même point commun. Chaque formulation contient 100 parts (poids équivalent en masse ou parties par poids) de polyol(s). À partir de cette quantité de polyols, il est possible de calculer le reste de la formulation, notamment la masse de polyisocyanate. Pour calculer cette masse, il faut d'abord définir l'indice caractéristique (Ic) de la mousse qui est donné par l'équation 2.1 :

$$Ic = \frac{Nombre\ de\ focntion\ NCO}{Nombre\ de\ fonction\ OH} \times 100 \qquad (2.1)$$

L'Ic est le point de départ de toute formulation de mousses polyuréthane (PUR) ou polyisocyanurate (PIR). Pour une mousse PUR le rapport Ic est compris entre 100 et 150. Pour une mousse PIR, il est généralement compris entre 300 et 400. Il faut donc commencer par exprimer le nombre de fonctions OH et NCO contenues dans le polyol et le polyisocyanate.

Pour les polyols et polyisocyanates, le nombre de fonctions OH et NCO est rarement indiqué. En général, les polyols sont caractérisés par leurs indices hydroxyles (IOH). L'IOH est défini par l'équation (2.2). Le nombre de fonctions OH d'un polyol est défini par l'équation (2.3).

$$IOH = \frac{Fonctionnalité\ du\ polyol\ \times 56109.37}{Masse\ molaire\ du\ polyol} \qquad (2.2)$$

exprimé en mg KOH/g avec la masse molaire du KOH de 56109.37 mg/mol

$$Nombre\ de\ fonction\ OH = \frac{IOH \times Masse\ de\ polyol\ (g)}{56109} \qquad (2.3)$$

L'IOH du polyol est obtenu par un dosage en retour. Les fonctions hydroxyles du polyol sont estérifiées par l'anhydride phtalique puis l'anhydride phtalique excédentaire est dosé par de la potasse selon la norme ASTM 4274-99 et est exprimé en mg KOH/g. L'indice d'isocyanate est obtenu par un dosage en retour de la dibutylamine selon la norme ISO 14896/3, également exprimé en mg KOH/g. Le calcul du taux de fonction NCO et du nombre de fonctions NCO est défini en équation (2.4) et (2.5).

$$\%NCO = \frac{Nombre\ de\ fonction\ NCO \times 42 \times 100}{Masse\ de\ polyisocyanate\ (g)} \qquad (2.4)$$

$$Nombre\ de\ fonction\ NCO = \frac{\%NCO \times Masse\ de\ polyisocyanate\ (g)}{4200} \qquad (2.5)$$

Il est important de déterminer la masse de polyisocyanate correspondant à l'Ic choisi et l'adapter à l'IOH du polyol utilisé pour la formulation d'une mousse. Cette masse est obtenue par l'équation (2.6). L'ensemble des composants contenant des fonctions OH dans la constitution de la mousse (éventuel solvant de catalyseur, agent gonflant chimique, etc…) doivent être pris en compte.

$$Masse\ \mathrm{NCO(g)} = \frac{\sum(Masse\ polyol \times IOH \times Ic) \times 4200}{56109 \times \%NCO \times 100} \qquad (2.6)$$

Des informations complémentaires sur le taux de gonflement des mousses, les ratios de catalyseur et surfactant, ainsi que des tableaux formulations de références sont exposées en annexe 1.

Ce Chapitre est subdivisé en deux sous-Chapitres qui se présente chacun sous la forme d'une publication.

Le Chapitre 2.1 intitulé « Synthesis *and characterization of polyurethane foams derived of fully renewable polyester polyols from sorbitol* » présentera la synthèse de différents polyols polyesters biosourcés à base de sorbitol. L'étude porte ensuite sur la sélection et la caractérisation du polyol polyesters présentant les caractéristiques les plus appropriées à la formulation de mousse PUR.

Le Chapitre 2.2 intitulé « *Elaboration and characterization of advanced biobased polyurethane foams presenting anisotropic behavior* » poursuit le premier sous Chapitre. Il porte sur l'étude approfondie de quatre systèmes de mousses PUR à base de polyols biosourcés. L'objectif de ce Chapitre est d'étudier les relations existantes entre les choix de formulation (systèmes d'agent gonflant, et choix des polyols) et les propriétés mécaniques des mousses PUR résultantes.

Ce Chapitre a fait aussi l'objet de deux dépôts de brevet à l'international (PCT/IB2017/055107 et PCT/IB2017/055116), protégeant les applications industrielles relatives à ces travaux.

Chapitre 2.1: Synthesis and characterization of polyurethane foams derived of fully renewable polyester polyols from sorbitol

Pierre Furtwengler[a], Rémi Perrin[b], Andreas Redl[c], Luc Avérous[a,*]

[a]*BioTeam/ICPEES-ECPM, UMR CNRS 7515,*

Université de Strasbourg, 25 rue Becquerel, 67087 Strasbourg, Cedex 2, France

[b]*Soprema,*

14 rue de Saint-Nazaire, 67025 Strasbourg, Cedex 1, France

[c]*Tereos,*

ZI et portuaire, BP 32, 67390 Marckolsheim, France

* Corresponding author: Prof. Luc Avérous, Phone: + 333 68852784, Fax: + 333 68852716, E-mail: luc.averous@unistra.fr

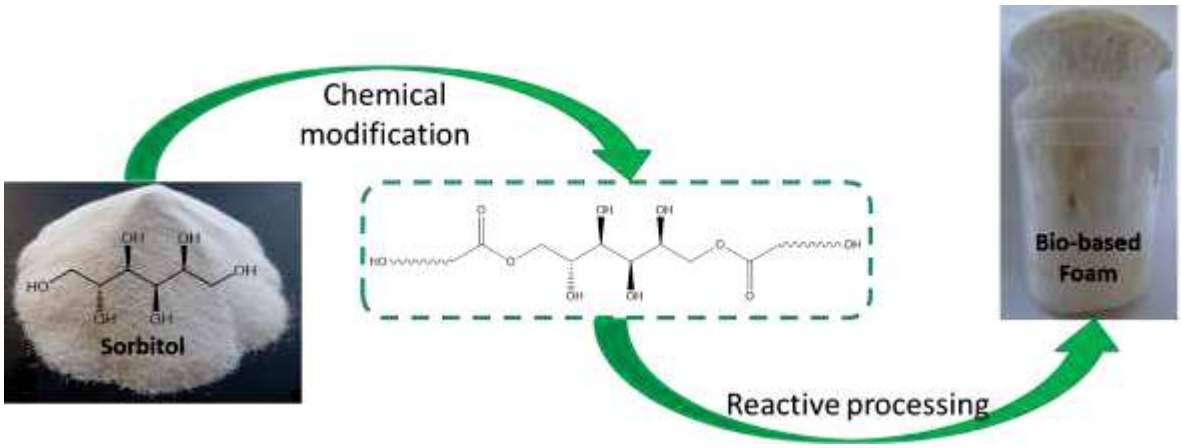

Published as P.Furtwengler, R.Perrin, A.Redl, L.Avérous, Eur. Polym. J., 2017, 97, 319-327

Abstract

This work globally redesigns the conventional approach in obtaining polyurethane foams (PUF), from sorbitol. Fully biobased polyester polyols were synthesized from sorbitol, adipic or succinic acid and different renewable C2 to C12 diols as the first step towards the elaboration of PUF. Sorbitol-based polyester polyols were synthesized through a two-step esterification without catalyst. The absence of a catalyst limits some side reactions and focuses the reaction on the primary hydroxyl groups of the sorbitol, to obtain the linear molecular structure. The global yields of the corresponding esterifications were above 80%. Hydroxyl values and acid values of the corresponding linear biobased polyester polyols ranged from 440 to 683 mg KOH/g, and from 11 to 49 mg KOH/g, respectively. Acid values were decreased below 10 mg KOH/g by neutralization. PUF were prepared with polyols blends containing this biobased polyester polyol (up to 75 wt%) and a conventional fossil based polyol e.g., oxypropylated glycerol, which present a high fossil content. The final biobased content of the PUF ranged up to 28 wt% in contrast to 9 wt% for the reference. Then the addition of neat glycerol to the polyol blend increased the final biobased contents of the PUF foams up to 31 wt%. In contrast with the traditional approach consisting of modifying the catalyst content, the activation of the reactive foaming process was improved through initial polyols blends. The final biobased PUF foaming kinetic was similar to that of the polyether polyol, used as a reference. Finally, the effects of chemical and physical blowing agents (water vs. isopentane) were compared on the foaming rate and foam structure. The use of chemical blowing agent efficiently decreased the foam gel time of 33% and increased the foaming rate of 1 mm/s with biobased systems. Besides, the polyols architecture has a strong influence on the foam tack free time which varied from 50 to 235 s for the studied PUF.

Introduction

Nowadays and worldwide, research inputs are focused on transforming renewable resources from biomass into useful biobased building blocks, solvents, polymers or materials for the chemical industry, while being in agreement with green chemistry. These approaches are asked to answer new ecological concerns, reduce the consumption of fossil resources and to develop new chemical architectures (Gandini et al., 2016; Langeveld et al., 2010).

Polyurethanes (PUs) are one of the main polymer families (Gandini, 2008), with a global production of 18 million tons in 2016, placing PUs at the 6th rank among polymer worldwide production. The global market of PUs is valuated around 53 billion Euros (Cornille et al., 2017a). They are used in different applications such as automotive, furniture, construction, footwear, acoustic and thermal insulations (Randall and Lee, 2002). Building insulation is a growing sector, in constant demand for innovative polymer materials to reduce building energy costs and noise pollution with PUs-based materials such as membranes or foams. To produce polyurethane foams (PUF) different basic components must be stirred such as polyisocyanate(s), polyol(s), catalyst(s) and blowing agent(s) (Reymore et al., 1975). Two types of blowing are used for the elaboration of PUF: physical and chemical blowings (Kattiyaboot and Thongpin, 2016). Physical blowing agents are low boiling point compounds such as chlorofluorocarbures and isopentane derivates which evaporate during the exothermic foaming process due to the polyaddition between isocyanates and hydroxyl groups (Figure 2.2, a) with a reactional enthalpy of 100.32 KJ/mol (Ionescu, 2005a). The most common chemical blowing agent is water which reacts with polyisocyanate to form urea, and liberates one mole of CO_2 per initial mole of water (Figure 2.2, b). Urea is a polar group which improves the hard segment content by increasing hydrogen bonding (weak interchain forces) in the foam polymer network.

(Chattopadhyay et al., 2006). The release in enthalpy of the reaction between water and isocyanate is twice that of the polyaddition of isocyanate and hydroxyl groups.

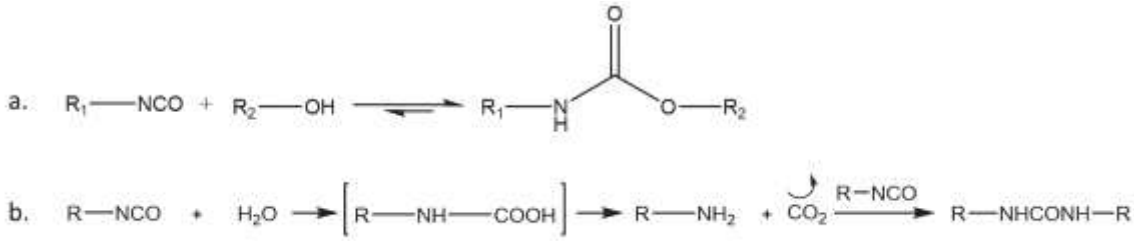

Figure 2.2:Reaction of Isocyanate with a. hydroxyl function to form urethane group, b. water to obtain urea and carbon dioxide released

Polyol polyethers represent 75% of the polyols used for PUF formulation with high hydrolysis resistance. However, polyesters polyols are used as they are highly thermally and oxidatively resistant. Polyol polyethers generally result from a alkoxylation reaction of a starter polyol (e.g. glycerol, sorbitol, sucrose). Polyester polyols are conventionally obtained by ring opening polymerization or by polycondensation between dicarboxylic acid with polyols in excess to ensure a high conversion of the diacid (Desroches et al., 2012). Polyether polyols represented a worldwide consumption of 4.5 million tons against only 0.9 million tons for polyester polyols, in 2000 (Randall and Lee, 2002). The annual global production capacities of the polyols for PUs have been recently estimated (2017) at 11, 2.2 and 0.2 million tons for polyether, polyester and biobased polyol, respectively ("D.Kyriacos, Polyols for PU. All producers and plant capacities. June 2017. ISBN 9789078546313,"). Polyester polyol consumption is growing at a rate of 4-5% per year due to their specific properties such as outstanding abrasion resistance (used e.g. in surface coating or footwear) (Randall and Lee, 2002).

More and more often PUs are biobased since polyols are becoming increasingly derived from renewable resources like sorbitol or glycerol, which are quoted in the Top 12 added value chemicals from biomass (determined by the U.S department of energy in 2004) (T.Werpy, 2004) or, more recently (2010), in an updated list (Bozell and Petersen, 2010) . Sorbitol and glycerol main properties and costs have been compared in Table SI 4 (in Annex) (Zhang et al., 2013; He et al., 2017; Aniceto et al., 2012). These two basic polyols present similar OH values which make them very complementary. Sorbitol can be compared as the equivalent of two glycerols in terms of functionality and molar mass.

As other basic polyols, sorbitol or glycerol are common starters for alkoxylation to synthesize suitable polyether polyols[8] due to their respective properties and low costs (Bozell and Petersen, 2010). The resulting biobased contents are then very low, around 30% for the polyether polyol and consequently 10% for the final corresponding PUs (Desroches et al., 2012). Besides, propylene oxide used for alkoxylation reaction, is highly toxic and the process implies high pressure and temperature (T.Werpy, 2004) which are major drawbacks with regards to energy savings and safety. Moreover, the chemical architecture of the obtained polyethers are not always fully controlled since all the available OH groups from the starter molecule are not obligatorily incorporated into the chemical modification (Arbenz and Avérous, 2014).

In the past, glycerol was mainly a by-product of the oleochemistry and biofuel transformation with a strong need of valorization (Mushrush and Hardy, 1998; Nanda et al., 2016; Stelmachowski et al., 2014). But nowadays, glycerol is a major chemical, in the core of different processes and (bio)synthesis for a very large range of applications ("Utilization of glycerol, a by-product of the transesterification process of vegetable oils: A review,".). Its strong demand leads to volatile pricing (Quispe et al., 2013) with now some short and partial unavailability. On the contrary, sorbitol is less

used and presents an extensively growing production from 5×10^5 tons (2010) to 6.5×10^5 tons (2013) (Kobayashi et al., 2014). Thus, sorbitol shows great promise for new means of valorization.

The current feedstock of sorbitol is starch, transformed through an aminolysis reaction and hydrogenation process (Zhang et al., 2013). Several new ways of production have been developed, especially from cellulosic material, which does not compete with food consumption (Kobayashi et al., 2011, 2013; Ribeiro et al., 2017; Yamaguchi et al., 2016). Sorbitol has been previously used to prepare PUs from sorbitol branched polyesters (Chang, 2002). Nevertheless the respective sorbitol content is rather low (2 wt% of the global composition). Sorbitol-based polyesters have also been reported with zinc acetate used as a catalyst at high temperature that reach 200°C (Anand et al., 2012). More recently, Gustini et al. (Gustini et al., 2015) synthetized sorbitol-based polyester polyol by enzymatic process at moderated temperature in range of 90 - 140°C. However, these final polyester polyols architectures present a low sorbitol content due the high polarity of the sorbitol (Gustini et al., 2015). Whereas, Gite et al.(Anand et al., 2016) developed a three step process to obtain polyester polyols with a high sorbitol content (27 mol% of the initial reactant) compared to previous cited works. Nevertheless, the final polyester polyols do not seem to be suitable for PUF foams production due to their high molar masses and then high viscosity at room temperature. All these sorbitol-based polyester polyols were developed for PUs coating applications. Recently, growing attention has been observed on the development of specific high resilient and antimicrobial PUF (Adnan et al., 2017; Udabe et al., 2017). For that, several biobased polyols were obtained from various renewable resources such as rapeseed oil, linseed, olive stone, crude glycerol, castor oil, microalgae or tannin to elaborate PUF and modified PUF (Arbenz et al., 2016; Hejna et al., 2017a; Matos et al., 2010; Prociak et al., 2017; Sharmin et al., 2017). Nevertheless, to the best of our knowledge, no recent published work deals with the transformation of crystalline sorbitol into low viscosity polyester polyol for PUF elaboration.

The aim of this work was to globally redesign the conventional approach in obtaining PUF, using sorbitol as an initial renewable compound. The main goal is to replace conventional polyether polyols, obtained from a harmful and unsafe alkoxylation process, while increasing the final biobased content of PUF. Furthermore, the polyol was synthesized in order to avoid side reactions, catalyzers and to be easily scaled up. The starting point is to transform the solid and crystalline sorbitol into a low viscous liquid from fully renewable polyester polyols. Based on esterification reactions, sorbitol was reacted with adipic acid and several potentially biobased and basic diols (from C2 to C12) to evaluate their impact on the properties of the resulting polyesters polyols. One of the original aspects of the polyester polyol synthesis was to focus the reaction only on the primary OH groups of the sorbitol in order to obtain linear polyesters polyols. The second part of this work was devoted to the elaboration of PUF based on the most suitable polyester polyol. Different PUF were prepared with a partial substitution (up to 75wt%) of a conventional polyether polyol (low biobased content), using the synthesized and fully renewable polyester polyol. The effects of various blowing agent systems, based on chemical (water), physical (isopentane) or dual blowing system (mix) were evaluated from the PUF properties.

Experimental part

Materials

Sorbitol was kindly provided by Tereos (Meritol, 98%, water content < 0.5%, reducing sugar content < 0.1%). Sorbitol was obtained from a process based on starch aminolysis. 1,2-ethanediol (1,2 ETH) (99.5%,) 1,4-butanediol (1,4 BDO) (99%), 1,6-hexanediol (1,6 HEX) (97%), 1,10-decanediol 1,10 DEC (98%), 1,12-dodecanediol (1,12 DD) (99%), deuterated dimethyl sulfoxide (DMSO-d_6) (99,9%),

and 2-chloro-4,4,5,5-tetramethyl-1,3,2-dioxaphospholane (Cl-TDP, 95%) were obtained from Sigma Aldrich. 1,8 octanediol (1,8 OCT) (98%), glycerol (GLY) (99%) were obtained from Fluka. 1,3 propanediol (1,3 PROP) (98%,) was obtained from Alfa Aesar. Adipic acid (AA) (99%) was obtained from Acros Organics. Succinic acid (SA) (99%) was obtained from BioAmber (France). SA was bio-produced by the fermentation of glucose (from wheat or corn) and obtained after a multistep process based on several purification, evaporation and crystallization stages. All diols were used without further purification. Sorbitol, AA and SA were dried one night in a vacuum oven at 45 °C and then stored in a desiccator under vacuum.

The polyether polyol was an oxypropylated polyol from Huntsman (Daltolac® R570), with an average functionality of 3.0 and an OH-value of 570 mg KOH/g and biobased content of around 30%. The polyisocyanate was polymeric 4,4'-methylenebis(phenyl isocyanate) (pMDI), N,N-Dimethylcyclohexylamine (DMCHA) from BorsodChem (Ongronat 2500) was the catalyst. The flame retardant was Tris (1-chloro-2-propyl) phosphate (TCPP) from Shekoy. The surfactant was polydimethylsiloxane from Evonik (B84501). Isopentane from Inventec was used as a physical blowing agent.

Methods

^{1}H- and ^{13}C-NMR spectra were performed with a Bruker 400 MHz. Deuterated dimethyl sulfoxide (DMSO-d_6) was used as solvent to prepare sample solutions at concentrations of 8-10 and 20-30 mg/mL for ^{1}H-NMR and ^{13}C-NMR, respectively. The number of scans was set to 128 for ^{1}H-NMR and at least 2048 for ^{13}C-NMR. The calibration of ^{1}H- and ^{13}C-NMR spectra was performed using the DMSO peak at 2.50 and 39.52 ppm, respectively. Water molecules present in DMSO-d_6 induced a supplementary peak in ^{1}H-NMR spectra at 3.33 ppm.

^{1}H-NMR were also used for the determination of the extent of the reaction by comparing the intensity of hydroxyl protons in the alpha position (α) from an ester group and in α of an acid end-group at δ = 2.29 ppm and δ = 2.20 ppm, respectively. The extent of the reaction is calculated using Equation 1.

$$Average\ acidic\ function = \frac{I_{2.2ppm}}{I_{2.29ppm}} \quad (1)$$

Where $I_{2.2ppm}$ and $I_{2.29ppm}$ represent the integral of the corresponding triplet.

^{31}P-NMR analysis were performed with a Bruker 400 MHz spectrophotometer after phosphitylation of the sample with 2-chloro-4,4,5,5-tetramethyl-1,3,2-dioxaphospholane according to standard protocols (Argyropoulos, 1995; Dais and Spyros, 2007, p. 45), the number of scans was set to 128 at 25°C. Peak analysis and quantitative analysis were performed according to previous reports (Granata and Argyropoulos, 1995).

Differential scanning calorimetry (DSC) was performed on a TA Instrument Q200 under nitrogen flux (50 mL/min). Samples of 1-3 mg were sealed in hermetic aluminum pans and analyzed using cyclic procedure involving an heating ramp from -80 to 160 °C at 10 °C/min, a cooling ramp down to -80 °C at 5 °C/min, then a second heating to 160 °C at 10 °C/min. Between each ramp, the temperature was hold for 2 min for stabilization.

Thermogravimetric analyses (TGA) were performed using a TA Instrument Hi-Res TGA Q5000 under argon (flow rate 25 mL/min) and/or reconstituted air (flow rate 25 mL/min). Sample of 1-3 mg were heated from room temperature to 600 °C (10 °C/min). The main characteristic degradation temperatures ($T_{deg,max}$) are those determined at the maximum of the weight loss derivative curve (DTG).

Infrared spectroscopy was performed with a Fourier transformed infrared spectrometer Nicolet 380 used in reflection mode equipped with an ATR diamond module (FTIR-ATR). An atmospheric background was collected before each sample analysis (32 scans, resolution 4 cm^{-1}).

Hydroxyl value (I_{OH}) was determined by esterification method using a 1M solution of phthalic anhydride in pyridine (ASTM 4274-99). 0.8 g of polyol were heated under reflux with 20 mL of phthalic anhydride solution for 45 minutes and cooled at room temperature. Then 10 mL of pyridine were added from the top of the reflux to collect all reactions products. Lastly 20mL of pyridine and 30 mL of water were added. The solution was titrated with 1M sodium hydroxide (NaOH) solution using an automatic titrating device (TitroLine 7000, SI Analytics**).** Hydroxyl index (I_{OH}) was determined in mg of $KOH.g^{-1}$, as described in Equation 2.

$$I_{OH} = \frac{((V_{blank} - V_s) * C * 56.1)}{W_s} \quad (2)$$

Where V_{blank} (mL) and V_S (mL) are the volumes of NaOH solution required for blank and polyol sample titrations, respectively. C ($mol.L^{-1}$) is the NaOH solution concentration and W_S (g) is the polyol weight.

Acid value (AV) was determined by traditional colorimetric method. 0.1 g of polyol was dissolved in 10 mL of methanol (MeOH), one drop of bromothymol blue solution (0.01 mmol/L in MeOH) was added to the polyol solution. Then titration was performed with 0.1M NaOH solution. AV is express in mg of $KOH.g^{-1}$ according to Equation 3.

$$AV = \frac{(V_{eq} * C) * 56.1}{Ws} \quad (3)$$

Where V_{eq} (mL) is the titration equivalent volume, C ($mol.L^{-1}$) is the NaOH solution concentration and W_s (g) is the polyol weight.

Dynamics viscosity was determined using an Anton Paar Physica MCR 301 rheometer device equipped with Peltier system and 50 mm diameter cone plate geometry (1.009°). Viscosity was measured at constant shear rate (10 s^{-1}) with a temperature range between 10 and 50 °C for viscous polyol at room temperature and up to 90 °C for solid one. Then, temperature was set to 20 and 25 °C to measured viscosity in function of shear rate from 0.001 to 100 s^{-1}.

Foams temperature, expansion heights and rate, density and pressure were recorded using a Foamat FPM 150 (Messtechnik GmbH) equipped with cylindrical recipient, 180 mm in height and 150 mm in diameter, an ultrasonic probe LR 2-40 PFT recording foaming rate and foam height, a NiCr/Ni type K thermocouple and a pressure sensor FPM 150. The data were recorded and analyzed using the *"Mouse" (Foam)* software.

Close cell content was determined using an Ultrapyc 1200e from Quantachrome instruments based on the technique of gas expansion (Boyle's law). Foams cubic samples (roughly2.5 cm × 2.5 cm × 2.5 cm) were cut for the first measurement then the sample was sectioned once more into eight pieces and measurement was re-run to correct the closed cells content based on close cells which were cut open during the trisecting.

Polyester polyol synthesis

A two-step synthesis was performed in a three-neck round bottom flask equipped with a distillation bridge and a gas inlet. The flask was charged with one molar equivalent sorbitol and two molar equivalents of diacids (*Table 2.1*, entries 1-2, 4-8). The mixture was stirred and heated to 150 °C for three hours. During the second step, two molar equivalents of each diol based on ending OH groups

(*Table 2.1*, entries 1-2, 4-8) were introduced to complete the reaction within 6 additional hours. The system was purged under vacuum after 5 or 7 h during 1 or 2 min, respectively, in order to remove the produced water to increase the reaction yield. Then, the corresponding products were analyzed.

Table 2.1: Synthesis of polyester polyols with the corresponding designations and the formulations.

Entry	Initials monomers	Terminal Diol	Polyester polyol designation
1	Sorbitol + AA	1,2 ETH (C2)	EASAE
2		1,3 PROP (C3)	PASAP
3		1,4 BDO (C4)	BASAB
4		1,6 HEX (C6)	HASAH
5		1,8 OCT (C8)	OASAO
6		1,10 DEC (C10)	DASAD
7		1,12 DD (C12)	DoASADo
8	Sorbitol + SA	1,4 BDO (C4)	BSASSAB

The synthesis was performed in a three-neck 250 mL glass. However, to obtain PUF in large quantity, BASAB polyester polyol (*Table 2.1*, entry 3) was synthesized into a 600 mL inox reactor according to the same protocol. In this case, 1,4 BDO quantity was adapted to 2.1 molar equivalent to compensate the potential loss of reactant and the self-condensation into tetrahydrofuran (Hu et al., 2010).

To control and decrease the acidic value, the synthesized polyols were neutralized using potassium hydroxide (KOH) after acidic titration. The KOH amount equivalent to the AV was previously dissolved in 100 mL flask that was filled with ethanol (EtOH) and stirred until complete KOH dissolution. In the meantime, the 600 mL inox reactor was heated at 60 °C to decrease the polyol viscosity. Under high stirring, the KOH solution was added and the system was maintained to 60 °C under high stirring for 2 h. Then EtOH was removed by vacuum distillation and the polyol was dried under vacuum over night at 45 °C.

Detailed foam processing

Different PUF were prepared with different ratio of BASAB, conventional polyether polyol which are partially fossil-based and neat short polyols e.g. sorbitol and glycerol. The pMDI was chosen as polyisocyanate due to the iso-reactivity of the isocyanate groups of the corresponding MDI. Chemical and physical blowing agent have been used, water and isopentane, respectively.

The different studied PUF formulations are presented in Table 2.2. The isocyanate/hydroxyl molar ratio (NCO/OH) was kept constant at 1.15 in all PUF formulation. Within this ratio, all the reactive OH groups were taken into account (including those of water). All other components were kept constant in proportion for each formulation. The pre-mix contains the polyols (100 parts), 2 parts of catalysts (DMCHA), 2 parts of surfactants (B84501), 10 parts of flame-retardant (TCPP), and the corresponding blowing agents (isopentane and / or water) were adjusted to kept the same blowing rate for each foams formulation (Table 2.2). The mixture was mechanically stirred until the obtaining of a fine white emulsion with the addition of the blowing agent. Separately, the temperatures of this mixture and the polyisocyanate (f = 2,8) were adjusted to 20 °C. The polyisocyanate is quickly added to the emulsion. The reactive mixture was vigorously stirred for 5 s and the foam was obtained (i) in an open 250 mL disposable beaker at room temperature (controlled to 20 °C) to follow the foam kinetic (Arbenz et al., 2016), or (ii) in a Foamat device.

Table 2.2: PUF formulations in wt. % and in parts to the total polyol content, with the final estimated biobased contents, the kinetic results, the Foamat data the and closed cell content

	Name	REF (Reference)	PUF 1	PUF 2	PUF 3	PUF 4	PUF5	PUF 6	PUF 7	PUF 8	PUF 9
Formulation	BASAB	0	0	85	85	25	50	75	60	80	90
	Polyether Polyol	100	100	0	0	75	50	25	0	0	0
	Neat glycerol	0	0	10	10	0	0	0	40	20	10
	Neat sorbitol	0	0	5	5	0	0	0	0	0	0
	Total polyols content	100	100	100	100	100	100	100	100	100	100
	Water	1.6	4.1	8.6	4.1	1.6	1.6	1.6	1.6	1.6	1.6
	Isopentane	15	7.4	0	13.2	14.3	13.7	12.9	23.3	17.8	15
Bio-based content	Biobased content of the total polyols (%)	30	30	100	100	48	65	83	100	100	100
	Foam biobased content (%)	9	8	22	26	15	22	28	22	27	31
Foam characteristic times	Cream time (s)	10	16	30	16	7	8	9	14	11	10
	Gel time (s)	40	35	60	90	38	45	40	74	70	70
	Tack free time (s)	66	62	235	210	50	55	100	91	107	120
Foamat records	Maximum rate (mm/s)	5	7.6	6.8	5.9	8.25	7.5	6.0	4.5	4.9	4.6
	Tmax (°C)	175	187	159	171	186	172	161	176	172	163
	Pmax (kPa)	4.7	10.6	11.8	3.4	19.9	3.6	0.9	7.7	3	1.3
	Density (g/L)	29.7	30.2	26.6	24.8	30	27.9	31.1	32.2	30.4	30.7
Close cells content (%)		95	92	35	15	69	14	4	4	2	3

Results and discussion

Synthesis and characterization of polyester polyols

The two-step synthesis yields a linear polyester polyol. The steric hindrance of sorbitol secondary OH and their lower reactivity compared to primary ones are key parameters to obtain linear structures. The corresponding structures have terminal carboxylic acid ending groups at the end of first synthesis step, or OH groups at the end of the second synthesis step as illustrated in Figure 2.3.

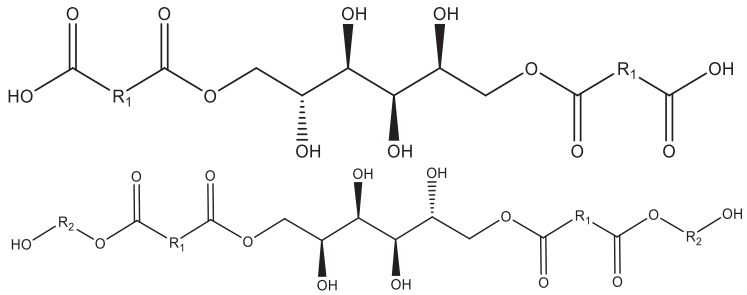

Figure 2.3: Structures of the sorbitol- based polyesters at the end of the first synthesis step (on the top) and at the end of the two-step reactions (on the bottom) with R_1 from C5 to C6, and R_2 from C2 to C12

In Figure 2.4, a FTIR spectrum of the intermediate product obtained after 3 h of the reaction exhibits the characteristic peaks of the reactional intermediate such as the large associated O-H stretching band at 3,400 cm^{-1} related to the different and preserved secondary OH from the initial sorbitol. Two signals are observed at 2,948 and 2,877 cm^{-1} and are assigned to the C-H symmetric and C-H asymmetric stretching vibration, respectively. The strong peak for C=O stretch of acidic ends groups appear at 1,693 cm^{-1}. Moreover, the C=O stretching band has a shoulder on the left side demonstrating the

presence of C=O stretch from ester linkage between sorbitol and diacids. These observations are in agreement with the expected structure, i.e. a molecule with ending carboxyl acids groups. Following the second reaction step, the C=O signal is now narrow and centered on 1,727 cm^{-1} corresponding to the C=O stretch from ester linkage. This is in agreement with the second step of the esterification process which involved the consumption of the previously available carboxyl acids groups.

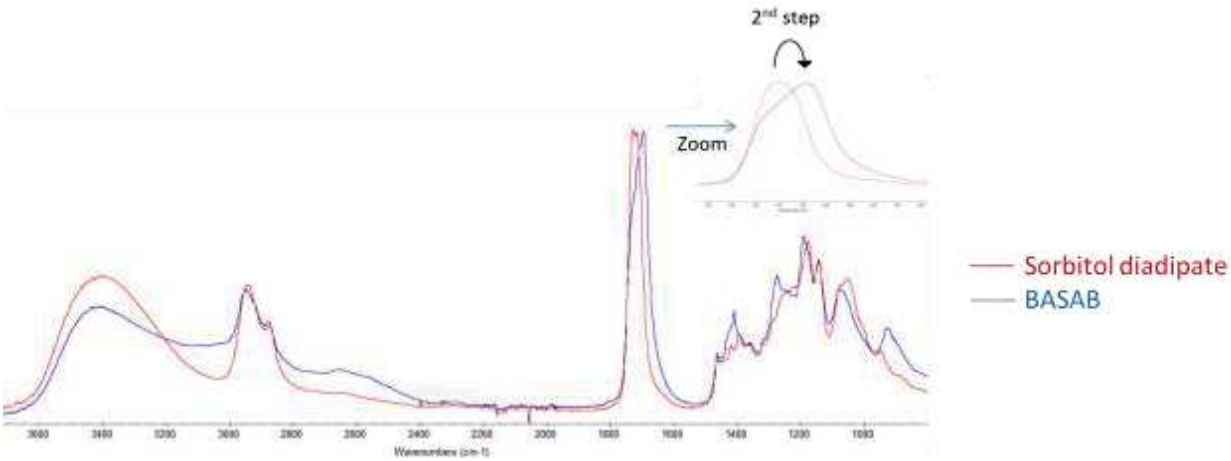

Figure 2.4 : FTIR spectra of the reactional intermediate and the final polyester polyol (Table 1, entry 3 at the end of the first synthesis step and final product

^{1}H-NMR spectra's are presented in the supporting information (*Figure SI 2* to Figure SI 8, in Annex). The signals attributions of the reactional intermediate are shown (*Figure SI 1*, in Annex). After the first reactional step, the average free acidic functions are of 56% (obtained using Equation 1). Then, this value drops to 16% after the second step of the reaction (*Figure SI 2* toFigure SI 8, in Annex). Table SI 5 shows the detailed yield for each polyester polyol synthesis. As expected, by the end of the first step, almost half of the acidic functions are consumed. The second step of the esterification efficiently increases the average content in agreement of ester function with the previous results from FTIR.^{13}C-NMR (Figure SI 9 to Figure SI 15, in Annex) of each polyester polyols shows the carbonyl linked to AA, the carbonyl of the ester linkage and the methylene carbons in α and β of the AA building blocks with ester linkage located at δ = 174.4, 172.9, 33.4 and 24.0 ppm, respectively. The signal of the sorbitol carbons bearing secondary OH groups are still visible but they become weaker, for each polyester polyol. Sorbitol signal intensity is lower as its concentration is weaker than the carbons from AA and 1,4 BDO. Only the two sorbitol carbons in α of the ester linkage exhibit a clear signal around δ = 62 ppm. ^{13}C-NMR spectra of sorbitol, AA, SA and reactional intermediate are presented in SI (Figure SI 16 to Figure SI 19, in Annex). ^{13}C-NMR of intermediate and final products permitted a clear identification of the carbonated structure in agreement with the expected products presented in Figure 2.3 and previous FT-IR observations.

^{31}P-NMR was performed with Cl-TDP as phospholane reagent. ^{31}P-NMR spectra and quantification results are available in Figure SI 20 to Figure SI 26 and Table SI 6 (in Annex). Phospilated product clearly indicated two strong signals linked to the OH area (145.5-149.5 ppm), except when 1,12 DD was used as a terminal diol. We assumed that the presence of two strong peaks is related to the primary OH. The strong signal of 1,12 DD corresponds to OH end groups in polyester, as already observed by Gustini *and al*. (Gustini et al., 2015). This phenomenon is due to the carbonated chain length of the 1,12 DD. The terminal OH groups are well separated from the ester linkage or from the available secondary OH, leading to a single signal. Table 3 shows the OH values determined from ^{31}P-NMR and the theoretical IOH. Theoretical IOH was determined from an ideal linear structure of a synthesized polyester polyol taking into account the polycondensation of the different initial

chemicals. ^{31}P-NMR seems to be an accurate way to determine the global IOH. The values of the global IOH determined from ^{31}P-NMR results are within a 5% difference of the theoretical IOH and then confirm the linear structure of the polyester. The Cl-TDP is used as a reagent, reacting with the primary and secondary OH groups as well as with carboxylic acid end-groups. Normally, in the case of the analysis of the aliphatic OH groups, 2-chloro-1.3.2-dioxaphospholane (phospholane reagent) is preferred to quantify primary and secondary OH since their respective signals can be separated in clear and distinct areas (Granata and Argyropoulos, 1995). But this reagent is highly sensitive to residual acid undergoing a fast degradation of the phophislated complex. Then the corresponding quantification is rather difficult to be performed, as reported in previous publications (Korntner et al., 2015). To avoid any deviance in the OH quantification, we decided exclusively to work with Cl-TDP to obtain an accurate global IOH.

Table 2.3 : IOH and AV data from the biobased polyester polyols

n.d. = not determined

Biobased polyester polyol	Theoretical IOH (mg KOH/g)	IOH determined from ^{31}P-NMR (mg KOH/g)	Titrated IOH (mg KOH/g)	AV determined from ^{31}P-NMR (mg KOH/g)	Titrated AV (mg KOH/g)
EASAE	640	634	347 ± 9	34	67 ± 3
PASAP	608	629	426 ± 19	22	58 ± 2
BASAB	578	574	382 ± 9	49	56 ± 1
HASAH	526	507	406 ±17	15	41 ± 1
OASAO	485	461	362 ±14	15	33 ± 1
DASAD	449	440	n.d.	12	34 ± 1
DoASADo	416	556	n.d.	11	38 ± 1
BSASSAB	640	683	409 ± 14	34	51 ± 14

OH titrations of the different synthesized polyester polyols were performed and can be compared with results obtained from ^{31}P-NMR data (Table 2.3). As expected, the IOH decreases when the diol chain length increases. However, results obtained from this method are very different from the ones determined by ^{31}P-NMR. The titration method is based on an esterification reaction with anhydride phthalic acid in pyridine. The use of anhydride phthalic could lead to transesterifications reactions, however this hypothesis can be justified since the corresponding formation of smaller diols should increases the IOH. Besides, these reactions are generally taking place at higher temperature in presence of metallic based catalyst. A more accurate hypothesis is the steric hindrance linked to the secondary OH from the sorbitol building block. To validate or not this hypothesis, neat sorbitol has been analyzed by this titration method. Theoretically sorbitol IOH value is 1847.7mg KOH/g against 1528.8 mg KOH/g obtained by titration, which means a maximum of only 5 OH equivalent functions for a neat sorbitol. Regarding to titration results (Table 2.3) it clearly appears that the phenomenon is amplified with the shortest polyesters polyols like EASAE, PASAP and BASAB. The steric hindrance and the numerous secondary OH are strong limitations for this titration method. Then ^{31}P-NMR seems to be a more accurate method due to the high reactivity of the phosphorous reagent which reacts on all the secondary and primary OH according to previous observations.

Table 2.3 shows AV data of polyester polyols and the results show a small amount of residual acidicity of 33-67 mg KOH/g, in agreement with previously determined reaction yields. Whereas AV determined by ^{31}P-NMR were range in 11 to 49 mg KOH/g, which is not in agreement with the titrated results.

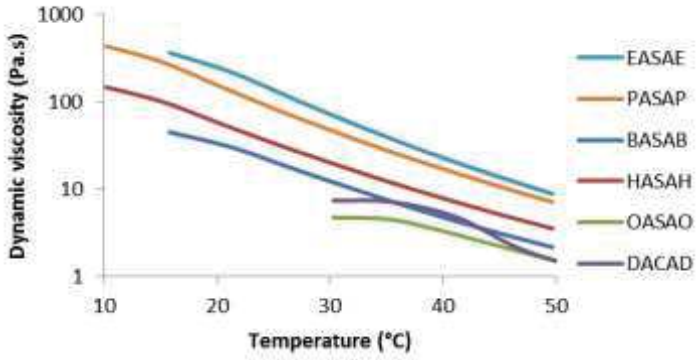

Figure 2.5: Polyester polyols dynamic viscosity in function of temperature

Figure 2.5 shows the evolution of the viscosity of the polyol as a function of temperature, at constant shear rate (10 s^{-1}). DoASADo, a waxy product at room temperature, with a melting point of 40 °C (Table 2.4) is not presented. Very high viscosities were obtained with OASAO and DACAD prior to 30 °C. In these cases, the evolutions of these viscosities have been determined after 30 °C. The analyzed polyester polyols present a fast viscosity decrease with the temperature due to their small chain lengths.

According to the literature, it is favorable that at room temperature, the polyol dynamic viscosity stays under 50 Pa.s for the foaming process (Ionescu, 2005). Then, DoASADo, OASAO and DACAD are not suitable and their behaviors will not be further investigated.

Figure SI 27 (in Annex) shows the polyol viscosity at 20 and 25 °C with a shear rate range from 0.01 to 100 s^{-1}. HASAH and BASAB show a Newtonian behavior in this shear rate and temperature range. BASAB has the lowest viscosity at both temperatures. HASAH and BASAB average viscosities are 48 and 28 Pa.s, respectively at 20 °C and their viscosities drop to 28 Pa.s and 17 Pa.s with a temperature increase from 20 to 25 °C, respectively. Since the difference of the chain lengths between these polyester polyols is negligible, the lowest viscosity of BASAB is mainly due to a plasticizing effect of the residual monomers with low viscosity (1.4 BDO). At contrario, residual HASAH monomer (1.6 HEX) is solid at 20 and 25 °C (Tm= 40 °C).

TGA analyses were performed to evaluate the weight loss of the polyol as a function of the temperature. Results are shown in Table 2.4. TGA curve of BASAB is given in Figure SI 28 (in Annex). All polyester polyols exhibit a first weight loss of 7-19 wt% starting at 40-50 °C, due to the unreacted monomer from the esterification and residual water. When monomers chain length increases, the weight of loss is above 10 wt% with a temperature range up to 210 °C, as is the case for entries 4-7 of Table 4. A second series of weight losses corresponding to ester degradations by α- and β-hydrogen bond scissions (Figure SI 30, in Annex) occur at higher temperature till 450-500 °C. For polyester polyols of Table 4, entries 4-7, it can be excluded that α- and β-hydrogen bond scissions occurs at the end of the first degradation step. According to these TGA results, BASAB is a good partner to ensure the exothermicity of the PUF foaming process implying temperature up to 90 °C, before the complete polymerization of the polyols with the available isocyanates.

Table 2.4 : Thermal behavior of the polyester polyols

Entry	Polyol	TGA			DSC	
		1st loss of weight		2nd serie of weight losses	T_g (°C)	T_m (°C)
		Temperature range	Weight loss (wt%)	Temperature range (°C)		
1	EASAE	50-130	7	150-450	-25	n.o
2	PASAP	50-135	8	135-450	-27	n.o
3	BASAB	40-130	7	130-450	-48	n.o
4	HASAH	40-162	11	162-450	-53	n.o
5	OASAO	40-175	12	175-500	n.o.	23
6	DASAD	40-200	16	200-450	-75	0-40
7	DoASADo	40-210	19	210-475	n.o.	30-40
8	BSASSAB	40-160	9	125-500	-40	n.o

n.o.: not observed

According to TGA results, there are no major degradations for DSC analysis in the studied temperature range. Polyester polyol DSC analyses are summarized in Table 2.4. OASAO, DASAD and DoASADo present a melting temperature (T_m) above 20°C confirming their semi-crystalline structure, which also explained their waxy behavior at room temperature. However, EASAE, PASAP, BASAB, HASAH and BSASSAB are amorphous polyesters. The polyester polyols show a sole glass transition (T_g) below -25 °C, till -75 °C. DSC results show the impact of the terminal diol at the end of the chains. When C2 to C6-based diols are used the corresponding polyester polyols are amorphous. However, with longer diol, crystallinity can occur.

From these results, it is clearly established that BASAB is the most suitable polyol for foaming applications. Then, this polyester was neutralized with KOH to decrease the AV from 56 to 10 mg KOH/g. Neutralization purpose is to increase BASAB reactivity in reactive foaming process and inhibited the residual free carboxyl acid (Ionescu, 2005). The neutralization was the only way to decrease the residual acidity since the esterification yield cannot be improved by increasing the reaction time of the second reaction step. Undesired reactions can occur with the formation of a polymer network between the residual carboxyl groups and the available secondary OH, giving a stiff solid material when increasing the reactional time of the second step.

Study of the polyurethanes foams

Foams morphology:

Figure 2.6 displays SEM images of two foams with two opposite structures (close vs. open cells). A classical polyhedral shape cell structure is observed (Figure 2.6-a) of the REF with high closed cells content. Cells are mainly orientated according to the rise direction of the foam. The shape is strongly dependent on the mold or recipient shape (Hawkins, 2005; Patterson et al., 2014). The SEM image of PUF 2 (Figure 2.6-b) is a representative image with open cells that can be described as a porous network without cell walls and only struts are present.

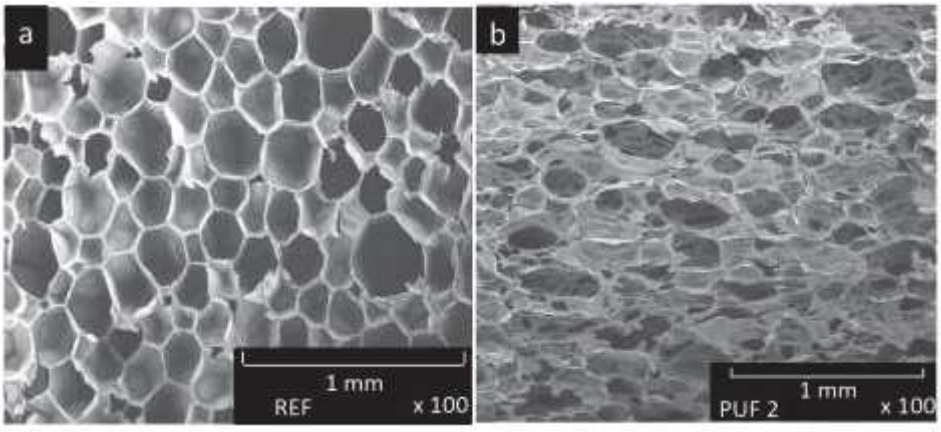

Figure 2.6: SEM images of PUF in the rise direction, a: close cell from the reference foam (REF). b: open cells from biobased PUF (PUF 2)

Study of the PUF kinetic

PUF kinetics were evaluated according to two different protocols. The first one is based on the determination of different conventional foam characteristic times such as the cream time (time of initiation of the isocyanate-water/polyol reaction), gel time and tack free time (Chuayjuljit et al., 2010; Septevani et al., 2015), respectively. The second method is based on a Foamat records.

Table 2.5 shows the results of the kinetics of the PUF formulated with un-neutralized and neutralized BASAB compared to the REF formulation (Table 2.2). The resulting kinetic of the foam made from un-neutralized BASAB is really long with a final tack free time 23 times longer than the REF and then, a small foam height (5 cm). Whereas the foams based on neutralized BASAB have similar kinetic than the REF (foam height: 17 cm). Foaming is an exothermic process due to different and concomitant or successive mechanisms. When un-neutralized BASAB is used, the blowing agent is vaporized prior to the foam structuration by polymerization with the elaboration of the PUs network. This low rate of polymerization is due to the polyol residual acidity which inhibits the effect of the catalyst by forming ammonium salts (Silva and Bordado, 2004). To obtain suitable PUF, studies were then conducted using neutralized BASAB.

Table 2.5 : Foam characteristic time comparison between a reference and with un-neutralized and neutralized BASAB (Formulations are similar than the reference, see Table 2)

	Reference	With Un-neutralized BASAB	With Neutralized BASAB
Cream time (s)	10	75	7
Gel time (s)	44	408	30
Tack free time (s)	66	1500	62
Foam high (cm)	19	5	17

Comparison of different blowing systems

From the results presented on Table 2.2, a comparison of two different blowing agents, water and isopentane, can be done on REF and PUF 1 (mainly fossil-based foam), PUF 2 and PUF 3 (biobased foams). The ensuing foam characteristic times are available in Table 2.2. The increase of water content increases the cream time of 6 s, from REF to PUF 1, and 16 to 30 s, for PUF 3 and PUF 2, respectively. Gel time experiences the opposite effect, PUF 3 gel time is 30 s longer than PUF 2 gel time. Whereas, PUF 1 is 5 s lower than REF. The cream time and gel time are evolving similarly

regardless of the origin of the polyol (fossil-based vs biobased) when water was used. Water effects were more effective with biobased polyol.

Table 2.2 also shows the data from Foamat. The values of the REF, PUF 1 to PUF 3 indicate that water tends to increase the maximum foaming rates, pressures and density. All these observations are in agreement with previous kinetic observations. The longer cream times of PUF 1 and PUF 2 can be explained by the thermal capacity of water that prevents the temperature increase and thus delays the beginning of the polymerization. Once this delay has passed, the high exothermicity of the reaction between water and isocyanate explains the lowest time required in PUF 1 and PUF 2 to reach the gel time as the highest foaming rate, temperature and pressure. These results clearly show the effect of the blowing agent on the foam characteristic time and kinetic.

A comparison of biobased foams PUF 2 and PUF 3 (Table 2.2) highlights the impact of isopentane as a physical blowing agent. The foam gel time and the maximum rates of expansion strongly vary. PUF 3 gel time is 1.5 times higher than PUF 2. The maximum foams rates are 5.9 and 6.8 mm/s, respectively. The isopentane, decreases the reaction rate by delaying the increase in temperature of the foams because it has a lower boiling point (27 °C) than water (100 °C).

Effect of the addition of biobased polyester polyol:

Table 2.2 shows kinetic parameters of foam PUF 1 and PUF 3 with the same blowing system. The same cream time (16 s) was observed for both formulations. But the gel time was 2.6 times longer and the tack free time was 3.4 times longer for PUF 3. The same effects were observed on the maximum rate of the expansion, on the temperature of foaming which clearly indicates a lowest reactivity of the biobased formulation PUF 3 compare to the mainly fossil-based PUF 1. The lowest reactivity of biobased polyols has already been observed in the literature. It is mainly caused by the presence of secondary hydroxyls (Chuayjuljit et al., 2010; Hu et al., 2002; Narine et al., 2007a; Septevani et al., 2015) . Besides, BASAB secondary hydroxyls are not close to the end of the chains and are then subject to high steric hindrance, compared to the secondary hydroxyls of the oxypropylated polyester.

Some foams, PUF 4 to PUF 6, were formulated with a partial substitution of the polyether polyol by the biobased BASAB polyester polyol (Polyether/BASAB (%wt/%wt): 75/25, 50/50, 25/50). Regarding the characteristic times and Foamat records from Table 2.2, it seems obvious that the increase of the BASAB content from 25 to 75wt% increases the cream time from 7 to 9 s and doubles the tack free time to reach 100 s. The foaming temperature decreases by 10 °C for each increment of 25wt% of BASAB incorporated. The pressure of the foam decreases from 19.9 to 0.9 kPa and the close cells content drops from 69 to 4% when the substitution rate increase from 25 to 75wt%. The cream times of PUF 4 to 6 are lower than REF. The partial substitution of the polyether polyol by the BASAB is effective to compensate its previously observed lowest reactivity up 50 wt%. It has to be mentioned that the tack free time increases with the biobased polyol content. As already described by Abdel Hakim et al. (Abdel Hakim et al., 2011) this tack free time increase is related to a longer time to cure the foams as a result of the lower reactivity of the secondary hydroxyl from the biobased polyol. This slower kinetic is responsible for the low level of closed cells of PUF 6 due to cell walls collapse with expansion. Only the strut structures of the foam are maintained (Andersons et al., 2016).

PUF 7 to PUF 9 (Table 2.2) were formulated with different ratios of biobased BASAB polyester polyol and glycerol. The glycerol content was 40, 20 and 10 wt% of the polyol total content for PUF 7, PUF 8 and PUF 9, respectively. PUF 8 and 9 present the same cream and gel times but the tack free time of PUF 8 is 13 s faster than PUF 9 ‘one. The foaming maximal temperature of PUF 9 is 10 °C lower than PUF 8. This is linked to the longer tack free time. Then, for PUF 7 the cream and gel times

are above the ones of PUF 8 whereas the tack free time is faster of 16 s. The same foaming temperatures are reach. Foamat records (Table 2.2) show a weak influence of the increasing glycerol content on the foaming rate, with only an increase of the density for PUF 7. The highest glycerol content, a short basic polyol compared to the BASAB polyester polyol, leads to a densification of the network. We can conclude that the glycerol (with one secondary hydroxyl against 4 groups for the BASAB) decreases the foam tack free time, due to a global increase in primary hydroxyl groups content, in the formulation (Septevani et al., 2015; Tan et al., 2011b).

Finally, the high content of open cells is a strong indication of weak cell walls that are broken when the blowing agent expands. This is mainly due to the long gel times of these foams (compared to REF). Prior or near the gel time cell struts can handle the foam weight, whereas the fine cell walls cannot stand the overpressure of the gas.

Biobased contents of the polyesters and foams:

Table 2.2 shows the final biobased content of the polyester poyols and foams. They are in a range of 30 to 100% for the polyester poyols and 9 to 31% for the foams. The REF-based foam has a low biobased content of 9% since the PUF 1 foam with a formulation similar to the REF has a lower final biobased content (8%). This difference is due to the water used as chemical blowing agent, which reacts with isocyanate (Figure 2.2, b). To compensate this consumption, the foam formulation required a higher polyisocyanate content to maintain the NCO/OH ratio at 1.15, reducing then the final biobased content of the foam. PUF 7 and PUF 9 are foams obtained with isopentane and are both based on a polyol with a biobased content of 100%. However, the corresponding foams biobased content are only 22 and 31%, respectively. PUF 7 and PUF 9 have been formulated with 40 and 10wt% of glycerol, respectively. The hydroxyl density is higher for glycerol than for BASAB polyester polyol. Then PUF7 required a higher polyisocyanate content in the initial formulation, decreasing the final biobased foam content. These different examples illustrate the clear impact of the formulation and the choice of blowing agent on the final biobased content of the PUF.

Conclusion

We successfully synthetized a range of biobased polyols from sorbitol specifically design for PUs synthesis. It has been demonstrated that sorbitol can be easily transformed into a low viscosity polyol while using very simple, safe and harmless chemical pathway based only on renewable building blocks to substitute polyether polyols from a more traditional chemistry. The most promising polyester polyol was obtained from sorbitol, adipic acid and 1,4-butanediol. This sorbitol-based polyol present an average IOH and viscosity of 574 mg KOH/g and 17 Pa.s (at 25 °C), respectively. These properties specifically match for the elaboration of advanced PUF. The partial or full substitution of the traditional polyether polyols by this promising polyol largely increased the final biobased content of PUF. The study of the kinetics of foaming was investigated and the effect of the blowing agent or the type of polyol were apprehended. They demonstrated to be key parameters to monitor the foam cream time and tack free time. The cream times of the biobased foams have been decrease of 33 % with the chemical blowing agent. Whereas the tack free time decrease from 120 to 91 s for a glycerol content from 10 to 40 wt% of the polyol blend. These results can be positively compared to the conventional approach based on the variation of the catalyst content. The corresponding biobased PUF were principally based on open cells (till 92%) and low density (30 g/L).

These biobased PUF should fulfill the requirements for a wide range of applications from furniture to building thermal or acoustic insulation. The foams structures let presume some unexpected mechanical

behaviors which will be investigated in our further work. In order to develop some applications, different studies need to be explored such as the behavior of these foams under climate ageing.

A lot of phenomena and observations cannot be fully explained and must be deeply considered in a close future. Foams are very complex systems, especially the foaming step which implied several successive and parallel mechanisms linked to a great number of parameters. The links between formulation, kinetic and final properties such a mechanical behavior for these PUF need to be more deeply investigated. Besides, the degradation-aging and the potential ends of life of these foams could be also analyzed.

Acknowledgements

The authors thank Dr. Alexandru Sarbu and Vincent Barraud (Soprema, France) for helpful discussions. They are grateful to Isabelle Dhenin (Soprema, France) for her technical assistance and to Pacôme Tomietto from University of Strasbourg for his contribution to BASAB synthesis. The authors also thank Kim Tremblay Parrado for the English corrections. This work has received funding from Alsace Region, Eurometropole and BPI-France.

References

Abdel Hakim, A.A., Nassar, M., Emam, A., Sultan, M., 2011. Mater. Chem. Phys. 129, 301–307.

Adnan, S., Tuan Noor, M.T.I., 'Ain, N.H., Devi, K.P.P., Mohd, N.S., Shoot Kian, Y., Idris, Z.B., Campara, I., Schiffman, C.M., Pietrzyk, K., Sendijarevic, V., Sendijarevic, I., 2017. J. Appl. Polym. Sci. 134, 45440.

Anand, A., Kulkarni, R.D., Gite, V.V., 2012. Prog. Org. Coat. 74, 764–767.

Anand, A., Kulkarni, R.D., Patil, C.K., Gite, V.V., 2016. RSC Adv 6, 9843–9850.

Andersons, J., Kirpluks, M., Stiebra, L., Cabulis, U., 2016. Mater. Des. 92, 836–845.

Aniceto, J.P.S., Portugal, I., Silva, C.M., 2012. ChemSusChem 5, 1358–1368.

Arbenz, A., Avérous, L., 2014. RSC Adv 4, 61564–61572.

Arbenz, A., Frache, A., Cuttica, F., Avérous, L., 2016a. Polym. Degrad. Stab. 132, 62–68.

Argyropoulos, D.S., 1995. Res. Chem. Intermed. 21, 373–395.

Bozell, J.J., Petersen, G.R., 2010. Green Chem. 12, 539.

Chang, W.L., 2002. Polyurethane prepared from sorbitol-branched polyesters. Google Patents.

Chattopadhyay, D.K., Sreedhar, B., Raju, K.V.S.N., 2006. J. Polym. Sci. Part B Polym. Phys. 44, 102–118.

Chuayjuljit, S., Maungchareon, A., Saravari, O., 2010. J. Reinf. Plast. Compos. 29, 218–225.

Cornille, A., Auvergne, R., Figovsky, O., Boutevin, B., Caillol, S., 2017. Eur. Polym. J. 87, 535–552.

Dais, P., Spyros, A., 2007. Magn. Reson. Chem. 45, 367–377.

Desroches, M., Escouvois, M., Auvergne, R., Caillol, S., Boutevin, B., 2012. Polym. Rev. 52, 38–79.

D.Kyriacos, Polyols for PU. All producers and plant capacities. June 2017. ISBN 9789078546313.

Gandini, A., 2008. Macromolecules 41, 9491–9504.

Gandini, A., Lacerda, T.M., Carvalho, A.J.F., Trovatti, E., 2016. Chem. Rev. 116, 1637–1669.

Granata, A., Argyropoulos, D.S., 1995. J. Agric. Food Chem. 43, 1538–1544.

Gustini, L., Noordover, B.A.J., Gehrels, C., Dietz, C., Koning, C.E., 2015. Eur. Polym. J. 67, 459–475.

Hawkins, M.C., 2005. J. Cell. Plast. 41, 267–285.

He, Q. (Sophia), McNutt, J., Yang, J., 2017. Renew. Sustain. Energy Rev. 71, 63–76.

Hejna, A., Kirpluks, M., Kosmela, P., Cabulis, U., Haponiuk, J., Piszczyk, Ł., 2017. Ind. Crops Prod. 95, 113–125.

Hu, L., Wu, L., Song, F., Li, B.-G., 2010. Macromol. React. Eng. 4, 621–632.

Hu, Y.H., Gao, Y., Wang, D.N., Hu, C.P., Zu, S., Vanoverloop, L., Randall, D., 2002. J. Appl. Polym. Sci. 84, 591–597.

Ionescu, M., 2005. Chemistry and technology of polyols for polyurethanes. Rapra Technology, Shawbury, Shrewsbury, Shropshire, U.K.

Kattiyaboot, T., Thongpin, C., 2016. Energy Procedia 89, 177–185.

Kobayashi, H., Ito, Y., Komanoya, T., Hosaka, Y., Dhepe, P.L., Kasai, K., Hara, K., Fukuoka, A., 2011. Green Chem 13, 326–333.

Kobayashi, H., Yabushita, M., Komanoya, T., Hara, K., Fujita, I., Fukuoka, A., 2013. ACS Catal. 3, 581–587.

Kobayashi, H., Yamakoshi, Y., Hosaka, Y., Yabushita, M., Fukuoka, A., 2014. Catal. Today 226, 204–209.

Korntner, P., Sumerskii, I., Bacher, M., Rosenau, T., Potthast, A., 2015. Holzforschung 69, 807–814.

Langeveld, J.W.A., Dixon, J., Jaworski, J.F., 2010. Crop Sci. 50, S-142.

Matos, M., Barreiro, M.F., Gandini, A., 2010. Ind. Crops Prod. 32, 7–12.

Mushrush, G.W., Hardy, D., 1998. Fuel system icing inhibitor and deicing composition. Google Patents.

Nanda, M.R., Zhang, Y., Yuan, Z., Qin, W., Ghaziaskar, H.S., Xu, C. (Charles), 2016. Renew. Sustain. Energy Rev. 56, 1022–1031.

Narine, S.S., Kong, X., Bouzidi, L., Sporns, P., 2007. J. Am. Oil Chem. Soc. 84, 65–72.

Patterson, B.M., Henderson, K., Gilbertson, R.D., Tornga, S., Cordes, N.L., Chavez, M.E., Smith, Z., 2014. Microsc. Microanal. 20, 1284–1293.

Prociak, A., Kurańska, M., Cabulis, U., Kirpluks, M., 2017. Polym. Test. 59, 478–486.

Quispe, C.A.G., Coronado, C.J.R., Carvalho Jr., J.A., 2013. Renew. Sustain. Energy Rev. 27, 475–493.

Randall, D., Lee, S. (Eds.), 2002. The polyurethanes book. Huntsman Polyurethanes] ; New York : Distributed by John Wiley & Sons, [Everberg, Belgium.

Reymore, H.E., Carleton, P.S., Kolakowski, R.A., Sayigh, A.A.R., 1975. J. Cell. Plast. 11, 328–344.

Ribeiro, L.S., Órfão, J.J. de M., Pereira, M.F.R., 2017. Bioresour. Technol. 232, 152–158.

Septevani, A.A., Evans, D.A.C., Chaleat, C., Martin, D.J., Annamalai, P.K., 2015. Ind. Crops Prod. 66, 16–26.

Sharmin, E., Shreaz, S., Zafar, F., Akram, D., Raja, V., Ahmad, S., 2017. Prog. Org. Coat. 105, 200–211.

Silva, A.L., Bordado, J.C., 2004. Catal. Rev. 46, 31–51.

Stelmachowski, M., Marchwicka, M., Grabowska, E., Diak, M., 2014. J. Adv. Oxid. Technol. 17, 167–178.

Tan, S., Abraham, T., Ference, D., Macosko, C.W., 2011. Polymer 52, 2840–2846.

T.Werpy, G.P., 2004.

Udabe, E., Isik, M., Sardon, H., Irusta, L., Salsamendi, M., Sun, Z., Zheng, Z., Yan, F., Mecerreyes, D., 2017. J. Appl. Polym. Sci. 134, 45473.

Utilization of glycerol, a by-product of the transesterification process of vegetable oils: A review.

Yamaguchi, A., Sato, O., Mimura, N., Shirai, M., 2016. Catal. Today 265, 199–202.

Zhang, J., Li, J., Wu, S.-B., Liu, Y., 2013. Ind. Eng. Chem. Res. 52, 11799–11815.

Chapitre2.2: Elaboration and characterization of advanced biobased polyurethane foams presenting anisotropic behavior

Pierre Furtwengler[a], Rodrigue Matadi Boumbimba[b], Luc Avérous[a,*]

[a]*BioTeam/ICPEES-ECPM, UMR CNRS 7515,*

Université de Strasbourg, 25 rue Becquerel, 67087 Strasbourg, Cedex 2, France

[b]*LEM3, UMR CNRS 7239, Université de Lorraine, 7 rue Félix Savart, 57045 Metz Cedex 1, France*

* Corresponding author: Prof. Luc Avérous, Phone: + 333 68852784, Fax: + 333 68852716, E-mail: luc.averous@unistra.fr

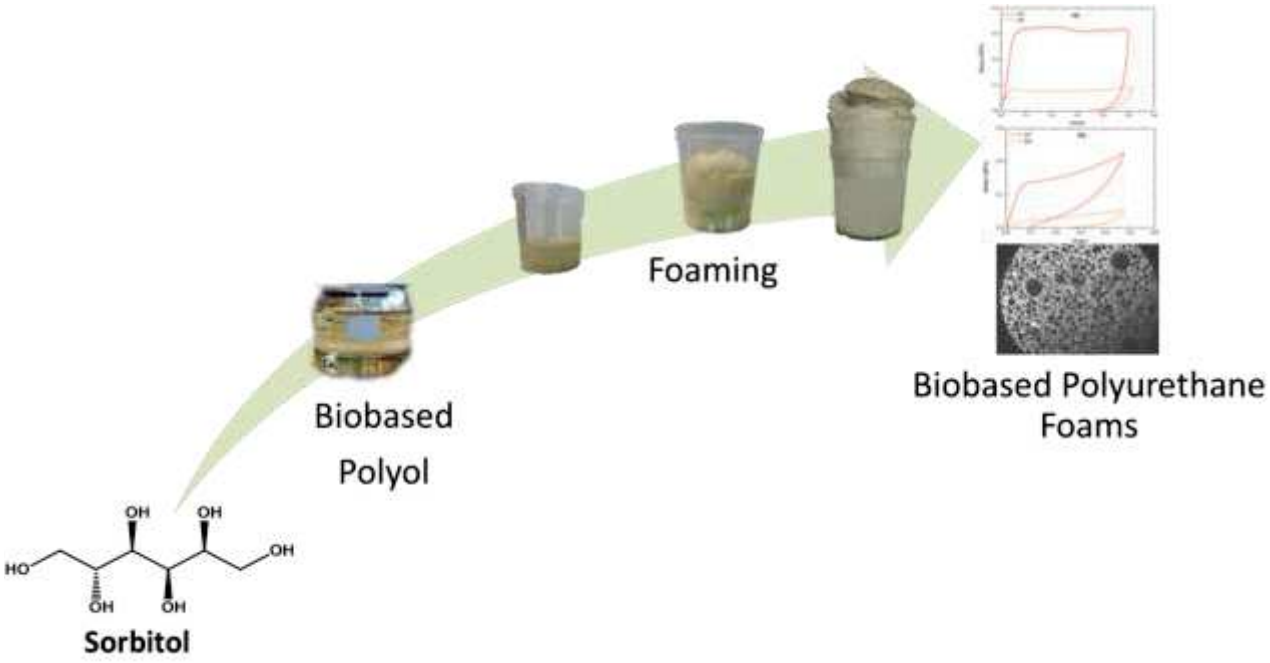

Published as P.Furtwengler, R.Matadi Boumbimba, L.Avérous, Macromolecular Materials and Engineering, 2018, doi: 10.1002/mame.201700501

Abstract:

Biobased and open cell polyurethane foams were produced from a synthesized sorbitol-based polyester polyol. Different formulations were developed with various blowing agent systems (chemical vs. physical blowing). Synthetized foams were fully characterized and compared. The cell morphology was carefully investigated by tomography and scanning electron microscopy. The chemical nature of the primary compounds, the foaming kinetics, the density, the thermal behavior and conductivity were fully studied, with also the main transition materials temperatures. We have shown that blowing agents especially impacts the foaming kinetics. In the case of chemically blowing foams, higher foaming rate and temperatures were obtained. The mechanical behavior was particularly analyzed using quasi-static compression tests, according two main axes compared to the rise direction. A direct relationship was observed between the formulation, the foam structure, the foam morphology and the corresponding mechanical properties. Results clearly highlight unexpected properties of biobased PU foams with unveil anisotropic mechanical properties.

Introduction

Polyurethanes (PUs) are versatile polymers, based on the reaction between a polyol and a polyisocyanate (Figure 2.7, a). They are used in a large range of applications, such as automotive, furniture, construction, footwear, acoustic and thermal insulation with a global production of 18 Millions Tons in 2016, placing PUs at the 6th rank among polymers in annual worldwide production (Gandini, 2008). Flexible foams represent the largest market of PU products (David Randall and steve Lee.) with more than 1600 kTons produced in Europe in 2011. Typically, PU foams are made from polyols, polyisocyanates, blowing agents and various catalysts to obtain chemically cross-linked cellular materials. Two types of blowing agents are used in PU foam synthesis based on chemical or physical systems. Chemical blowing agents are based on compounds that chemically react in the foaming process to liberate gases. Water reacts with the isocyanate function to form urea and liberate one mole of CO_2 per mole of water (Figure 2.7, b) (David Randall and steve Lee.). Physical blowing agents are compounds with a low boiling point such as isopentane derivates, which evaporate during the exothermic foaming process.

Generally, flexible and semi-flexible PU foams are obtained from polyols with low hydroxyl values (OHV) (OHV $\leq$ 100 mg KOH/g) and relatively high number-average molar masses (3,000 g/mol $\leq$ Mn $\leq$ 6,000 g/mol) (Pawlik and Prociak, 2012) in order to increase material flexibility and decrease the cross-link density. Semi-flexible slabstock foams are very important part of PU foams since they can fulfil some requirements to solve a modern problem, the noise pollution (Gama et al., 2015; Gwon et al., 2016). Since their open cell structure is permeable to moisture (Marcovich et al., 2017), these materials are highly demanded in insulation applications to avoid moisture and wet surfaces, with biofilms formation and fungi growth. These materials generally have a low apparent density, low thermal conductivity and are rather cheap materials. Semi-flexible slabsblock foams are versatile building insulation materials (both acoustic and thermal) which are less described in the literature.

Flexible and semi-flexible PU foams properties come in part from the phase separation of hard and soft segments. Soft segments are stretchable chains, mainly from the polyols, that give the material its elasticity (Bernardini et al., 2015b). Generally hard segments (HS) are described as rigid structures. HS are are often based on the chain extenders and the isocyanates (Laurichesse et al., 2014). HS could be for instance also linked to an excess of diisocyanate components. This excess leads to an increase in biuret (Figure 2.7, d), allophanate (Figure 2.7, c) or isocyanurate linkage (Figure 2.7, e). Another way to improve HS content is to increase the weak interchain forces within the hard domains by adding polar groups such as urea (Chattopadhyay et al., 2006).

PU industry is strongly dependent on fossil-based polyols and polyisocyanates (Saunders and Slocombe, 1948). Developing new and original sustainable polyols from valuable biobased building blocks for PU industry is a first step for a strong and durable development. Such a step develops a green chemistry approach, reduces the greenhouse gases emissions, responds to several societal demands, and introduces materials with new properties, using the polyfunctionality and wide diversity of the biomass.

Sorbitol is a building block of interest. It has been quoted as one of the top 12 added value chemicals from biomass by the U.S department of energy in 2004 (Holladay et al., 2007), and more recently in an updated list from Bozell et al. (Bozell and Petersen, 2010). Sorbitol is a highly functional, crystalline sugar alcohol bearing two primary hydroxyl groups and four secondary hydroxyl groups, for chemical modification such as polyurethane chemistry. The sorbitol modification into convenient polyols must be controlled to fulfill some basic requirements. Indeed, the polyol functionality i.e. OHV and / or polyol viscosity have a strong impact on PU network formation, PU foams density, and the closed or open characters of the foam cells (Septevani et al., 2015). The size, shape and spatial distribution of the cells are also some other parameters which control the physical properties (Andersons et al., 2016). PU foams thermal and mechanical properties are closely dependent of the foam morphology.

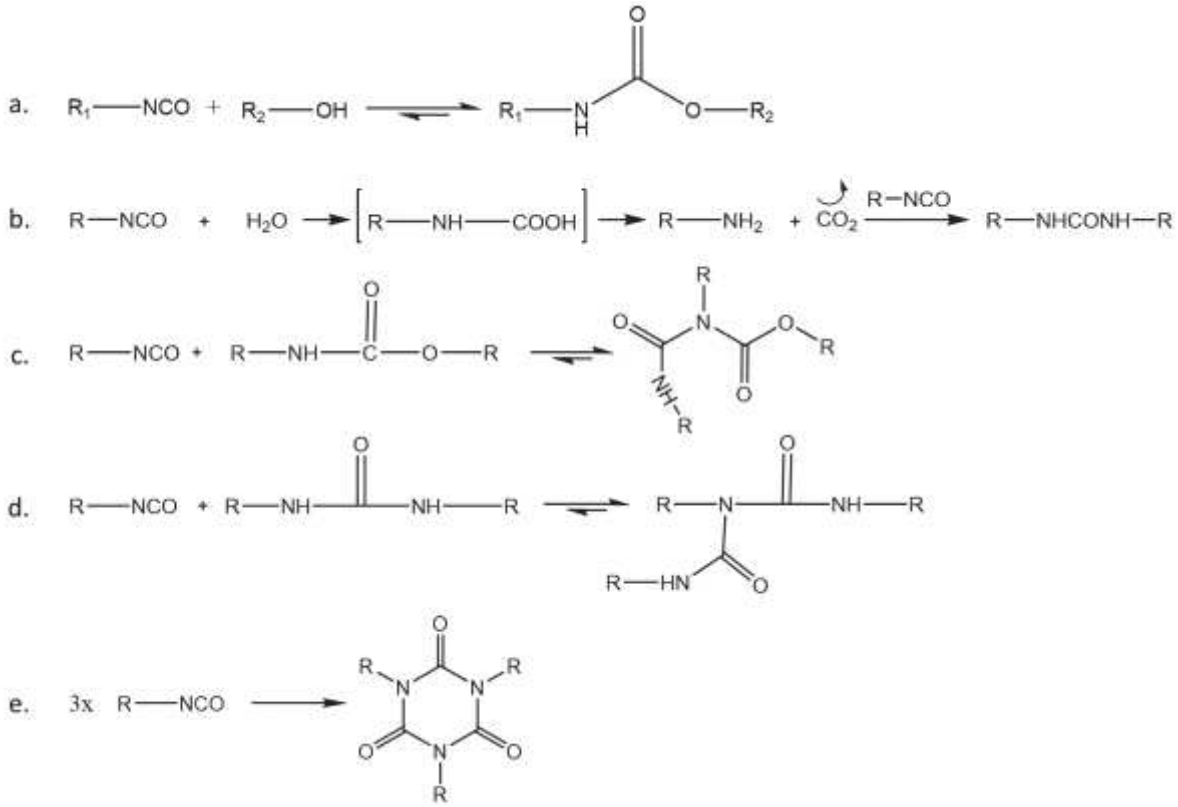

Figure 2.7: Isocyanate reactivity with alcohol (a), water (b), urethane (c), urea or isocyanate trimerization (e).

Several researchers have studied the elaboration and the physical characterization of biobased polymer foams by using different approaches (Chuayjuljit et al., 2010; Paruzel et al., 2017; Patterson et al., 2014; Tan et al., 2011b). However, the mechanical and thermal properties of these materials have been less investigated. For instance, only few works deal with the study and modelling of the mechanical properties in connection with thermal properties (Gibson et al., 1989; Gupta et al., 2010). According to the classical model developed by Gibson and Ashby, the Young's modulus exhibits a square dependence to the relative density but no dependence on cell size (Gibson and Ashby, 1997). The effect of foam density is well established (Chen et al., 2002; Jin et al., 2007; Maiti et al., 1984), nevertheless there have been few studies related to (i) the

influence of the cell size at constant density, and to (ii) the effect of the initial foam formulation (Brezny and Green, 1990).

The aim of this work is to extend and complete a previous and recent preliminary publication (Furtwengler et al, 2017), where polyurethane foams were produced from a synthesized sorbitol-based polyester polyol. A more conventional polyether-based foam was used as a reference. The properties of the foams were tuned by the addition of small polyols (glycerol, sorbitol). Mixed physical and chemical blowing systems, based on isopentane and water, respectively, were also tested at different ratios.

More specifically, the goal of this specific study is to establish a deeper comparative study and correlations between different foam formulations with a specific focus on the mechanical properties. Mechanical characterization, including dynamical mechanical analysis in longitudinal direction, and quasi-static compression tests, in both transversal (T) and longitudinal (L) directions according to the foam rising direction, were performed. Mechanical results were correlated with cells morphology, apparent density and closed cells content. Moreover, the thermal conductivity studies of all foams grades were investigated and associated to the foams structures, investigated by both scanning electron microscopy and micro-tomography.

Experimental Section

Chemical

Sorbitol was kindly provided by Tereos (Meritol, 98%, water content < 0.5%, reducing sugar content < 0.1%). 1,4-butanediol (BDO, 99%) was obtained from Sigma Aldrich. Adipic acid (AA) (99%) was obtained from Acros Organics. Polyether polyol was a common oxypropylated polyol from Huntsman (Daltolac® R570), with an average functionality of 3.0 and an OH-value of 570 mg KOH/g. The polyisocyanate was polymeric 4,4'-methylenebis(phenyl isocyanate) (MDI) from BorsodChem (Ongronat 2500). Two typical polyurethane foam catalysts were used: N,N-Dimethylcyclohexylamine (DMCHA) and 15 %wt potassium octoate solution (Ko), from Momentive and BorsodChem, respectively. Flame retardant which also act as rheofluidifiant was Tris (1-chloro-2-propyl) phosphate (TCPP) from Shekoy, surfactant was polydimethylsiloxane (B84501) from Evonik and glycerol (gly) (99.5%) was obtained from Fisher Scientific. Isopentane from Inventec was used as physical blowing agent. All these chemicals were used as received without further purification.

Synthesis of the sorbitol-based polyol

Sorbitol-based polyester polyol was synthesized following a two-step bulk polycondensation from sorbitol, 1.4-butanediol and adipic acid. One molar equivalent of sorbitol and two molar equivalents of adipic acid were charged into a 600 mL Parr thermo-regulated reactor (model N°4568) equipped with a heating mantle, mechanical stirrer and a thermocouple. The media was heated to 150°C for three hours, then the reactor was stopped and open to add 2 molar equivalents of 1.4-butanediol in respect to the sorbitol. The reaction was relaunched for six additional hours. Finally, the reactor was cooled down to 60°C and the residual acidity of unreacted adipic acid was neutralized by addition of the proper amount of K_2CO_3. A viscous yellow polyol (BASAB) was recovered from the reactor. BASAB general properties are summarized and compared to fossil-based polyether polyol in Table 2.6. The details linked to this synthesis or structural characterization of the BASAB can be found in Annex (Figure SI 31 to Figure SI 35). More details are also found in a recent publication (Furtwengler et al, 2017).

Table 2.6 : Main properties of the polyether and biobased BASAB polyester polyols.

	Dynamic viscosity at 25°C (mPa.s)	Titrated OHV (mg KOH/g)	Titrated IA value (mg KOH/g	Average functionality	
				Primary hydroxyl	Secondary hydroxyl
Polyether polyol	670	570	≤ 5	3.0 (terminal)	
BASAB polyol	24 300 ± 200	382 ± 9	3.4 ± 0.8	2	4

PU foams synthesis

PU foams were prepared with an isocyanate / hydroxyl molar ratio (NCO / OH) of 1.15. To determine the isocyanate content, all reactive hydroxyl groups were taken into account, *i.e.* polyols and water. Based on the two components foaming process a pre-mix containing polyol(s), catalysts, surfactants (polydimethylsiloxane, B84501), flame retardant (TCPP) and blowing agent was prepared. Blowing agents were chosen between isopentane (physical blowing agent) and water (chemical blowing agent). Based on the ideal gas law, the total volume of blowing agent was kept constant in respect to the total amount of foaming material. In each preparation, the number of parts by weight (pbw) of TCPP and surfactants were constant at 10 and 2.5 pbw, respectively, and the total amount of polyols is fixed to 100 pbw. In the case of neat crystalline polyol such as sorbitol, the component was previously dissolved in water to increase its efficiency. The mixture was mechanically stirred until obtaining a fine white emulsion with the full incorporation of the blowing agent. Such as the polyisocyanate, the initial mixture temperature was controlled and adjusted to 20°C. The right amount of polyisocyanate was quickly added to the emulsion and the whole reactive mixture was vigorously stirred for 5 s. Then, the foam rises freely in 250 mL disposable beaker e.g., in the Foamat device. Before further analysis foams samples were kept for three days at room temperature for a dimensional stability.

Characterizations

Thermogravimetric analyses (TGA) were performed using a Hi-Res TGA Q5000 (TA Instruments, US) under reconstituted dry air with a blend of oxygen and nitrogen gas (flow rate 25 mL/min). Samples of 1-3 mg were heated from room temperature to 700°C (10°C/min) in heating ramp mode controlled and monitored by the TA Instrument proprietary software: Q series. The main characteristic degradation temperatures are those at the maximum of the weight loss derivative curve (DTG) ($T_{deg,max}$).

Infrared spectroscopy was performed with a Fourier-transform infrared spectrometer Nicolet™ 380 (Thermo Scientific, US) used in reflection mode equipped with an ATR diamond module (ATR-FTIR). An atmospheric background was collected before sample analysis (64 scans, resolution 4 cm^{-1}). All spectra were analyzed with OMNIC™ Spectra software and normalized on C-H stretching peak at 2950 cm^{-1}.

Dynamic mechanical analysis (DMA) were conducted on TRITEC 2000 DMA apparatus (Triton Technology Ltd, UK) in compressive mode. Samples were analyzed at constant frequency of 1Hz for temperature range from 30 to 270°C with a heating rate of 2°C/min and a constant static strength of 0.5 N. Samples were cubic-shaped (7.5 × 7.5 × 7.5 mm^3). Three samples cut from the center of the foam were analyzed for each foam.

The quasi-static compression tests were carried out with an compression testing machine (E1000, Instron-USA), equipped by a load sensor of 1 KN, at 25°C and at a constant strain rates of 2.5 mm/min. Samples were cubic-shaped (25 × 25 × 25 mm^3) and three different samples per foams were analyzed. They were tested in L and T directions, according to the sense of the foam expansion. The Young's modulus was defined as the slope of stress-strain curves in the elastic region and the yield stress as the first maximum of the stress strain curve.

Thermal conductivity was measured from the conduction heat flux. Typically, the device consists of a heating element with two thermocouples to obtain the temperature at the front and back faces. The device is also equipped by two sensors dedicated to the measurement of the heat and the cycle times. These latter are used to correct the maximum conduction heat flux. It is necessary for the calculation of the thermal conductivity coefficient, by the means of the Fourier law, used in steady state thermal conduction. Plates of different materials, with dimensions of 300*400*3 mm^3 have been used for the determination of the thermal conductivity coefficient. Measurements were repeated three times per sample.

Foams temperature, expansion heights and rates, density and foaming pressure were recorded using a Foamat FPM 150 (Messtechnik GmbH, Germany) equipped with cylindrical recipients, 180 mm height and 150 mm in diameter, an ultrasonic probe LR 2-40 PFT recording foaming heights, a NiCr/Ni type K thermocouple, and a pressure sensor FPM 150. The data were recorded and analyzed with a specific software.

Closed cells content is determined using an Ultrapyc 1200e (Quantachrome Instruments, US) based on the technique of gas expansion (Boyle's law). Foams cubic samples (around 2.5 × 2.5 × 2.5 cm^3) are cut for a first measurement. Then, the cubic sample was sectioned into eight equivalent pieces and the measurement was run again. This second run allows to correct the closed cells content from the closed cells due to the sample cutting. Measurements were performed according to EN ISO4590 and ASTM 6226.

Foams apparent density measurements were performed according to EN 1602 standard method. Ten foam samples of 15,625 x 10^{-6} m^3 (equivalent to 2,5 x 2,5 x 2,5 cm cubic samples) per foam grade were prepared and weight. The density was calculated according to Equation 1.

$$\rho = \frac{m}{V} \qquad (1)$$

where m (kg) is the sample masse and V (m^3) is the sample volume.

Foams cells morphology was observed on a HITACHI TM-1000 (Japan) tabletop field emission scanning electron microscope (SEM). Cubic foams samples were cut with a microtome blade and analyzed in two characteristic orientations, L and T from the foam rises direction.

Results and discussion

Table 2.7: PU foams formulations and the main corresponding characteristic times linked to the foaming process

Designation:		REF (Reference)	B85-2	B85-4	B100-2	B100-4
Formulations	Polyol	Polyether	BASAB + gly + sorbitol	BASAB + gly + sorbitol	BASAB	BASAB
	Polyol ratio (pbw)	100	85 + 10 + 5	85 + 10 + 5	100	100
	Physical blowing agent (isopentane in pbw)	15.04	19.28	13.20	12.25	4.14
	Chemical blowing agent (water in pbw)	1.60	1.60	4.14	1.60	4.14
	Total of blowing agent content in respect to the total foam composition (%)	12.66	12.66	12.66	12.66	12.66
Characteristic times	Cream time (s)	10	27	16	15	22
	Gel time (s)	44	122	90	70	60
	Tack free time (s)	66	300	210	115	110

Table 2.7 presents the main formulations and some characteristic times linked to the foaming steps with different biobased polyols. Foam characteristic times and Foamat records of REF and B85-4 have been previously described (Furtwengler et al, 2017) and will be mainly used for comparison purposes. REF presents the faster cream time of 10 s, whereas all biobased foams are up to 15 s. The tack free time is an indication linked to the surface of the foam and does not indicate the end of the full foaming process. However according to this parameter, the polymerization step starts to stop in 66 s for REF, whereas all other biobased foams present times higher than 100 s. Foamat records indicated that REF foam reaches its highest foaming rate of 5 mm/s (Figure 2.8, c) in 60 s, and in 70 s it reaches its maximum height of 160 mm (Figure 2.8, b). It is a direct consequence of the exothermic polyaddition reaction between the polyol and the polyisocyanate which present an enthalpy of 100.32 kJ/mol (Ionescu, 2005). For instance, the internal temperature of REF is stabilized only after 210 s (Figure 2.8, a), the time to fully cure the PU network. B100-2 foam is the biobased equivalent of REF, the Foamat record (Figure 2.8) clearly indicates the effect of the chemical structure of the polyol. Its foaming rate is five times lower than REF, as a consequence of a lower foam temperature. This indicates that the polyester polyol is less reactive than the polyether polyol as expected since the secondary hydroxyls groups are less accessible and reactive than the terminal hydroxyl group of the polyether (Tan et al., 2011b). The B100-2 temperature curve (Figure 2.8, a) shows a delay of almost 60 s before the indication of the temperature increase. This value corresponds to the time needed by the mix to start the foaming process and to the time that the expanding system enters in contact with the Foamat temperature probe. This delay is noticeable on all biobased temperature curves and it is linked to the foaming rate. Compared to B100-2 and REF, B100-4 was formulated with higher water content. The foaming process parameters of B100-4 are improved since the reaction between isocyanate and water is twice as exothermic than with an alcool. The exothermicity of the water-isocyanate reaction is clearly visible on the foam temperature evolution which skyrockets from 30 to 140°C, in 47 s. The foaming rate for B100-4 is 1.6 or 4 times higher than REF or B100-2, respectively, for an equivalent foam height.

Even if the addition of water in the formulation is an efficient way to improve the foaming reactivity, we extend our previous investigation (Furtwengler et al, 2017) based on the study of the impact of non-volatile and highly reactive short polyols to foam B85-2. Sorbitol and glycerol were used to improve the starting-step of the multistep foaming process (Table 2.7). The corresponding foams (B85-2 and B85-4) reach a similar height compared to REF, with variations of the foaming rate and temperature. The foam B85-2 temperature starts to increase after 60 s and a low foaming rate of 2 mm/s is maintained constant for 80 s, attributed to the reaction of small diols. Then, when the temperature reaches 80°C, the BASAB polyol starts to vigorously react and the foaming rate of B85-2 increased from 2 to 3 mm/s. This increase of reactivity is also visible on the B85-2 temperature curve (Figure 2.8-a) which presents a change of slope at 110 s and then continues to increase. Instead, the highest water content for B85-4 induces a strong temperature increase which masks the reactivity gap between the small diols and the BASAB. As it is visible in Figure 2.8-a, b, c the temperatures and the foaming rates increased drastically and the foam reaches its maximum height in 20 s. These observations are similar and in agreement with our previous work on small diol and blowing agent nature effect on the foaming reaction (Furtwengler et al, 2017). We can notice that for B100-4 and B85-4 foams, the temperature curves decrease before the end of the recorded time. These foams show the highest temperature increase whereas the temperature evolved more gradually for the other foams. Foams B100-4 and B85-4 heat release finished before the end of the Foamat recording time and the observed temperature decrease is related to the foams cooling after reaction.

The comparison of B85-2 and B100-2 foaming rate curves presented in Figure 2.8, clearly demonstrated the well-known high reactivity of the small diols, compared to longer diols such as BASAB. The foaming rate of B100-2 never exceeds 2 mm/s, whereas B85-2 foaming rate reaches 3 mm/s. The consequence is also visible on the foaming temperature of B100-2, presented in Figure 2.8-a, which is 40°C lower than that of B85-2.

The resulting expansion of the foam is affected by the lower temperature (Figure 2.8-b). The height of the B85-2 foam is twice the B100-2 foam's one, whereas they have the same amount of chemical blowing agent. When formulated with higher water content, i.e. foam sample B100-4, the foam reaction profiles are greatly improved. Foam height and temperature are now similar for B85-2 and B85-4 (Figure 2.8-a and b). The foaming rate evolution between B100-2 and B100-4 is drastic. B100-4 maximal foaming rate is reached at 8 mm/s in 50 s and then it decreases rapidly. This kinetic is faster than for B85-4. The main hypothesis to explain this phenomenon is based on the formation of funnels inside the foam, instead of cell formation, promoted by the small diol, which could act as cross-linker agent. This hypothesis has been confirmed by SEM images.

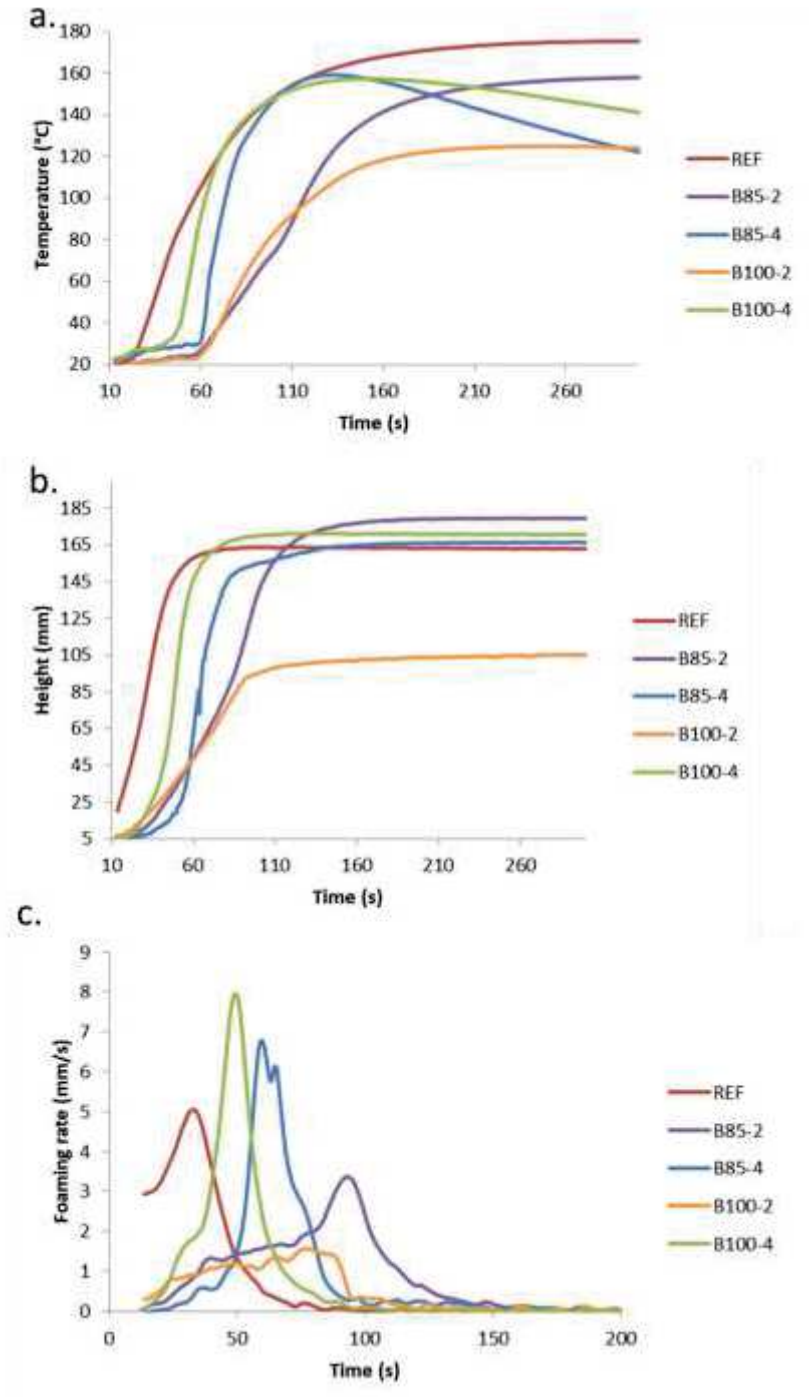

Figure 2.8: Foaming reaction profiles: evolution of the temperature (a), maximum height (b), and foaming rate (c) vs. time during the foaming step

Water as a chemical blowing agent is a convenient and the easiest way to increase the foaming rate, but also leads to an increase of the urea content in the foam. As urea induces HS, the foam mechanical properties are impacted. Then to limit the urea content, it is possible to partially replace water by the use of small and highly reactive polyols which act also as foaming starter.

The analysis of the chemical architectures of the PU foams was investigated by FTIR. Functional groups linked to PU and polyisocyanurates (PIR) synthesis were targeted (Figure 2.9-a). The large peak at 3300 cm^{-1} is related to the stretching of N-H groups. The peak at 2270 cm^{-1} is consistent with residual free NCO (Guelcher et al., 2005), which is coherent with a formulation NCO/OH molar ratio of 1.15. Hydroxyl groups are visible with the baseline drag up to 3600 cm^{-1}. These hydroxyl groups are certainly unreacted secondary hydroxyl from BASAB. N-H groups also exhibit a bending signal (Rogulska et al., 2013) at 1510 cm^{-1}. The broad peak at 2950 cm^{-1} corresponds to stretching of C-H bond from the PU backbone and the signal at 1595 cm^{-1} corresponds to Ar-H stretching from phenyl groups of the polyisocyanate (Modesti and Lorenzetti, 2001). Several peaks were attributed to the urethane group including the H-bonded C=O stretching at 1709 cm^{-1}, the C-O stretching at 1220 cm^{-1} and then the two merge peaks at 1062 cm^{-1} and 1017 cm^{-1} are associated to the symmetric stretching of N-CO-O bonds and the stretching of C-O bonds (Barrioni et al., 2015). Urea functions have been previously reported (Mustafe., 2005) as a broad peak at 1647 cm^{-1}. We assumed that their low contents compared to urethane groups induce a weaker signal which is at the origin of the non-return to the baseline of the spectra in the 1700-1600 cm^{-1} area. Then, the last important peak appearing on all spectra at 1412 cm^{-1} is attributed to isocyanurate absorption band (Modesti and Lorenzetti, 2001; Romero, 2005; Vitkauskiene et al., 2011). It indicates that even in PU formulation with low excesses of isocyanate function, a small amount of isocyanurate is formed. The quantity of isocyanurate related to the peak intensity (Figure 2.9, b) shows a good correlation with previously recorded foam temperature. This is in agreement with the high temperature needed to obtain PIR materials (Hofmann., 1870) In conclusion, these systems are poly(urethane-isocyanurate) (PUIR) foams.

Figure 2.10 presents the TGA and DTG thermograms of the foams. REF shows a first loss of weight characterized by a bimodal thermal degradation. The first weight loss corresponds to the urethane and polyol polyether decompositions, with a maximum of the DTG curve at 250°C. The second stage is assigned to the carbon-carbon bond cleavage with a maximum on the DTG curve at 560°C. These results are in agreement with several data reported in the literature (Arbenz et al., 2017; Celzard et al., 2011; Ulrich, 1981). The thermal stability of the foams is influenced by several parameters depending on the formulations. For instance, the temperature of urethane decomposition group is influenced by the nearby chemical groups. It has been reported that urethane function surrounded by two alkyls presents an initial decomposition at 250°C, whereas surrounded by two aryl groups will start at 120°C (Simon et al., 1988). This decomposition is mainly induced by the thermal reversibility of the urethane function. The main decomposition pathways are due to the reverse reaction, the dissociation, the amine formation and the transcarbamoylation (Delebecq et al., 2013).

All the biobased foams present a lower thermal stability than REF, with a weight loss starting at 170°C. The degradation steps are complex due to the addition of different chemical groups brought by the polyester polyol. The polyesters are subject to two main degradations, which are α- and β-hydrogen bond scissions (Abe, 2006), resulting in a competitive degradation with the urethane function degradation. We cannot clearly notice a particular effect of the addition of the short polyols in the corresponding architectures, as DTG thermograms are rather similar for most of biobased foams. Only B85-4 shows a variation on TGA and DTG thermograms since its weight loss is slower than other biobased foams. This is coherent with its formulation based on high water addition which induces higher urea content. Urea groups are more thermally stable than the urethane's ones (Chattopadhyay et al., 2006).

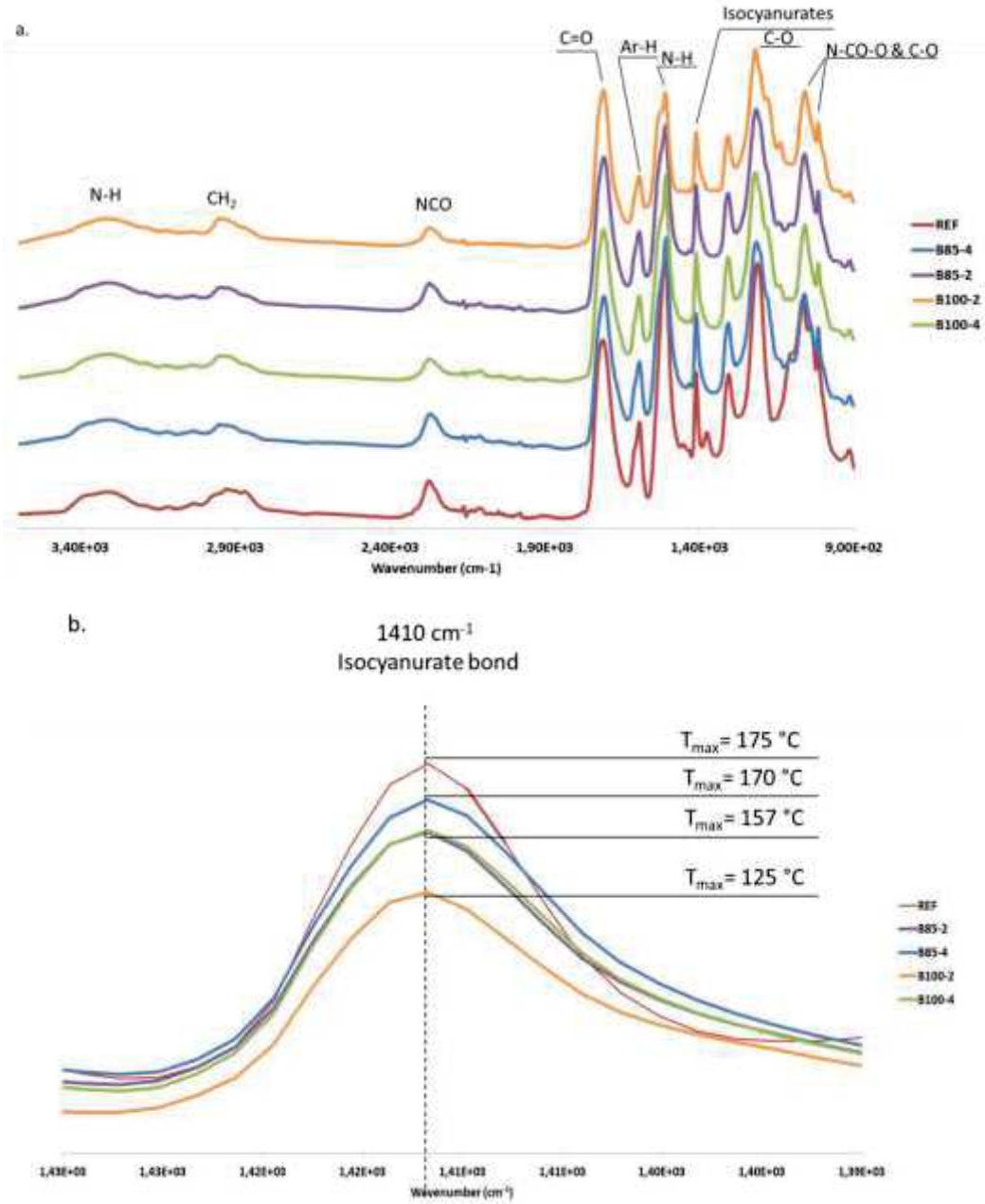

Figure 2.9: a. FTIR spectra of formulated foams, b. FTIR spectra zoom on isocyanurate absorption band area

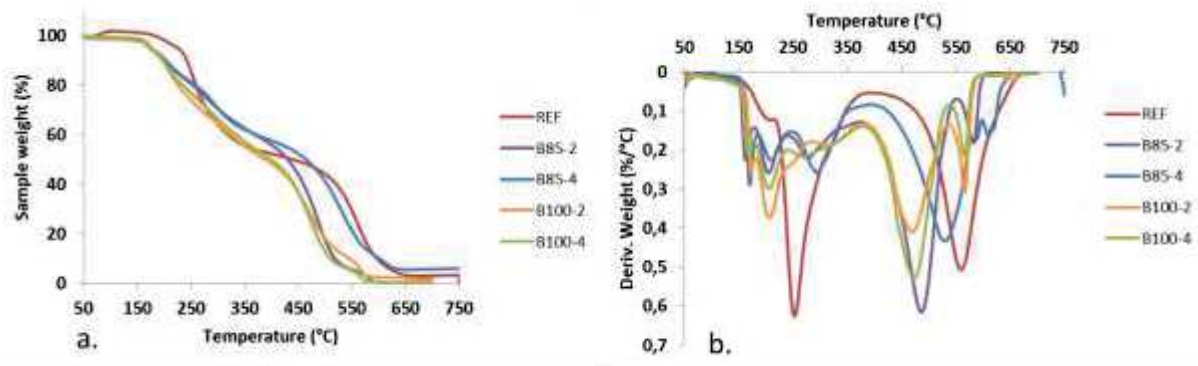

Figure 2.10 : TGA (a) and DTG (b) curves for PU-based foams under dry air

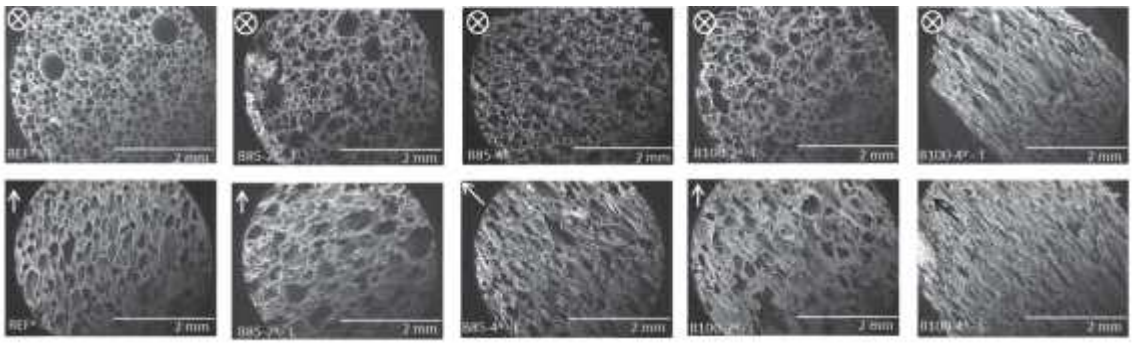

Figure 2.11: SEM images of PU foam samples in T (top) and L direction (bottom)

Table 2.8: PU foam cell morphology

		REF	B85-2	B85-4	B100-2	B100-4
L direction	Feret max, D_F^{max} (µm)	376 ± 91	432 ± 157	443 ± 146	362 ± 134	408 ± 122
	Feret min, D_F^{min} (µm)	194 ± 39	227 ± 69	174 ± 47	173 ± 58	110 ± 25
	$R= D_F^{max} / D_F^{min}$	1.96 ± 0.35	1.92 ± 0.47	2.60 ± 0.8	2.17 ± 0.76	3.78 ± 0.93
T direction	Feret max, D_F^{max} (µm)	217 ± 33	350 ± 114	232 ± 66	277 ± 100	380 ± 88
	Feret min, D_F^{min} (µm)	182 ± 33	245 ± 77	170 ± 47	171 ± 52	104 ± 28
	$R= D_F^{max} / D_F^{min}$	1.21 ± 0.15	1.46 ± 0.36	1.38 ± 0.25	1.65 ± 0.42	3.79 ± 0.97

Figure 2.11 displays foams samples morphologies from SEM images in L and T directions, with respect to the foam rise. Different and inhomogeneous structures with open-cell PU foams are obtained except for REF, which presents homogeneous closed cells foam.

In L direction, all cells are polyhedral-shaped with a clear anisotropy (R) (Table 2.8) and ellipsoid shapes ($1.9 \leq R \leq 3.8$). This phenomenon is increased by the partially free foaming process with a foam growth in L direction. In contrary, cells are more spherical in T direction ($1.21 \leq R \leq 1.65$) except for B100-4 where the cells are ellipsoidal in both directions. SEM images can also give the global foam structure. B100-4 exhibits widely elongated cells which initiate small funnels in the material. Whereas B100-2 is closer to a conventional open cell structure. This difference can be easily explained by the high water content in B100-4, which promotes a rapid and strong liberation of carbon dioxide, creating orientated funnel with a partial breakage of the closed cells. In comparison, the physical blowing agent has a softer expansion controlled by its evaporation located in the air of the microbubbles created by the mechanical agitation of the polyol premix (Ramesh et al., 1994), resulting in a sponge-like structure. Instead, B85-2 and B85-4 show a cellular structure with a lower R coefficient than B100-2 and B100-4. Their cellular structures are linked to higher cross-link density of the PU network, which is induced by the addition of the short polyfunctional polyols (glycerol and sorbitol) limiting the gas expansion, with an increase of the material stiffness. In supporting information, Figure SI 36 (in Annex) gives the tomographic images of REF and biobased foams. The tomographic image displays thus a very complex structure, with non-homogeneous shape and size, in agreement with SEM observations. The variability of the morphologies of biobased foams were in agreement with the formulations and foams reactive profiles previously presented. Compared to the structure of REF, the use of renewable polyester polyol is an efficient way to obtain cellular structures with a large variation in morphologies and properties.

Table 2.9 : Main foams parameters

Nomenclature	Chemical blowing agent (parts)	Apparent density (kg/m^3)	Longitudinal direction cell size (µm)	Closed cells content (%)	Thermal conductivity coefficient λ (mW/m K)
REF	1.6	30.7 ± 0.8	194 ± 39	93	25.0 ± 0.1
B85-2	1.6	25.4 ± 1.6	227 ± 69	2	51.0± 0.4
B85-4	4.14	23.1 ± 0.3	174 ± 47	2	51.0 ± 0.2
B100-2	1.6	41.2 ± 3.5	173 ± 58	10	40.0 ± 0.4
B100-4	4.14	25.3 ± 1.8	110 ± 25	9	35.0 ± 0.2

Table 2.9 presents the thermal conductivity coefficients and apparent density of all the studied foams. Biobased foams densities range from 23 to 41 kg/m^3, close to REF density (31 kg/m^3). B100-2 presents the highest value (41 kg/m^3), compared to the others biobased foams which present more or less similar densities at around 23-25 kg/m^3. The foams with higher water content are more expanded. This is in good correlation with previous observations. Table 2.9 shows that all biobased foams with higher water content exhibited an increase in foaming rate and temperature with originated the increase of the gas expansion. The phenomenon was enhanced from B100-2 to B100-4. Obviously, REF shows the lowest thermal conductivity value due to its high closed cells content. Surprising information is coming from the biobased PU foams thermal conductivity. They present a lower closed cells content and show a relatively good thermal conductivity comprise between 35 and 51 mW/mK, on agreement with commercial equivalent fossil-based foams. The closed cells content is responsible of 60-65% of the low density foam thermal properties (Fleurent and Thijs, 1995). The complement (40-35%) depends of the expansion gas and the polymeric material. Non-foamed polyurethanes and polyurethane urea present a heat capacity (Cp) in a range of 0.422 to 0.665 cal.g^{-1}.°C^{-1} and 0.389 to 0.513 J.g^{-1}.K, respectively (Mark, 2009). Generally, low Cp values are linked to low thermal conductivity of the foams. B85-4 and B85-2 or B100-4 and B100-2 foams show closer thermal conductivity values, probably due to their relative closed cells content and cells dimension. Direct relationship between relative densities and thermal conductivities can be found. Thermal conductivities of B100-4 or B100-2 are lower than B85-4 or B85-2. Since the biobased foams present mainly open cell, the main differences between B100-4 and B100-2 are their densities which however induce an equivalent thermal conductivity coefficient. B85-4 and B85-2 have the same apparent densities, closed cells contents, and approximately the same cell sizes and equivalent thermal conductivity coefficients.

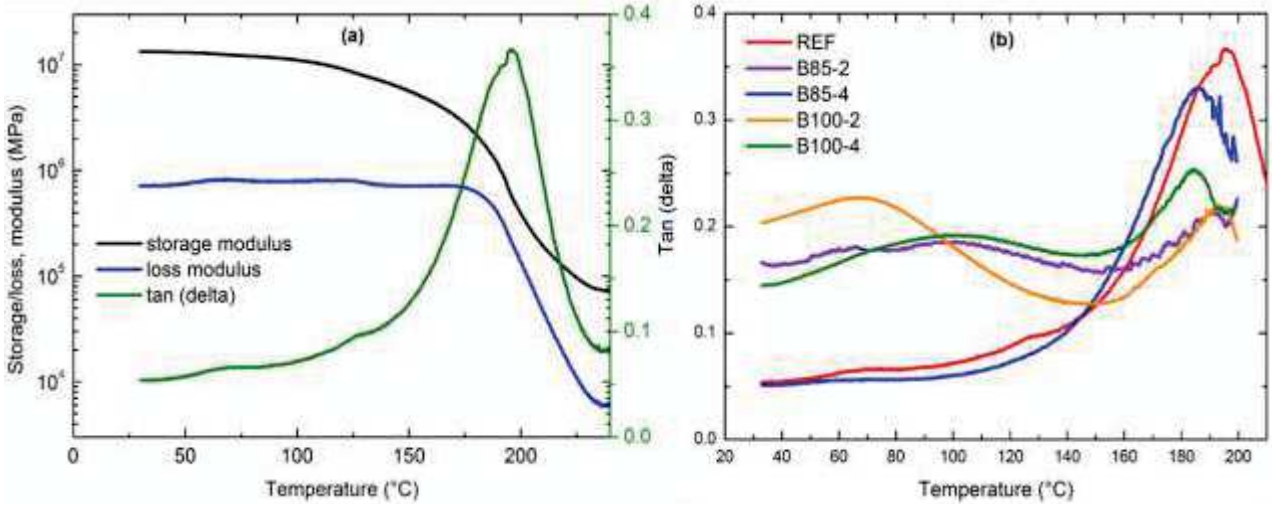

Figure 2.12: -a) storage, loss modulus and Tan δ evolution of REF, and -b) polyester-based PU foam B100-2

The evolution of the storage modulus, loss modulus and loss factor (Tanδ) versus temperature of REF is presented in Figure 2.12-a). As commonly observed, both storage and loss modulus, stay higher in the glassy region, before a sudden drop in the glass transition region. The Tanδ spectrum only presents one peak. The relaxation temperature is determined at the maximum, and can be associated to the glass transition temperature (Tg). This temperature is around 200°C for PU foams sample. DMA tests performed on the polyester-based PU foams, shows as expected a decrease of the visco-elastic properties and Tg (Figure 2.12-b and Table 2.10), confirming that the polymer chain mobility is increased. The chain mobility increase is induced by a lower cross-linking density of the PU network as the biobased polyol has a lower OHV compared to REF, which is based on polyether. It clearly appears, from results reported in Table 2.10, that the storage modulus of biobased foams increases from B85-2 to B85-4, probably due to the chemical blowing agent which generates hard urea parts. B100-2 and B100-4 present intermediate and closed values. For the polyester-based foams, Tg values vary in a short range from 184 to 192°C. All these thermal and viscoelastic properties variations will be better explained through the analysis of the mechanical properties.

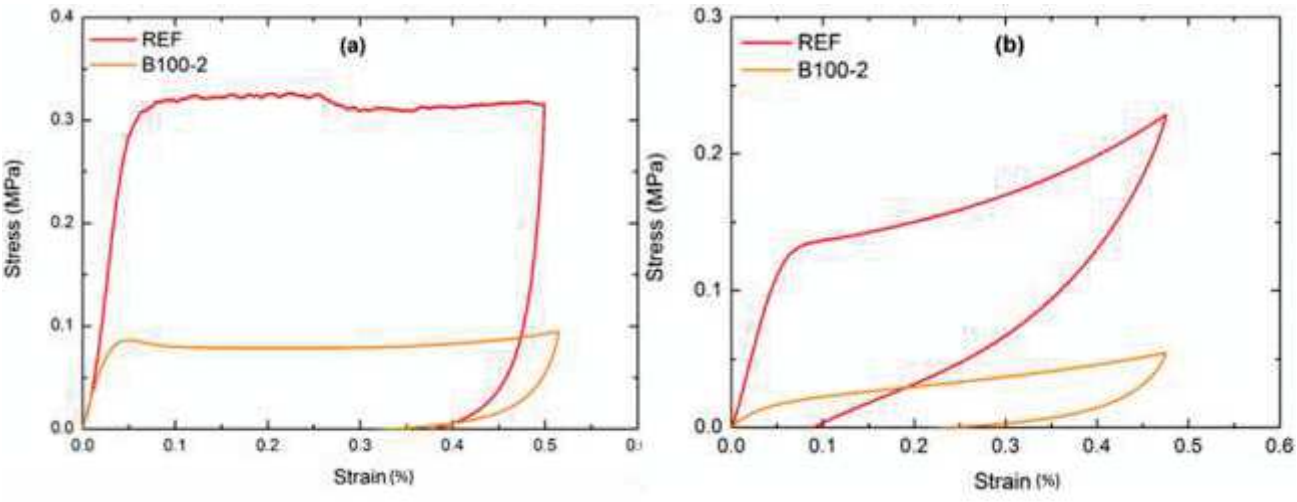

Figure 2.13: Stress strain curves of both REF and polyester-based PU foam (B100-2) , in –a) L direction (top), -b) T direction (bottom)

Figure 2.13 shows the comparison of the mechanical properties between REF and the biobased B100-2, at room temperature in both L and T directions. As previously described (Chen et al., 2002), in the L direction (Figure 2.13-a), the stress increases linearly with the strain (due to the elastic behavior of the foams), before reaching the yield point. Up to the yield point, the stress stays quasi-constant due to the foam densification. In the T direction, the behavior is rather different. After an elastic region until the yield point, the stress continues to increase, corresponding to the foam densification. It was also noticed that the residual strain after unloading is less than the one in the L direction, as a consequence of the foam cells structure, orientated in the foam rise direction (Delebecq et al., 2013). This alignment, leads to the development of an anisotropic behavior, which contributes to increase the mechanical properties in the L direction, compared to the T one. SEM observations and Feret diameters values confirm the cells orientations. After the elastic region, the cells-based structures orientated in the L direction break under loading originating the observed residual strain. Whereas in T direction, the elongated cells are able to undergo larger deformation before failure. These hypotheses are supported by Andersons and al (Andersons et al., 2016), whom worked on stiffness and strength of closed cells PUIR foams.

Compared to REF, the biobased foam depicts lower mechanical properties, with a lower young's modulus and yield stress. Hence Young modulus and yield stress were 8.5 and 0.3 MPa for REF and, 3.0 and 0.08 Mpa for B100-2, respectively (Table 2.10). The same trends are observed in the T direction. This drastic

change is mainly based on the chemical structure of the corresponding foams (Septevani et al., 2015). In addition, the closed cells content decreases from 90 to 10% for REF and B100-2, respectively. Under compression loading, the enclosed gas of the closed cells is pressured and contributes to increase some mechanical properties (D'Souza et al., 2014).

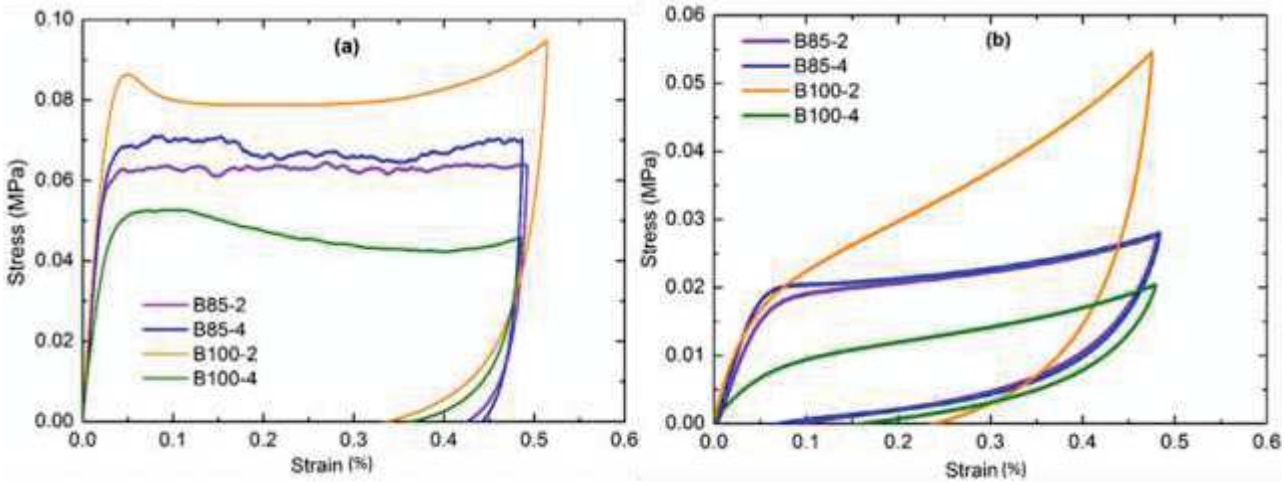

Figure 2.14: Stress-strain curves of different polyester-based PU foam, in –a) L direction (top), -b) T direction (bottom)

Figure 2.14-a. shows the stress-strain curves of the biobased foams. B100-2 presents higher performances. Obviously, the young modulus and the yield stress of B100-2 are the highest. The mechanical properties enhancement of B100-2 is explained by its higher density. In addition, under compression loading, both a quick densification and a good load repartition, lead to an increase of the mechanical properties. In opposite, B100-4 presents the lowest mechanical properties, mainly due to its high open cell content and lowest density.

The slight increase of mechanical properties of B85-4 compared to B85-2 is also due to the chemical structure of both materials. The B85-4 foam is elaborated with a higher water content than B85-2. In addition, it is also important to notice that the presence of glycerol and sorbitol in B85-4 and B85-2, increases the cross-link density, which could also explain the higher mechanical properties of B85-4, compared to B100-4.

The transversal compressive stress-strain curves of the biobased foams are shown in Figure 2.14-b. The difference in mechanical properties observed between these biobased foams follows the same trend than that observed in L direction. However, Figure 2.14-b, shows that the stress-strain behavior is very different than the one in L direction, showing a clear anisotropic behavior of the biobased foams. An accurate examination of the slopes of stress-strain curves in the elastic region indicates that the Young's modulus measured in T direction is 10 times lower than the one in L direction, for B85-4 and B100-4. This ratio is around 14 and 6 for B85-2 and B100-2, respectively. This decrease is less pronounced for the yield stress. For B100-2, for example, the yield stress in T direction is just 3 times lower than the one determined in L direction.

Table 2.10 : Main mechanical properties and glass transition temperatures.

	REF	**B85-2**	**B85-4**	**B100-2**	**B100-4**
Apparent density (Kg/m^3)	30.7 ± 0.8	25.4 ± 1.6	23.1 ± 0.3	41.2 ± 3.5	25.3 ± 1.8
Storage modulus (MPa)	13.08	1.95	3.23	2.35	2.30
Glass transition temperature (°C)	194.0 ± 0.5	189.8 ± 0.5	184.2 ± 0.5	192.0 ± 0.5	185.3 ± 0.5
Longitudinal modulus (MPa)	8.5 ± 0.8	5.8 ± 0.3	5.2 ± 0.7	3.0 ± 0.3	2.1 ± 0.5
Transversal modulus (MPa)	1.80 ± 0.12	0.43 ± 0.08	0.52 ± 0.03	0.50 ± 0.02	0.21 ± 0.06

Longitudinal yield stress (MPa)	0.320 ± 0.030	0.063 ± 0.003	0.069 ± 0.003	0084 ± 0.005	0.052 ± 0.002
Transversal yield stress (MPa)	0.130 ± 0.004	0.016 ± 0.002	0.020 ± 0.003	0.023 ± 0.007	0.004 ± 0.0006

Conclusion

Open cell biobased PU foams were successfully elaborated from a sorbitol-based polyester polyol. A large panel of PU foams with different behaviors was obtained. The blowing agent, the polyols natures and contents demonstrated to be keys parameters on the modulation of the elaboration of the biobased foam in term of structures and properties. The obtained results are in total agreement with the viscoelastic properties determined by DMA. The Tg decreases in the case of the polyester polyol as consequence of the lowest OHV of the biobased polyol. In addition, for the biobased foams, chemical and physical blowing agents lead to variations in apparent density, closed cells content, and microstructure.

The PU foams present a large variation of the mechanical behaviors. The compression mechanical tests show that the mechanical properties were highly distinctive according to the L or T directions. These foams present unexpected results with a significant anisotropy which could bring some specific applications.

These biobased PUR foams should fulfill the requirements for a wide range of applications from furniture to thermal and acoustic insulation for building, as they display a limited low thermal conductivity on agreement with their structures. These biobased PU foams seem to especially fit for some novel markets with both thermal and sound insulation, added with an elastic behavior. In this way, additional tests such as the acoustics properties, ageing, durability linked to their ends-of life will be deeply investigated in a future work.

Acknowledgements

The authors thank the Alsace Region, Eurometropole, BPI-France, Soprema, and Tereos for their financial supports. The authors are also grateful to Adrien Baldi (LEM, Université de Lorraine, France) for sharing its compression testing equipment.

Keywords: Open cells, Sorbitol, Biobased Polyurethane Foams, Morphology, Mechanical properties

Text for the Table of Contents

Novel biobased polyurethanes foams were elaborate from a synthetized sorbitol based polyester polyol. The obtained foams kinetic and mechanical properties were deeply investigated. A direct relationship between the foams elaboration components and the mechanical properties was observed. Unexpected results were obtained, such as unveil anisotropic mechanical properties for these biobased foams.

References

Abe, H., 2006. Macromol. Biosci. 6, 469–486.

Andersons, J., Kirpluks, M., Stiebra, L., Cabulis, U., 2016. Mater. Des. 92, 836–845.

Arbenz, A., Perrin, R., Avérous, L., 2017. J. Polym. Environ.

Barrioni, B.R., de Carvalho, S.M., Oréfice, R.L., de Oliveira, A.A.R., Pereira, M. de M., 2015. Mater. Sci. Eng. C 52, 22–30.

Bernardini, J., Cinelli, P., Anguillesi, I., Coltelli, M.-B., Lazzeri, A., 2015. Eur. Polym. J. 64, 147–156.

Bozell, J.J., Petersen, G.R., 2010. Green Chem. 12, 539.

Brezny, R., Green, D.J., 1990. Acta Metall. Mater. 38, 2517–2526.

Celzard, A., Fierro, V., Amaral-Labat, G., Pizzi, A., Torero, J., 2011. Polym. Degrad. Stab. 96, 477–482.

Chattopadhyay, D.K., Sreedhar, B., Raju, K.V.S.N., 2006. J. Polym. Sci. Part B Polym. Phys. 44, 102–118.

Chen, W., Lu, F., Winfree, N., 2002. Exp. Mech. 42, 65–73.

Chuayjuljit, S., Maungchareon, A., Saravari, O., 2010. J. Reinf. Plast. Compos. 29, 218–225.

David Randall, steve Lee. The Polyurethanes book. Wiley.

Delebecq, E., Pascault, J.-P., Boutevin, B., Ganachaud, F., 2013. Chem. Rev. 113, 80–118.

D'Souza, J., Camargo, R., Yan, N., 2014. J. Appl. Polym. Sci. 131, n/a-n/a.

Fleurent, H., Thijs, S., 1995. J. Cell. Plast. 31, 580–599.

Furtwengler, P., Perrin, R., Redl, A., Avérous, L., 2017. Eur. Polym. J. 97, 319–327.

Gama, N.V., Soares, B., Freire, C.S.R., Silva, R., Neto, C.P., Barros-Timmons, A., Ferreira, A., 2015. Mater. Des. 76, 77–85.

Gandini, A., 2008. Macromolecules 41, 9491–9504.

Gibson, L.J., Ashby, M.F., 1997. Cellular Solids: Structure and Properties, Cambridge Solid State Science Series. Cambridge University Press.

Gibson, L.J., Ashby, M.F., Zhang, J., Triantafillou, T.C., 1989. Int. J. Mech. Sci. 31, 635–663.

Guelcher, S.A., Gallagher, K.M., Didier, J.E., Klinedinst, D.B., Doctor, J.S., Goldstein, A.S., Wilkes, G.L., Beckman, E.J., Hollinger, J.O., 2005. Acta Biomater. 1, 471–484.

Gupta, N., Ye, R., Porfiri, M., 2010. Compos. Part B Eng. 41, 236–245.

Gwon, J.G., Kim, S.K., Kim, J.H., 2016. Mater. Des. 89, 448–454.

Hofmann-1870-Berichte_der_deutschen_chemischen_Gesellschaft.pdf.

Holladay, J.E., Bozell, J.J., White, J.F., Johnson, D., 2007. DOE Rep. PNNL 16983.

Ionescu, M., 2005. Chemistry and technology of polyols for polyurethanes. Rapra Technology, Shawbury, Shrewsbury, Shropshire, U.K.

Jin, H., Lu, W.-Y., Scheffel, S., Hinnerichs, T.D., Neilsen, M.K., 2007. Int. J. Solids Struct. 44, 6930–6944.

Laurichesse, S., Huillet, C., Avérous, L., 2014. Green Chem. 16, 3958.

Maiti, S.K., Gibson, L.J., Ashby, M.F., 1984. Acta Metall. 32, 1963–1975.

Marcovich, N.E., Kurańska, M., Prociak, A., Malewska, E., Kulpa, K., 2017. Ind. Crops Prod. 102, 88–96.

Mark, J.E. (Ed.), 2009. Polymer data handbook, 2nd ed. ed. Oxford University Press, Oxford ; New York.

Modesti, M., Lorenzetti, A., 2001. Eur. Polym. J. 37, 949–954.

MUSTAFE, A.M.B.M., 2005. FTIR studies on 2K polyurethane paint.

Paruzel, A., Michałowski, S., Hodan, J., Horák, P., Prociak, A., Beneš, H., 2017. ACS Sustain. Chem. Eng. 5, 6237–6246.

Patterson, B.M., Henderson, K., Gilbertson, R.D., Tornga, S., Cordes, N.L., Chavez, M.E., Smith, Z., 2014. Microsc. Microanal. 20, 1284–1293.

Pawlik, H., Prociak, A., 2012. J. Polym. Environ. 20, 438–445.

Ramesh, N.S., Rasmussen, D.H., Campbell, G.A., 1994. Polym. Eng. Sci. 34, 1685–1697.

Rogulska, M., Kultys, A., Olszewska, E., 2013. J. Therm. Anal. Calorim. 114, 903–916.

Romero, R.R., 2005. J. Cell. Plast. 41, 339–359.

Saunders, J.H., Slocombe, R.J., 1948. Chem. Rev. 43, 203–218.

Septevani, A.A., Evans, D.A.C., Chaleat, C., Martin, D.J., Annamalai, P.K., 2015. Ind. Crops Prod. 66, 16–26.

Simon, J., Barla, F., Kelemen-Haller, A., Farkas, F., Kraxner, M., 1988. Chromatographia 25, 99–106.

Sorenson, W.R., 1959. J. Org. Chem. 24, 978–980.

Tan, S., Abraham, T., Ference, D., Macosko, C.W., 2011. Polymer 52, 2840–2846.

Ulrich, H., 1981. J. Cell. Plast. 17, 31–34.

Vitkauskiene, I., Makuska, R., Stirna, U., Cabulis, U., 2011. J. Cell. Plast. 47, 467–482.

Conclusion et perspectives du Chapitre

Dans le Chapitre 2 il a été montré que l'obtention de polyols polyesters linéaires à partir de sorbitol, de diacides et de diols était possible en contrôlant les conditions réactionnelles. Ceci a été fait en exploitant la différence de réactivités des groupements hydroxyles du sorbitol (primaire vs. secondaire) afin de concentrer les réactions d'estérifications principalement sur les hydroxyles primaires. Le suivi de la réaction par RMN a montré que c'etait un outil de contrôle efficace de la réaction afin de suivre la conversion des fonctions acides carboxyliques en fonctions ester et déterminer les temps de réaction de chaque étape d'estérification. Les polyols polyesters synthétisés ont été obtenus à partir de synthons biosourcés ou biosourçables (acide adipique, acide succinique, diols en C2 à C12). L'ensemble des réactions d'estérifications présentent des taux de conversion de plus de 80% des fonctions acides en travaillant dans un ratio stœchiométrique entre les fonctions alcools et acides. Travailler à la stœchiométrie permet de n'avoir qu'un seul sous-produit de réaction, l'eau, et de s'affranchir de l'élimination de réactifs excédentaires. Cela permet d'améliorer l'économie d'atome de la réaction.

La caractérisation de ces polyols a dévoilé plusieurs comportements inattendus ou déviances des méthodes de caractérisations pour des polyols de fonctionnalité élévée. La méthode traditionnelle de caractérisation de l'indice hydroxyles des polyols, basée sur un dosage en retour d'acide a montré certaines limitations, très certainement liées à l'encombrement stérique des fonctions hydroxyles secondaires portées par le sorbitol. Ainsi la méthode alternative de titration par RMN du phosphore s'est révélée être une technique de choix pour doser la teneur réelle en fonctions hydroxyles de ces polyols hautement fonctionnalisés. L'utilisation de ces deux techniques de dosage présente l'avantage de pouvoir doser la quantité de groupements hydroxyles accessibles (par titrage en retour) et les groupements hydroxyles présents dans le polyol (par RMN du phosphore). Le second point inattendu concernant ces polyols est l'évolution de la viscosité des polyols finaux à base de diadipate de sorbitol. En effet, l'évolution de la viscosité des polyols ne présente pas de lien direct avec la taille du diol terminal.

Dans ce Chapitre nous avons démontré notre capacité à élaborer des mousses polyuréthanes à partir du BASAB. Cela a permis de synthetiser des polyols à partir de 100% de ressource renouvelable, ce qui ameliore le contenu final des mousses en matière renouvelable. Les mousses polyuréthane peuvent atteindre 30% de contenu biosourcé en ne travaillant que sur le polyol.

L'étude sur les mousses polyuréthane dévoile également que la cinétique d'une mousse est fortement impacté par le choix de l'agent gonflant. Cet impact bien que relativement attendu est peu décrit dans la littérature. L'effet de l'agent gonflant sur le temps de crème des mousses polyuréthane est difficile à appréhender puisque selon les systèmes, des effets de retard ou d'accélération ont pu être observés. Il est par contre evident que la présence d'un agent gonflant physique tel que l'isopentane retarde les temps de gel et de hors poisse des mousses par rapport aux mêmes mousses contenant un agent chimique tel que l'eau. De plus la réaction de l'eau avec les isocyanates crée des liaisons amides et urées qui ont tendance à rigidifier les mousses polyuréthane. Dans la littérature, ce paramètre est bien trop souvent négligé.

CHAPITRE 3 : ELABORATION DE MOUSSES POLYISOCYANURATES A PARTIR DE POLYOLS BIOSOURCES

Introduction du Chapitre 3

Dans le Chapitre précédent il a été démontré que le BASAB est un très bon polyol polyester pour l'élaboration de mousses polyuréthanes, principalement de par sa faible viscosité. Il est également apparu que les catalyseurs employés pour la synthèse de mousses polyuréthanes étaient particulièrement sensibles à l'acidité résiduelle des polyols obtenus par réaction d'estérification. Il n'a été possible d'obtenir des systèmes expansés qu'avec le BASAB sous sa forme neutralisée. Les mousses polyuréthanes semi-rigides ainsi obtenues présentaient de bonnes cinétiques de moussage et des morphologies variables en fonctions des choix de formulation.

Dans le Chapitre 3, nous nous intéresserons au développement d'autres produits expansés spécifiquement adaptés pour l'isolation des bâtiments : les mousses polyisocyanurate rigides. L'obtention de telles mousses est plus délicate que l'obtention de mousses polyuréthanes, car les réactions mises en jeux sont plus complexes et plus exigeantes. Notamment, la trimérisation des isocyanates qui ne peut avoir lieu qu'à haute température ce qui impose de travailler avec des systèmes moussant fortement exothermiques, donc très réactifs. Néanmoins, il n'existe pas de température seuil à atteindre garantissant la bonne obtention du réseau polyisocyanurate. Il a donc été choisi de travailler avec une mousse polyisocyanurate de type industrielle, servant de référence, et de substituer progressivement le polyol polyester pétrosourcé par du BASAB. En conservant la formulation référence, les profils cinétiques et les propriétés des mousses polyisocyanurates obtenues sont étudiées en fonction du taux de substitution.

Le second volet du développement des mousses polyisocyanurates a donc été l'optimisation et l'adaptation de la formulation de telles mousses avec uniquement du polyol biosourcé. L'utilisation de catalyseurs de la même famille que celui de référence, mais présentant des masses molaires plus faibles a montré une activité interessante. Cependant, l'incorporation d'un petit diol theoriquement hautement réactif tel que l'éthylène glycol a été un moyen efficace pour améliorer les profils de moussage des systèmes polyisocyanurates.

L'ensemble des mousses présentées dans ce Chapitre ont pour vocation d'être utilisées comme matériau d'isolation. De ce fait, une caractérisation spécifique a été faite pour appréhender les propriétés de conductivités thermiques, de résistance à l'inflammabilité, et les propriétés mécaniques des mousses biosourcées par rapport à une référence pétrosourcée traditionnelle.

Les résultats de ces travaux sont présentés sous la forme d'une publication scientifique intitulée « Novel rigid polyisocyanurate foams from synthesized biobase polyester polyol with enhanced properties » soumise dans ACS Sustainable Chemistry & Engineering ». Ce Chapitre fait également l'objet de deux dépôts de brevet à l'international et national (PCT/IB2017/055110 & FR 18/00072).

Novel rigid polyisocyanurate foams from synthesized biobased polyester polyol with enhanced properties

Pierre Furtwengler[a], Rodrigue Matadi Boumbimba[b], Alexandru Sarbu[c], Luc Avérous[a]

[a]*BioTeam/ICPEES-ECPM, UMR CNRS 7515,*

Université de Strasbourg, 25 rue Becquerel, 67087 Strasbourg, Cedex 2, France

[b]*LEM3, UMR CNRS 7239, Université de Lorraine, 7 rue Félix Savart - BP 15082, 57013 -* METZ *CEDEX 03, France*

[c]*Soprema,*

14 rue de Saint-Nazaire, 67025 Strasbourg, Cedex 1, France

* Corresponding author: Prof. Luc Avérous, Phone: + 333 68852784, Fax: + 333 68852716, E-mail: luc.averous@unistra.fr

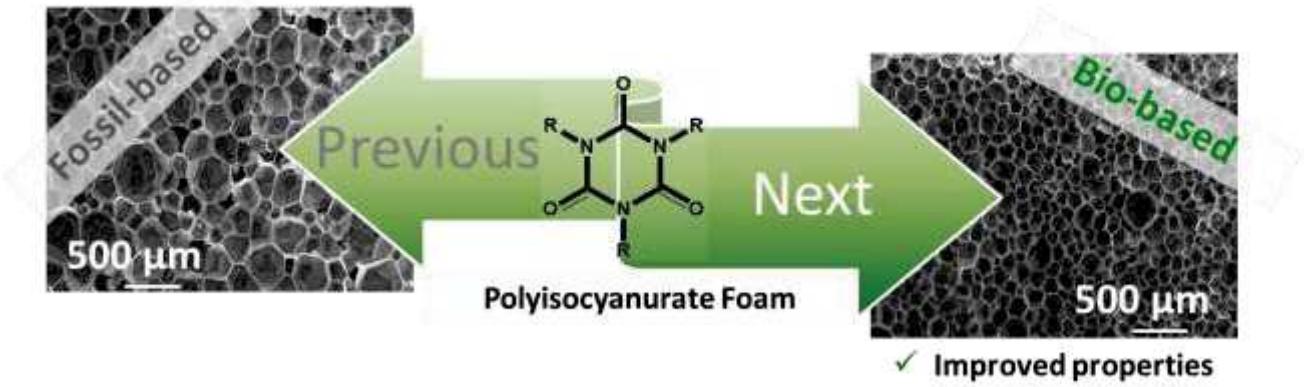

Submitted in ACS Sustainable Chemistry & Engineering

Abstract:

Novel rigid polyurethane-polyisocyanurate foams (PUIR) produced from different polyesters polyols, such as a conventional fossil-based polyester polyol (as a reference) and a synthesized sorbitol-based polyester polyol, have been fully investigated. PUIR foams were prepared by gradual substitution of the fossil-based by the biobased polyester polyol until a full substitution with adapted conditions. The foaming reactive process was monitored in continuous to evaluate the impact of the temperature, the isocyanate trimerization and the biobased polyester polyol, on the foaming rate. The different foams were fully characterized and compared. Foams with 25 wt% of biobased polyester polyol show an impressive increase of 96 and 142% of their respective longitudinal and transversal Young's modulus, compared to the equivalent fossil-based reference. Mechanical properties of such foams are linked to their morphologies as they presented significant smaller cell sizes compared to the reference, for a similar density (30 g/L). Foams thermal conductivity, degradation and flammability were also studied. Biobased foams show remarkable thermal conductivities till 22 mW/mK, whereas conventional values of equivalent fossil based foams range from 23 to 30 mW/mK. Foams prepared with 100% of biobased polyol present the highest thermal resistance.

Synopsis: Advanced rigid polyisocyanurates foams from renewable, eco-friendly synthesized, sorbitol based polyol for high performance insulation applications, were developed and analyzed.

Keywords: Sorbitol based polyol, rigid polyisocyanurate foams, small cells size, closed-cells foams, renewable foams, thermal analysis, mechanical properties

Introduction

Polyurethanes (PU) present versatile thermoplastics and thermosets architectures which are widely used in a large range of applications based on foams, membranes, coating for automotive, furniture, construction, footwear, acoustic and thermal insulation. PU are at the 6th rank among polymers based on their worldwide production, with a market of e.g., around 50 billion $ in 2016 (Cornille et al., 2017a; David Randall and steve Lee.; Gandini, 2008).

Nowadays the PU industry is strongly dependent on fossil-based components such as polyethers polyols obtained by alkoxylation (Arbenz and Avérous, 2014) or isocyanates, which are historically made from phosgene or diphosgene chemistry (Ozaki and others, 1972; Saunders and Slocombe, 1948; Sigurdsson et al., 1996). According to various legislations, especially Kyoto Protocol (Almer and Winkler, 2017; Gupta, 2016), it is now mandatory to reduce greenhouse gas emissions. This reduction can be brought by the improvement of the building insulation (L. Liu et al., 2017). Foams, based on closed cell materials, are performance insulation solutions. Different types of insulating gases can be entrapped in the closed cells to enhance the global insulation properties (Fleurent and Thijs, 1995). The mechanical characteristics of these foams assure their uses in applications where the rigidity is a key point.

Four main types of polymer-based foams are currently used in building insulation: polyurethane based foams (PUF), extruded expanded polystyrene (XPS), molded expanded polystyrene (EPS) and phenolic foam (PF), according to ISO 10456 standard. They present a thermal conductivity from 20 (mainly for PF) to 30 mW/mK, PUF and PF outperform other foams such as XPS or EPS (30-45 mW/mK)(Jelle, 2011).

Taking a closer look in the chemical structure of PUF, 2 types of architectures can be obtained with polyurethane (PUR) and polyisocyanurate (PIR), respectively. Polyisocyanurate-polyurethane (PUIR) foams are a mixed of both systems. PUR foams are based on the polyaddition of polyfunctional polyols and polyisocyanate to obtain thermoset architectures. Compared to PUR, PIR systems are synthesized with different conditions (temperature, catalyst,), when the isocyanate/hydroxyl groups ratio is around 3:1. PIR foams are based on the trimerization of di-isocyanates at high temperature into isocyanurate rings (Slotta and Dressler, 1930b) (Figure 3.1) in presence of specific catalysts (Silva and Bordado, 2004). Then the PIR structure is obtained by polyaddition between these rings and polyols. PUIR foams network is based on both chemistry and synthesized according different steps. In a first step, the polyol reacts with the polyisocyanate to form the PUR systems. Then under the exothermic condition, at higher temperature and with a specific catalyst system, polyisocyanates in excess trimerize into isocyanurate rings to form chemical crosslinks points with the residual polyols. At a certain point, the high crosslink density of PIR foams could constitute their main drawback, since it could induce a high fragility (Reymore et al., 1975). However, the PIR friability is largely balanced by their improved properties compared to a more conventional PUR foam, due to their higher thermal and fire resistances (Dick et al., 2001). The thermal stability of isocyanurate groups varies from 365 to 500 °C (Reymore et al., 1975) compared to 120 to 250 °C (Simon et al., 1988) for the urethane, according to their chemical environment. The elaboration of PUIR is a good balance between both constitutive systems. Then, PUIR are now attractive to fulfill the latest requirements in building insulation. However we can notice that only few researches have been carried out on biobased PUIR. Only very recently, rapeseed oil, crude glycerol, castor oil, microalgae and tannin based polyols were reported in the fabrication of biobased PUIR foams (Arbenz et al., 2016, 2017; Hejna et al., 2017a; Prociak et al., 2017).

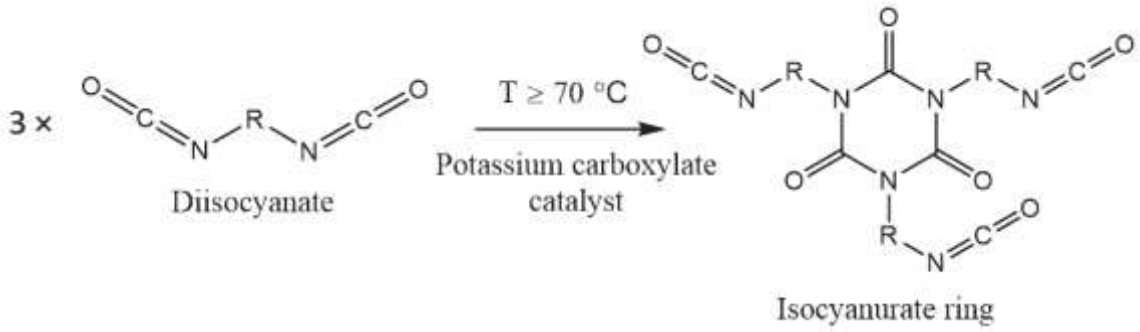

Figure 3.1: Diisocyanate trimerization in presence of potassium carboxylate catalyst

PUIR foams properties are mainly related to their morphologies and structures, which are linked to their thermal conductivities and mechanical behavior. It is well-established that thermal properties of foamed materials are mainly dependent on the closed cell content, the morphology, and the entrapped gas (Fleurent and Thijs, 1995). The literature shows a lot of examples on the relationships between mechanical properties and densities for a large range of polymer foams (Guan and Hanna, 2004; Mosiewicki et al., 2009). However, such studies are rather rare with PUIR systems. The mechanical properties of PUIR foams have not been deeply investigated. Andersons et al. (Andersons et al., 2016) worked on partially biobased, low density, and closed cells polyisocyanurate foams. They studied the anisotropy of the foams stiffness and strength. They showed that the ratios of Young's moduli and strength according to the rise and transverse directions were around 3 and 1.4, respectively.

The aim of this study was to fully investigate novel biobased PUIR foams prepared with a synthesized sorbitol-based polyester polyol vs. a conventional fossil based polyester polyol, used as a reference. Different foams were produced by gradual replacement of the fossil-based polyester polyol with the biobased polyol, until a full substitution. The impact of the addition of biobased polyester polyol was then investigated on the foaming process and reactivity. The foaming behavior, the foam parameters, the thermal degradation and the fire resistance were studied and compared in connection with the formulation. The study of the mechanical behavior has been particularly focused in this study. Shore hardness, quasi-static compression tests, in both transversal and longitudinal directions towards the foam rising direction, were performed. Results were correlated with cell morphology, apparent density, and the ratio of closed cells determined by electronic microscopy. Moreover, the thermal conductivities of all foams were investigated and compared.

Materials and methods

The polyisocyanate was polymeric 4,4'-methylenebis(phenyl isocyanate) (named as pMDI, Ongronat 2500 from BorsodChem). Various catalysts such as the N, N-dimethylcyclohexylamine (named as DMCHA) from BorsodChem, the 1,3,5-tris(3-[dimethylamino]propyl)-hexahydro-s-triazine (named as triazine, Tegoamin C41 from Evonik), potassium propionate (named as KP, Struksilon KPROP14 from Schill+Seilacher GmbH, Germany), bis(2-dimethylaminoethyl)ether (named as BDMAEE, trade name Lupragen N205 from BASF), 15% wt. potassium 2-ethylhexanoate solution (named as KE, trade name K-ZERO 3000 from Momentive) were used. The flame retardant was Tris (1-chloro-2-propyl) phosphate (TCPP from Shekoy Chemicals Europe). The surfactant was polyether polysiloxane based (named as PDMS, TEGOSTAB® B84501 from Evonik). Ethylene glycol (EG) was obtained from Alfa Aesar (purity 99%). Isopentane from Inventec, was used as physical blowing agent. All these chemicals were used as received without further purification.

The fossil polyol was an aromatic polyester polyol obtained from phthalic anhydride (Stepanpol® PS-2412, from Stepan). This polyol was used as a conventional reference and further referred as the fossil-based polyol. The biobased polyester polyol (BASAB) was synthesized from sorbitol according to a multistep protocol previously described (Furtwengler et al., 2017). Briefly, BASAB polyester polyol results from a two-step esterification between sorbitol, adipic acid and 1,4-butanediol (1,4 BDO). The first step is based on the reaction of one molar equivalent of sorbitol with two molar equivalents of adipic acid. The second step consist of the addition of one molar equivalent of 1,4 BDO in respect to the residual carboxylic groups. The reaction was performed in bulk without catalyst at 150°C on agreement with green chemistry principles. This specific process results in a linear polyester polyol. The main properties of both polyols are compared in Table 3.1.

Table 3.1: Comparison of the fossil-based and BASAB polyols properties

Polyester Polyol	Hydroxyl-value (mg KOH/g)	Acid-value (mg KOH/g)	Viscosity (25 °C, mPa.s)	Primary hydroxyl	Secondary hydroxyl	Surface tension (mN/m)
Fossil-based polyol	230-250	1.9-2.5	4,000	2	0	33.6 ± 0.9
BASAB	490-510	Inf. 3	14,000	2	4	40 ± 0.8

Preparation of PUIR foams

Isocyanate/hydroxyl molar ratio (NCO/OH) was kept at 3.2, in all PUIR formulations. To determinate the isocyanate quantity, all reactive hydroxyl groups are taken into account, *i.e.* polyols, water and some solvents used in the catalysts composition. A blend containing polyols, catalysts, surfactant (PDMS), flame retardant

(TCPP), blowing agent (isopentane) and water was prepared. In each formulation (Table 3.2), water, TCPP, and surfactants were kept constant at 0.9, 15, and 2.5 parts by weight (pbw), respectively. The total amount of polyol was kept at 100 pbw. Based on the ideal gas law, the total volume of blowing agent was kept constant in respect to the total amount of foaming material. The mixture was mechanically stirred until obtaining a fine white emulsion with the incorporation of the blowing agent. The temperatures of the different components were adjusted to 20 °C. Then, the right amount of polyisocyanate was quickly added with a syringe into the emulsion. The whole reactive mix was vigorously stirred for 5 s. Then, the foam rose freely in a 250 mL disposable beaker at room temperature (controlled at 20 °C) or in the Foamat device. The main characteristic reaction times i.e., cream time, gel time and tack free time were recorded. Before further analysis, the foam samples were kept at room temperature for three days to obtain a full structural and dimensional stability, without withdrawal.

Table 3.2: Detailed formulations for the elaboration of the PUIR foams.

		REF	PU-90/10/0-KE	PU-75/25/0-KE	PU-65/35/0-KE	PU-55/45/0-KE	PU-35/65/0-KE	PU-0/85/15-KE	PU-0/85/15-KP
Molar ratio	NCO/OH	3.2	3.2	3.2	3.2	3.2	3.2	3.2	3.2
Polyol (pbw)	Fossil-based polyol	100	90	75	65	55	35	0	0
	BASAB	0	10	25	35	45	65	85	85
	EG	0	0	0	0	0	0	15	15
Catalyst (%wt)	KE	0.12	0.12	0.12	0.12	0.12	0.12	0.17	0
	Triazine	0.08	0.08	0.08	0.08	0.08	0.08	0.21	0.11
	BDMAEE	0.03	0.03	0.03	0.03	0.03	0.03	0.08	0.22
	KP	0	0	0	0	0	0	0	0.97
Surfactant (pbw)	PDMS	2.5	2.5	2.5	2.5	2.5	2.5	2.5	2.5
Flame retardant (pbw)	TCPP	15	15	15	15	15	15	15	15
Blowing agent (pbw)	Water	1	1	1	1	1	1	1	1
	Isopentane	22	23	25	27	29	32	42	44
	Total blowing agent content in respect to the total foam composition (%)	13.0	13.0	13.0	13.0	13.1	13.0	12.7	12.7

Some foams were prepared with a partial substitution of the fossil-based polyester polyol by the BASAB polyol. Substitution ratio were from 0 (reference, REF) to 65 wt%. PUIR foams were labeled according to fossil-based polyol (wt%)/BASAB (wt%)/EG (wt%) ratio as REF, PU-90/10/0-KE, PU-75/25/0-KE, PU-65/35/0-KE, PU-55/45/0-KE, PU-45/55/0-KE and PU-35/65/0-KE. Whereas, 100 wt% biobased polyol foams were labelled PU-0/85/15-KE, and PU-0/85/15-KP. Detailed formulations are presented in Table 3.2.

Characterizations

Thermogravimetric analyses (TGA) were performed using a TA Instrument Hi-Res TGA Q5000 (TA Instruments, US) under reconstituted air (flow rate 25 mL/min). Samples of 1-3 mg were heated from room temperature to 700 °C (10 °C/min). The main characteristic degradation temperatures are those of the maximum of the weight loss derivative curve (DTG) ($T_{deg,\ max}$) and the characteristic temperatures at which 50% ($T_{deg50\%}$) and 100% ($T_{deg100\%}$) weight loss were reported.

Infrared spectroscopy was performed with a Fourier-transform infrared spectrometer Nicolet™ 380 (Thermo Scientific, US) used in reflection mode equipped with an ATR diamond module (FTIR-ATR). An atmospheric background was collected before each sample analysis (64 scans, resolution 4 cm^{-1}). All spectra were normalized on the C-H stretching peak at 2950 cm^{-1}.

Foams temperature, expansion heights, rates, density and pressure were recorded using a Foamat FPM 150 (Messtechnik GmbH) equipped with cylindrical recipients, 180 mm height and 150 mm in diameter, an ultrasonic probe LR 2-40 PFT recording foaming heights, a NiCr/Ni type K thermocouple, and a pressure sensor FPM 150. The data was recorded and analyzed with a specific software.

Closed cell content was determined using an Ultrapyc 1200e from Quantachrome Instruments (US) based on the technique of gas expansion (Boyle's law). Cubic foam samples (around 2.5 × 2.5 × 2.5 cm^3) are cut for the first measurement then the sample was sectioned once more into eight pieces and the measurement was run again. The second run corrects the content of closed cells based on closed cells which were damaged due to the sample cutting. Measurements were performed according to EN ISO4590 and ASTM 6226 techniques.

Foam fire resistance was evaluated according to EN ISO 11925-2 standard method. This flammability test consists of a small direct flame (20 mm high) exposure of plane foam samples for 15 s. This flammability test is evaluated by measuring of the maximum flame propagation on the plane surface of the foam. The test result is positive if the flame propagation stops before reaching 15 cm high on the foam sample.

Foam cell morphology was observed with a Jeol JSM-IT100 (Japan) emission scanning electron microscope (SEM). Cubic foam samples were cut with a microtome blade and were analyzed in two characteristic orientations: parallel and perpendicular to the foam rise direction. Using ImageJ software (Open source processing program) cell average size was measured as the cell aspect ratio defined by eq.1(Andersons et al., 2016).

$$R = \frac{1}{n}\sum_{i=1}^{n}\frac{D_F^{max}}{D_F^{min}} \qquad (1)$$

where D_F^{max} and D_F^{min} are maximum and minimum cell Feret diameters, n is the number of measured cells for a given sample.

The foam hardness was measured with a Shore 00 Hardness Tester from Hilderbrand (Germany) according to the ASTM D 2240 standard. Each sample was tested ten times, the measurements average value and standard deviations were determined.

The quasi-static compression tests were carried out with an Instron compression testing machine (E1000, USA), equipped by load sensor of 1 kN, at room temperature and at a constant strain rate of 2.5 mm/min. The cubic samples used for compression tests have dimensions of 25 × 25 × 25 mm^3. Samples were tested in the longitudinal direction (corresponding to the rise expansion) and in the transversal direction. The Young's modulus was defined as the slope of stress-strain curves in the elastic region and the yield stress as the first maximum of the stress strain curve.

Thermal conductivity was measured from the conduction of heat flux. Typically, the setup consists of a heating element with two thermocouples to determine the temperatures on the front and back faces. The device is also equipped with sensors dedicated to the measurement of the heating time and the cycle time. The heat and cycle times are used to correct the maximum conduction heat flux, which is necessary for the determination of the thermal conductivity coefficient, by the means of the Fourier law, used in steady state

thermal conduction. Plates of different materials, with dimensions of 300 × 400 × 3 mm^3, have been used for the determination of the thermal conductivity coefficient.

Results and discussions

Study of the compatibility between the polyols

The Hansen solubility parameters for both polyols were determined according to a previously reported protocol (Zhang and Kessler, 2015) (briefly described in the supporting information), by qualitatively measuring their dissolutions in fourteen well-known solvents (detailed inTable SI 7, in Annex).

Prior to any substituted foam formulation, the compatibility of both polyols was investigated. Figure SI 37 (in Annex) shows the predicted solubility spheres of both polyols according to the three parameters determined by Hansen with (i) the dispersion parameters (δ_d), (ii) the polar parameters (δ_p) and (iii) the hydrogen bonding parameters (δ_h). It clearly appears that both spheres are largely overlapped. The spheres centers are separated by a distance inferior to their respective radius. From these observations, we can assume that both polyols are compatible and should undergo a stable emulsion preparation prior foaming.

PUIR foam reaction times and kinetics

The fossil-based PUIR foam reference (REF) exhibits short reaction times, as presented in Table 3.3. Recorded characteristic times for REF were 10, 60 and 148 s for the cream, gel and tack free times, respectively. The PUIR foam (Figure 3.4-a) presents a typical collar due to the second expansion step induced by the isocyanate trimerization. This second step is also visible on Foamat measurements, presented in Figure 3.2-b. The foam expansion rate starts to decrease after 30 s of reaction and increases again after 60 s of reaction. The foam temperature curve (Figure 3.2-a) also shows a local plateau at 50 s with an increase up to 150 °C, which is linked to the isocyanate trimerization. The same phenomenon is visible in Figure 3.2-c. After 50 s, a change in the slope is observed and the normalized height increases rapidly from 80 to 100% with the isocyanate trimerization.

Figure SI 38 (in Annex) presents the reference times of substituted foams. Cream times slightly increase with the increase of BASAB content, caused by the lowest reactivity of the secondary hydroxyl (Tan et al., 2011b). The gel times are similar to REF from PU90/10/0-KE to PU-65/35/0-KE. However, the tack free time is subject to variations. When the BASAB content increase, the tack free time decreases, close to the gel time. This reduced time gap between the gel and the tack free times indicate that biobased PU foams network polymerization is clearly enhanced due to the higher BASAB functionality.

Figure 3.2-a represents the foam temperature as a function of time. The exothermicity of the reaction between polyol and isocyanate is higher for REF and PU-90/10/0-KE. Then, it gradually decreases for higher substitution ratios due to the lower reactivity of the secondary hydroxyl of the BASAB polyol (Tan et al., 2011b). All temperature curves show an inflection point around 70 °C followed by an increase in temperature. This is related to the exothermicity of the catalyzed isocyanate trimerization reaction and the networks formation (Schwetlick and Noack, 1995). Figure 3.2-b represents the foam rising rate. The foaming rate is influenced by the gas expansion. It was thus expected that its evolution was correlated to the foam temperature evolution. The increase in biobased polyol content delayed the temperature increase and then decelerate the foam expansion. Thus, the foaming rate peak become wider and its maximum decreased from 3.5 (REF), to 1.5 mm/s (PU-35/65/0-KE). The second increase of the foaming rate related to the isocyanate trimerization, is consequently delayed. The evolution of foams normalized height (H/Hmax) as a

function of time is presented in Figure 3.2-c. The second increase of normalized height is linked to the foaming rate and the isocyanurate trimerization. For up to 35 wt% (PU-65/35/0-KE) of biobased polyol substitution, the normalized height increases linearly. Then, when the isocyanate trimerization occurs, we can show a change of this evolution. For the others samples, the normalized height presents a kind of plateau before the inflection, due to the trimerization delay as previously observed on the foaming rate.

Based on previous foaming profile parameters, we established that the foaming rate was decreasing for PU-35/65/0-KE compared to REF. To improve the foaming step, it was needed to increase the foaming temperature when higher amounts of BASAB were used. The chosen strategy was to use a very reactive small diol i.e. EG, to promote an initial exothermicity boost of the reaction. We also used a catalyst with a lower molar mass to increase its mobility and activity in the media. The optimized formulation PU-0/85/15-KE and PU-0/85/15-KP are detailed in Table 3.2.

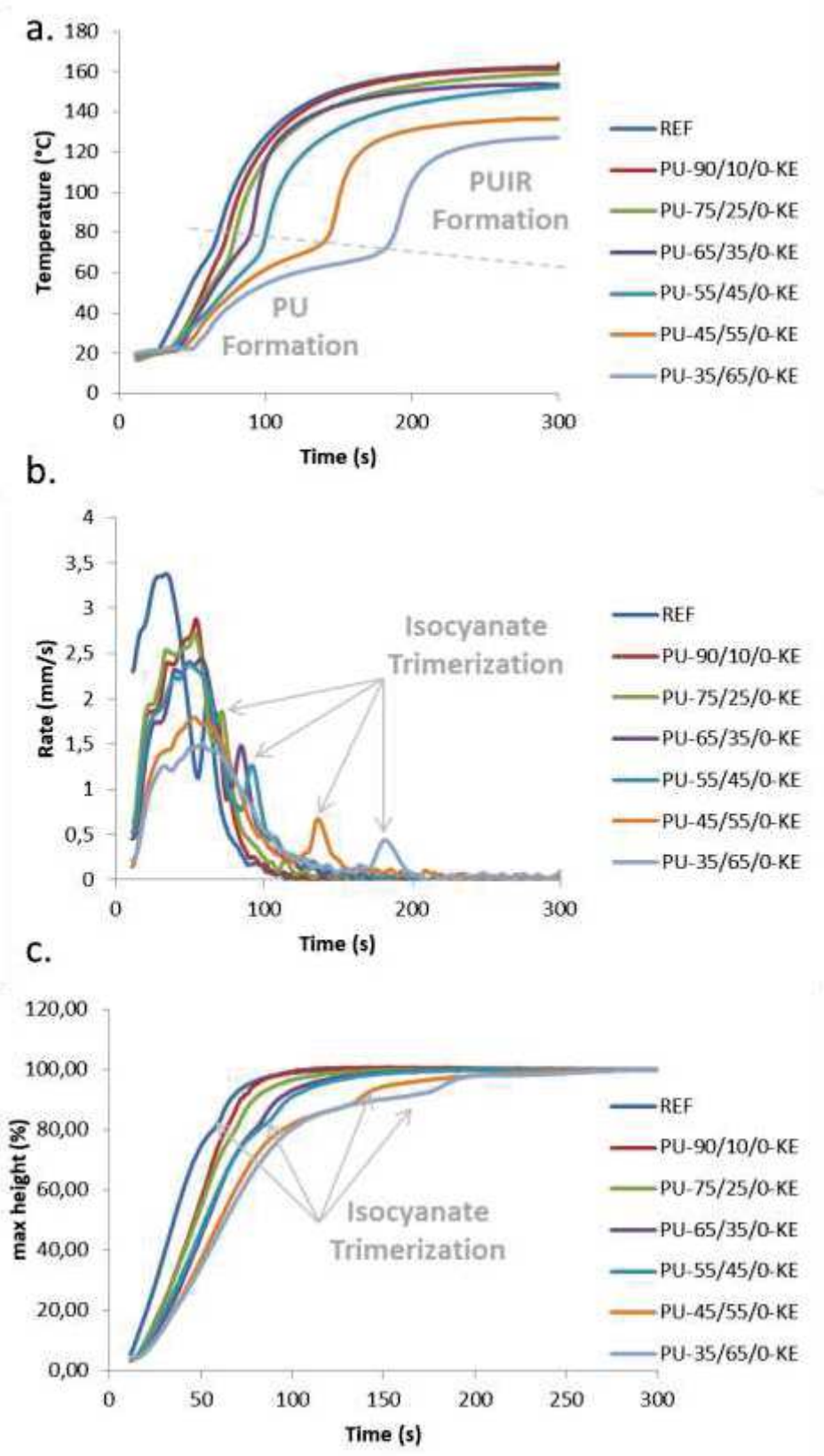

Figure 3.2: PUIR foaming. Evolution of (a) temperature, (b) foaming rate, and (c) normalized height (H/Hmax) vs. time.

Table 3.3: Characteristic time of REF, PU-0/85/15-KE and PU-0/85/15-KP foams

		REF	PU-0/85/15-KE	PU-0/85/15-KP
Characteristic times	Cream time (s)	10	12	11
	Gel time (s)	60	134	82
	Tack free time (s)	148	166	120

PU-0/85/15-KE foam was catalyzed with the same catalyst as REF (KE), but with a higher amount, whereas PU-0/85/15-KP was catalyzed by KP. Table 3.3 shows PU-0/85/15-KE and PU-0/85/15-KP characteristic times. PU-0/85/15-KE cream time is similar to REF, but the gel and the tack free times show a delay of 74 and 18 s, respectively. PU-0/85/15-KP cream time is equivalent than REF. The tack free time is even largely faster than REF. But, the gel time is a little bit slower.

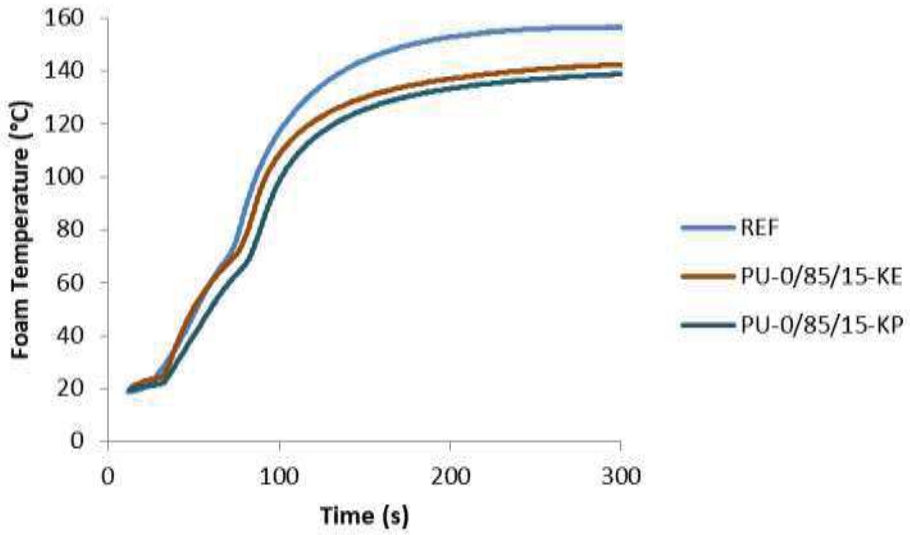

Figure 3.3: Evolution of the foam temperature vs. time for REF, PU-0/85/15-KE and PU-0/85/15-KP

However, the most important differences between these foams with different formulations can be macroscopically shown. Figure 3.4-c depicts a PU-0/85/15-KP formulation with a smooth surface and a similar top skin as REF, whereas PU-0/85/15-KE (Figure 3.4-b) presents an irregular surface. The main hypothesis is based on the longer gel time of 134 against 82 s for PU-0/85/15-KE and PU-0/85/15-KP, respectively. Since these three foams are based on PUIR, a longer gel time translates a longer time to reach a same polymerization degree. Under the expansion gas pressure, this longer time tends to increase the cell walls collapse and then generate visible cracks and bubbles on the foam surface. According to these different observations, KP catalyst seems to be the most appropriate catalyst to increase the biobased foam kinetic, to obtain a right foam morphology.

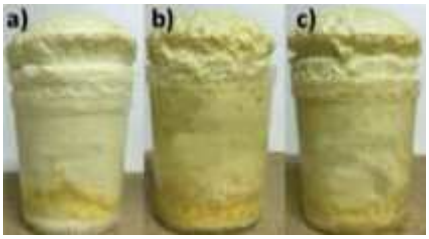

Figure 3.4: Images of the PUIR foams (a) REF, (b) PU-0/85/15-KE and (c) PU-0/85/15-KP (from left to right)

Figure 3.3 shows PU-0/85/15-KE and PU-0/85/15-KP temperature profiles. The foams temperature evolutions are similar than REF. The exothermicity which is linked to the polyisocyanate trimerization was less delayed compared to previous results obtained from PU-45/55-KE and PU-35/65/0-KE (Figure 3.2-a). In connection with previously observed characteristic times (Table 3.3), it is obvious that the KP catalyst is more efficient than the KE at similar temperature. Thus, the more promising results are obtained with a combination of two biobased polyols: BASAB and EG with a ratio of 85 and 15 wt%, respectively. Such a formulation presents a high and final biobased content.

Closed cell content and Foams morphologies (SEM)

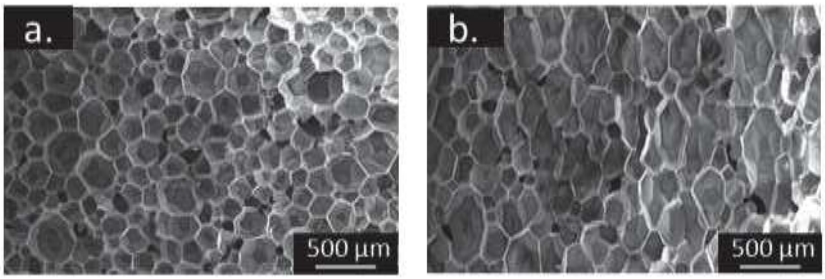

Figure 3.5: REF PUIR foam SEM images, magnify x40 (see scale bars). a. in transversal direction to the foam rise, b. in the foam rise direction (from bottom to top).

Figure 3.5 shows the SEM images of REF foam in the transverse and longitudinal directions compared to the foam rise. A typical honeycomb structure in the transverse direction is clearly observed. The cell stretch in the longitudinal direction is characteristic of partially free foaming process performed in an open cylindrical container (Hawkins, 2005). This is really visible through the anisotropic coefficient R of all PUIR foams presented in Table 4. R coefficients of the REF are close to 2.0 in the longitudinal direction (oval shape), whereas in the rise direction, R is around 1.2 (close to spherical cell shape). Surprisingly, the introduction of BASAB polyol in the formulation has a great influence on the cell size as observed on SEM images presented in Figure SI 39 (in Annex). The minimum cell diameter drops from 275 to 155 µm in the transversal direction for PU-75/25/0-KE compared to REF (Table 3.4). The same phenomenon is observed in longitudinal direction (Table 3.4). With a substitution from 35 to 45 wt%, the cells size increases compared to PUIR foam with 25 wt% of substitution. Nevertheless, foams with 25 to 45 wt% still have smaller cell sizes than REF (Table 3.4). Above 45 wt% of substitution, PUIR foams (PU-45/55/0-KE, PU-35/65/0-KE, PU-0/85/15-KE and PU-0/85/15-KP) present larger cells compared to REF in all directions (Table 3.4). The lowest temperatures are reached for the foaming of PU-45/55/0-KE, PU-35/65/0-KE, PU-0/85/0-KE and PU-0/85/15-KP (Figure 3.2 and Figure 3.3), which induce a growing delay before the isocyanate trimerization, and then lower reaction rates (e.g., longer gel time). The resulting longer reaction time linked to expansion, induces higher coalescence phenomena before the stabilization/"freezing" of the morphology through the

final polymerization of the network, inducing larger cells.

Figure 3.6 shows the cell size distribution of PUIR foams in transversal direction for substitution of the fossil-based polyester polyol until PU-55/45/0-KE. Cell size distributions are narrow and average cells diameters decrease gradually with the increase of BASAB content in the foam up to PU-65/35/0-KE. The PUIR foam presenting a substitution ratio of 45 wt% (PU-55/45/0-KE), marks a change of trend compared to PU-65/35/0-KE, since the cells diameters increase. Figure SI 40 (in Annex) shows the cell size distributions of the PUIR foams in both, longitudinal and transversal directions. Compared to REF, from PU-90/10/0-KE to PU-55/45/0-KE, the foams present a narrower cell distribution. In addition, their average cells sizes are smaller than REF. Foams with a BASAB content higher than 45 wt% present larger cells compared to REF, on agreement with the change of trend observed on PU-45/55/0-KE.

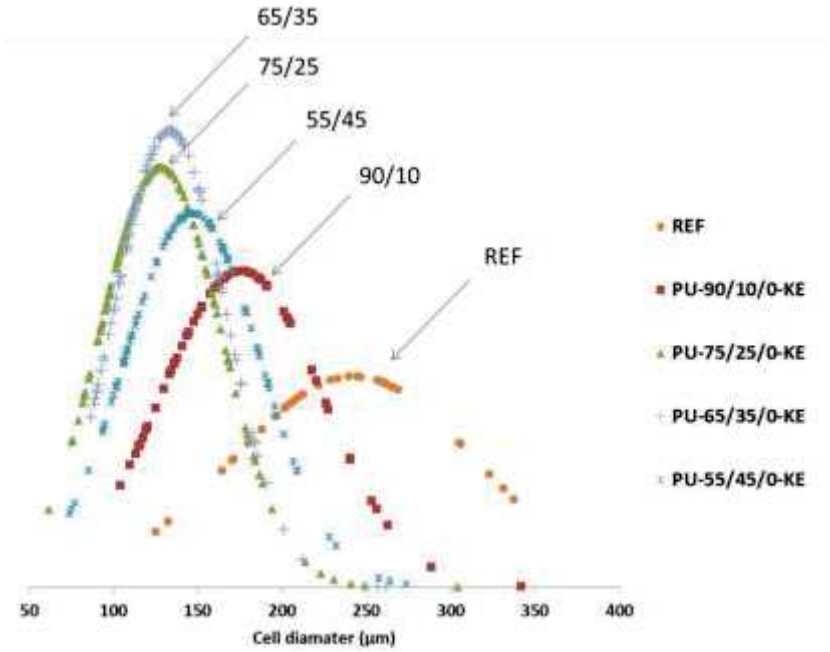

Figure 3.6: Cells diameters distribution in transversal direction to the foam rise of diffrent PUIR foams

Three main factors were identified to explain the cell size decrease when BASAB polyol was introduced up to PU-65/35/0-KE (all SEM images are shown in Figure SI 39, in Annex). First, the introduction of BASAB in the formulation increases the medium viscosity (see Table 3.1). It is known that decreasing the medium viscosity generally leads to larger and less regular cells. Instead, a viscosity increase induces a cells size decrease by limiting the cells coalescence and the expansion (Chuayjuljit et al., 2010; Fan et al., 2013; Tan et al., 2011b). Increasing viscosity also increases the shear rate in the mixing step of the foam components. The shear rate increase introduces more air bubbles to the initial emulsion with smaller average size, which will act as germination sites with the blowing agent (Minogue, 2000; Ramesh et al., 1994). Moreover, the surface tension of the BASAB (Table 3.1) is slightly higher than the fossil-based polyol' one. This increase slows down the bubble growth according to Laplace equation (2) as the pressure inside the bubble must overcome the surface tension to grow (Minogue, 2000).

$$\Delta P = \frac{2\gamma}{r} \quad (2)$$

Where ΔP is the bubble gas pressure excess, γ the surface tension and r the bubble radius. Then, the higher functionality of BASAB could lead to a faster structural organization of the cell wall by decreasing the gel time, preventing cells coalescence resulting with higher cell sizes (Septevani et al., 2015).

Foams closed cell content are presented in Table 3.5. REF and PU-90/10/0-KE to PU-65/35/0-KE present closed cell contents higher than 90 %. Closed cell content of foam samples PU-55/45/0-KE, PU-45/55/0-KE and PU-35/65/0-KE drop to 87, 47, and 28%, respectively. Additionally, PU-0/85/15-KP and PU-0/85/15-KE have a respective closed cell content of 85 and 86 %. These foams present lower foaming temperatures and slower reaction times according to aforementioned results. This means that the cell walls are collapsed during the foam expansion step (Septevani et al., 2015).

Table SI 8 displays the Shore hardness data. Shore results can be divided into two main populations. PU-90/10/0-KE to PU-65/35/0-KE, present values similar to REF. The Shore results are similar to REF for PU-90/10/0-KE to PU-55/45/0-KE. The others Shore hardness are slightly lower indicating a rigidity decrease.

Table 3.4: Feret diameters and anisotropic coefficients R in longitudinal and transversal directions, for PUIR foams.

		REF	PU-90/10/0-KE	PU-75/25/0-KE	PU-65/35/0-KE	PU-55/45/0-KE	PU-45/55/0-KE	PU-35/65/0-KE	PU-0/85/15-KE	PU-0/85/15-KP
Longitudinal direction	Feret max, D_F^{max} (µm)	408 ± 117	269 ± 70	254 ± 66	251 ± 59	301 ± 93	728 ± 218	938 ± 260	524 ± 215	521 ± 123
	Feret min, D_F^{min} (µm)	223 ± 44	145 ± 34	118 ± 22	126 ± 27	147 ± 37	320 ± 77	421 ± 87	295 ± 112	298 ± 67
	R= D_F^{max} / D_F^{min}	1.83	1.86	2.15	2.00	2.05	2.28	2.23	1.78	1.75
Transverse direction	Feret max, D_F^{max} (µm)	275 ± 72	208 ± 47	155 ± 39	158 ± 39	183 ± 45	495 ± 126	643 ± 189	386 ± 123	448 ± 122
	Feret min, D_F^{min} (µm)	242 ± 72	176 ± 48	128 ± 36	134 ± 33	147 ± 40	392 ± 110	518 ± 147	324 ± 116	347 ± 122
	R= D_F^{max} / D_F^{min}	1.14	1.18	1.21	1.18	1.24	1.26	1.24	1.19	1.29

Foams properties and performances

Table 3.5: All formulated PUIR foams apparent density and close cells content

	REF	PU-90/10/0-KE	PU-75/25/0-KE	PU-65/35/0-KE	PU-55/45/0-KE	PU-45/55/0-KE	PU-35/65/0-KE	PU-0/85/15-KE	PU-0/85/15-KP
Apparent density (kg/m^3)	31.1	30.2	32.3	32.9	32.1	36.1	39.8	33.8 ± 2	32.8 ± 0.8
Closed cell content (%)	95	94	92	92	87	47	28	86	85

n.d: not determined

Apparent density values presented in Table 3.5 are similar for all PUIR formulations, except for samples PU-45/55/0-KE and PU-35/65/0-KE. Since the blowing agent content is maintained constant for each formulation, densifications of PU-45/55/0-KE and PU-35/65/0-KE are linked to their lower foaming reactivity, resulting in lower foams temperatures. These latter decrease with the blowing agent expansion rates.

FT-IR spectra of the foams are presented in Figure SI 41-a, b (in Annex). All foams present characteristic peaks, such as stretching vibration of N-H groups at 3400-3200 cm^{-1}, and C=O stretching vibration at 1705 cm^{-1} for urethane functions (Barrioni et al., 2015). Signals located at 2955 cm^{-1} and 2276 cm^{-1} are respectively attributed to the C-H bond stretching of the polyurethane backbone and the residual unreacted NCO groups (Guelcher et al., 2005). The signal at 1596 cm^{-1} corresponds to Ph-H stretching in the phenyl groups from the polymeric polyisocyanate (Modesti and Lorenzetti, 2001). The N-H groups bending signal(Jin et al., 2007) is located at 1509 cm^{-1}. The C-O stretching is at 1220 cm^{-1}. The strong signal at 1408 cm^{-1} is assigned to the isocyanurate rings (Hejna et al., 2017a; Sheridan and Haines, 1971), typical of PUIR foams.

Thermal stability of PUIR foam samples were investigated by thermogravimetric analysis. Figure SI 42 (in Annex) shows TGA and DTG curves of all PUIR foams. All PUIR foams present a classical two-step weight loss (Sheridan and Haines, 1971). PUIR foams with higher BASAB contents (PU-45/55/0-KE, PU-35/65/0-KE, PU-0/85/15-KE and PU-0/85/15-KP) show a higher thermal stability compared to REF. Table 3.6 shows the temperatures at the maximum of the weight loss derivative curve: $T_{deg\ max1}$ and $T_{deg\ max2}$. $T_{deg\ max1}$ are in the 200 – 300 °C range. $T_{deg\ max2}$ is observed around 500 °C for all substituted PUIR foams. Whereas, the $T_{deg\ max2}$ of PU-0/85/15-KE and PU-0/85/15-KP foams appears at 538 and 534 °C, respectively. In addition, a shoulder appears in the DTG curve at above 600 °C. $T_{deg\ max1}$ corresponds to the urethane bond decomposition. The urethane bond decomposition mechanism is generally described as three simultaneous processes such as (i) the dissociation of isocyanate and alcohol, (ii) the formation of primary and secondary amines and (iii) the olefin formation (Javni et al., 2000; Reulier et al., 2016). $T_{deg\ max2}$ is more pronounced than the first $T_{deg\ max1}$ and it is assigned to the dual degradation of isocyanurate and carbon-carbon bond cleavage (Sheridan and Haines, 1971). The first weight loss is less important due to the isocyanurate groups. Isocyanurate groups are more thermally stable than urethane due to the absence of labile hydrogen and the corresponding degradation is then mainly due to carbon-carbon bond cleavage (Chattopadhyay and Webster, 2009; Reymore et al., 1975). In the specific case of PU-0/85/15-KE and PU-0/85/15-KP, the higher $T_{deg\ max2}$ is attributed to their higher BASAB contents. The higher OH value of BASAB compared to the fossil-based polyol, increases the formation of urethane functions and the crosslinking of the PUIR network (Javni et al., 2000; Septevani et al., 2015).

Table 3.6 presents two temperatures corresponding to 50 % ($T_{deg\ 50\%}$) and 100 % ($T_{deg\ 100\%}$) of PUIR foams weight loss, respectively. $T_{deg\ 50\%}$ and $T_{deg\ 100\%}$ are similar for all PUIR foams formulations, excepted for PUIR samples PU-35/65/0-KE and PU-0/85/15-KP which present higher $T_{deg\ 50\%}$ and $T_{deg\ 100\%}$. These two foams present the highest biobased contents. This is in agreement with previous observation on the TGA and DTG results.

The flammability results of the different foams are presented in Figure SI 43 (in Annex). All foams passed the test, excepted PU-0/85/15-KE and PU-0/85/15-KP, where the flame stayed persistent and above the acceptable height limit. PU-0/85/15-KE and PU-0/85/15-KP are the only foams with 85 wt% of BASAB, an aliphatic compound The aromatic fossil polyol present an aromatic structure and it is well known that aromaticity brings higher fire-resistant, promoting charring on the surface, which decrease the flammability (Celzard et al., 2011; M. Zhang et al., 2014a).

Table 3.6: PUIR foams degradation temperature at 50% and 100% of weight loss and DTG results

Sample	TGA		DTG	
	$T_{deg50\%}$ (°C)	$T_{deg100\%}$ (°C)	$T_{deg\ max1}$	$T_{deg\ max2}$
REF	448	645	301	523
PU-90/10/0-KE	425	628	290	519
PU-75/25/0-KE	432	604	294	512
PU-65/35/0-KE	440	605	295	511
PU-55/45/0-KE	437	614	292	507
PU-45/55/0-KE	466	646	302	509
PU-35/65/0-KE	473	702	303	505
PU-0/85/15-KE	458	632	300	538
PU-0/85KP/15-KP	499	690	295	534

Figure 3.7 show the stress-strain curves of all PUIR foams, obtained in longitudinal and transversal directions. As previously described (Chen et al., 2002), in the longitudinal direction (Figure 3.7-a), the stress increases linearly with the strain (due to the elastic behavior of the foams), before reaching the yield point. After the yield point, the stress stays quasi-constant due to the foam cell collapsing. In the transversal direction (Figure 3.7-b), the foam behaves differently. After an elastic part, until the yield point, the stress continues to increase, corresponding to the foam densification. The difference between the foam behaviors in the longitudinal and transversal directions is due to the anisotropic foam character. This behavior has been well explained in a previous work (Furtwengler et al., 2017.). It is confirmed by the longitudinal and transversal Young's modulus ratio which decreases from 5.75 to 3.08 for foam samples REF to PU-65/35/0-KE, respectively. The lowest Young's modulus ratio of PU-65/35/0-KE reflects the least anisotropic behavior. This observation is in agreement with previous results regarding the foam cell anisotropic coefficient R (presented in Table 3.4) as PU-65/35/0-KE presents the smallest R value.

In the longitudinal direction, it clearly appears that the mechanical properties, including Young's modulus and yield stress, as presented in Table 3.7, describe successively two main trends. Both Young's modulus and yield stress firstly increase when the biobased polyol concentration increased from 0 to 25 wt% (foam samples REF to PU-75/25/0-KE), where a threshold loads is reached. Afterwards, a decrease of mechanical properties is observed for biobased polyol concentration going from 35 to 65 wt%. During the mechanical properties ascending phase, the longitudinal Young's modulus increases from 6.9 to 13.5 MPa for foam samples REF and PU-75/25/0-KE, respectively. This corresponds to an increase of the longitudinal Young's modulus of about 96%. According to previous observations, the mechanical properties follows a similar trend. When the average cells size decreases, the load repartition is more homogeneous in the foam sample resulting in higher Young's moduli. Then after the threshold loads, in direct link with the foams architectures, samples become more brittle because of the BASAB polyfunctionality. It results in a Young's modulus decreased of about 45%, between PU-65/35/0-KE and PU-35/65/0-KE. In the transversal direction, a similar and less pronounced evolution can be observed with a rise of Young's modulus from 1.2 to 2.9 MPa (Table 3.7), from REF to PU-75/25/0-KE foams. Then, such as in the longitudinal direction, a decrease of Young's modulus from 2.4 to 1.0 MPa is noticed from PU-65/35/0-KE to PU-35/65/0-KE foam. As mentioned above, from REF to PU-65/35/0-KE, the foam cell size decreased when the BASAB amount increased. The good load distribution, combined with the closed cells content, leads to an increase in performance. The enclosed gas in the cells is generating a resistant pressure to the compressive load, enhancing the foam mechanical properties (D'Souza et al., 2014). In contrast, when the biobased polyol content increases from 45 to 65 wt%, the content of closed cells decreases significantly. At the same time, the size of the cells increased and some defects appear in the foam morphology, as shown on SEM images in Figure SI 39 (in Annex). All these factors contribute to the loss in mechanical properties. Additionally,

Figure SI 44 (in Annex) presents the evolution of the Young's modulus in transversal and longitudinal direction.

In contrast to what was observed in the longitudinal direction, the yield stress in the transversal direction continuously decreases when BASAB content increased. From mechanical properties in the transversal direction (Figure 3.7-b), two groups of biobased foams can be distinguished. The first one is composed of the systems REF, PU-90/10/0-KE, PU-75/25/0-KE and PU-65/35/0-KE, which behaves like REF, with good recovery. The second one includes PU-55/45/0-KE, PU-45/55/0-KE and PU-35/65/0-KE, which present a poor recovery behavior. This latter behavior could be explained by the brittle nature of these foams due to the high cross-links structures due to the high functionality of BASAB.

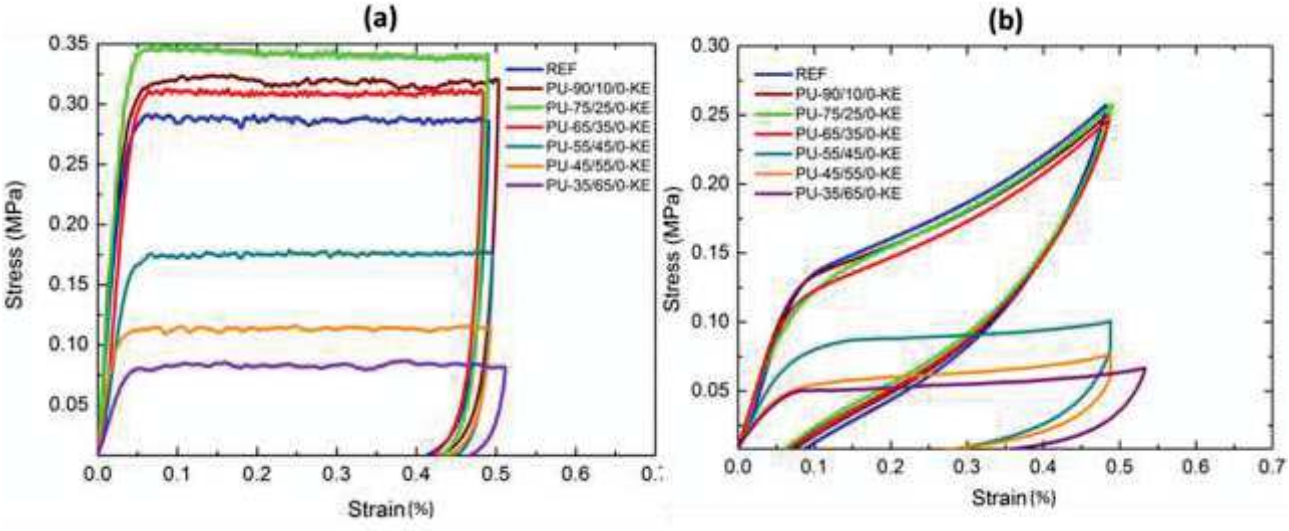

Figure 3.7: Stress-strain curves in (a) longitudinal and (b) transversal direction to the foam rise, for foam systems from the reference to 65% of substitution

Table 3.7: Mechanical and thermal conductivity parameters of the different PUIR Foams

Sample designation	Young's modulus in longitudinal direction (MPa)	Yield stress in longitudinal direction (MPa)	Young's modulus in transversal direction (MPa)	Yield stress in transversal direction (MPa)	Longitudinal and transversal Young's modulus ratio	Thermal conductivity coefficient λ in longitudinal direction (mW/m K)
REF	6.9	0.29	1.2	0.14	5.75	24
PU-90/10/0-KE	11.7±0.1	0.28	2.3	0.12	5.09	23
PU-75/25/0-KE	13.5±0.5	0.35	2.9	0.10	4.66	22
PU-65/35/0-KE	7.4±0.3	0.31	2.4	0.10	3.08	23
PU-55/45/0-KE	6.2±0.10	0.17	1.3	0.08	4.77	22.5
PU-45/55/0-KE	5.9±0.4	0.11	1.2	0.05	4.91	25
PU-35/65/0-KE	4.1±0.3	0.08	1.0± 0.1	0.05	4.1	n.d

n.d: not determined

The thermal conductivity (Table 3.7) slightly decreased when the amount of biobased polyol increased. The corresponding values are closed to 20 mW/(m.K) for REF, PU-90/10/0-KE, PU-75/25/0-KE, and PU-65/35/0-KE, respectively. Foams PU-75/25/0-KE conductivity value of 22 mW/mK is remarkable. For instance, on recently published work on sorbitol based rigid PU foams, the average conductivity value was 36 mW/mK (Ugarte et al., 2015). With other types of polyols these values generally range between 23 to 30 mW/mK (Gao et al., 2013; Kurańska et al., 2017; Piszczyk et al., 2014; Tan et al., 2011b). The thermal conductivity (λt) of such foams depends on four different conductivity coefficients (λ) namely λ_{gas}, λ_{PUIR},

$\lambda_{radiation}$ and $\lambda_{convection}$, as described in equation (3) (Ashida, 2006). In PU foams, conduction in the gaseous phase account for 65-80 % of the heat transfer, whereas the solid and radiative component account for 35-20 %. As these PUIR foams are obtained with isopentane, and present similar densities and close-cells content, the thermal conductivity is mainly influenced by the cell-size decrease. The smaller cell-size impacts the extinction coefficient (K) of $\lambda_{radiation}$ expressed by Equations (4) and (5) (Hejna et al., 2017b; Septevani et al., 2015).

$$\lambda_t = \lambda_{gas} + \lambda_{PUIR} + \lambda_{radiation} + \lambda_{convection} \quad (3)$$

$$\lambda_{\text{radiation}} = \frac{16\sigma T^3}{3K} \quad (4)$$

$$K = 4.1\frac{\sqrt{\frac{\rho_f}{\rho_p}f_s}}{d} \quad (5)$$

Where σ is Stephan-Boltzmann constant ($5.67*10^{-8}$ W/m^2K^4), T is the temperature, d is cell diameter, f_s is the polymer fraction contained in foams cell struts, ρ_f and ρ_p are foams and polymer density, respectively. So, the lowest thermal conductivity of foams sample PU-75/25/0-KE is a consequence of combined effect of closed cell content and cell size reduction compare to the REF. For biobased polyol content between 35 and 45 wt%, the thermal conductivity stays constant around 23 mW/mK. Then slightly increases to 25 mw/mK when the biobased polyol content reaches 55 wt%. In this particular case, the thermal conductivity increase is mainly caused by the closed cell content decrease and the increase of the cells size. The closed cell content decrease strongly affects λ_{gas} value as open-cells are mainly filled by air a less efficient gas, instead of isopentane (Fleurent and Thijs, 1995; Hejna et al., 2017b).

Conclusion

Innovative biobased PUIR foams were successfully elaborated from a synthesized polyol based on sorbitol as a building block to obtain high-performance cellular materials. Different formulations have been developed; a conventional fossil-based polyester polyol has been incrementally replaced or substituted by this synthesized biobased polyol. The corresponding PUIR foams present for instance a high content of closed cell. Compared to the fossil-based reference, the cell sizes were reduced by 44 % with corresponding and remarkable reduced thermal conductivity till 22 mW/mK. Mechanical properties also benefit from the cell-size decrease in both, longitudinal and transversal directions to the foam rise.

Main results show that the developed biobased PUIR foams fulfill the main requirements in connection with the targeted application fields (thermal insulation) such as:

- ✓ good fire resistance,
- ✓ mechanical performance,
- ✓ low density,
- ✓ high closed cell content,
- ✓ low thermal conductivity.

In a future work, additional test will be investigated to determine for instance, the aging behavior and the durability of these biobased foams.

Acknowledgements

The authors are grateful to Alsace Region, BPI France, Soprema, and Tereos for their financial supports.

Réferences

Almer, C., Winkler, R., 2017. J. Environ. Econ. Manag. 82, 125–151.

Andersons, J., Kirpluks, M., Stiebra, L., Cabulis, U., 2016. Mater. Des. 92, 836–845.

Arbenz, A., Avérous, L., 2014. RSC Adv 4, 61564–61572.

Arbenz, A., Frache, A., Cuttica, F., Avérous, L., 2016. Polym. Degrad. Stab.

Arbenz, A., Perrin, R., Avérous, L., 2017. J. Polym. Environ.

Ashida, K., 2006. Polyurethane and related foams: chemistry and technology. CRC press.

Barrioni, B.R., de Carvalho, S.M., Oréfice, R.L., de Oliveira, A.A.R., Pereira, M. de M., 2015. Mater. Sci. Eng. C 52, 22–30.

Celzard, A., Fierro, V., Amaral-Labat, G., Pizzi, A., Torero, J., 2011. Polym. Degrad. Stab. 96, 477–482.

Chattopadhyay, D.K., Webster, D.C., 2009. Prog. Polym. Sci. 34, 1068–1133.

Chen, W., Lu, F., Winfree, N., 2002. Exp. Mech. 42, 65–73.

Chuayjuljit, S., Maungchareon, A., Saravari, O., 2010. J. Reinf. Plast. Compos. 29, 218–225.

Cornille, A., Auvergne, R., Figovsky, O., Boutevin, B., Caillol, S., 2017. Eur. Polym. J. 87, 535–552.

David Randall, steve Lee, n.d. The Polyurethanes book. Wiley.

Dick, C., Dominguez-Rosado, E., Eling, B., Liggat, J.., Lindsay, C.., Martin, S.., Mohammed, M.., Seeley, G., Snape, C.., 2001. Polymer 42, 913–923.

D'Souza, J., Camargo, R., Yan, N., 2014. J. Appl. Polym. Sci. 131, n/a-n/a.

Fan, H., Tekeei, A., Suppes, G.J., Hsieh, F.-H., 2013. J. Appl. Polym. Sci. 127, 1623–1629.

Fleurent, H., Thijs, S., 1995. J. Cell. Plast. 31, 580–599.

Furtwengler, P., Perrin, R., Redl, A., Avérous, L., 2017. Eur. Polym. J. 97, 319–327.

Gandini, A., 2008. Macromolecules 41, 9491–9504.

Gao, L., Zheng, G., Zhou, Y., Hu, L., Feng, G., Xie, Y., 2013. Ind. Crops Prod. 50, 638–647.

Guan, J., Hanna, M.A., 2004. Ind. Crops Prod. 19, 255–269.

Guelcher, S.A., Gallagher, K.M., Didier, J.E., Klinedinst, D.B., Doctor, J.S., Goldstein, A.S., Wilkes, G.L., Beckman, E.J., Hollinger, J.O., 2005. Acta Biomater. 1, 471–484.

Gupta, A., 2016. Climate Change and Kyoto Protocol, in: Handbook of Environmental and Sustainable Finance. Elsevier, pp. 3–23.

Hawkins, M.C., 2005. J. Cell. Plast. 41, 267–285.

Hejna, A., Kirpluks, M., Kosmela, P., Cabulis, U., Haponiuk, J., Piszczyk, Ł., 2017a. Ind. Crops Prod. 95, 113–125.

Hejna, A., Kosmela, P., Kirpluks, M., Cabulis, U., Klein, M., Haponiuk, J., Piszczyk, Ł., 2017b. J. Polym. Environ.

Javni, I., Petrovi?, Z.S., Guo, A., Fuller, R., 2000. J. Appl. Polym. Sci. 77, 1723–1734.

Jelle, B.P., 2011. Energy Build. 43, 2549–2563.

Jin, H., Lu, W.-Y., Scheffel, S., Hinnerichs, T.D., Neilsen, M.K., 2007. Int. J. Solids Struct. 44, 6930–6944.

Kurańska, M., Prociak, A., Cabulis, U., Kirpluks, M., Ryszkowska, J., Auguścik, M., 2017. Ind. Crops Prod. 95, 316–323.

Liu, L., Li, H., Lazzaretto, A., Manente, G., Tong, C., Liu, Q., Li, N., 2017. Renew. Sustain. Energy Rev. 69, 912–932.

Minogue, E., 2000. An in-situ study of the nucleation process of polyurethane rigid foam formation. Dublin City University.

Modesti, M., Lorenzetti, A., 2001. Eur. Polym. J. 37, 949–954.

Mosiewicki, M.A., Dell'Arciprete, G.A., Aranguren, M.I., Marcovich, N.E., 2009. J. Compos. Mater. 43, 3057–3072.

Ozaki, S., others, 1972. Chem Rev 72, 457–496.

Pierre Furtwengler, Rodrigue Matadi Boumbimba, Luc Avérous, n.d. Macromol. Mater. Eng.

Piszczyk, Ł., Strankowski, M., Danowska, M., Hejna, A., Haponiuk, J.T., 2014. Eur. Polym. J. 57, 143–150.

Prociak, A., Kurańska, M., Cabulis, U., Kirpluks, M., 2017. Polym. Test. 59, 478–486.

Ramesh, N.S., Rasmussen, D.H., Campbell, G.A., 1994. Polym. Eng. Sci. 34, 1685–1697.

Reulier, M., Boumbimba, R.M., Rasselet, D., Avérous, L., 2016. J. Appl. Polym. Sci. 133, n/a-n/a.

Reymore, H.E., Carleton, P.S., Kolakowski, R.A., Sayigh, A.A.R., 1975. J. Cell. Plast. 11, 328–344.

Saunders, J.H., Slocombe, R.J., 1948. Chem. Rev. 43, 203–218.

Schwetlick, K., Noack, R., 1995. J. Chem. Soc. Perkin Trans. 2 395.

Septevani, A.A., Evans, D.A.C., Chaleat, C., Martin, D.J., Annamalai, P.K., 2015. Ind. Crops Prod. 66, 16–26.

Sheridan, J.E., Haines, C.A., 1971. J. Cell. Plast. 7, 135–139.

Sigurdsson, S.T., Seeger, B., Kutzke, U., Eckstein, F., 1996. J. Org. Chem. 61, 3883–3884.

Silva, A.L., Bordado, J.C., 2004. Catal. Rev. 46, 31–51.

Simon, J., Barla, F., Kelemen-Haller, A., Farkas, F., Kraxner, M., 1988. Chromatographia 25, 99–106.

Slotta, K.H., Dressler, H., 1930. Eur. J. Inorg. Chem. 63, 888–898.

Tan, S., Abraham, T., Ference, D., Macosko, C.W., 2011. Polymer 52, 2840–2846.

Ugarte, L., Gómez-Fernández, S., Peña-Rodríuez, C., Prociak, A., Corcuera, M.A., Eceiza, A., 2015. ACS Sustain. Chem. Eng. 3, 3382–3387.

Zhang, C., Kessler, M.R., 2015. ACS Sustain. Chem. Eng. 3, 743–749.

Zhang, M., Pan, H., Zhang, L., Hu, L., Zhou, Y., 2014. Ind. Crops Prod. 59, 135–143.

Conclusion et perspectives du Chapitre

Le Chapitre 3 a été consacré à l'élaboration de mousses polyisocyanurates. Les mousses ont été obtenues par un procédé de substitution progressive d'un polyol pétrosourcé de référence par un polyol biosourcé à base de sorbitol, le BASAB.

Dans le Chapitre précédent il a été montré que le BASAB permettait l'obtention de mousses polyuréthanes semi-rigides pouvant satisfaire un grand nombre d'applications, mais leur propriété en tant qu'isolant thermique n'était pas optimale du fait d'un haut taux de cellules ouvertes dans les matériaux. La synthèse de mousses polyisocyanurates rigides à haut taux de cellules fermées est plus adaptée à l'obtention de matériaux isolants. Le BASAB a présenté une bonne compatibilité avec le polyol pétrosourcé de référence permettant d'obtenir, avant ajout du polyisocyanate, une émulsion fine de polyol, catalyseur, surfactant, d'ignifugeant et d'agent gonflant physique. L'efficacité de ce système a été démontrée jusqu'à l'incorporation de 45 %pds de BASAB dans le polyol pétrosourcé avec un optimum lorsque le ratio de polyols est de 25/75 (%pds / %pds, BASAB / polyol pétrosourcé). Par contre, au-delà de 45 %pds d'incorporation de BASAB, les cinétiques d'obtention des mousses polyisocyanurate se dégradent, principalement à cause de la plus basse réactivité du BASAB dans les conditions de synthèse utilisées qui étaient spécifiques au polyol pétrosourcé. Ainsi en travaillant avec un système biosourcé, il a été démontré qu'en ajustant la catalyse de la réaction, et plus précisément la catalyse de trimérisation des isocyanates, il été possible d'obtenir des mousses polyisocyanurate sans polyols d'origine fossile. Dans cette configuration réactionnelle, le propionate de potassium s'est avéré être un catalyseur plus actif que le 2-éthylhexanoate de potassium permettant la bonne formation du réseau polyisocyanurate à de plus faibles températures.

Par la suite, la morphologie, les propriétés mécaniques et thermiques des mousses ont pu être étudiées. La morphologie des mousses polyisocyanurates contenant jusqu'à 45 %pds de BASAB a démontré une diminution de la taille des cellules des mousses. La diminution des tailles de cellules a pu être reliée à l'émulsion fine du mélange réactionnel associée à la fonctionnalité et viscosité du BASAB. Les mousses partiellement biosourcées développées dans ce Chapitre présentent donc des tailles de cellules considérablement inférieures à ce qui est classiquement observé pour des mousses de cette gamme de densité. La réduction de la taille des cellules fermées dans les mousses est à l'origine des améliorations observées sur la résistance à la compression et de la réduction des coefficients de conductivité thermique des différents matériaux.

Ces résultats, très encourageants ont été poursuivis par un essai réalisé à l'échelle d'un pilote industriel allant de la synthèse du BASAB à l'élaboration de panneaux de mousses PUIR en continu sur ligne de production. Les résultats de cet essai pilote concluant sont présentés en Annexe 6. Ainsi l'introduction d'un polyol polyesters biosourcé dans l'élaboration de matériaux polymères durables pour l'industrie de l'isolation des bâtiments a prouvé être à l'origine de l'amélioration des propriétés de ces derniers.

CHAPITRE 4 : DEVELOPPEMENT D'UNE NOUVELLE MOLECULE PLATEFORME BIOSOURCEE A PARTIR DU SORBITOL

Introduction du Chapitre 4

Dans les précédents Chapitres, le sorbitol a été impliqué dans plusieurs réactions d'estérification en association avec des diols de différentes tailles. S'en est suivi la synthèse de différentes mousses polyuréthanes (Chapitre 2) et polyisocyanurates (Chapitre 3).

La polyfonctionnalité du sorbitol peut être mise à profit pour développer de nouvelles molécules plateformes. Le développement d'une molécule plateforme revient à développer une structure de base qui permettrait d'accéder à de nouvelles architectures moléculaires et macromoléculaires.

Afin d'assurer la continuité de ce travail, la molécule visée doit entre autres permettre la synthèse de polyuréthanes, dans ce cas sans isocyanate. Une solution est donc l'élaboration de carbonates cycliques puisque ceux-ci peuvent servir de monomères pour des polymérisations par ouverture de cycles ou être impliquée dans des réactions d'aminolyse avec des diamines biosourcées. L'aminolyse reste la voie de synthèse la plus développée pour l'obtention de liaison carbamate sans utiliser d'isocyanate. L'utilisation de diamines biosourcées est une bonne stratégie pour travailler avec des monomères issus de ressource renouvelable. Ce type de diamines peut être obtenue par catalyse hétérogène de synthons issus de la biomasse (Pelckmans et al., 2017). Par exemple, des diamines en C4, C6 ou C36 peuvent être obtenues respectivement à partir de protéines, d'alcools ou de dimère d'acide gras.

Ce Chapitre présente les conditions de synthèse d'une molécule plateforme, le bis(cyclocarbonate) à partir de sorbitol en milieu non solvanté hétérogène. Le caractère « plateforme » de la molécule obtenue est demontré en l'impliquant dans la synthèse d'un diol, de polyéthers et de polyuréthanes sans isocyanate entièrement biosourcé. L'étude est présentée sous la forme d'une publication scientifique intitulée « *From D-sorbitol to five-membered bis(cyclo-carbonate) as a platform for the synthesis of different original biobased chemicals and polymers* » soumise dans ACS Sustainable Chemistry & Engineering. Cette étude fait également l'objet d'un dépôt de brevet national FR 17/00351.

From D-sorbitol to five-membered bis(cyclo-carbonate) as a platform for the synthesis of different original biobased chemicals and polymers.

Pierre Furtwengler[a], Luc Avérous[a]

[a]*BioTeam/ICPEES-ECPM, UMR CNRS 7515,*

Université de Strasbourg, 25 rue Becquerel, 67087 Strasbourg, Cedex 2, France

* Corresponding author: Prof. Luc Avérous, Phone: + 333 68852784, Fax: + 333 68852716, E-mail: luc.averous@unistra.fr

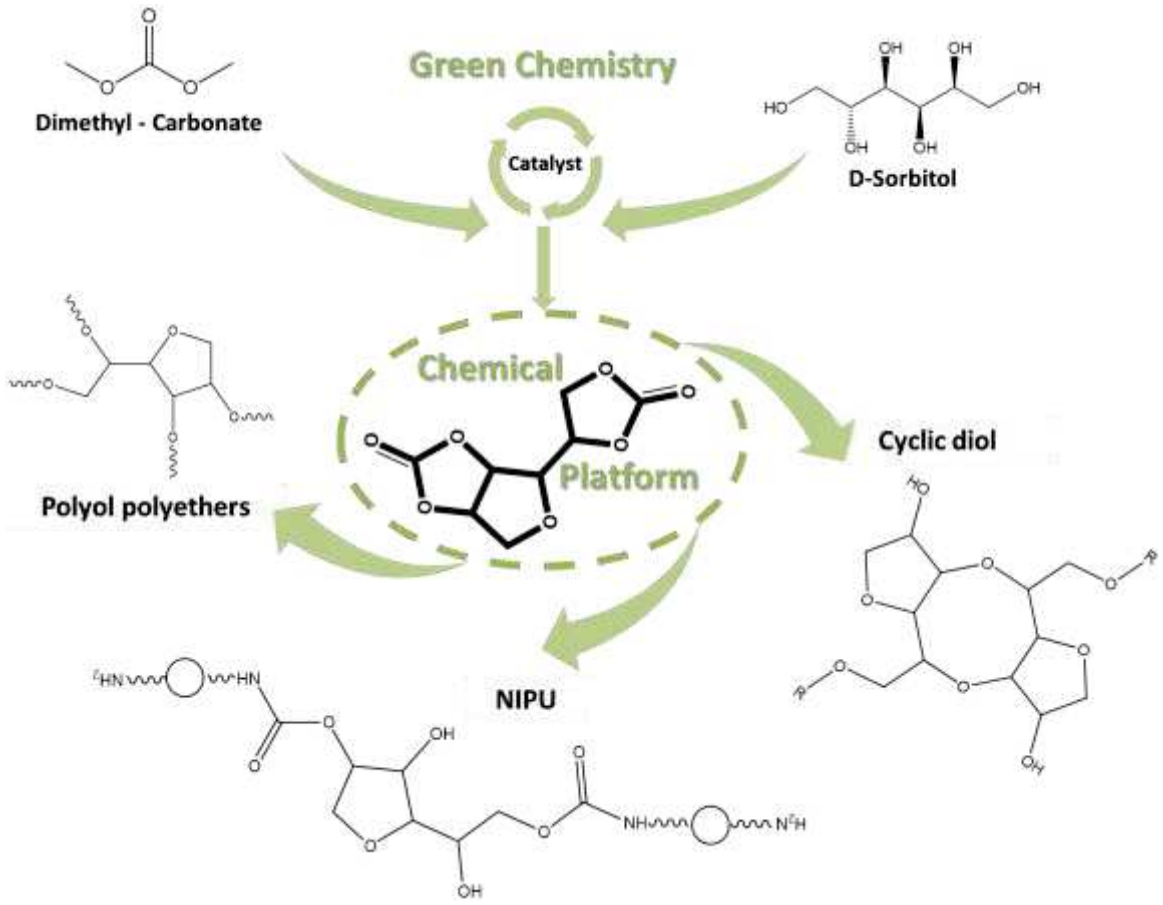

Submitted in ACS Sustainable Chemistry & Engineering

Abstract

Bis(cyclo-carbonate) (D-BisCC) was successfully synthesized from D-sorbitol through an environmentally friendly process with dimethyl carbonate (DMC) as a reactant. In agreement with green chemistry principles, solvent free reactions were catalyzed and took place at low temperature, 75 °C. The D-BisCC was then recovered by precipitation in distilled water. The reaction yield was increased till 50%, due to the use of a continuous DMC feed in order to limit the side-reactions and the loss of reactant by azeotropic flux with methanol, a subsidiary product of the reaction. The obtained D-BisCC is a remarkable chemical platform which could compete with others polycyclic chemical platforms (isosorbide,). D-BisCC can be for instance used to synthesize different chemicals such as short and long polyols, or novel biobased non-isocyanate polyurethanes (NIPU). Two D-BisCC molecules have been coupled to obtain novel cyclic diols with pendant side chains. Polyethers polyol were also obtained by anionic ring opening polymerization. According to the synthesis conditions, these synthetized polyether polyols range from partially to highly cross-linked materials. Finally, NIPU were synthesized with short and biobased fatty diamines. The glass transition temperatures of these NIPU can be tuned from – 9 to 42 °C, as well as their OH-value, ranged from 3 to 9 mmol/g of hydroxyl groups. These different modifications and synthesis highlight the versatility of the synthesized D-BisCC and demonstrated the high potential of this building block. D-BisCC can be considered as a chemical platform to open the way to different original and biobased chemical architectures.

Introduction

D-sorbitol (Table 4.1) is a widely available and low cost sugar alcohol which is mainly obtained from D-glucose hydrogenation (Zhang et al., 2013). D-sorbitol is a remarkable building block, selected by the Department of Energy (DoE-US) as one of the TOP 12 renewable value added chemicals from biomass in 2004 or more recently in 2010 (Bozell and Petersen, 2010; Holladay et al., 2007). It is for instance an important precursor for the synthesis of L-ascorbic acid (vitamin C) (Gallezot et al., 1994). Sorbitol is widely used as food, drug and cosmetic additives and for the elaboration of chemical such as long polyols (Desroches et al., 2012).

D-sorbitol has been directly used as monomers or building blocks in polyester synthesis through multistep pathways (Anand et al., 2012, 2016; Furtwengler et al., 2017). To develop eco-friendly synthesis process, D-sorbitol has also been involved in enzymatic reactions (Gustini et al., 2015, 2016). As previously reported, polyhydric chemical were implicated in ester exchange reaction with a cyclic carbonate reactants such as diphenyl carbonate to obtained poly(cyclocarbonate) (Hough et al., 1962; Komura et al., 1973). For example, D-mannitol tricarbonate was synthesized in severe conditions from D-mannitol and ethylene glycol at 150 °C under a reduce pressure of 20 mmHg (Komura et al., 1973). Whereas, D-sorbitol tricarbonate was synthesized from diphenyl carbonate in N,N-dimethylformamide and catalyzed by sodium hydrogen carbonate at 110 °C (Hough et al., 1962). More recently, such reactions were enhanced on agreement with the principles of a green chemistry, with the use of another carbonate, dimethyl carbonate (DMC) (Tomczyk et al., 2012). DMC is an environmentally friendly reactive solvent according to its nontoxicity and represent an alternative to phosgene for methylation and

carbonylation process (Tundo and Selva, 2002). 85% of the DMC Europe's production is based on the Enichem process (Romano et al., 1982; Romano and Rivetti, 1993; Garcia-Herrero et al., 2016). The Enichem process use carbon monoxide and oxygen as reactants, but its current production derived of CO_2 is on the rise, positioning DMC as a green reactive solvent (Garcia-Herrero et al., 2016). In this contexte, Tomczyk et *al*. (Tomczyk et al., 2012) used DMC instead of the diphenyl carbonate in reaction with D-sorbitol (10 eq.) catalyzed by potassium carbonate but 1,4-dioxane was used as solvent. The reaction product was the (1R,4S,5R,6R)-6-(1,3-dioxolan-2-one-4-yl)-2,4,7trioxa-3-oxy-bicyclo[3.3.0]octane, a D-sorbitol based five-membered bis(cyclo-carbonate) (D-BisCC) with a yield of 43% after recrystallization in acetonitrile instead of the D-sorbitol tricarbonate. Mazurek-Budzynska et *al*. (Mazurek-Budzyńska et al., 2016) also reported the synthesis of this molecule working with 10 eq. of DMC toward D-sorbitol in methanol catalyzed by potassium carbonate with a global yield of 40%. However, to the best of our knowledge, D-BisCC were always conducted in solvent conditions.

The D-BisCC molecule is composed of two cyclo-carbonate groups and a tetrahydrofuran ring witch can be compared (Table 4.1) to another important polycyclic sorbitol derivative which is largely used as a building block with a large industrial production: the isosorbide (Ginés-Molina et al., 2017; Rose and Palkovits, 2012). Isosorbide results from a double dehydration of the sorbitol, which directly influences the carbon / oxygen ratio (C/O) (Table 4.1). The C/O ratio of D-BisCC (Table 4.1) indicates a conservation of the richness in oxygen atoms from D-sorbitol (close to 1) compared to isosorbide, for instance. Obviously the annual production and price of the D-BisCC cannot be assessed as it is not produce at industrial scale.

Table 4.1: Chemical structures and properties of building blocks. D-sorbitol and different polycyclic sorbitol derivatives.

Chemical structure	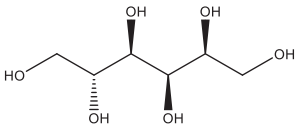	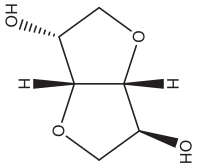	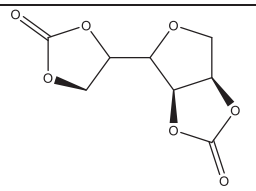
Chemical name	D-sorbitol	Isosorbide	D- BisCC
Molar mass (g/mol)	182	146	216
Functionality	6	2	2
Functionality nature	Hydroxyl	Hydroxyl	Cyclic Carbonate
Melting temperature (°C)	95-100	61-62	214-216
C/O ratio	1	1.50	1.14
Annual production (Tons)	6.5 x 10^5	Less than 10^3	0

Isosorbide has been largely developed and investigated as an innovative biobased rigid diol during the two last decades (Fenouillot et al., 2010). For instance, polyesters such as polyisosorbide terephthalate (PIT) or polyethylene isosorbide terephthalate (PEIT) were developed (Rose and Palkovits, 2012). The replacement of ethylene glycol by isosorbide improved the rigidity and the behavior of the final polyester. Tg of PIT is 200 °C whereas the Tg of PEIT evolved from 70 to 180 °C (Feng et al., 2011; Rose and Palkovits, 2012).

D-BisCC presents an equivalent molar mass than isosorbide with also a bifunctionality. However, its melting temperature (T_m) is more than three time the isosorbide' one. This higher T_m indicates a strong rigidity and thermal resistance of the D-BisCC. As isosorbide which can be directly valorized towards biobased polymers by esterification (Noordover et al., 2006) or Williamson etherification (Caouthar et al., 2007), BisCC molecules can open a variety of routes with diverse polymerization types. D-BisCC is a versatile molecule which can be considered as a chemical platform to extend the development of advanced oligomers and polymers such as non-isocyanate polyurethanes (NIPU) (Carré et al., 2016; Cornille et al., 2016b; Maisonneuve et al., 2015; Tryznowski et al., 2015), polyol polyethers (Wu et al., 2008), or by ring opening polymerization (ROP) to obtain various macromlecular architectures such as polycarbonates (Suriano et al., 2011).

BisCC can be for instance used for the synthesis of aliphatic polycarbonates at low temperature (≤ 60 °C) via anionic ROP (Haba et al., 2005; Tezuka et al., 2015). These authors assumed that the reactivity is linked to the particular ring strain to polymerize at low temperature. Such low temperatures have been only reported on aldohexopyranosides monomers (Tezuka et al., 2015). Most of the ROP based on BisCC are thermodynamically unfavorable and operate at high temperature (≈ 150 °C) leading to the elimination of carbon dioxide to produce linear copolymers with carbonates and ethers groups.

On the same way, the synthesis of non-isocyanate polyurethanes (NIPU) can rely on BisCC. NIPU are mainly synthesizing according to three types of reaction which are (i) AB-type azide condensation (More et al., 2012), (ii) transurethane polycondensation (Deepa and Jayakannan, 2008b) and (iii) aminolysis (Kihara and Endo, 1993b). The aminolysis reaction is based on the reaction between a cyclocarbonate and an amine function. It is until now, the most promising way to avoid the use of toxic polyisocyanate in polyurethane synthesis. Resulting materials are called polyhydroxyurethanes (PHU), as hydroxyl groups are generated, close to the urethane group (Carré et al., 2014). BisCC presents a lower reactional rate toward amine functions than six-membered cyclic carbonate but they are widely used (Tomita et al., 2001). Compared to six, seven or even height-membered cyclic carbonate, BisCC are more economically viable as they are easily obtained with high yield and high renewable content (Cornille et al., 2017a; Ochoa-Gómez et al., 2012; Xu et al., 2015). Additionally, their synthesis does not require phosgene derivatives whereas six-membered cyclic carbonate does (Cornille et al., 2015).

The aim of this study was to synthetized a biobased chemical platform, BisCC from an attractive renewable building-block, the D-sorbitol. The D-BisCC synthesis parameters were investigated and enhanced to improved D-sorbitol conversion and limit side reactions with respect to green chemistry principles (solvent-

free, low temperature and catalyzed reactions). To show that D-BisCC is a chemical platform, it was used as a basis leading to the elaboration of different products. Synthetized D-BisCC was implicated in the elaboration of different and new biobased molecular architectures such as a new diol, cross-linked polyethers and NIPU with also renewable diamines. All products from the D-BisCC to its derivatives chemical structures and properties were fully characterized and analysed.

Experimental part

Materials:

D-sorbitol was kindly provided by Tereos (Meritol, 98%, water content < 0.5%, reducing sugar content < 0.1%). 1.3.5-triazabicyclo[4.4.0]dec-5-ene (TBD), 1.8-diazabicyclo[5.4.0]undec7-ene (DBU), tert-butylimino-tri(pyrrolidino)phosphorarane (purity ≥ 97%, BTPP), dimethyl carbonate (purity ≥ 99%, DMC), diethyl carbonate (purity ≥ 99%, DEC) ethylene carbonate (purity 99+ %, EC), 1-octanol (purity ≥ 99%), cis-1,2-cyclopentanediol (98%), (±)-trans-1,2-cyclopentanediol (97%) and 2-chloro-4,4,5,5-tetramethyl-1,3,2-dioxaphospholane (Cl-TDP, 95%) were obtained from Sigma Aldrich. Sodium hydroxide (NaOH) was obtained from Carlo Erba Reagents. Potassium Hydroxide (KOH), potassium carbonate (K_2CO_3) and 1.5-diamino-2-methylpentane (1.5 MD, 99%) were obtained from VWR Chemical**.** Titanium (IV) isopropoxide (TTIP), and titanium (IV) butoxide (TNBT) were obtained from Acros Organics. 1,4 diaminobutane (1.4 B, 98+ %) and stannous octoate (Sn(oct), 95%) were obtained from Alfa Aesar. Hexamethylene diamine (1.6 H, 98%) was provided by BASF. A diamine based on dimer fatty (DDA), obtained from the dimerization of two fatty acids (Javni et al., 2008) was kindly provided by Croda (Priamine 1075). At room temperature, DDA is a yellowish, slightly viscous liquid. Some DDA properties are summarized in *Table 4.2*. All reagents were used without further purification.

Table 4.2: DDA main properties *(Carré et al., 2015)*

Designation	Amine Value (mmol/g)	Functionality	Dimer content (wt%)	Carbon chain length	Tg (°C)
DDA	3.64	2.0	> 99	36	<-50

Synthesis with catalyst of D-sorbitol-based Bis(cyclo-carbonate):

A round-bottom flask equipped with a distillation bridge or vigreux fractionating columns, or reflux device was charged with one molar equivalent of D-sorbitol. 5 mol% of catalyst (TBD, DBU, BTPP, KOH, NaOH, K_2CO_3, TTIP, TNBT or stannous octoate (Sn(oct)) were added, in respect to D-sorbitol (Table 4.3).

Table 4.3: BisCC synthesis from D-sorbitol and DMC or EC, under different conditions and catalyst systems

Entry	Reactional device	D-sorbitol / carbonate molar ratio	Catalyst	Reaction time (h)	Yield (%) Synthesis of BisCC
1	Distill. Bridge	4[a]	None	14.5	18
2	Distill. Bridge	3.5[b]	TTIP	16	0
3		3.5[b]	TNBT	16	0
4		3.5[b]	Sn(oct)	16	0
5		3.5[b]	KOH	16	0
6		3.5[b]	NaOH	16	0
7		3.5[b]	K_2CO_3	16	0
8		3.5[b]	BTPP	1-16	21
9		3.5[b]	DBU	1-16	24
10		3.5[b]	TBD	1-16	22
11		7	BTPP	16	35
12		9	BTPP	1-16	42
13		5[b]	TBD	1-16	40
14		7[b]	TBD	1-16	41
15	Reflux	3.5[b]	TBD	16	10
16	Vigreux.	3.5[b]	TBD	16	15
17		5	TBD	16	14
18		7[b]	TBD	1-24	36
19		9[b]	TBD	1-48	45
20		12[b]	TBD	16	Mainly byproducts
21		15[b]	TBD	16	Mainly byproducts
22		18[b]	TBD	16	Mainly byproducts

[a]: EC, under vacuum reaction
[b]: DMC
n.d: not determined

Then, different amounts of DMC, comprised between 3.5 and 18.0 molars equivalents with respect to D-sorbitol, were added. In the case of continuously feed reaction, a syringe pump (Fischer Scientific No 9034914) was used to keep constant the DMC flow rate (Table 4.4). The mixture was stirred and heated to 75 °C, for 16 to 48 h (Table 4.3 and 4.4). At the end, the media was cool down to room temperature. Then, distilled water was added to precipitate the product. Reaction products were filtrated over 0.45 µm polyvinylidene fluoride (PVDF) membrane and wash with distilled water. Finally, the product was dry overnight at 50 °C under vacuum. When reaction kinetic was investigated, each yield was calculated from a dedicated reaction.

Table 4.4: Synthesis of BisCC from D-sorbitol using a continuous feed of DMC

Entry	DMC initial feed in respect to D-sorbitol (mole/mole)	Aditional feedI of DMC, in respect to D-sorbitol (mole/mole)		Reaction total time (h)	Yield (%)
		Molar ratio	Flow rate (mL/h)		
1	3.35	3.35	0.15	16	50
2	3.35	6.70	0.30	16	43
3	1.00	6.70	0.30	16	35

Synthesis without catalyst of D-sorbitol-based Bis(cyclo-carbonate):

A 50 mL round-bottom flask equipped with a distillation bridge was charged with one molar equivalent of D-sorbitol and four molar equivalents of EC. The mixture was stirred, heated to 150 °C, and maintained under controlled vacuum (23-33 mbar) to remove reaction byproducts (ethylene glycol). Different Reaction

times were investigated (6, 14.5, 24 or 48 h). A brown mixture was obtained at the end. The medium was cool down to room temperature and brought back to atmospheric pressure. 10 mL of ethanol were added and the medium was heated until full dilution in ethanol. The mixture was then poured into a beaker and let for two days at 4 °C, for crystallization. Brown crystals were obtained and recovered by filtration. They were finally washed with glacial acetic acid to obtain white crystal and then dried overnight, at 50 °C under vacuum.

Synthesis of cyclopentanediol by trans-esterification:

A 25 mL round flask equipped with a distillation bridge was charged with one molar equivalent of cis-1,2-cyclopentanediol or trans-1,2-cyclopentanediol, 3.5 molar equivalent of DMC with respect to the diol and 5 mol% equivalent to the diol of TBD. The mixture was stirred and heated at 75 °C for 16 h. At the end, the DMC excess was distilled under vacuum. The corresponding product and the residual TBD were directly analyzed, without further purification.

NIPU synthesis:

A 50 mL round flask was charged with different diamines such as 1,4 diminobutane, 1,2-diamino-2-methylpentane, 1,6 hexamethylene diamine, DDA with an equimolar ratio of D-BisCC (Table 4.5). 10 mL of methanol were added as a solvent (Cornille et al., 2017b). Then the medium was heated until reflux temperature (66 °C) for 72 h. Then, the methanol was eliminated by evaporation. The viscous product was poured on a non-adhesive Teflon® sheet and placed into an oven at 80 °C for 72 additional hours before being hot pressed at 80 °C, to obtain material plates. Then, two series of NIPU with a blend of DDA with 1.4 B or 1.5 MD were prepared according to the same protocol (Table 4.5).

Table 4.5: Detailed PHU name and composition

Entry	Sample name	Diamine 1	Diamine 2	Diamine 1/Diamine 2 (Molar ratio)
1	PHU-P	DDA	none	1/0
2	PHU-B	1.4 B	none	1/0
3	PHU-D	1.5 MD	none	1/0
4	PHU-H	1.6 H	none	1/0
5	PHU-0.2B	DDA	1.4 B	0.8 / 0.2
6	PHU-0.4B	DDA	1.4 B	0.6 / 0.4
7	PHU-0.6B	DDA	1.4 B	0.4 / 0.6
8	PHU-0.8B	DDA	1.4 B	0.2 / 0.8
9	PHU-0.2D	DDA	1.5 MD	0.8 / 0.2
10	PHU-0.4D	DDA	1.5 MD	0.6 / 0.4
11	PHU-0.6D	DDA	1.5 MD	0.4 / 0.6
12	PHU-0.8D	DDA	1.5 MD	0.2 / 0.8

Synthesis of polyether polyols

A 50 mL round flask was charged with different molar ratio of D-BisCC and 1-octanol at 150 °C, for 2 to 24 h with 0.7 or 5 mol% of K_2CO_3 as a catalyst, regarding D-BisCC content (Table 4.6). 1 mL of dimethylsufoxide was added as solvent. Then, the flask was closed with a septum. The reactional system was

flush under argon for 10 minutes before launching. During the reaction, the septum was pierced with a needle to evacuate the potential gaseous coproducts . The final product was a dark product. In most cases, the product was a liquid, which was precipitated in 50 mL of toluene. The solid materials were washed in 50 mL of water.

Table 4.6: Conditions of synthesis to obtain polyether / polycarbonate from D-BisCC.

Entry	Initiator	Initiator / D-BisCC molar ratio	K_2CO_3- catalyst (%mol)	Temperature (°C)	Time (h)
1	1-octanol	1/1	5 %	150	2
2	1-octanol	1/100	5 %	150	17
3	1-octanol	1/50	5 %	150	24
4	1-octanol	1/25	5 %	150	17
5	1-octanol	1/100	0.7 %	150	2
6	1-octanol	1/100	0.7 %	150	24
7	1-octanol	1/50	0.7 %	150	24
8	1-octanol	1/25	0.7 %	150	24
9	1-octanol	1/10	0.7 %	150	24

Acetylation of samples

To enhance samples solubility in tetrahydrofuran for SEC analysis, acetylation of the hydroxyl groups was performed when required. Acetylation was done in a pyridine / acetic anhydride mixture (1:1 v/v) at room temperature for 24 h to increase sample solubility for analysis as previously reported (Arbenz and Avérous, 2015).

General methods and analysis:

^{1}H- and ^{13}C-NMR spectra were performed with a Bruker 400 MHz (US). Deuterated dimethyl sulfoxide (DMSO-d_6) was used as solvent to prepare sample solutions with concentrations of 8-10 and 20-30 mg/mL for ^{1}H-NMR and ^{13}C-NMR, respectively. The number of scans was set to 64 for ^{1}H-NMR and at least 2048 for ^{13}C-NMR. The calibrations of ^{1}H- and ^{13}C-NMR spectra were performed using the DMSO peak at 2.50 and 39.52 ppm, respectively. The water molecules present in DMSO-d_6 eventually introduce an additional peak in ^{1}H-NMR spectra at 3.33 ppm.

^{31}P-NMR analyses were performed with a Bruker 400 MHz (US) spectrophotometer after phosphitylation of the sample with Cl-TDP according to standard protocols (Argyropoulos, 1995; Dais and Spyros, 2007), the number of scans was set to 128 at 25 °C. Peak analysis and quantitative analysis were performed according to previous reports (Granata and Argyropoulos, 1995).

Elementary analyses were performed on a ThermoFisher Scientific ‘’Flash 2000’’ device (absolute precision of 0.3%) with 1 mg sample burned up to 950 °C.

Electrospray ionization mass (MS) experiments were performed on a Bruker Daltonics microTOF spectrometer (Bruker Daltonik GmgH, Bremen, Germany) equipped with an orthogonal electrospray interface (ESI). Calibration was performed using a solution of 10 mM sodium formiate. Sample solutions

were introduced into the spectrometer source with a syringe pump (Harvard type 55 1111: Harvard Apparatus Inc., South Natick, MA, USA) with a flow rate of 5 µL.min^{-1}.

Differential scanning calorimetry (DSC) was performed on a TA Instrument Q200 (Q5000 (TA Instruments, US) under nitrogen flux (50 mL/min). Samples of 1-3 mg were sealed in hermetic aluminum pans and analyzed using cyclic procedure involving a heating ramp comprises between -50 to 260 °C at 10 °C/min, a cooling ramp at 5 °C/min, then a second heating up to 260 °C at 10 °C/min. Between each ramp, the temperature was held 2 min for stabilization. For the DSC analysis of PHU, the heating ramp does not exceed 100 °C.

Thermogravimetric analyzes (TGA) were performed using a TA Instrument Hi-Res TGA Q5000 (TA Instruments, US) under reconstituted air (flow rate 25 mL/min). Samples of 1-3 mg were heated from room temperature to 700 °C (10 °C/min). Characteristic temperature of 5 %wt ($T_{deg5\%}$) and 50 wt% ($T_{deg50\%}$) of weight of loss were noted. The main characteristic degradation temperatures were those at the maximum of the weight loss derivative curve (DTG) (T_{deg}).

Infrared spectroscopy was performed with a Fourier transformed infrared spectrometer Nicolet^{TM} 380 from Thermo Scientific (US) used in reflection mode equipped with an ATR diamond module (FTIR). An atmospheric background was collected before each sample analysis (32 scans, resolution 4 cm^{-1}).

Size exclusion chromatography (SEC) measurements were performed in tetrahydrofuran (THF, HPLC grade) in Waters (US) Acquity APC system equipped with a 1.7 µm, 45 Å 150 mm APC XT column, 2.5 µm, 200 Å 150 mm APC XT column and a 2.5 µm, 450 Å, 150 mm APC XT column, a Acquity RI refractive index detector and a Acquity TUV diode array (UV) detector. The instrument was calibrated with linear polystyrene standards from 162 to 1,650,000 g/mol and reported molar masses are the molar masses at the peak. Sample presenting low solubility in THF were acetylated prior to the performed analysis. In the case of small molar masses (i.e. oligomers) the degree of polymerization (DPn) is evaluated according to equation (1).

$$DPn = \frac{(Mn - Mn_{ini})}{Mn_0} \quad (1)$$

Where Mn is the obtain number-average, Mn_{ini} the molar masses of the initiator and Mn_0 the molar masses of the monomer.

Results and discussion

Synthesis of D-BisCC

In order to study the D-sorbtiol conversion into D-BisCC several reactional conditions and setting were investigated and detailed in Table 4.3. The product of each successful reaction presented in Table 4.3, entry 8 to 19 was a white powder directly obtained by precipitation in water, with the exception of the product presented in Table 4.3, entry 1 which was recovered after re-crystallization (white powder too). Elementary

analysis and ESI results were in perfect agreement with the values obtained from the theoretical D-BisCC chemical structure (Figure 4.1), as presented in Table 4.7.

Table 4.7: ESI and elementary analysis of D-BisCC. Theoretical and experimental results.

		Theoretical values	Results
Elementary Analysis	Carbon (%)	44.46	44.61
	Hydrogen (%)	3.73	3.88
	Nitrogen (%)	0.00	0.00
ESI	$[M+K^+]$ (g/mol)	255.00	254.99

The absence of nitrogen in the product is a strong argument which shows the efficiency of the removal of TBD and DBU. The DSC analysis of D-BisCC (Figure SI 45 in Annex) shows a sole endothermic peak at 214 °C corresponding to the fusion. FTIR spectra (*Figure SI 46* in Annex) present typical C=O stretching vibration of five membered cyclic carbonate at 1778 cm^{-1} and the peak at 1130 cm^{-1} is related to the C-O-C stretch. Finally, C-H_2 and C-H linkage stretching vibration are visible at 2995-2992 and 2880 cm^{-1}, respectively. The D-BisCC structure was confirmed by ^1H and ^{13}C-NMR, (Figure SI 47-a and b in SI, with fully attributed signals).

^1H-NMR, δ (ppm): 5.4 (m, 2H, CH-CH(O)), 5.0 (m,1H, CHO), 4.6 (t, 1H, C$\underline{H_2}$O), 4.5 (m, H, C$\underline{H_2}$O), 4.2 (d, 1H, C$\underline{H_2}$O), 4.0 (d, 1H, C$\underline{H}$O), 3.8 (d, 1H, CH_2O), (fully attributed ^1H-NMR spectra available in Figure SI 47-a in Annex).

^{13}C-NMR, δ (ppm): 154.7 (C=O), 153.9 (C=O), 81.1 (CH-O), 80.8 (CH-CHOC(O)), 79.6 (CH2-CHO-C(O)), 74 (CHO-C(O)-CH2O), 71.8 (CH2O), 66.3 (CH2O) (fully attributed ^{13}C-NMR spectra available in Figure SI 47-b in Annex).

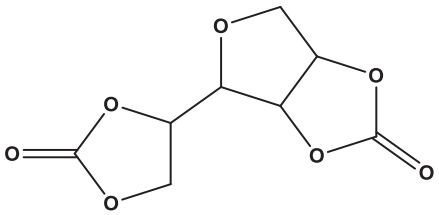

Figure 4.1: D-BisCC from D-sorbitol

According to all these different characterizations, the unique synthesized product was the D-BisCC.

A preliminary protocol has been tested with the same conditions previously described on the synthesis of tri-cyclocarbonate from D-mannitol (Komura et al., 1973), but in this case with the D-sorbitol as a starting reagent (Table 4.3, Entry 1). The corresponding conditions (high temperature, controlled vacuum) are not adequate and did not permit the obtaining of tri-cyclocarbonate. After recrystallization, the obtained product was D-BisCC with a low yield (18%), largely lower than the one previously reported with D-mannitol (65 %). Contrary to the D-mannitol, D-sorbitol has a high tendency to undergo a first dehydration with these

conditions. This is explained by the stereochemistry differences of both isomers (Figure 4.2). In the D-sorbitol, several hydroxyl groups present *cis* configuration along the backbone. In the case of D-mannitol, three pairs of hydroxyl groups present three distinct planes. This last configuration highly promotes the formation of five-membered cyclocarbonate.

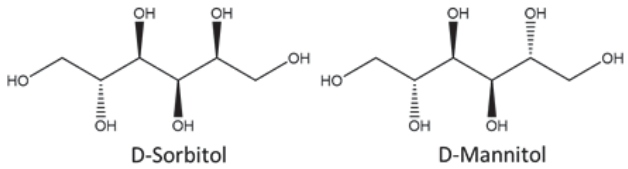

Figure 4.2: D-sorbitol and D-mannitol structures

Mazurek-Budzynsky and al (Mazurek-Budzyńska et al., 2016) also faced a limited D-sorbitol conversion into D-BisCC when reacted with DMC. These authors proposed a reactional pathway (Figure 4.3) with the dehydration of the D-sorbitol firstly occurs and with two reactional intermediates, 1,4- and 3,6-sorbitan, respectively. However, only the pairs of diols of 1,4-sorbitan, in *cis* configuration, can undergo the transesterification with DMC. Whereas, diols in *trans* configuration are not suitable for the formation of five-membered cyclic carbonates because of the ring strength which lead to linear carbonates. Our observations are on perfect agreement with Mazurek-Budzynsky and al. (Mazurek-Budzyńska et al., 2016) results, leading to the same conclusions. The stereochemistry and the number of available diols strongly affect the formation of five-membered cyclocarbonates, regardless the structure (linear or cyclic) of the carbonates (DMC or EC, respectively) involved in the transesterification.

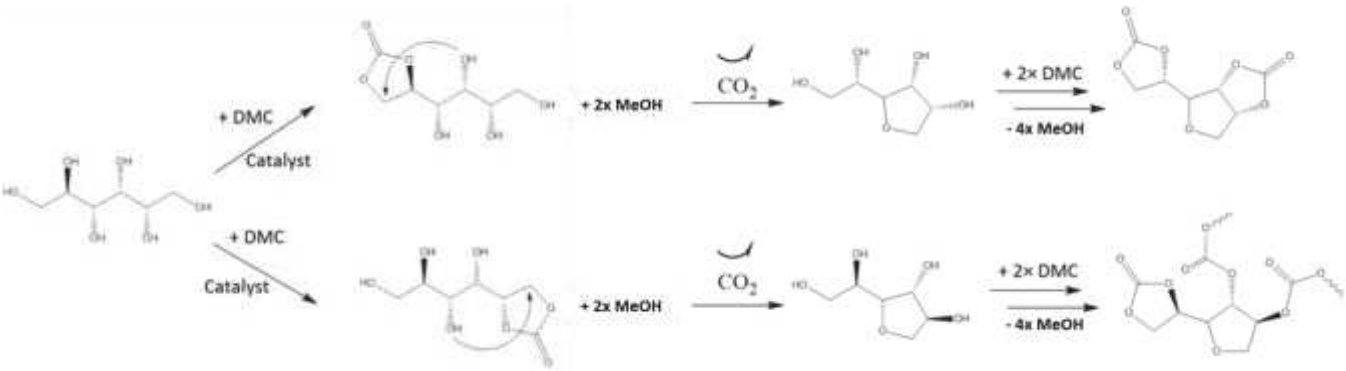

Figure 4.3: Proposed reaction path-way of D-sorbitol with DMC, from Mazurek-Budzynsky et al.(Mazurek-Budzyńska et al., 2016)

To confirm the previous hypothesis concerning the effect of the spatial configuration of the hydroxyl groups on the final yield, different model molecules based on cis-1,2-cyclopentanediol (^{1}H-NMR spectrum available in Figure SI 48 in Annex) and trans-1,2-cyclopentanediol (^{1}H-NMR spectrum available in Figure SI 49 in Annex) corresponding to the cyclic diols present in 3,6-sorbitan and 1,4-sorbitan, respectively, were studied. ^{1}H-NMR signal attribution (Figure SI 50 in Annex) of the synthesis product obtained from cis-1,2-cyclopentanediol was a cyclic carbonate, with a typical chemical displacement of δ (ppm)= 5.4 (m, 2H, CH-CH(O)). Additionally, the absence of the alcohol signal at δ (ppm) = 4.2 (m, 2H, CH(OH)) is a strong

confirmation of the full conversion of the cis-1,2-cyclopentanediol. Instead, ^{1}H-NMR signals attributions (Figure SI 51 in Annex) of the products from trans-1,2-cyclopentanediol were less obvious. A total conversion of the two hydroxyl functions with the absence of the signal at δ (ppm) = 4.4 (m, 2H, CH(O<u>H</u>)) was noticed. However, the sharpest singlet at δ (ppm) = 3.7 (s, 3H, CH_3<u>O</u>) was related to a methyl carbonate structure and the absence of signals at δ (ppm)= 5.4 (m, 2H, CH-CH(O)) is relevant to the absence of cyclic carbonate. These results on model molecules confirm the initial hypothesis; the diol *cis* stereochemistry promotes cyclic carbonate based on esters exchange reaction. Then, the limiting step is the first dehydration leading to 3,6-sorbitan and 1,4-sorbitan. However, only 1,4-sorbitan presents the suitable stereochemistry to ensure five-membered cyclic carbonate formation.

Catalyst screening and D-BisCC kinetic study

Table 4.3 presents the results of a catalyst screening. In a first part, different tests were based on metallic catalysts since they are widely used on polymer synthesis and transesterification (Debuissy et al., 2017). The results of these tests based on a transesterification between DMC and D-sorbitol with a distillation bridge, during 16 h are given in Table 4.3, Entries 2-4. No reaction occurs (yield of 0 %) since the reaction temperature is too low to activated metallic catalysts, which are generally used in a temperature range of 150-250 °C (Jacquel et al., 2011; Tserki et al., 2006). Then, most efficient catalyst systems have been tested with two families based on strong bases associated with mineral (Table 4.3, Entries 5-7) or organic structures (Table 4.3, Entry 8-10). These latter can be divided into two main groups based on strong bases with (i) the phosphazene family, which are the strongest bases, and particularly BTPP which presents a pK_{BH+}= 28.89 (Schwesinger et al., 1994) (Table 4.3, Entry 8), and (ii) the guanidine family with TBD and DBU, pK_{BH+}= 25.98 and 24.33, respectively (Table 4.3, Entries 9-10). BTPP gave similar results than DBU and TBD with a low yield, 20-25%. These results were surprising as it was expected that the strongest bases could increase the reaction rate and the yield. In fact, we could assume that the basicity of BTPP is too high and then promote side-reactions. In particular, it could be assumed that the carbonate rings are deprotonated to create an equilibrium between ring and linear-based carbonates. Table 4.3, Entries 5-7 present results with mineral bases. No reaction occurs with the strong mineral bases which have been also tested by Mazurek-Budzyńska and al. (Mazurek-Budzyńska et al., 2016) They performed reactions with methanol as solvent and then obtain 41% of D-sorbitol conversion with K_2CO_3 as catalyst.

The use of a solvent should be taken into account to explain this difference of results, since the solvent can increase the mobility of the chemicals and the homogeneity of the medium. However, it is very well known that reactions without solvent present strong advantages for the environment and a green chemistry, for the scaling up, and on the final product cost. Based on these previous observations, the solubilities of the different catalysts at room temperature and 75 °C (i.e. the reactional temperature) were investigated. It appears that all the mineral catalysts were insoluble in DMC at both temperatures. However, TBD, DBU and BTPP were soluble in DMC at 75 °C. These solubility results confirmed the deprotonation of D-sorbitol in a

tri-phase medium under ester-exchange conditions was impossible. Instead, when the catalyst is soluble in the reactional medium, its activity is promoted, and a solid / liquid reaction is then possible.

To conclude this screening part, strong organo-catalysts seem to be the most appropriate catalysts to perform this kind of reaction. This also highlights the fact that working in a green way i.e. in a reactive solvent with bi-phase medium implies an appropriate choice of catalyst. According to these previous results, organo-catalysts were selected after this screening step. More precisely, a system based on TBD was chosen since it presents a lower toxicity with similar yield results compared to DBU or BTPP.

Figure 4.4 displays the results of kinetic evolutions with 3.5 and 7eq. of DMC toward sorbitol with a distillation bridge (Table 4.3, Entries 10 and 14).

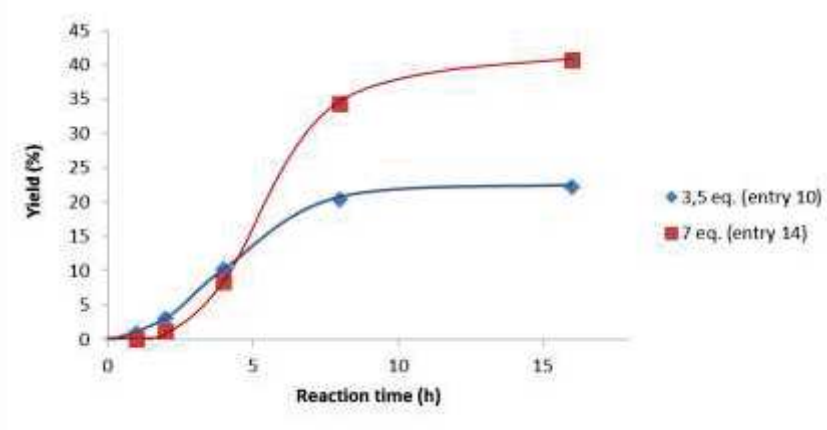

Figure 4.4: Influence of the number of equivalent of DMC on the kinetic profile with a distillation bridge device

With 3.5eq. of DMC, a yield plateau at around 20 % was reached after 8 h of reaction. With 7eq. of DMC, the same phenomenon occurs at 41 %, also after around 8 h of reaction. These results were surprising considering the proposed reactional mechanism (Figure 4.3), working with more than 3.5eq. of DMC equivalent is theoretically not needed. Figure SI 52 (in Annex) shows ^{1}H-NMR analysis of the reaction distillate indicating DMC and methanol (MeOH) molecules in the medium. It pointed out the formation of an azeotrope between DMC and MeOH. Such an azeotrope has been previously reported (Clements, 2003) with a DMC/MeOH molar ratio close to 30/70. Additionally, the evaporation of DMC by vapor pressure cannot be excluded.

The effect of different experimental conditions and devices were investigated to increase the reaction yield and to compensate the potential loss of reactant. Optimum results were 40 % yield with 5 eq. of DMC and 10% yield with distillation bridge (Table 4.3, entry 13) and reflux device (Table 4.3, entry 15), respectively. Finally, with vigreux fractionating column, several synthesis were performed with various content of DMC. The main kinetic results of the corresponding study are presented on Figure 4.5. The profiles are similar to the previous one and present a plateau at 24-48h of reaction. Nevertheless, the option of breaking the azeotrope with a vigreux fractionating column cannot be selected. Indeed, a remaining amount of DMC is still distilled with the methanol and the reaction was not shifted in favor of the synthesis of the BisCC. The

global yield only increases of 5% with a 32 h long reaction compared to the obtained result with a distillation bridge. More detailed information are available in the Annex 6 section. All results are summarized in Table 4.3.

This kinetic study shows that the optimum yield at low reactional temperature was 40% with 5eq. of DMC, TBD as catalysts with a distillation bridge device over 16 h reaction. However, a maximum yield of 45% can be reached using a vigreux fractionating column during 48 h. This reactional time is three times superior than those performed with a distillation bridge. These results are promising since the formation of 1,4 sorbitan with 3,6 sorbitan cannot be avoided, limiting consequently the yield, according to the mechanism proposed on Figure 4.3.

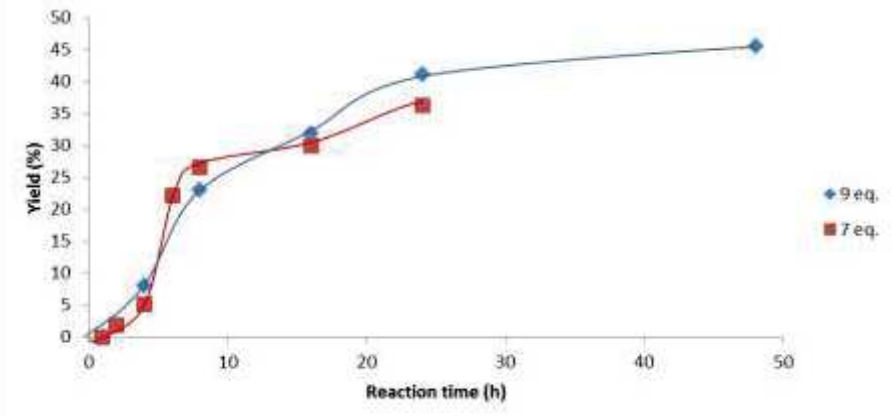

Figure 4.5: Influence of the number of equivalent of DMC on the kinetic profile with vigreux distillation column

D-BisCC yield optimization based on continuous flow rate system

To optimize the DMC intake and increase the conversion of D-sorbitol into D-BisCC; another reactional setup with a continuous feeding of DMC was incremented. The DMC feed was regulated at 0.3 mL/h (Table 4.4, Entry 2-3) and initial DMC/D-sorbitol (mole/mole) ratios were fixed at 1 (Table 4.4, Entry 3) and 3.5 (Table 4.4, Entry 2). Reactions yield were 35 and 43 %, respectively. Compared to previous results, the yield increase was not significant in these conditions. When initial DMC/D-sorbitol ratio was set to 1, the low content of reactive solvent prevents a correct homogenization of the medium and the global reactivity of the system is decreased. Then, with the ratio set to 3.35, the conditions are very similar to the optimum one with a distillation bridge. It is thus coherent to obtain a similar reaction yield.

According to these observations, reactional settings were adjusted. The DMC/D-sorbitol ratio was maintained at 3.5, but the DMC flow rate was decreased to 0.15 mL/h to maintain the reactant content as low as possible in the reactional medium in order to minimize reactant loss by vapor tensor and maintain the azeotrope formation. In this case, a total of 8.5 eq. of DMC in respect to the D-sorbitol were used i.e. an excess of 5.5 eq. Similar conditions were used for the reaction presented in Table 4.3, entry 19 with a classical reaction setup, leading to 45% yield in 48h. Instead the use of continuous feeding of DMC successfully increased the yield to 50% in 16h.

Synthesis of polyether/polycarbonate by ROP of D-BisCC

The conditions of reactions between 1-octanol and BisCC are presented in Table 4.6. A gas release was observed for all reactions on agreement with the mechanism presented in Figure 4.6 (Kühnel et al., 2015).

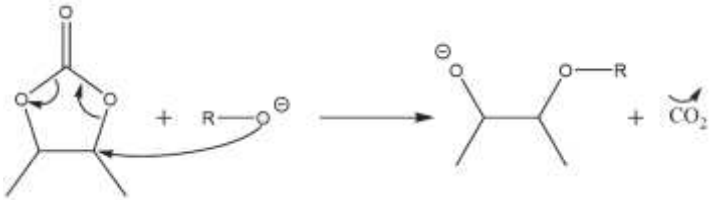

Figure 4.6: General mechanism to obtain ether linkage from five-membered BisCC, with CO_2 formation

Table 4.6, Entry 1 corresponds to a model reaction between an alcohol initiator and the D-BisCC to control the reactivity of the five-membered carbonate cycles. After two hours of reaction, the medium was directly analyzed by ^{1}H-NMR (Figure 4.7, b)), ^{13}C-NMR (Figure 4.7, c)) since the reaction was performed in DMSO-d_6. Results were compared to the initial medium (before the reaction starting) (Figure 4.7, a)). The full consumption of the five-membered carbonate and hydroxyls groups was controlled through the absence of the peak at δ (ppm): 5.4 (m, 2H, CH-CH(O)) and δ (ppm): 4.3 (s, 1H, CH_2-OH)). D-BisCC is highly reactive in these conditions and released hydroxyl groups from the ROP were able to react on another D-BisCC to coupled two initiated D-BisCC. The resulting coupled molecule is a diol and is presented in Figure 4.7, b-c. Thus, a D-BisCC molecule can act as cross-linking point, once the two cyclic(carbonate) are opened, two hydroxyls groups are released and available to initiate another D-BisCC molecule.Figure SI 53, (1), (2) and (3) (in Annex) present the three main molecules which can be theoretically obtained by this reaction. According to ^{13}C-NMR spectrum (Figure 4.7, c), the reactional product is 5,10-bis((octyloxy)methyl)octahydro-2H,5H-difuro[3,2-b:3',2'-f][1,5]dioxocane-3,8-diol (Figure SI 53 (3) in Annex).

Anionic ROP were conducted with 10 to 100eq. of D-BisCC, in respect to the 1-octanol, with 0.7% mol of catalyst (Table 4.6, Entries 6-9). Brown viscous products were obtained, (Table 4.6, Entries 6 and 7), and sticky brown materials (Table 4.6, Entries 8 and 9). SEC analyzes (Figure SI 54 in Annex) show two main oligomers populations with degree of polymerization (DPn) of 5 and 10 (Table 4.8), respectively (determined from Equation (1)). When 10eq. of initiator were used (Entry 9), only one population was detected with a DPn = 5 (Table 4.8). Similar DPn were observed when the reaction was conducted with 25 or 100eq. of D-BisCC. (Table 4.8, Entry 6, 8). Consequently, 25eq. of D-BisCC seems to be an optimum. A low molar masses peak (i.e. 355 g/mol) was sometimes observed, corresponding to residual D-BisCC.

According to the proposed opening mechanism (Figure 4.6), primary and secondary hydroxyl groups can be obtained. Each time, a five-membered cyclic carbonate is opened. The hydroxyl contents of each oligomer were determined by quantitative ^{31}P-NMR (Figure SI 55 in Annex) and show a low content in primary hydroxyl groups. The global OH value is comprised between 4.5 and 5.5 mmol/g (Table 4.8).

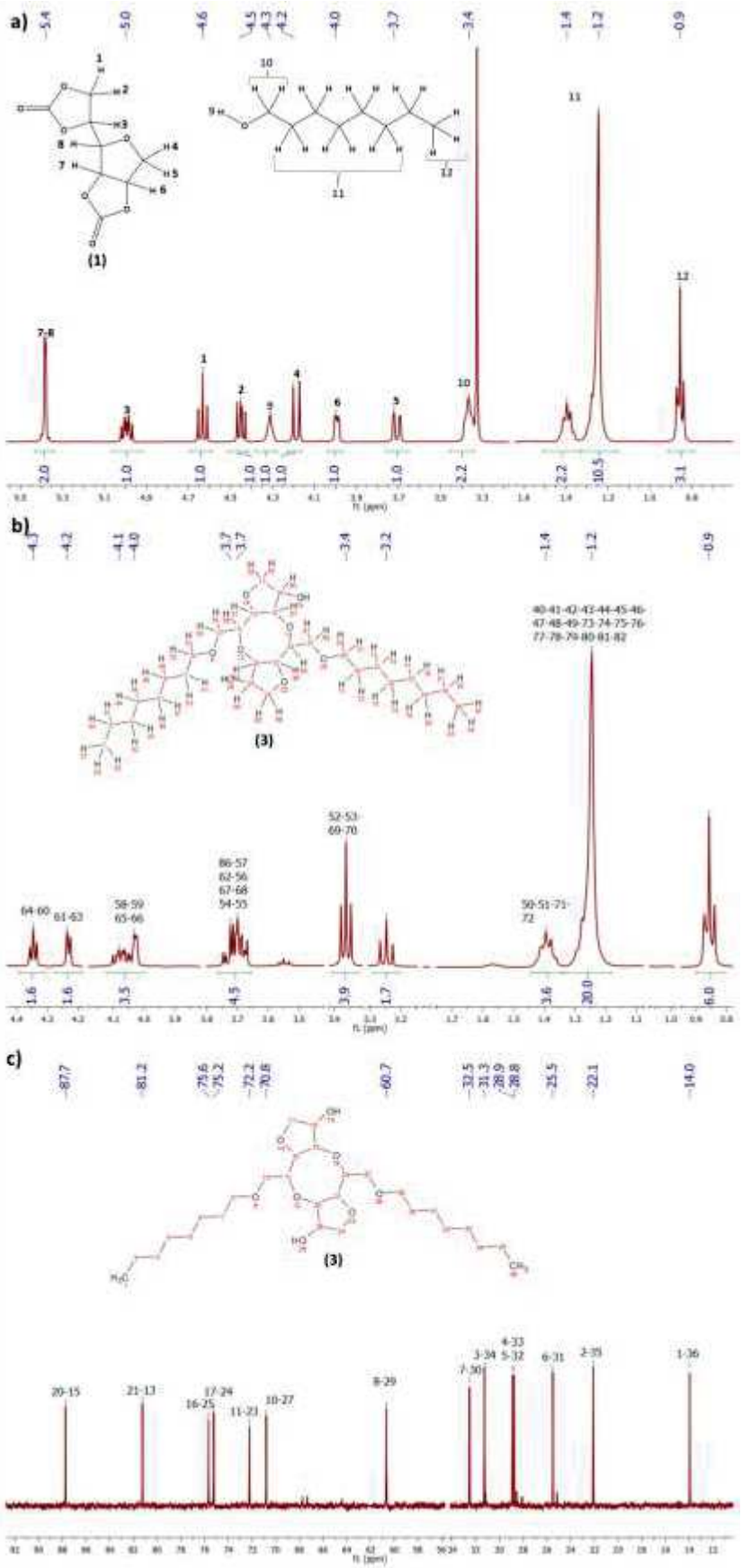

Figure 4.7: NMR spectra: (a) ^{1}H-NMR of the D-BisCC and 1-octanol mixture (b) ^{1}H-NMR and (c) ^{13}C-NMR of the synthesized product.

From the synthesis presented in Table 4.4, Entries 2-4 present a higher content in catalyst in order to increase the reaction rate. In each case, a solidified and brittle brown material was obtained. Figure SI 56 (in Annex) shows FTIR analysis of the corresponding materials. The absence of the characteristic peak at 1778cm^{-1} (C=O, five-membered cyclic carbonates) and the large signal at 3200 cm^{-1} corresponding to O-H elongation are strong indications that the full conversion of the BisCC occurs. The presence of the bands at 1680 and 1040 cm^{-1} are related to C=O stretching of the linear carbonate and the C-O stretching of ethers linkage (Duval and Avérous, 2016), respectively. Nevertheless, these three different products were insoluble in most of the common solvents even after acetylation due to the cross-linked architectures. Then, the NMR quantification of ether and carbonate linkage contents were impossible to be correctly performed.

Table 4.8: Properties of main synthetized macromolecular architectures

Entry	Mn_1 (g/mol)	Mn_2 (g/mol)	Mn_3 (g/mol)	DPn	I-OH content (mmol/g)	II-OH content (mmol/g)	Global OH value (mg KOH/g)	$T_{deg\ 5\%}$	$T_{deg50\%}$	Chars (% wt)
2								140	440	0
3					*Insoluble*			98	200	25
4								92	271	35
5	1588	n.o.	n.o.	7	0.6	4.6	288	114	196	0
6	335	1355	2377	10	0.9	4.1	276	138	258	0
7	335	1340	2315	10	0.7	4.2	273	90	228	2
8	1385	2500	n.o.	10	0.8	4.7	305	125	248	8
9	255	1280	n.o	5	0.9	3.6	250	119	244	9

n.o.: not observed

Synthesis of polyhydroxyurethanes

Four PHU were synthetized from different short diamines (C4 to C6) and DDA (C36) (Table4.5, Entries 1-4). Then, two families of PHU were synthetized from a blend of DDA and short diamines to investigate the effect of the fatty diamines on the chemical and thermal properties of the resulting PHU (Table 4.5, Entries 5-12).

Figure 4.8 presents the FTIR spectra of the initial monomer (D-BisCC) and PHU-P, PHU-B, PHU-D and PHU-H. D-BisCC presents, as previously described, a characteristic peak at 1783 cm^{-1} corresponding to the carbonyl bond. This peak is missing for the different synthetized PHUs showing the full consumption of the BisCC. All PHUs present the distinctive bands of the urethane groups located at 3300-3400 cm^{-1} (–NH stretching merge with the –OH stretching), 1690 cm^{-1}, 1530 cm^{-1} (-NH, bending) and 1250 cm^{-1} (=CO, stretching) (Cornille et al., 2016b). The O-H stretching band at 3300-3400 cm^{-1} is due to the aminolysis reaction presented in Figure 4.9, on perfect agreement with the expected chemical structure of PHUs. A shoulder or second peak located around 1650 cm^{-1} is characteristic of amide formation. This peak is absent since the monomers do not present ester linkages for PHU-B, PHU-D, PHU-H and PHU-P (Carré et al., 2014). The PHU obtained from the diamines blend present similar FT-IR spectra (Figure SI 57 in Annex).

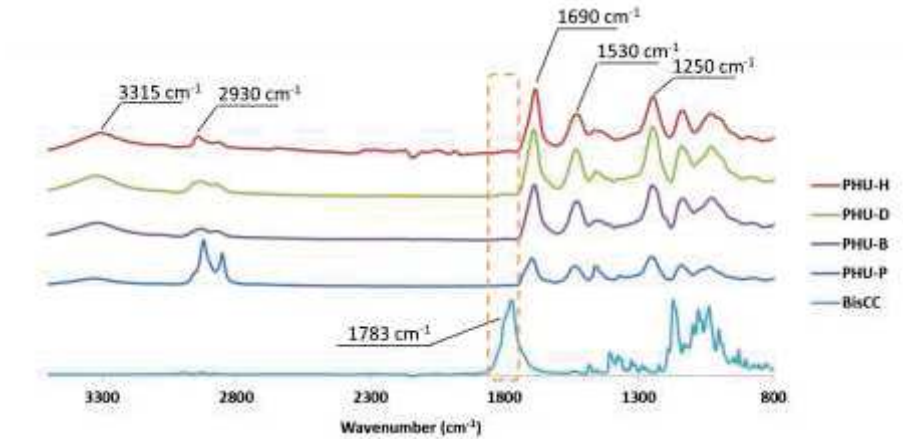

Figure 4.8: FT-IR spectra of BisCC, PHU-P, PHU-B, PHU-D, PHU-D and PUH-H

Table 4.8 presents the number-average molar mass (Mn) of the synthetized PHUs. All SEC curves are available in Figure SI 58 and Figure SI 59 (in Annex). Mn values are rather low, comprise between 1450 and 2430 g.mol^{-1} for all PHUs. However, it is well known that PHUs generally present low Mn and high Đ (Table 4.9) due to different factors such as a wide number of side reactions. (Besse et al., 2015) The molar masses obtained in this study are comparable to other published NIPU systems(Boyer et al., 2010; Carré et al., 2014).

The PHUs OH-values presented in Table 4.9 evolve from around 9 mmol/g for PHU-B, PHU-D, PHU-H to 3 mmol/g for PHU-P, in full agreement with the aminolysis reaction, presented on Figure 4.9**.**

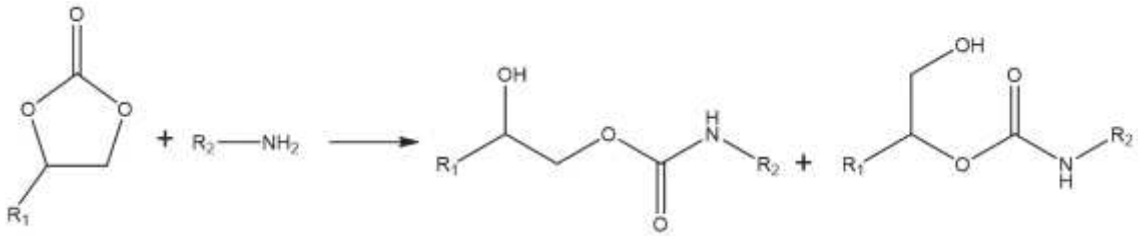

Figure 4.9: aminolysis reactional pathway between a five-membered BisCC and a primary amine

It is obvious that hydroxyl groups content decrease with the diamine chain length increase. Then the PHUs functionality can be tuned. Indeed, the diamine blend strategy provides a wide range of OH-values. These hydroxyl groups can be used for PHU crosslinking to modify the properties by increasing the molar masses of the PHUs.

Figure SI 60 to Figure SI 63 and Figure SI 64 to Figure SI 67 (in Annex) present the ^{1}H-NMR and ^{13}C-NMR spectra of PHU-P, PHU-B, PHU-D, PHU-H, respectively, with the main peaks attribution. These NMR spectra confirm the macromolecular architectures of the PHUs on agreement with previous FT-IR observations.

TGA and DTG curves of PHU-P (Figure 10, a-b) present a three-step weight loss. This complex thermal degradation is linked to the urethane function reversibility within a temperature range from 120 to 250 °C

depending of the neighbor groups (Simon et al., 1988). At higher temperature, irreversible degradation mechanism of the urethane bond followed by carbon-carbon bonds cleavages take place. However, PHUs obtained from shorter diamines present a two-stage weight loss based on urethane function reversible and irreversible degradation mechanism. The resulting low molar masses PHUs fragments, linked to the short monomers compared to DDA, are vaporized before that carbon-carbon bonds cleavages could occur. As previously described (Javni et al., 2000), PHUs with the highest urethane bonds content present the lower thermal stability such as PHU-B or PHU-H, for instance compared to PHU-P. PHU-H presents the lowest thermally stability, certainly due to the presence of methyl groups along the backbone due to the chemical structure of 1.5-diamino-2-methylpentane. It is very well known that the methyl group is electron donor which promotes the urethane degradation into primary amines and olefins (Javni et al., 2000).

Finally, PHU obtained from diamines blends presents weight loss profiles comprised between the PHU-P profile and the PHU-B or the PHU-D profile, as shown in Figure SI 68 (in Annex). The characteristic temperature at 50% of weight loss ($T_{deg50\%}$) ranges between 216 and 318 °C for PHUs based on 1.4 B (Table 4.9). $T_{deg50\%}$ of PHU based on 1.5 MD evolved from 217 to 304 °C (Table 4.9). As previously described, the increase of the DDA content in the macromolecular architecture, decreases the global thermal instability linked to the urethane bonds.

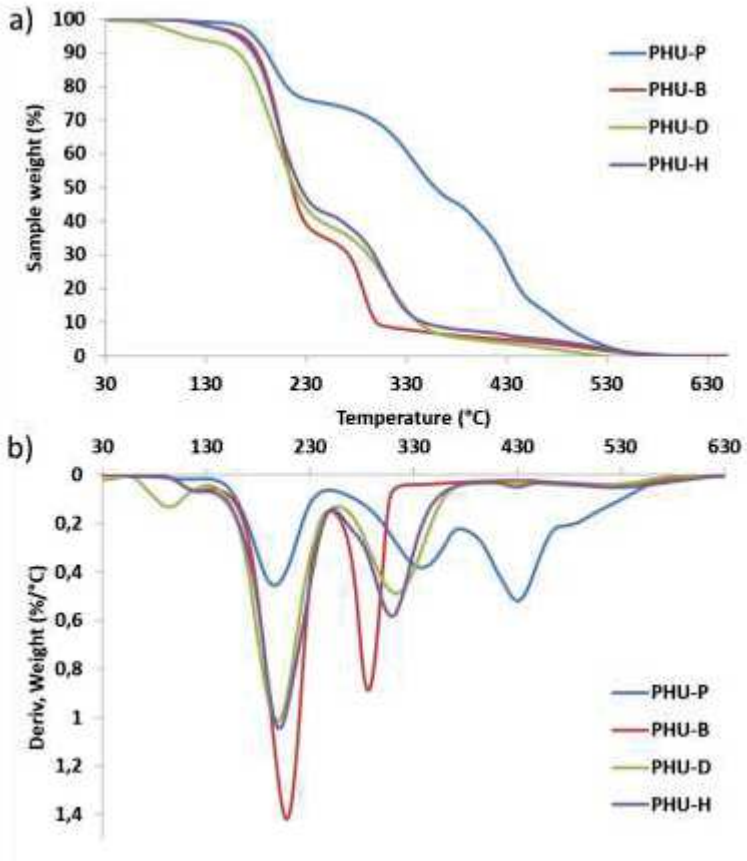

Figure 4.10: a) TGA and b) DTG curves of PHU-P, PHU-B, PHU-D and PHU-H

TGA analyses have shown that no major degradation occurs during the the studied temperature range of the DSC analysis. Tg of the PHUs are presented in Table 4.9. PHU-B, PHU-D and PHU-H have similar Tg (around 41°C), whereas PHU-P presents a Tg below 0°C. This low Tg is linked with DDA building block and its pending chains since they bring chains mobility and a Tg decrease (Gargallo et al., 1987, 1988; Yazdani-Pedram et al., 1986). As previously shown on thermal properties, the diamine blending can allow to tune the Tg of the corresponding PHU. As presented in Figure SI 69 (in Annex), Tg from PHU-0.2B to PHU-0.8B and from PHU-0.2D to PHU-0.8D gradually evolved from below zero to room temperature (Table 4.9) as a function of the DDA content and evolved according to a polynomial fit presented in Equation SI. 2-3 in Annex 6).

Table 4.9: Main properties of the synthetized PHUs

Sample	$T_{deg\ 50\%}$ (°C)	Tg (°C)	OH-Value (mmol /g)	Mn (g/mol)	Mw (g/mol)	Đ
PHU-P	359	-3	3.25	2433	5367	2.21
PHU-B	216	41	8.84	1906	4478	2.35
PHU-D	217	42	8.69	2266	5845	2.58
PHU-H	224	41	4.83	1446	2722	1.88
PHU-0.2B	318	-9	3.90	1815	3124	1.72
PHU-0.4B	326	-4	4.58	1927	4360	2.26
PHU-0.6B	280	12	5.26	1843	4189	2.28
PHU-0.8B	257	20	6.26	1685	5032	2.99
PHU-02D	304	-2	4.06	2769	5038	1.82
PHU-0.4D	324	2	4.48	2139	4874	2.28
PHU-0.6D	276	20	5.15	2402	5518	2.30
PHU-0.8D	270	37	6.01	1502	5176	3.45

Conclusion

The D-BisCC, a promising biobased chemical platform, was successfully synthetized from D-sorbitol in eco-friendly condition i.e. low temperatures, catalyzed reactions, reactive solvents and renewable reactants. A deep study of the reactional conditions and setups was conduct to determine the optimum pathway resulting in a strong increase of the synthesis yield (+25 %) compared to previous works based on green reactions. One of the key parameter was the catalyst solubility in DMC, the reactive solvent. The most fruitful results were obtained with TBD as catalyst and a continuous feed of DMC into the reactional medium. To show that D-BisCC is a chemical platform, it was used as a basis leading to the elaboration of different products with specific architectures: (i) a diol (ii) crosslinked polyethers and (iii) PHUs. All D-BisCC derivate present non-conventional molecular architectures from the fused tetrahydrofuran ring, with the resulting hydroxyl groups obtained from the rings opening. In the case of polyether's synthesis, these hydroxyl groups show a reactivity high enough to polymerize with another D-BiCC to form a chain. This chemical platform was also involved in PHUs synthesis with different short and fatty diamines. The chain length of the diamine was an effective leverage on PHUs glass transition. The resulting non-isocyanate polyurethanes present a large range of glass transition temperatures from– 9 to 42 °C.

To conclude, D-BisCC has proved to be an efficient biobased chemical platform, leading to a large range of products, using different chemical pathways, with a large portfolio of properties.

Acknowledgements

The authors are grateful to Alsace Region, Eurometropole, BPI-France, Tereos and Soprema for their financial supports.

References

Anand, A., Kulkarni, R.D., Gite, V.V., 2012. Prog. Org. Coat. 74, 764–767.

Anand, A., Kulkarni, R.D., Patil, C.K., Gite, V.V., 2016. RSC Adv 6, 9843–9850.

Arbenz, A., Avérous, L., 2015. Ind. Crops Prod. 67, 295–304.

Argyropoulos, D.S., 1995. Res. Chem. Intermed. 21, 373–395.

Besse, V., Camara, F., Méchin, F., Fleury, E., Caillol, S., Pascault, J.-P., Boutevin, B., 2015. Eur. Polym. J. 71, 1–11.

Boyer, A., Cloutet, E., Tassaing, T., Gadenne, B., Alfos, C., Cramail, H., 2010. Green Chem. 12, 2205.

Bozell, J.J., Petersen, G.R., 2010. Green Chem. 12, 539.

Caouthar, A., Roger, P., Tessier, M., Chatti, S., Blais, J.C., Bortolussi, M., 2007. Eur. Polym. J. 43, 220–230.

Carré, C., Bonnet, L., Avérous, L., 2014. RSC Adv 4, 54018–54025.

Carré, C., Bonnet, L., Avérous, L., 2015. RSC Adv 5, 100390–100400.

Carré, C., Zoccheddu, H., Delalande, S., Pichon, P., Avérous, L., 2016. Eur. Polym. J. 84, 759–769.

Clements, J.H., 2003. Ind. Eng. Chem. Res. 42, 663–674.

Cornille, A., Auvergne, R., Figovsky, O., Boutevin, B., Caillol, S., 2017a. Eur. Polym. J. 87, 535–552.

Cornille, A., Blain, M., Auvergne, R., Andrioletti, B., Boutevin, B., Caillol, S., 2017b. Polym Chem 8, 592–604.

Cornille, A., Dworakowska, S., Bogdal, D., Boutevin, B., Caillol, S., 2015. Eur. Polym. J. 66, 129–138.

Cornille, A., Michaud, G., Simon, F., Fouquay, S., Auvergne, R., Boutevin, B., Caillol, S., 2016. Eur. Polym. J. 84, 404–420.

Dais, P., Spyros, A., 2007. Magn. Reson. Chem. 45, 367–377.

Debuissy, T., Pollet, E., Avérous, L., 2017. Eur. Polym. J. 90, 92–104.

Deepa, P., Jayakannan, M., 2008. J. Polym. Sci. Part Polym. Chem. 46, 2445–2458.

Desroches, M., Escouvois, M., Auvergne, R., Caillol, S., Boutevin, B., 2012. Polym. Rev. 52, 38–79.

Duval, A., Avérous, L., 2016. ACS Sustain. Chem. Eng. 4, 3103–3112.

Feng, X., East, A.J., Hammond, W.B., Zhang, Y., Jaffe, M., 2011. Polym. Adv. Technol. 22, 139–150.

Fenouillot, F., Rousseau, A., Colomines, G., Saint-Loup, R., Pascault, J.-P., 2010. Prog. Polym. Sci. 35, 578–622.

Furtwengler, P., Perrin, R., Redl, A., Avérous, L., 2017. Eur. Polym. J. 97, 319–327.

Gallezot, P., Cerino, P., Blanc, B., Fleche, G., Fuertes, P., 1994. J. Catal. 146, 93–102.

Garcia-Herrero, I., Cuéllar-Franca, R.M., Enríquez-Gutiérrez, V.M., Alvarez-Guerra, M., Irabien, A., Azapagic, A., 2016. ACS Sustain. Chem. Eng. 4, 2088–2097.

Gargallo, L., Hamidi, N., Radić, D., 1987. Thermochim. Acta 114, 319–328.

Gargallo, L., Soto, E., Tagle, L.H., RadiĆ, D., 1988. Thermochim. Acta 130, 289–297.

Ginés-Molina, M.J., Moreno-Tost, R., Santamaría-González, J., Maireles-Torres, P., 2017. Appl. Catal. Gen. 537, 66–73.

Granata, A., Argyropoulos, D.S., 1995. J. Agric. Food Chem. 43, 1538–1544.

Gustini, L., Lavilla, C., Janssen, W.W.T.J., Martínez de Ilarduya, A., Muñoz-Guerra, S., Koning, C.E., 2016. ChemSusChem 9, 2250–2260.

Gustini, L., Noordover, B.A.J., Gehrels, C., Dietz, C., Koning, C.E., 2015. Eur. Polym. J. 67, 459–475.

Haba, O., Tomizuka, H., Endo, T., 2005. Macromolecules 38, 3562–3563.

Holladay, J.E., Bozell, J.J., White, J.F., Johnson, D., 2007. DOE Rep. PNNL 16983.

Hough, L., Priddle, J.E., Theobald, R.S., 1962. J. Chem. Soc. Resumed 1934–1938.

Jacquel, N., Freyermouth, F., Fenouillot, F., Rousseau, A., Pascault, J.P., Fuertes, P., Saint-Loup, R., 2011. J. Polym. Sci. Part Polym. Chem. 49, 5301–5312.

Javni, I., Hong, D.P., Petrović, Z.S., 2008. J. Appl. Polym. Sci. 108, 3867–3875.

Javni, I., Petrovic, Z.S., Guo, A., Fuller, R., 2000. J. Appl. Polym. Sci. 77, 1723–1734.

Kihara, N., Endo, T., 1993. J. Polym. Sci. Part Polym. Chem. 31, 2765–2773.

Komura, H., Yoshino, T., Ishido, Y., 1973. Bull. Chem. Soc. Jpn. 46, 550–553.

Kühnel, I., Podschun, J., Saake, B., Lehnen, R., 2015. Holzforschung 69.

Maisonneuve, L., Lamarzelle, O., Rix, E., Grau, E., Cramail, H., 2015. Chem. Rev. 115, 12407–12439.

Mazurek-Budzyńska, M.M., Rokicki, G., Drzewicz, M., Guńka, P.A., Zachara, J., 2016. Eur. Polym. J. 84, 799–811.

More, A.S., Gadenne, B., Alfos, C., Cramail, H., 2012. Polym. Chem. 3, 1594.

Noordover, B.A.J., van Staalduinen, V.G., Duchateau, R., Koning, C.E., van Benthem, Mak, M., Heise, A., Frissen, A.E., van Haveren, J., 2006. Biomacromolecules 7, 3406–3416.

Ochoa-Gómez, J.R., Gómez-Jiménez-Aberasturi, O., Ramírez-López, C., Belsué, M., 2012. Org. Process Res. Dev. 16, 389–399.

Romano, U., Rivetti, F., 1993. Process for preparing di-alkyl carbonates. Google Patents.

Romano, U., Rivetti, F., Di Muzio, N., 1982. Process for producing dimethylcarbonate. Google Patents.

Rose, M., Palkovits, R., 2012. ChemSusChem 5, 167–176.

Schwesinger, R., Willaredt, J., Schlemper, H., Keller, M., Schmitt, D., Fritz, H., 1994. Chem. Ber. 127, 2435–2454.

Simon, J., Barla, F., Kelemen-Haller, A., Farkas, F., Kraxner, M., 1988. Chromatographia 25, 99–106.

Suriano, F., Coulembier, O., Hedrick, J.L., Dubois, P., 2011. Polym Chem 2, 528–533.

Tezuka, K., Koda, K., Katagiri, H., Haba, O., 2015. Polym. Bull. 72, 615–626.

Tomczyk, K.M., Guńka, P.A., Parzuchowski, P.G., Zachara, J., Rokicki, G., 2012. Green Chem. 14, 1749.

Tomita, H., Sanda, F., Endo, T., 2001. J. Polym. Sci. Part Polym. Chem. 39, 162–168.

Tryznowski, M., Świderska, A., Żołek-Tryznowska, Z., Gołofit, T., Parzuchowski, P.G., 2015. Polymer 80, 228–236.

Tserki, V., Matzinos, P., Pavlidou, E., Vachliotis, D., Panayiotou, C., 2006. Polym. Degrad. Stab. 91, 367–376.

Tundo, P., Selva, M., 2002. Acc. Chem. Res. 35, 706–716.

Wu, M., Guo, J., Jing, H., 2008. Catal. Commun. 9, 120–125.

Xu, B.-H., Wang, J.-Q., Sun, J., Huang, Y., Zhang, J.-P., Zhang, X.-P., Zhang, S.-J., 2015. Green Chem. 17, 108–122.

Yazdani-Pedram, M., Soto, E., Tagle, L.H., Diaz, F.R., Gargallo, L., Radić, D., 1986. Thermochim. Acta 105, 149–160.

Zhang, J., Li, J., Wu, S.-B., Liu, Y., 2013. Ind. Eng. Chem. Res. 52, 11799–11815.

Conclusion et perspectives du Chapitre

Au cours de ce Chapitre, la synthèse d'un synthons de référence entre le sorbitol et le carbonate de diméthyle a été démontrée. Pour cela, il est necessaire que le catalyseur de réaction soit soluble dans le diméthyle carbonate à la température de réaction. Une température de réaction fixée à 75 °C pendant 16h avec un pont de distillation sont les conditions les plus performantes pour obtenir une conversion inférieure a 50% du sorbitol en bis(cyclo-carbonate). Un des points limitants de la réaction est la présence d'un azéotrope entre le carbonate de diméthyle et le sous-produit de la réaction (le méthanol) à une température de réaction proche du point d'ébullition du carbonate de diméthyle. Ainsi en travaillant avec un milieu pauvre en diméthyle carbonate (par ajout continu) le rendement de conversion du sorbitol a pu atteindre 50%.

La molécule ainsi obtenue est une molécule plateforme. Celle-ci a pu être impliquée dans différentes réactions chimiques ou procédés de polymérisation. Cela a permis l'obtention d'un diol, de polyéthers courts réticulés et différents polyuréthanes sans isocyanate. Le diol obtenu est une molécule intéressante, car les deux chaines pendantes peuvent être modifiées pour incorporer une fonctionnalité supplémentaire, ouvrant l'accès à de nombreuses architectures macromoléculaires complexes.

Le bis(cyclo-carbonate) a montré qu'il était possible de le polymériser par polymérisation par ouverture de cycle en l'initiant avec un diol. Le degré de polymérisation reste néanmoins difficile à appréhender puisqu'un réseau réticulé est obtenu.

Enfin, le monomère bis(cyclo-carbonate) a été utilisé pour synthétiser des polyuréthanes sans isocyanate linéaire avec différentes diamines biosourcées ou biosourçables. Il a été démontré que la taille de la diamine avait un effet considérable sur la température de transition vitreuse des matériaux finaux. Ainsi, en incorporant différentes diamines, il est possible d'adapter les propriétés du matériau pour répondre à une plus grande variété d'applications. En revanche, la faible réactivité des cycles carbonate à cinq membres ne peut être oubliée. Malgré des temps de réaction relativement longs, les masses molaires des produits de synthèse restent relativement faibles. Ce qui est classique dans la synthèse des polyuréthanes sans isocyanate obtenus par réaction d'aminolyse. Cependant on pourrait exploiter les fonctions hydroxyles créées par réticulation. Cela positionne les NIPU de cette étude comme des pré-polymères biosourcés pouvant être réticulés en vue de futures applications de revêtement de surface, par exemple.

CONCLUSION GENERALE ET PERSPECTIVES

Ce projet de thèse avait pour objectif de transformer un synthon biosourcé et commun, issu de matière agricole, le sorbitol, en polyols respectueux de l'environnement pour l'élaboration de mousses d'isolation polyuréthane ou polyisocyaurate pour le bâtiment. Ce travail de doctorat pluridisciplinaire a associé la synthèse de polymères, la formulation de matériaux, leurs caractérisations physico-chimiques, et les procédés de moussage. De plus, en fin de thèse une démonstration de preuve de concept avec un changement d'échelle jusqu'à la tonne a été faite avec la production de grands volumes de mousses d'isolation sur des lignes de production industrielles.

La démarche scientifique s'est axée sur le développement d'architectures moléculaires et macromoléculaires originales pour l'élaboration de matériaux polymères biosourcés et durables.

L'étude bibliographique présentée dans le **Chapitre 1** de ce manuscrit présente un état de l'art des différentes voies de transformation de la biomasse en polyols biosourcés possédant les propriétés adaptées pour la formulation de mousses de type polyuréthane ou polyisocyaurate. L'analyse de la littérature scientifique a permis de mettre en exergue le spectre des principaux polyols analysé dans la littérature et de faire le lien entre l'origine de la ressource (biomasse) et les propriétés finales des polyols et mousses résultantes. Il ressort de cette étude que l'abondance, la richesse et la variété des synthons ou matériaux issus de la biomasse génère une gamme large de polyols d'architectures variées pour des mousses polyuréthanes et polyisocyanurates. Il apparait que la biomasse lignocellulosique, les huiles végétales et le glycérol brut issu de l'industrie du biodiesel a fait l'objet d'une abondante recherche en raison de leur faible coût et grande disponibilité. A contrario, les synthons polyfonctionnels issus de matière renouvelable traditionnellement utilisée dans l'élaboration de polyols tel que le sorbitol ont été moins developpés. Fort de ce constat, la transformation du sorbitol en nouvelles molécules plateformes et polyols de faible viscosité destinés à l'élaboration de polyuréthane sans isocyanate et mousse polyuréthane a été développée et approfondie dans ce travail de recherche original et productif dans les **Chapitres 2 à 4**. Les **Chapitres 2 à 3** présentent les stratégies de synthèse du sorbitol en polyols polyesters biosourcés suivit de sa formulation et mise en œuvre pour l'obtention de mousses polyuréthane performantes. Différents autres monomères ont été impliqués dans la synthèse des polyols polyesters permettant d'étudier les relations existantes entre la structure de ces monomères et les propriétés finales des polyols. À partir de ces polyols biosourcés, différentes mousses polyuréthanes et polyisocynaurates ont pu être formulées. L'ensemble des polyols et matériaux obtenus on fait l'objet d'une caractérisation chimique, thermique, mécanique et morphologique. Le **Chapitre 4** développe une voie originale de transformation en solvant réactif pour l'élaboration d'une molécule plateforme bifonctionnelle et biosourcée, en partant du sorbitol. Pour démontrer le caractère plateforme de cette molécule, elle a été impliquée dans l'élaboration de différentes architectures (macro)moléculaires. Les synthèses on fait l'objet d'études cinétiques. L'ensemble des produits de réaction a été caractérisé. Ces différentes approches sont résumées dans la Figure C 1**.**

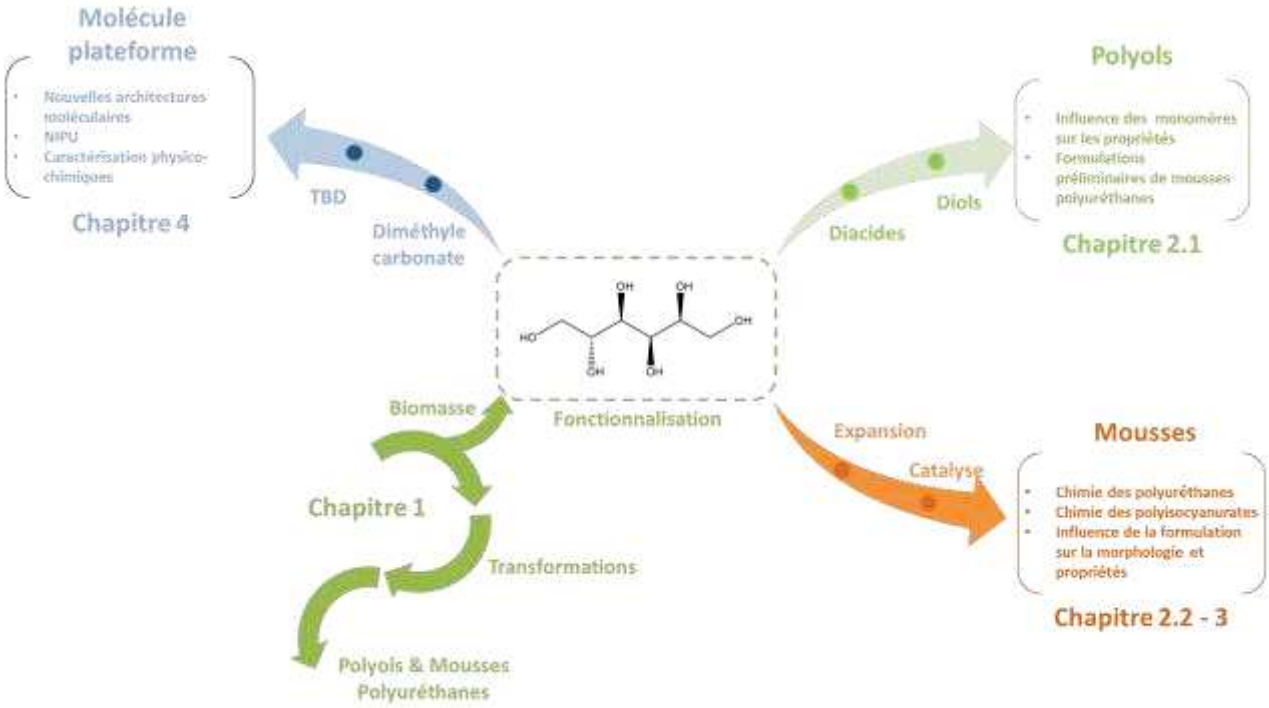

Figure C 1 : Schéma récapitulatif des différents produits obtenus à partir du sorbitol

Les synthèses des différents polyols polyesters linéaires à partir d'un synthon plurifonctionnel, le sorbitol, et de différents diols courts en l'absence de catalyseur et de solvant ont été abordées dans le **Chapitre 2**. L'étude a montré que l'obtention de polyols polyesters linéaires n'est possible que lorsque les conditions opératoires sont contrôlées de manière à localiser la réaction sur les hydroxyles primaires du sorbitol. Il est également ressorti de ce travail que la longueur du diol influence peu les temps de réaction et de rendement d'estérification. Par contre, la longueur finale de chaîne des polyols polyesters induite par les changements de tailles des diols utilisés à une grande influence sur la teneur en groupements hydroxyles et la viscosité du polyol final. La viscosité et la teneur en groupement hydroxyle d'un polyol sont deux caractéristiques essentielles dans l'élaboration de mousse polyuréthane. Seul le polyol synthétisé à partir de sorbitol, acide adipique et 1,4-butanediol (BASAB) présente une viscosité inférieure à 20 000 mPa.s à 20°C permettant une bonne incorporation des différents constituants pour générer une mousse polyuréthane dans de bonnes conditions. À partir du BASAB, plusieurs mousses polyuréthanes ont été obtenues avec différentes formulations. Il a ainsi été montré qu'un point particulièrement impactant des formulations est le choix du ou des agent(s) gonflant(s). Sur les systèmes à base de polyol biosourcé, l'utilisation de l'eau comme agent gonflant favorise énormément la fin de réaction de moussage en diminuant les temps caractéristiques de gel et de hors poisse. Les mousses biosourcées à base d'eau sont plus expansées et présentent donc des densités plus faibles que les mousses expansées avec un agent gonflant physique tel que l'isopentane. Ce phénomène bien que facilement expliqué par l'exothermicité de la réaction entre l'eau et les fonctions isocyanate est moins visible sur des systèmes à base de polyols pétrosourcés. L'avantage majeur des mousses polyuréthanes obtenues à partir de BASAB est leur caractère semi-flexible à haut taux de cellules ouvertes tout en conservant des valeurs de coefficient de conductivité thermique de l'ordre de ceux de la laine minérale.

Toute une gamme de mousses d'isolation commercialisées est constituée de mousses d'isolation thermique hautes performances présentant des coefficients de conductivité thermique inférieurs ou égale à 25 mW/mK. Dans le **Chapitre 3,** l'étude de mousse polyisocyanurates à haut taux de cellules fermées a été étudiée avec pour objectif d'augmenter la teneur en polyol biosourcé de ces matériaux et leurs propriétés. L'étude de la

substitution d'un polyol pétrosourcé par le BASAB a montré qu'il était possible d'obtenir des mousses avec un taux de cellules fermées supérieures à 85 % jusqu'à une substitution totale du polyol pétrosourcé à condition d'utiliser des catalyseurs adéquats. La stratégie la plus prometteuse reste l'incorporation de 25-35 %pds de BASAB au polyol pétrosourcé pour en augmenter la viscosité et la fonctionnalité. Ces deux paramètres sont des éléments clefs pour contrôler la taille des cellules et éviter la coalescence ou une trop grande expansion. En effet, les observations MEB des mousses polyisocynaurates élaborées ont montré des cellules 44% plus petites que celles habituellement obtenues. La diminution de la taille des cellules des mousses permet une meilleure répartition des charges compressives et par conséquent augmente la résistance à la compression des matériaux polymères alvéolaires finaux. L'amélioration la plus conséquente liée à la diminution de la taille des cellules est l'amélioration des propriétés isolantes des mousses polyisocyanurates. Cette stratégie a démontré que l'incorporation de BASAB aux mousses polyisocyanurate améliore les propriétés finales d'un matériau durable destiné à l'industrie du bâtiment. Les résultats encourageants de ces travaux scientifiques ont mené à l'élaboration d'une « preuve de concept » sur ligne de production, qui est présentée en annexe 6.

Le quatrième et dernier chapitre de ce mémoire est consacré à une approche différente de valorisation du sorbitol en une nouvelle molécule plateforme de type bis(cyclo-carbonate). Dans une démarche de respect des principes de la chimie verte, les conditions de synthèse ont été largement optimisées. Ceci porte sur l'utilisation de solvant réactif limitée et de catalyseurs adéquats. Le système réactionnel a permis d'obtenir des taux de conversion du sorbitol en molécule D-BisCC de 50% en parfait accord avec des données comparables de la littérature, à une température de réaction inférieure à 80 °C et à pression atmosphérique. Il a été montré qu'une telle molécule pouvait être impliquée dans des réactions par ouverture de cycle pour former un nouveau diol avec un ratio 1/1 entre l'amorceur et le D-BisCC. Le diol synthétisé comporte deux chaînes pendantes liées à l'amorceur, ce qui permet un grand nombre de fonctionnalisations supplémentaires par modification de ces chaines pendantes. En modifiant le ratio amorceur / D-BisCC, une polymérisation par ouverture de cycle a pu être observée. Le D-BisCC peut donc être considéré comme un nouveau monomère pour l'obtention de réseau polyéther. Enfin, la synthèse de polyuréthanes sans isocyanate par réaction d'aminolyse avec différentes diamines et le D-BisCC a été étudiée. L'ensemble de ces synthèses démontrent la versatilité de la chimie des carbonates cycliques, positionnant le D-BisCC comme une molécule plateforme biosourcée qui pourrait rentrer en compétition avec d'autres molécules commercialisées équivalentes.

Cette thèse rédigée sous forme d'articles scientifiques a permis de soumettre 4 publications scientifiques dans des journaux à comité de lecture et un article de synthèse bibliographique (*review*) sera prochainement soumis. Parallèlement à ces soumissions d'articles scientifiques, 5 brevets ont été déposés dont 3 à l'international. Ces publications scientifiques et brevets permettent de valoriser le travail doctoral auprès de la communauté scientifique académique et industrielle. Deux publications scientifiques sont déjà publiées dans *European Polymer Journal,* 2017, 97, 319-327 et Macromolecular Materials and Engineering DOI : 10.1002/mame.201700501.

****

Ce travail doctoral se positionne à la frontière entre recherche industrielle et académique et présente de nombreux résultats de synthèse et transformation à partir du sorbitol. Le résultat le plus marquant est la synthèse à l'échelle pilote du BASAB, apportant de nouvelles connaissances dans la synthèse de polyol polyester et ouvre de nouveaux débouchés une nouvelle voie de valorisation industrielle du sorbitol. Une synthèse pilote au niveau de la Tonne a pu être exploitée jusqu'à la production de panneaux de mousse polyisocyanurate à l'échelle industrielle. Cet essai industriel réussi marque bien évidemment l'aboutissement du projet de thèse et la réussite du partenariat mené avec les 2 partenaires industriels.

L'essai pilote a permis de soulever de nouvelles problématiques, différentes de celles de l'échelle laboratoire. Par exemple lors de la synthèse du BASAB, le lancement de l'agitation en présence des monomères solides n'est pas possible et retarde grandement le démarrage de la réaction d'estérification. Lors de la formulation des mousses, le rapprochement des temps de gel et de hors poisse observé sur les mousses contenant du BASAB diminue la fenêtre de processabilité, en terme de temps permettant une bonne conformation de panneaux de mousses isolantes. Également, il pourrait être intéressant d'optimiser la formulation de mousses polyisocyanurates pour augmenter la teneur en BASAB des mousses polyisocyanuates.

Bien que les résultats obtenus soient très positifs, un grand nombre travaux complémentaires restent à faire afin d'acquérir une meilleure connaissance des polyols polyesters obtenus et des matériaux synthétisés. Premièrement un seul polyol polyester a été exploité jusqu'à l'élaboration de matériaux. Il pourrait être intéressant de synthétiser des polyuréthanes thermoplastiques à très haut taux en renouvelable en associant les polyols polyesters développés dans le Chapitre 2.1 avec un diisocyanate biosourcé à base, par exemple, d'isosorbide présenté dans le Chapitre 1. Cela permettrait d'étudier les différences de réactivité entre les hydroxyles primaires et secondaires des polyols polyesters et/ou d'observer les variations de comportement mécanique et thermique des polyuréthanes thermoplastiques en associant des polyols polyesters de tailles différentes. Ensuite, la synthèse des polyuréthanes sans isocyanate développé pourrait être optimisée, car même si les masses molaires de tels polymères restent faible à cause de nombreuses réactions secondaires, des voies de développement ont été identifiées. À titre d'exemple, le choix du solvant ou le ratio molaire des monomères ont démontré être des paramètres pouvant profiter à l'augmentation des masses molaires des polyuréthanes sans isocyanates obtenus par réaction d'aminolyse.

Enfin, une voie de recherche à explorer pourrait être la formulation de mousses polyuréthanes flexible à partir de polyol polyesters biosourcés développé au cours de ce travail doctoral. En effet ce type de mousses élargirait le champ d'application et d'utilisation des polyols à base de sorbitol au-delà du domaine du bâtiment.

BIBLIOGRAPHIE GENERALE

Abdel Hakim, A.A., Nassar, M., Emam, A., Sultan, M., 2011. Mater. Chem. Phys. 129, 301–307.

Abe, H., 2006. Macromol. Biosci. 6, 469–486.

Adnan, S., Tuan Noor, M.T.I., 'Ain, N.H., Devi, K.P.P., Mohd, N.S., Shoot Kian, Y., Idris, Z.B., Campara, I., Schiffman, C.M., Pietrzyk, K., Sendijarevic, V., Sendijarevic, I., 2017. J. Appl. Polym. Sci. 134, 45440.

Ahvazi, B., Wojciechowicz, O., Ton-That, T.-M., Hawari, J., 2011. J. Agric. Food Chem. 59, 10505–10516.

Ain, N.H., Tuan Noor, M.T., Mohd Noor, M.A., Srihanum, A., Devi, K.P., Mohd, N.S., Mohdnoor, N., Kian, Y.S., Hassan, H.A., Campara, I., Schiffman, C.M., Pietrzyk, K., Sendijarevic, V., Sendijarevic, I., 2017. J. Cell. Plast. 53, 65–81.

Alma, M.H., Yoshioka, M., Yao, Y., Shiraishi, N., 1996. Holzforschung 50, 85–90.

Almeida, E.L. de, Goulart, G.A.S., Claro Neto, S., Chierice, G.O., Siqueira, A.B. de, 2016. Polímeros 26, 176–184.

Almer, C., Winkler, R., 2017. J. Environ. Econ. Manag. 82, 125–151.

Álvarez-Barragán, J., Domínguez-Malfavón, L., Vargas-Suárez, M., González-Hernández, R., Aguilar-Osorio, G., Loza-Tavera, H., 2016. Appl. Environ. Microbiol. 82, 5225–5235.

Anand, A., Kulkarni, R.D., Gite, V.V., 2012. Prog. Org. Coat. 74, 764–767.

Anand, A., Kulkarni, R.D., Patil, C.K., Gite, V.V., 2016. RSC Adv 6, 9843–9850.

Andersons, J., Kirpluks, M., Stiebra, L., Cabulis, U., 2016. Mater. Des. 92, 836–845.

Aniceto, J.P.S., Portugal, I., Silva, C.M., 2012. ChemSusChem 5, 1358–1368.

Aou, K., Schrock, A.K., Baugh, D., Gamboa, R.R., Ulmer, L.C., 2017. Polymer 117, 183–197.

Arbenz, A., Avérous, L., 2014. RSC Adv 4, 61564–61572.

Arbenz, A., Avérous, L., 2015. Ind. Crops Prod. 67, 295–304.

Arbenz, A., Frache, A., Cuttica, F., Avérous, L., 2016. Polym. Degrad. Stab. 132, 62–68.

Arbenz, A., Perrin, R., Avérous, L., 2017. J. Polym. Environ.

Argyropoulos, D.S., 1995. Res. Chem. Intermed. 21, 373–395.

Arnold, R.G., Nelson, J.A., Verbanc, J.J., 1957. Chem. Rev. 57, 47–76.

Arshanitsa, A., Vevere, L., Telysheva, G., Dizhbite, T., Gosselink, R.J.A., Bikovens, O., Jablonski, A., 2015. Holzforschung 69.

Ashida, K., 2006. Polyurethane and related foams: chemistry and technology. CRC press.

Ashida, K., Morimoto, K., Yufu, A., 1995. J. Cell. Plast. 31, 330–355.

Austin, A.L., Levis, W.W., Pizzini, L.C., Hartman, R.J., 1978. Polyurethane foam from an oxyalkylated product. US 4105597.

Austin, A.L., Levis, W.W., Pizzini, L.C., Hartman, R.J., 1979. Process for preparing a polyurethane foam from an oxyalkylated product. US 4177335.

Avar, G., Meier-Westhues, U., Casselmann, H., Achten, D., 2012. Polyurethanes, in: Polymer Science: A Comprehensive Reference. Elsevier, pp. 411–441.

Badri, K.H., Ahmad, S.H., Zakaria, S., 2000. J. Mater. Sci. Lett. 19, 1355–1356.

Badri, 2001-The production of a high-functionality RBD palm kernel-based polyester polyol.

Badri, K.H., Ahmad, S.H., Zakaria, S., 2001. J. Appl. Polym. Sci. 82, 827–832.

Barber, T.A., 2004. Rigid urethane foams using saccharides as reactive components. WO2004060948A2.

Barrioni, B.R., de Carvalho, S.M., Oréfice, R.L., de Oliveira, A.A.R., Pereira, M. de M., 2015. Mater. Sci. Eng. C 52, 22–30.

Basso, M., Pizzi, A., Lacoste, C., Delmotte, L., Al-Marzouki, F., Abdalla, S., Celzard, A., 2014. Polymers 6, 2985–3004.

Basso, M.C., Giovando, S., Pizzi, A., Pasch, H., Pretorius, N., Delmotte, L., Celzard, A., 2014. J. Appl. Polym. Sci. 131, n/a-n/a.

Baur, X., Marek, W., Ammon, J., Czuppon, A.B., Marczynski, B., Raulf-Heimsoth, M., Roemmelt, H., Fruhmann, G., 1994. Int. Arch. Occup. Environ. Health 66, 141–152.

Bayer, O., 1947. Angew. Chem. 59, 257–272.

Bednarek, M., 2016. Prog. Polym. Sci. 58, 27–58.

Beneš, H., Vlček, T., Černá, R., Hromádková, J., Walterová, Z., Svitáková, R., 2012. Eur. J. Lipid Sci. Technol. 114, 71–83.

Bennett, S.J., 2012. Energy Policy 50, 95–108.

Bernardini, J., Anguillesi, I., Coltelli, M.-B., Cinelli, P., Lazzeri, A., 2015a. Polym. Int. 64, 1235–1244.

Bernardini, J., Cinelli, P., Anguillesi, I., Coltelli, M.-B., Lazzeri, A., 2015b. Eur. Polym. J. 64, 147–156.

Besse, V., Camara, F., Méchin, F., Fleury, E., Caillol, S., Pascault, J.-P., Boutevin, B., 2015. Eur. Polym. J. 71, 1–11.

Bhaumik, P., Dhepe, P.L., 2015. Chapter 1. Conversion of Biomass into Sugars, in: Murzin, D., Simakova, O. (Eds.), Green Chemistry Series. Royal Society of Chemistry, Cambridge, pp. 1–53.

Blagbrough, I.S., Mackenzie, N.E., Ortiz, C., Scott, A.I., 1986. Tetrahedron Lett. 27, 1251–1254.

Blattmann, H., Lauth, M., Mülhaupt, R., 2016. Macromol. Mater. Eng. 301, 944–952.

Boyer, A., Cloutet, E., Tassaing, T., Gadenne, B., Alfos, C., Cramail, H., 2010. Green Chem. 12, 2205.

Bozell, J.J., Petersen, G.R., 2010. Green Chem. 12, 539.

Brezny, R., Green, D.J., 1990. Acta Metall. Mater. 38, 2517–2526.

Britain, J.W., Gemeinhardt, P.G., 1960. J. Appl. Polym. Sci. 4, 207–211.

Calle, M., Lligadas, G., Ronda, J.C., Galià, M., Cádiz, V., 2016. Eur. Polym. J. 84, 837–848.

Calvo-Correas, T., Mosiewicki, M.A., Corcuera, M.A., Eceiza, A., Aranguren, M.I., 2015. J. Renew. Mater. 3, 3–13.

Campanella, A., Bonnaillie, L.M., Wool, R.P., 2009. J. Appl. Polym. Sci. 112, 2567–2578.

Campbell, T.W., Smeltz, K.C., 1963. J. Org. Chem. 28, 2069–2075.

Caouthar, A., Roger, P., Tessier, M., Chatti, S., Blais, J.C., Bortolussi, M., 2007. Eur. Polym. J. 43, 220–230.

Carothers, W.H., 1929. J. Am. Chem. Soc. 51, 2548–2559.

Carothers, W.H., 1931. Chem. Rev. 8, 353–426.

Carothers, W.H., 1936. Trans. Faraday Soc. 32, 39.

Carothers, W.H., Dorough, G.L., Natta, F.J. van, 1932. J. Am. Chem. Soc. 54, 761–772.

Carr, C., 1992. Starch-Stärke 44, 183–187.

Carr, R.H., Hernalsteen, J., Devos, J., 1994. J. Appl. Polym. Sci. 52, 1015–1022.

Carré, C., Bonnet, L., Avérous, L., 2014. RSC Adv 4, 54018–54025.

Carré, C., Bonnet, L., Avérous, L., 2015. RSC Adv 5, 100390–100400.

Carré, C., Zoccheddu, H., Delalande, S., Pichon, P., Avérous, L., 2016. Eur. Polym. J. 84, 759–769.

Carriço, C., Fraga, T., Carvalho, V., Pasa, V., 2017. Molecules 22, 1091.

Carriço, C.S., Fraga, T., Pasa, V.M.D., 2016. Eur. Polym. J. 85, 53–61.

Cateto, C.A., Barreiro, M.F., Ottati, C., Lopretti, M., Rodrigues, A.E., Belgacem, M.N., 2014. J. Cell. Plast. 50, 81–95.

Cateto, C.A., Barreiro, M.F., Rodrigues, A.E., Belgacem, M.N., 2009. Ind. Eng. Chem. Res. 48, 2583–2589.

Çaylı, G., Küsefoğlu, S., 2008. J. Appl. Polym. Sci. 109, 2948–2955.

Celzard, A., Fierro, V., Amaral-Labat, G., Pizzi, A., Torero, J., 2011. Polym. Degrad. Stab. 96, 477–482.

Chang, W.L., 2002. Polyurethane prepared from sorbitol-branched polyesters. Google Patents.

Charlon, M., Heinrich, B., Matter, Y., Couzigné, E., Donnio, B., Avérous, L., 2014. Eur. Polym. J. 61, 197–205.

Chattopadhyay, D.K., Sreedhar, B., Raju, K.V.S.N., 2006. J. Polym. Sci. Part B Polym. Phys. 44, 102–118.

Chattopadhyay, D.K., Webster, D.C., 2009. Prog. Polym. Sci. 34, 1068–1133.

Chaudhary, S., Surekha, P., Kumar, D., Rajagopal, C., Roy, P.K., 2013. J. Appl. Polym. Sci. 129, 2779–2788.

Chen, F., Lu, Z., 2009. J. Appl. Polym. Sci. 111, 508–516.

Chen, W., Lu, F., Winfree, N., 2002. Exp. Mech. 42, 65–73.

Chmiel-Szukiewicz, E., 2013. J. Appl. Polym. Sci. 127, 1595–1600.

Christopher L. WIlson, C.L., L, C.J.B., 1958. Method of making polyester composition. 2863855A.

Chuayjuljit, S., Maungchareon, A., Saravari, O., 2010. J. Reinf. Plast. Compos. 29, 218–225.

Chuayjuljit, S., Sangpakdee, T., Saravari, O., 2007. J. Met. Mater. Miner. 17.

Chuayjuljit, 2007-Processing and Properties of Palm Oil-Based Rigid Polyurethane Foam.

Clements, J.H., 2003. Ind. Eng. Chem. Res. 42, 663–674.

Cook, W., Hostettler, F., Lombardi, F., 1974. Polyurethane foams based on liquid poly (e-caprolactone) polyester polyols. 3806473.

Cornille, A., Auvergne, R., Figovsky, O., Boutevin, B., Caillol, S., 2017a. Eur. Polym. J. 87, 535–552.

Cornille, A., Blain, M., Auvergne, R., Andrioletti, B., Boutevin, B., Caillol, S., 2017b. Polym Chem 8, 592–604.

Cornille, A., Dworakowska, S., Bogdal, D., Boutevin, B., Caillol, S., 2015. Eur. Polym. J. 66, 129–138.

Cornille, A., Guillet, C., Benyahya, S., Negrell, C., Boutevin, B., Caillol, S., 2016a. Eur. Polym. J. 84, 873–888.

Cornille, A., Michaud, G., Simon, F., Fouquay, S., Auvergne, R., Boutevin, B., Caillol, S., 2016b. Eur. Polym. J. 84, 404–420.

Cregut, M., Bedas, M., Durand, M.-J., Thouand, G., 2013. Biotechnol. Adv. 31, 1634–1647.

Čuk, N., Fabjan, E., Grželj, P., Kunaver, M., 2015. J. Appl. Polym. Sci. 132, n/a-n/a.

Cunningham, R.L., Gordon, S.H., Felker, F.C., Eskins, K., 1998. J. Appl. Polym. Sci. 69, 957–964.

Czupryński, B., Liszkowska, J., Paciorek-Sadowska, J., 2012. J. Appl. Polym. Sci. 126, E44–E53.

Dais, P., Spyros, A., 2007. Magn. Reson. Chem. 45, 367–377.

Datta, J., Kopczyńska, P., 2016. Crit. Rev. Environ. Sci. Technol. 46, 905–946.

David Randall, steve Lee, n.d. The Polyurethanes book. Wiley.

De, G.M., Pettingill, O.H., 1963. Certain oxyalkylated polyols. US 3110737.

Debuissy, T., Pollet, E., Avérous, L., 2017. Eur. Polym. J. 97, 328–337.

Debuissy, T., Sangwan, P., Pollet, E., Avérous, L., 2017c. Polymer 122, 105–116.

Deepa, P., Jayakannan, M., 2008a. J. Polym. Sci. Part Polym. Chem. 46, 2445–2458.

Deepa, P., Jayakannan, M., 2008b. J. Polym. Sci. Part Polym. Chem. 46, 2445–2458.

Defaye, J., Gadelle, A., Pedersen, C., 1990. Carbohydr. Res. 205, 191–202.

Delebecq, E., Pascault, J.-P., Boutevin, B., Ganachaud, F., 2013. Chem. Rev. 113, 80–118.

Desroches, M., Escouvois, M., Auvergne, R., Caillol, S., Boutevin, B., 2012. Polym. Rev. 52, 38–79.

Deutschmann, R., Dekker, R.F.H., 2012. Biotechnol. Adv. 30, 1627–1640.

Dick, C., Dominguez-Rosado, E., Eling, B., Liggat, J.., Lindsay, C.., Martin, S.., Mohammed, M.., Seeley, G., Snape, C.., 2001. Polymer 42, 913–923.

D.Kyriacos, Polyols for PU. All producers and plant capacities. June 2017. ISBN 9789078546313, n.d.

Dominguez-Rosado, E., Liggat, J.J., Snape, C.E., Eling, B., Pichtel, J., 2002. Polym. Degrad. Stab. 78, 1–5.

Dong, K., Guo, X., Xu, J., Yang, D., Qiu, F., 2012. Polym.-Plast. Technol. Eng. 51, 754–759.

D'Souza, J., Camargo, R., Yan, N., 2014. J. Appl. Polym. Sci. 131, 40599.

D'Souza, J., Camargo, R., Yan, N., 2017. Polym. Rev. 57, 668–694.

Duval, A., Avérous, L., 2016. ACS Sustain. Chem. Eng. 4, 3103–3112.

Elbers, N., Ranaweera, C.K., Ionescu, M., Wan, X., Kahol, P.K., Gupta, R.K., 2017. J. Renew. Mater. 5, 74–83.

Engels, H.-W., Pirkl, H.-G., Albers, R., Albach, R.W., Krause, J., Hoffmann, A., Casselmann, H., Dormish, J., 2013. Angew. Chem. Int. Ed. 52, 9422–9441.

F, S., M, M., A, R.S., 1987. Cell. Polym. 6, 27–41.

Fan, H., Tekeei, A., Suppes, G.J., Hsieh, F.-H., 2013. J. Appl. Polym. Sci. 127, 1623–1629.

Fang, Z., Smith, R.L., Qi, X. (Eds.), 2017. Production of Platform Chemicals from Sustainable Resources, Biofuels and Biorefineries. Springer Singapore, Singapore.

Feng, X., East, A.J., Hammond, W.B., Zhang, Y., Jaffe, M., 2011. Polym. Adv. Technol. 22, 139–150.

Fenouillot, F., Rousseau, A., Colomines, G., Saint-Loup, R., Pascault, J.-P., 2010. Prog. Polym. Sci. 35, 578–622.

Flèche, G., Huchette, M., 1986. Starch - Stärke 38, 26–30.

Fleurent, H., Thijs, S., 1995. J. Cell. Plast. 31, 580–599.

Fritz, H., Young, D.M., 1965. Polyurethane polymers from lactone polyesters. 3186971.

Furtwengler, P., Perrin, R., Redl, A., Avérous, L., 2017. Eur. Polym. J. 97, 319–327.

Galanis, S., Dasgupta, P.K., 2001. Anal. Chim. Acta 429, 101–110.

Gallezot, P., Cerino, P., Blanc, B., Fleche, G., Fuertes, P., 1994. J. Catal. 146, 93–102.

Gama, N., Silva, R., Carvalho, A.P.O., Ferreira, A., Barros-Timmons, A., 2017. Polym. Test. 62, 13–22.

Gama, N.V., Silva, R., Costa, M., Barros-Timmons, A., Ferreira, A., 2016. Polym. Test. 56, 200–206.

Gama, N.V., Soares, B., Freire, C.S.R., Silva, R., Neto, C.P., Barros-Timmons, A., Ferreira, A., 2015. Mater. Des. 76, 77–85.

Gandhi, T.S., Patel, M.R., Dholakiya, B.Z., 2015. J. Polym. Eng. 35.

Gandini, A., 2008. Macromolecules 41, 9491–9504.

Gandini, A., Belgacem, M.N., 2008. The State of the Art, in: Monomers, Polymers and Composites from Renewable Resources. Elsevier, pp. 1–16.

Gandini, A., Lacerda, T.M., 2015. Prog. Polym. Sci. 48, 1–39.

Gandini, A., Lacerda, T.M., Carvalho, A.J.F., Trovatti, E., 2016. Chem. Rev. 116, 1637–1669.

Gao, L., Zheng, G., Zhou, Y., Hu, L., Feng, G., Xie, Y., 2013. Ind. Crops Prod. 50, 638–647.

Gao, L.-L., Liu, Y.-H., Lei, H., Peng, H., Ruan, R., 2010. J. Appl. Polym. Sci. NA-NA.

Garcia-Herrero, I., Cuéllar-Franca, R.M., Enríquez-Gutiérrez, V.M., Alvarez-Guerra, M., Irabien, A., Azapagic, A., 2016. ACS Sustain. Chem. Eng. 4, 2088–2097.

Gargallo, L., Hamidi, N., Radić, D., 1987. Thermochim. Acta 114, 319–328.

Gargallo, L., Soto, E., Tagle, L.H., RadiĆ, D., 1988. Thermochim. Acta 130, 289–297.

Ge, J., Shi, X., Cai, M., Wu, R., Wang, M., 2003. J. Appl. Polym. Sci. 90, 2756–2763.

Ge, J., Zhong, W., Guo, Z., Li, W., Sakai, K., 2000. J. Appl. Polym. Sci. 77, 2575–2580.

George, N., Kurian, T., 2014. Ind. Eng. Chem. Res. 53, 14185–14198.

Gibson, L.J., Ashby, M.F., 1997. Cellular Solids: Structure and Properties, Cambridge Solid State Science Series. Cambridge University Press.

Gibson, L.J., Ashby, M.F., Zhang, J., Triantafillou, T.C., 1989. Int. J. Mech. Sci. 31, 635–663.

Ginés-Molina, M.J., Moreno-Tost, R., Santamaría-González, J., Maireles-Torres, P., 2017. Appl. Catal. Gen. 537, 66–73.

Granata, A., Argyropoulos, D.S., 1995. J. Agric. Food Chem. 43, 1538–1544.

Grause, G., Buekens, A., Sakata, Y., Okuwaki, A., Yoshioka, T., 2011. J. Mater. Cycles Waste Manag. 13, 265–282.

Grignard, B., Thomassin, J.-M., Gennen, S., Poussard, L., Bonnaud, L., Raquez, J.-M., Dubois, P., Tran, M.-P., Park, C.B., Jerome, C., Detrembleur, C., 2016. Green Chem 18, 2206–2215.

Grimminger, J., Muha, K., 1995. J. Cell. Plast. 31, 48–72.

Guan, J., Hanna, M.A., 2004. Ind. Crops Prod. 19, 255–269.

Guelcher, S.A., Gallagher, K.M., Didier, J.E., Klinedinst, D.B., Doctor, J.S., Goldstein, A.S., Wilkes, G.L., Beckman, E.J., Hollinger, J.O., 2005. Acta Biomater. 1, 471–484.

Guo, A., Cho, Y., Petrović, Z.S., 2000. J. Polym. Sci. Part Polym. Chem. 38, 3900–3910.

Guo, A., Zhang, W., Petrovic, Z.S., 2006. J. Mater. Sci. 41, 4914–4920.

Gupta, A., 2016. Climate Change and Kyoto Protocol, in: Handbook of Environmental and Sustainable Finance. Elsevier, pp. 3–23.

Gupta, N., Ye, R., Porfiri, M., 2010. Compos. Part B Eng. 41, 236–245.

Gupta, R.K., Ionescu, M., Radojcic, D., Wan, X., Petrovic, Z.S., 2014. J. Polym. Environ. 22, 304–309.

Gupta, R.K., Ionescu, M., Wan, X., Radojcic, D., Petrovic, Z.S., 2015. J. Polym. Environ. 23, 261–268.

Gustini, L., Lavilla, C., Janssen, W.W.T.J., Martínez de Ilarduya, A., Muñoz-Guerra, S., Koning, C.E., 2016. ChemSusChem 9, 2250–2260.

Gustini, L., Noordover, B.A.J., Gehrels, C., Dietz, C., Koning, C.E., 2015. Eur. Polym. J. 67, 459–475.

Gwon, J.G., Kim, S.K., Kim, J.H., 2016. Mater. Des. 89, 448–454.

Haba, O., Tomizuka, H., Endo, T., 2005. Macromolecules 38, 3562–3563.

Han, M.S., Choi, S.J., Kim, J.M., Kim, Y.H., Kim, W.N., Lee, H.S., Sung, J.Y., 2009. Macromol. Res. 17, 44–50.

Hartstra, L., Van, W.H.A., 1950. Hydrogenation of carbohydrates. 2518235.

Hawkins, M.C., 2005. J. Cell. Plast. 41, 267–285.

Hayden, D.E., Foucht, M.E., 1978. Polyurethane foam system. US 4072623.

He, Q. (Sophia), McNutt, J., Yang, J., 2017. Renew. Sustain. Energy Rev. 71, 63–76.

Hejna, A., Kirpluks, M., Kosmela, P., Cabulis, U., Haponiuk, J., Piszczyk, Ł., 2017a. Ind. Crops Prod. 95, 113–125.

Hejna, A., Kosmela, P., Kirpluks, M., Cabulis, U., Klein, M., Haponiuk, J., Piszczyk, Ł., 2017b. J. Polym. Environ.

Herzberger, J., Niederer, K., Pohlit, H., Seiwert, J., Worm, M., Wurm, F.R., Frey, H., 2016. Chem. Rev. 116, 2170–2243.

Himabindu, M., Kamalakar, K., Karuna, M., Palanisamy, A., 2017. J. Renew. Mater. 5, 124–131.

Hofmann-1870-Berichte_der_deutschen_chemischen_Gesellschaft.pdf, n.d.

Hojabri, L., Kong, X., Narine, S.S., 2009. Biomacromolecules 10, 884–891.

Holladay, J.E., Bozell, J.J., White, J.F., Johnson, D., 2007. DOE Rep. PNNL 16983.

Hopmann, C., Latz, S., 2015. Polymer 56, 29–36.

Hostettler, F., 1965. Lactone polyesters. 3169945.

Hough, L., Priddle, J.E., Theobald, R.S., 1962. J. Chem. Soc. Resumed 1934–1938.

Hu, L., Wu, L., Song, F., Li, B.-G., 2010. Macromol. React. Eng. 4, 621–632.

Hu, M., Hwang, J.-Y., Kurth, M.J., Hsieh, Y.-L., Shoemaker, C.F., Krochta, J.M., 1997. J. Agric. Food Chem. 45, 4156–4161.

Hu, S., Luo, X., Li, Y., 2014. ChemSusChem 7, 66–72.

Hu, S., Luo, X., Wan, C., Li, Y., 2012. J. Agric. Food Chem. 60, 5915–5921.

Hu, Y.H., Gao, Y., Wang, D.N., Hu, C.P., Zu, S., Vanoverloop, L., Randall, D., 2002. J. Appl. Polym. Sci. 84, 591–597.

Huang, G., Wang, P., 2017. Polym. Test. 60, 266–273.

Ionescu, M., 2005. Chemistry and technology of polyols for polyurethanes. Rapra Technology, Shawbury, Shrewsbury, Shropshire, U.K.

Ionescu, M., Petrović, Z.S., 2010. J. Cell. Plast. 46, 223–237.

Ionescu, M., Radojčić, D., Wan, X., Shrestha, M.L., Petrović, Z.S., Upshaw, T.A., 2016. Eur. Polym. J. 84, 736–749.

Ionescu, M., Wan, X., Bilić, N., Petrović, Z.S., 2012. J. Polym. Environ. 20, 647–658.

Jacobs, P., Hinnekens, H., 1989. Single-step catalytic process for the direct conversion of polysaccharides to polyhydric alcohols. 0329923.

Jacquel, N., Freyermouth, F., Fenouillot, F., Rousseau, A., Pascault, J.P., Fuertes, P., Saint-Loup, R., 2011. J. Polym. Sci. Part Polym. Chem. 49, 5301–5312.

Javni, I., Hong, D.P., Petrović, Z.S., 2008. J. Appl. Polym. Sci. 108, 3867–3875.

Javni, I., Petrovi?, Z.S., Guo, A., Fuller, R., 2000. J. Appl. Polym. Sci. 77, 1723–1734.

Jefferson, R.T., Salyer, I.O., 1971. Process for closed-cell rigid polyurethane foams. 355,85,31.

Jelle, B.P., 2011. Energy Build. 43, 2549–2563.

Jeong, H., Park, J., Kim, S., Lee, J., Ahn, N., 2013. Fibers Polym. 14, 1301–1310.

Jeong, H., Shim, W.J., 2017. Pol. Marit. Res. 24.

Ji, D., Fang, Z., He, W., Luo, Z., Jiang, X., Wang, T., Guo, K., 2015. Ind. Crops Prod. 74, 76–82.

Ji, D., Fang, Z., Wan, Z.D., Chen, H.C., He, W., Li, X.L., Guo, K., 2013. Adv. Mater. Res. 724–725, 1681–1684.

Jiang, L., Zhang, J., 2017. Biodegradable and Biobased Polymers, in: Applied Plastics Engineering Handbook. Elsevier, pp. 127–143.

Jiang, Y., Loos, K., 2016. Polymers 8, 243.

Jin, H., Lu, W.-Y., Scheffel, S., Hinnerichs, T.D., Neilsen, M.K., 2007. Int. J. Solids Struct. 44, 6930–6944.

Jin, J.F., Chen, Y.L., Wang, D.N., Hu, C.P., Zhu, S., Vanoverloop, L., Randall, D., 2002. J. Appl. Polym. Sci. 84, 598–604.

Jin, Y., Ruan, X., Cheng, X., Lü, Q., 2011. Bioresour. Technol. 102, 3581–3583.

Kacperski, M., Spychaj, T., 1999. Polym. Adv. Technol. 10, 620–624.

Kairytė, A., Vėjelis, S., 2015. Ind. Crops Prod. 66, 210–215.

Kang, S.M., Kang, M.S., Kwon, S.H., Park, H., Kim, B.K., 2014. J. Polym. Eng. 34.

Karadeniz, K., Çalıkoğlu, Y., Sen, M.Y., 2017. Polym. Bull. 74, 2819–2839.

Karayannidis, G.P., Achilias, D.S., 2007. Macromol. Mater. Eng. 292, 128–146.

Kattiyaboot, T., Thongpin, C., 2016. Energy Procedia 89, 177–185.

Kaushiva, B.D., McCartney, S.R., Rossmy, G.R., Wilkes, G.L., 2000. Polymer 41, 285–310.

Kaushiva, B.D., Wilkes, G.L., 2000. J. Appl. Polym. Sci. 77, 202–216.

Kharbas, H.A., McNulty, J.D., Ellingham, T., Thompson, C., Manitiu, M., Scholz, G., Turng, L.-S., 2017. J. Cell. Plast. 53, 373–388.

Kihara, N., Endo, T., 1993a. J. Polym. Sci. Part Polym. Chem. 31, 2765–2773.

Kihara, N., Endo, T., 1993b. J. Polym. Sci. Part Polym. Chem. 31, 2765–2773.

Kobashigawa, K., Tokashiki, T., Naka, H., Hirose, S., Hatakeyama, H., 2001. Recent Adv. Environ. Compat. Polym. Camb. Woodhead Publ. 229–34.

Kobayashi, H., Ito, Y., Komanoya, T., Hosaka, Y., Dhepe, P.L., Kasai, K., Hara, K., Fukuoka, A., 2011. Green Chem 13, 326–333.

Kobayashi, H., Yabushita, M., Komanoya, T., Hara, K., Fujita, I., Fukuoka, A., 2013. ACS Catal. 3, 581–587.

Kobayashi, H., Yamakoshi, Y., Hosaka, Y., Yabushita, M., Fukuoka, A., 2014. Catal. Today 226, 204–209.

Komura, H., Yoshino, T., Ishido, Y., 1973. Bull. Chem. Soc. Jpn. 46, 550–553.

Korntner, P., Sumerskii, I., Bacher, M., Rosenau, T., Potthast, A., 2015. Holzforschung 69, 807–814.

Kosmela, P., Kazimierski, P., Formela, K., Haponiuk, J., Piszczyk, Ł., 2017. J. Ind. Eng. Chem.

Kühnel, I., Podschun, J., Saake, B., Lehnen, R., 2015. Holzforschung 69.

Kurańska, M., Prociak, A., 2016. Ind. Crops Prod. 89, 182–187.

Kurańska, M., Prociak, A., Cabulis, U., Kirpluks, M., Ryszkowska, J., Auguścik, M., 2017. Ind. Crops Prod. 95, 316–323.

Kurańska, M., Prociak, A., Kirpluks, M., Cabulis, U., 2015. Ind. Crops Prod. 74, 849–857.

Kurimoto, Y., Doi, S., Tamura, Y., 1999. Holzforschung 53.

Lan, Z., Daga, R., Whitehouse, R., McCarthy, S., Schmidt, D., 2014. Polymer 55, 2635–2644.

Langeveld, J.W.A., Dixon, J., Jaworski, J.F., 2010. Crop Sci. 50, S-142.

Lapprand, A., Boisson, F., Delolme, F., M?chin, F., Pascault, J.-P., 2005. Polym. Degrad. Stab. 90, 363–373.

Laurichesse, S., Huillet, C., Avérous, L., 2014. Green Chem. 16, 3958.

Layer, O., 1988.

Lee, S.-H., Teramoto, Y., Shiraishi, N., 2002. J. Appl. Polym. Sci. 83, 1482–1489.

Lee, S.-H., Yoshioka, M., Shiraishi, N., 2000. J. Appl. Polym. Sci. 78, 319–325.

Li, Chenguo, Li, S., Zhao, J., Zhang, Z., Zhang, J., Yang, W., 2014. J. Polym. Res. 21.

Li, Cong, Luo, X., Li, T., Tong, X., Li, Y., 2014. Polymer 55, 6529–6538.

Li, H., Mahmood, N., Ma, Z., Zhu, M., Wang, J., Zheng, J., Yuan, Z., Wei, Q., Xu, C. (Chunbao), 2017. Ind. Crops Prod. 103, 64–72.

Li, H.-Q., Shao, Q., Luo, H., Xu, J., 2016a. J. Appl. Polym. Sci. 133, 43261.

Li, Q.F., Feng, Y.L., Wang, J.W., Yin, N., Zhao, Y.H., Kang, M.Q., Wang, X.W., 2016. Plast. Rubber Compos. 45, 16–21.

Li, S., Bouzidi, L., Narine, S.S., 2017. Eur. Polym. J. 93, 232–245.

Li, S., Zhao, J., Zhang, Z., Zhang, J., Yang, W., 2014. RSC Adv. 4, 23720.

Li, Y., Ragauskas, A.J., 2012. J. Wood Chem. Technol. 32, 210–224.

Lin, L., Yoshioka, M., Yao, Y., Shiraishi, N., 1994. J. Appl. Polym. Sci. 52, 1629–1636.

Liszkowska, J., 2017. Polym. Bull. 74, 283–305.

Liu, C., Long, Y., Xie, J., Xie, X., 2017. Polymer 116, 240–250.

Liu, L., Li, H., Lazzaretto, A., Manente, G., Tong, C., Liu, Q., Li, N., 2017. Renew. Sustain. Energy Rev. 69, 912–932.

Liu, Y., He, J., Yang, R., 2017. J. Mater. Sci. 52, 4700–4712.

Long, Y., Sun, F., Liu, C., Huang, D., Xie, X., 2016. J. Appl. Polym. Sci. 133.

Lowe, A.B., 2014. Polymer 55, 5517–5549.

Lucas, N., Bienaime, C., Belloy, C., Queneudec, M., Silvestre, F., Nava-Saucedo, J.-E., 2008. Chemosphere 73, 429–442.

Luo, X., Hu, S., Zhang, X., Li, Y., 2013. Bioresour. Technol. 139, 323–329.

Luo, X., Li, Y., 2014. J. Polym. Environ. 22, 318–328.

Machado, T.O., Sayer, C., Araujo, P.H.H., 2017. Eur. Polym. J. 86, 200–215.

Mahmood, N., Yuan, Z., Schmidt, J., Tymchyshyn, M., Xu, C. (Charles), 2016. Green Chem 18, 2385–2398.

Maisonneuve, L., Lamarzelle, O., Rix, E., Grau, E., Cramail, H., 2015. Chem. Rev. 115, 12407–12439.

Maiti, S.K., Gibson, L.J., Ashby, M.F., 1984. Acta Metall. 32, 1963–1975.

Majumdar, K.K., Kundu, A., Das, I., Roy, S., 2000. Appl. Organomet. Chem. 14, 79–85.

Maldas, D., Shiraishi, N., 1996. Int. J. Polym. Mater. 33, 61–71.

Marcovich, N.E., Kurańska, M., Prociak, A., Malewska, E., Kulpa, K., 2017. Ind. Crops Prod. 102, 88–96.

Mark, J.E. (Ed.), 2009. Polymer data handbook, 2nd ed. ed. Oxford University Press, Oxford ; New York.

Matos, M., Barreiro, M.F., Gandini, A., 2010. Ind. Crops Prod. 32, 7–12.

Matsumiya, Y., Murata, N., Tanabe, E., Kubota, K., Kubo, M., 2009. J. Appl. Microbiol.

Mazurek-Budzyńska, M.M., Rokicki, G., Drzewicz, M., Guńka, P.A., Zachara, J., 2016. Eur. Polym. J. 84, 799–811.

McAdams, C.A., Farmer, S., 2003. J. Cell. Plast. 39, 369–386.

Mielewski, D.F., Flanigan, C.M., Perry, C., Zaluzec, M.J., Killgoar, P.C., 2005. Ind. Biotechnol. 1, 32–34.

Minogue, E., 2000. An in-situ study of the nucleation process of polyurethane rigid foam formation. Dublin City University.

Modesti, M., Lorenzetti, A., 2001. Eur. Polym. J. 37, 949–954.

Molero, C., de Lucas, A., Rodríguez, J.F., 2006. Polym. Degrad. Stab. 91, 221–228.

Molero, Carolina, de Lucas, A., Rodríguez, J.F., 2008. Polym. Degrad. Stab. 93, 353–361.

Molero, C., de Lucas, A., Romero, F., Rodríguez, J.F., 2008. J. Appl. Polym. Sci. 109, 617–626.

More, A.S., Gadenne, B., Alfos, C., Cramail, H., 2012. Polym. Chem. 3, 1594.

Mosiewicki, M.A., Dell'Arciprete, G.A., Aranguren, M.I., Marcovich, N.E., 2009. J. Compos. Mater. 43, 3057–3072.

Mosiewicki, M.A., Rojek, P., Michałowski, S., Aranguren, M.I., Prociak, A., 2015. J. Appl. Polym. Sci. 132, 41602.

Mushrush, G.W., Hardy, D., 1998. Fuel system icing inhibitor and deicing composition. Google Patents.

MUSTAFE, A.M.B.M., 2005. FTIR studies on 2K polyurethane paint.

Nadji, H., Bruzzèse, C., Belgacem, M.N., Benaboura, A., Gandini, A., 2005. Macromol. Mater. Eng. 290, 1009–1016.

Nagy, T., Antal, B., Czifrák, K., Papp, I., Karger-Kocsis, J., Zsuga, M., Kéki, S., 2015. J. Appl. Polym. Sci. 132, n/a-n/a.

Nakashima, K., Takeshita, T., Morimoto, K., 2002. Environ. Health Prev. Med. 7, 1–6.

Nanda, M.R., Zhang, Y., Yuan, Z., Qin, W., Ghaziaskar, H.S., Xu, C. (Charles), 2016. Renew. Sustain. Energy Rev. 56, 1022–1031.

Narine, S.S., Kong, X., Bouzidi, L., Sporns, P., 2007a. J. Am. Oil Chem. Soc. 84, 65–72.

Narine, S.S., Yue, J., Kong, X., 2007b. J. Am. Oil Chem. Soc. 84, 173–179.

NF EN ISO 10456 - Juin 2008, n.d.

Ng, W.S., Lee, C.S., Chuah, C.H., Cheng, S.-F., 2017. Ind. Crops Prod. 97, 65–78.

Nikje, A., Mohammad, M., Haghshenas, M., Garmarudi, A.B., 2007. Polym.-Plast. Technol. Eng. 46, 265–271.

Nikje, M.M.A., Garmarudi, A.B., 2006. Polym.-Plast. Technol. Eng. 45, 1101–1107.

Nikje, M.M.A., Garmarudi, A.B., Idris, A.B., 2011. Des. Monomers Polym. 14, 395–421.

Nikje, M.M.A., Mohammadi, F.H.A., 2010. Polym.-Plast. Technol. Eng. 49, 818–821.

Nikles, D.E., Farahat, M.S., 2005. Macromol. Mater. Eng. 290, 13–30.

Noordover, B.A.J., van Staalduinen, V.G., Duchateau, R., Koning, C.E., van Benthem, Mak, M., Heise, A., Frissen, A.E., van Haveren, J., 2006. Biomacromolecules 7, 3406–3416.

Noreen, A., Zia, K.M., Zuber, M., Tabasum, S., Zahoor, A.F., 2016. Prog. Org. Coat. 91, 25–32.

Ochoa-Gómez, J.R., Gómez-Jiménez-Aberasturi, O., Ramírez-López, C., Belsué, M., 2012. Org. Process Res. Dev. 16, 389–399.

Ochoa-Gómez, J.R., Roncal, T., 2017. Production of Sorbitol from Biomass, in: Fang, Z., Smith, R.L., Qi, X. (Eds.), Production of Platform Chemicals from Sustainable Resources. Springer Singapore, Singapore, pp. 265–309.

Ogunniyi, D., 2006. Bioresour. Technol. 97, 1086–1091.

Olivier Coulembier Philippe Dubois, Jean-Marie Raquez, 2009. Handbook of Ring-Opening Polymerization. Wiley-VCH, Weinheim.

Oliviero, M., Verdolotti, L., Stanzione, M., Lavorgna, M., Iannace, S., Tarello, M., Sorrentino, A., 2017. J. Appl. Polym. Sci. 134, 45113.

Ozaki, S., others, 1972. Chem Rev 72, 457–496.

P. Madden, J., Baker, G.K., H. Smith, C., 1972. J. Cell. Plast. 8, 201–207.

Palanisamy, A., Karuna, M.S.L., Satyavani, T., Rohini Kumar, D.B., 2011. J. Am. Oil Chem. Soc. 88, 541–549.

Palaskar, D.V., Boyer, A., Cloutet, E., Alfos, C., Cramail, H., 2010. Biomacromolecules 11, 1202–1211.

Paruzel, A., Michałowski, S., Hodan, J., Horák, P., Prociak, A., Beneš, H., 2017. ACS Sustain. Chem. Eng. 5, 6237–6246.

Patterson, B.M., Henderson, K., Gilbertson, R.D., Tornga, S., Cordes, N.L., Chavez, M.E., Smith, Z., 2014. Microsc. Microanal. 20, 1284–1293.

Pavier, Claire, Gandini, A., 2000. Ind. Crops Prod. 12, 1–8.

Pavier, C., Gandini, A., 2000. Carbohydr. Polym. 42, 13–17.

Pawar, M.S., Kadam, A.S., Dawane, B.S., Yemul, O.S., 2016a. Polym. Bull. 73, 727–741.

Pawar, M.S., Kadam, A.S., Singh, P.C., Kusumkar, V.V., Yemul, O.S., 2016b. Iran. Polym. J. 25, 59–68.

Pawlik, H., Prociak, A., 2012. J. Polym. Environ. 20, 438–445.

Pelckmans, M., Renders, T., Van de Vyver, S., Sels, B.F., 2017. Green Chem. 19, 5303–5331.

Petrovic, Z.S., Ferguson, J., 1991. Prog. Polym. Sci. 16, 695–836.

Petrovic, Z., 2008. Polym. Rev. 48, 109–155.

Petrović, Z.S., Wan, X., Bilić, O., Zlatanić, A., Hong, J., Javni, I., Ionescu, M., Milić, J., Degruson, D., 2013. J. Am. Oil Chem. Soc. 90, 1073–1078.

Petrović, Z.S., Zhang, W., Javni, I., 2005. Biomacromolecules 6, 713–719.

Pfister, D.P., Xia, Y., Larock, R.C., 2011. ChemSusChem 4, 703–717.

Pierre Furtwengler, Rodrigue Matadi Boumbimba, Luc Avérous, n.d. Macromol. Mater. Eng.

Pillai, P.K.S., Li, S., Bouzidi, L., Narine, S.S., 2016. Ind. Crops Prod. 84, 273–283.

Piszczyk, Ł., Strankowski, M., Danowska, M., Hejna, A., Haponiuk, J.T., 2014. Eur. Polym. J. 57, 143–150.

Posen, I.D., Jaramillo, P., Griffin, W.M., 2016. Environ. Sci. Technol. 50, 2846–2858.

Posner, T., 1905. Berichte Dtsch. Chem. Ges. 38, 646–657.

Prociak, A., Kurańska, M., Cabulis, U., Kirpluks, M., 2017. Polym. Test. 59, 478–486.

Quadrini, F., Bellisario, D., Santo, L., 2013. Polym. Eng. Sci. 53, 1357–1363.

Quispe, C.A.G., Coronado, C.J.R., Carvalho Jr., J.A., 2013. Renew. Sustain. Energy Rev. 27, 475–493.

Raiford, L.C., Freyermuth, H.B., 1943. J. Org. Chem. 08, 230–238.

Ramesh, N.S., Rasmussen, D.H., Campbell, G.A., 1994. Polym. Eng. Sci. 34, 1685–1697.

Randall, D., Lee, S. (Eds.), 2002. The polyurethanes book. Huntsman Polyurethanes] ; New York : Distributed by John Wiley & Sons, [Everberg, Belgium.

Rashmi, B.J., Rusu, D., Prashantha, K., Lacrampe, M.F., Krawczak, P., 2013. J. Appl. Polym. Sci. 128, 292–303.

Rehkopf, J.D., Mcneice, G.M., Rudin, A., 1994. J. Cell. Plast. 30, 34–43.

Reichmann, W.W., Phillips, B.A., 1988. J. Cell. Plast. 24, 601–610.

Reulier, M., Boumbimba, R.M., Rasselet, D., Avérous, L., 2016. J. Appl. Polym. Sci. 133, n/a-n/a.

Reymore, H.E., Carleton, P.S., Kolakowski, R.A., Sayigh, A.A.R., 1975. J. Cell. Plast. 11, 328–344.

Ribeiro da Silva, V., Mosiewicki, M.A., Yoshida, M.I., Coelho da Silva, M., Stefani, P.M., Marcovich, N.E., 2013. Polym. Test. 32, 665–672.

Ribeiro, L.S., Órfão, J.J. de M., Pereira, M.F.R., 2017. Bioresour. Technol. 232, 152–158.

Rieger, B., Amann, M. (Eds.), 2012. Synthetic biodegradable polymers, Advances in polymer science. Springer, Heidelberg ; New York.

Robles, H., 2014. Urethane, in: Encyclopedia of Toxicology. Elsevier, pp. 889–891.

Rogge, T.M., Stevens, C.V., Vandamme, A., Booten, K., Levecke, B., D'hooge, C., Haelterman, B., Corthouts, J., 2005. Biomacromolecules 6, 1992–1997.

Rogulska, M., Kultys, A., Olszewska, E., 2013. J. Therm. Anal. Calorim. 114, 903–916.

Rokicki, G., Piotrowska, A., 2002. Polymer 43, 2927–2935.

Romano, U., Rivetti, F., 1993. Process for preparing di-alkyl carbonates. Google Patents.

Romano, U., Rivetti, F., Di Muzio, N., 1982. Process for producing dimethylcarbonate. Google Patents.

Romero, R.R., 2005. J. Cell. Plast. 41, 339–359.

Rose, M., Palkovits, R., 2012. ChemSusChem 5, 167–176.

Rossmy, G.R., Kollmeier, H.J., Lidy, W., Schator, H., Wiemann, M., 1977. J. Cell. Plast. 13, 26–35.

Rotaru, I., Ionescu, M., Donescu, D., Vuluga, M., 2008. Mater. Plast. 45, 23–28.

Roy, P.K., Mathur, R., Kumar, D., Rajagopal, C., 2013. J. Environ. Chem. Eng. 1, 1062–1069.

Saunders, J.H., Slocombe, R.J., 1948. Chem. Rev. 43, 203–218.

Schuster, F., Ngako Ngamgoue, F., Goetz, T., Hirth, T., Weber, A., Bach, M., 2017. J Mater Chem C 5, 6738–6744.

Schwesinger, R., Willaredt, J., Schlemper, H., Keller, M., Schmitt, D., Fritz, H., 1994. Chem. Ber. 127, 2435–2454.

Schwetlick, K., Noack, R., 1995. J. Chem. Soc. Perkin Trans. 2 395.

Senger, J.S., Yilgor, I., McGrath, J.E., Patsiga, R.A., 1989. J. Appl. Polym. Sci. 38, 373–382.

Septevani, A.A., Evans, D.A.C., Chaleat, C., Martin, D.J., Annamalai, P.K., 2015. Ind. Crops Prod. 66, 16–26.

Serrano, L., Alriols, M.G., Briones, R., Mondragón, I., Labidi, J., 2010. Ind. Eng. Chem. Res. 49, 1526–1529.

Sharmin, E., Shreaz, S., Zafar, F., Akram, D., Raja, V., Ahmad, S., 2017. Prog. Org. Coat. 105, 200–211.

Sheridan, J.E., Haines, C.A., 1971. J. Cell. Plast. 7, 135–139.

Sigurdsson, S.T., Seeger, B., Kutzke, U., Eckstein, F., 1996. J. Org. Chem. 61, 3883–3884.

Silva, A.L., Bordado, J.C., 2004. Catal. Rev. 46, 31–51.

Simón, D., Borreguero, A.M., de Lucas, A., Molero, C., Rodríguez, J.F., 2013. J. Mater. Cycles Waste Manag.

Simón, D., Borreguero, A.M., de Lucas, A., Rodríguez, J.F., 2014. Polym. Degrad. Stab. 109, 115–121.

Simón, D., Borreguero, A.M., de Lucas, A., Rodríguez, J.F., 2015a. Polym. Degrad. Stab. 121, 126–136.

Simón, D., Borreguero, A.M., de Lucas, A., Rodríguez, J.F., 2015b. Polym. Degrad. Stab. 116, 23–35.

Simón, D., de Lucas, A., Rodríguez, J.F., Borreguero, A.M., 2016. Polym. Degrad. Stab. 133, 119–130.

Simon, J., Barla, F., Kelemen-Haller, A., Farkas, F., Kraxner, M., 1988. Chromatographia 25, 99–106.

Slotta, K.H., Dressler, H., 1930a. Berichte Dtsch. Chem. Ges. B Ser. 63, 888–898.

Slotta, K.H., Dressler, H., 1930b. Eur. J. Inorg. Chem. 63, 888–898.

Smith, C.H., 1963. Ind. Eng. Chem. Prod. Res. Dev. 2, 27–31.

Sonnenschein, M.F., Wendt, B.L., 2013. Polymer 54, 2511–2520.

Sonnenschein, M.F., Werness, J.B., Patankar, K.A., Jin, X., Larive, M.Z., 2016. Polymer 106, 128–139.

Sorenson, W.R., 1959. J. Org. Chem. 24, 978–980.

Soto, G., Castro, A., Vechiatti, N., Iasi, F., Armas, A., Marcovich, N.E., Mosiewicki, M.A., 2017. Polym. Test. 57, 42–51.

Soto, G.D., Marcovich, N.E., Mosiewicki, M.A., 2016. J. Appl. Polym. Sci. 133.

Stelmachowski, M., Marchwicka, M., Grabowska, E., Diak, M., 2014. J. Adv. Oxid. Technol. 17, 167–178.

Stirna, U., Fridrihsone, A., Lazdiņa, B., Misāne, M., Vilsone, D., 2013. J. Polym. Environ. 21, 952–962.

Storey, R.F., Wiggins, J.S., Puckett, A.D., 1994. J. Polym. Sci. Part Polym. Chem. 32, 2345–2363.

Suh, H.S., Ha, J.Y., Yoon, J.H., Ha, C.-S., Suh, H., Kim, I., 2010. React. Funct. Polym. 70, 288–293.

Suriano, F., Coulembier, O., Hedrick, J.L., Dubois, P., 2011. Polym Chem 2, 528–533.

Szycher, M., 2013. Szycher's handbook of polyurethanes. CRC Press, Boca Raton, Fla.

T, P.J.J., F, S.W., 1965. Process for oxyalkylating solid polyols. US 3190927.

Takeyasu, H., Sonobe, T., Yamaguchi, Y., Doi, T., 1992. Polyurethane flexible foam and method for its production. Google Patents.

Tan, S., Abraham, T., Ference, D., Macosko, C.W., 2011a. Polymer 52, 2840–2846.

Tan, S., Abraham, T., Ference, D., Macosko, C.W., 2011b. Polymer 52, 2840–2846.

Tanaka, R., Hirose, S., Hatakeyama, H., 2008. Bioresour. Technol. 99, 3810–3816.

Tezuka, K., Koda, K., Katagiri, H., Haba, O., 2015. Polym. Bull. 72, 615–626.

Tibério Cardoso, G., Claro Neto, S., Vecchia, F., 2012. Front. Archit. Res. 1, 348–356.

Tomczyk, K.M., Guńka, P.A., Parzuchowski, P.G., Zachara, J., Rokicki, G., 2012. Green Chem. 14, 1749.

Tomita, H., Sanda, F., Endo, T., 2001. J. Polym. Sci. Part Polym. Chem. 39, 162–168.

Tondi, G., Pizzi, A., 2009. Ind. Crops Prod. 29, 356–363.

Tryznowski, M., Świderska, A., Żołek-Tryznowska, Z., Gołofit, T., Parzuchowski, P.G., 2015. Polymer 80, 228–236.

Tserki, V., Matzinos, P., Pavlidou, E., Vachliotis, D., Panayiotou, C., 2006. Polym. Degrad. Stab. 91, 367–376.

Tundo, P., Selva, M., 2002. Acc. Chem. Res. 35, 706–716.

T.Werpy, G.P., 2004.

Udabe, E., Isik, M., Sardon, H., Irusta, L., Salsamendi, M., Sun, Z., Zheng, Z., Yan, F., Mecerreyes, D., 2017. J. Appl. Polym. Sci. 134, 45473.

Ugarte, L., Fernández-d'Arlas, B., Valea, A., González, M.L., Corcuera, M.A., Eceiza, A., 2014a. Polym. Eng. Sci. 54, 2282–2291.

Ugarte, L., Gómez-Fernández, S., Peña-Rodríuez, C., Prociak, A., Corcuera, M.A., Eceiza, A., 2015. ACS Sustain. Chem. Eng. 3, 3382–3387.

Ugarte, L., Saralegi, A., Fernández, R., Martín, L., Corcuera, M.A., Eceiza, A., 2014b. Ind. Crops Prod. 62, 545–551.

Ulrich, H., 1981. J. Cell. Plast. 17, 31–34.

Ulrich, H., Odinak, A., Tucker, B., Sayigh, A.A.R., 1978. Polym. Eng. Sci. 18, 844–848.

Uprety, B.K., Reddy, J.V., Dalli, S.S., Rakshit, S.K., 2017. Bioresour. Technol. 235, 309–315.

Utilization of glycerol, a by-product of the transesterification process of vegetable oils: A review, n.d.

Vaidya, U.R., Nadkarni, V.M., 1987. J. Appl. Polym. Sci. 34, 235–245.

Vaidya, U.R., Nadkarni, V.M., 1988. J. Appl. Polym. Sci. 35, 775–785.

Van Maris, R., Tamano, Y., Yoshimura, H., Gay, K.M., 2005. J. Cell. Plast. 41, 305–322.

Velencoso, M.M., Gonzalez, A.S., García-Martínez, J.C., Ramos, M.J., De Lucas, A., Rodriguez, J.F., 2013. Polym. Int. 62, 783–790.

Vert, M., Doi, Y., Hellwich, K.-H., Hess, M., Hodge, P., Kubisa, P., Rinaudo, M., Schué, F., 2012. Pure Appl. Chem. 84.

Viswanathan, T., Burrington, D., Richardson, T., 2008. J. Chem. Technol. Biotechnol. Biotechnol. 34, 52–56.

Vitkauskiene, I., Makuska, R., Stirna, U., Cabulis, U., 2011. J. Cell. Plast. 47, 467–482.

Wilson, M.E., Hu, M., Kurth, M.J., Hsieh, Y.-L., Krochta, J.M., 1996. J. Appl. Polym. Sci. 59, 1759–1768.

WO03028644A2.

Woods, G., 1982. Flexible polyurethane foams: chemistry and technology. Applied Science Publishers, London ; Englewood, N.J.

Worley, W.G., Shah, H.M., Athey, P.S., Bruchertseifer, C., Mueller, G., 2008. Polyurethane polymer systems. 20110098417.

Wu, C.-H., Chang, C.-Y., Cheng, C.-M., Huang, H.-C., 2003. Polym. Degrad. Stab. 80, 103–111.

Wu, C.-H., Chang, C.-Y., Li, J.-K., 2002. Polym. Degrad. Stab. 75, 413–421.

Wu, L.C.-F., Glasser, W.G., 1984. J. Appl. Polym. Sci. 29, 1111–1123.

Wu, M., Guo, J., Jing, H., 2008. Catal. Commun. 9, 120–125.

Xu, B.-H., Wang, J.-Q., Sun, J., Huang, Y., Zhang, J.-P., Zhang, X.-P., Zhang, S.-J., 2015. Green Chem. 17, 108–122.

Xu, J., Jiang, J., Hse, C.-Y., Shupe, T.F., 2014. J. Appl. Polym. Sci. 131, 40096.

Xue, B.-L., Huang, P.-L., Sun, Y.-C., Li, X.-P., Sun, R.-C., 2017. RSC Adv 7, 6123–6130.

Yamaguchi, A., Hiyoshi, N., Sato, O., Shirai, M., 2011. Green Chem. 13, 873.

Yamaguchi, A., Sato, O., Mimura, N., Shirai, M., 2016. Catal. Today 265, 199–202.

Yao, W., Wang, H., Guan, D., Fu, T., Zhang, T., Dou, Y., 2017. Adv. Mater. Sci. Eng. 2017, 1–7.

Yao, Y., Yoshioka, M., Shiraishi, N., 1996. J. Appl. Polym. Sci. 60, 1939–1949.

Yasunaga, K., Neff, R.A., Zhang, X.D., Macosko, C.W., 1996. J. Cell. Plast. 32, 427–448.

Yazdani-Pedram, M., Soto, E., Tagle, L.H., Diaz, F.R., Gargallo, L., Radić, D., 1986. Thermochim. Acta 105, 149–160.

Yeganeh, H., Hojati-Talemi, P., 2007. Polym. Degrad. Stab. 92, 480–489.

Yoshioka, M., Miyata, A., Nishio, Y., 2004a. J. Wood Sci. 50, 504–510.

Yoshioka, M., Miyata, A., Yagi, T., Nishio, Y., 2004b. J. Wood Sci. 50, 511–518.

Young, D.M., Fritz, H., n.d. Foamed polymer of isocyanate modified lactone polyesters and method of preparing same. 2990379.

Yu, C.-Y., Lee, W.-J., 2014. Polym. Degrad. Stab. 101, 60–64.

Yu, F., Saha, P., Suh, P.W., Kim, J.K., 2015. J. Appl. Polym. Sci. 132, 41410.

Yue, D., Oribayo, O., Rempel, G.L., Pan, Q., 2017. RSC Adv 7, 30334–30344.

Yukuta, T., Yagura, K., Fuchigami, N., 1981. Method of producing flexible reticulated polyether polyurethane foams.

Zarzyka, I., 2016. J. Cell. Plast. 52, 545–561.

Zenner, M.D., Xia, Y., Chen, J.S., Kessler, M.R., 2013. ChemSusChem 6, 1182–1185.

Zhang, C., Kessler, M.R., 2015. ACS Sustain. Chem. Eng. 3, 743–749.

Zhang, G., Zhang, Q., Wu, Y., Zhang, H., Cao, J., Han, D., 2017. J. Appl. Polym. Sci. 134, 45582.

Zhang, J., Li, J., Wu, S.-B., Liu, Y., 2013. Ind. Eng. Chem. Res. 52, 11799–11815.

Zhang, L., Jeon, H.K., Malsam, J., Herrington, R., Macosko, C.W., 2007. Polymer 48, 6656–6667.

Zhang, L., Zhang, M., Hu, L., Zhou, Y., 2014. Ind. Crops Prod. 52, 380–388.

Zhang, M., Pan, H., Zhang, L., Hu, L., Zhou, Y., 2014a. Ind. Crops Prod. 59, 135–143.

Zhang, Q., Zhang, G., Han, D., Wu, Y., 2016. J. Appl. Polym. Sci. 133.

Zhang, X.., Macosko, C.., Davis, H.., Nikolov, A.., Wasan, D.., 1999. J. Colloid Interface Sci. 215, 270–279.

Zheng, Z.-Q., Liu, Y., Li, D., Wang, L., Adhikari, B., Chen, X.D., 2017. Int. J. Food Eng. 13.

Zhou, X., Sain, M.M., Oksman, K., 2016. Compos. Part Appl. Sci. Manuf. 83, 56–62.

Zia, K.M., Bhatti, H.N., Ahmad Bhatti, I., 2007. React. Funct. Polym. 67, 675–692.

Zieleniewska, M., Leszczyński, M.K., Kurańska, M., Prociak, A., Szczepkowski, L., Krzyżowska, M., Ryszkowska, J., 2015. Ind. Crops Prod. 74, 887–897.

Zieleniewska, M., Ryszkowska, J., Bryskiewicz, A., Auguscik, M., Szczepkowski, L., Swiderski, A., Wrzesniewska-Tosik, K., 2017. Polimery 62, 127–135.

Zlatanić, A., Javni, I., Ionescu, M., Bilić, N., Petrović, Z.S., 2015. J. Cell. Plast. 51, 289–306.

Zlatanić, A., Lava, C., Zhang, W., Petrović, Z.S., 2004. J. Polym. Sci. Part B Polym. Phys. 42, 809–819.

Zou, X., Qin, T., Huang, L., Zhang, X., Yang, Z., Wang, Y., 2009. Energy Fuels 23, 5213–5218.

2011. Focus Powder Coat. 2011, 7–8.

ANNEXES

Annexe 1 : Définitions et exemples relatifs à la formulation de mousses polyuréthane ou polyisocyanurate

Expression du nombre de part

Très généralement lorsqu'une formulation de mousse PUR ou PIR est donnée, les quantités de matière sont exprimées en partie par poids (parts) ou poids équivalent en masse. Pour établir l'ensemble des quantités de matière impliquées dans la formulation de la mousse, on se base sur 100 parts en poids équivalent de polyol (fixe). Puis est déterminé le nombre de parts équivalentes de polyisocyanate en fonction de l'Ic.

Taux de gonflement de la mousse

Afin d'obtenir des mousses similaires en termes de densité ou de densité comparable, il est essentiel de travailler avec un taux d'agent gonflant identique dans chaque formulation. Le taux d'agent gonflant n'est autre que le rapport entre le volume de gaz introduit dans la formulation et la masse totale des constituants de la formulation. Pour cela il est considéré que les gaz d'expansion utilisés se comportent comme des gaz parfaits et occupent 22,4 L/mol. Il est également considéré dans le cas de l'eau qu'une mole d'eau libère une mole de dioxyde de carbone. Ainsi, le taux d'agent gonflant, une fois fixé, permet de travailler avec des systèmes ayant le même « potentiel » d'expansion. Les différences de hauteur ou de densité des mousses seront donc uniquement liées à la température atteinte pendant le procédé de moussage ; soit en lien direct avec la réactivité du mélange.

Quantité d'agents gonflants

La quantité d'agents gonflants est choisie en fonction de la densité de mousse finale souhaitée. En général la quantité d'agents gonflants dépasse rarement 5 %pds de l'ensemble de la formulation.

Quantité de catalyseur

La quantité et la nature du / des catalyseur(s) d'une mousse diffèrent que l'on travaille sur un système PUR ou PIR. La quantité en elle-même est faible et généralement inférieure à 2 %pds de l'ensemble de la formulation. Elle est ajustée au cas par cas pour obtenir des temps caractéristiques de moussages voulus. Ou bien, elle est maintenue constante pour évaluer l'impact d'autres paramètres sur les temps caractéristiques de moussages.

Quantité de surfactant

La quantité de surfactant n'a pas besoin d'être très élevée pour être efficace. Il n'est pas rare que sa quantité soit inférieure à 1 %pds de l'ensemble de la formulation.

Protocole succinct de préparation d'une mousse

Le bon mélange des différents constituants de la mousse est essentiel. Ainsi un premier mélange appelé A est réalisé. Ce mélange contient l'ensemble des réactifs (polyol, catalyseur, agent gonflant, surfactant, etc…) à l'exception du polyisocyanate. Le mélange A est homogénéisé jusqu'à l'obtention d'un mélange monophasique. Le deuxième mélange, appelé B est uniquement constitué de la quantité de polyisocyanate prédéterminés par le calcul.

Ensuite A et B sont rapidement mélangés l'un à l'autre (moins de 20 s) puis la réaction de moussage commence.

Exemple de formulation

- ***Exemple 1 – mousse PUR***

Cas d'une mousse ne contenant qu'un seul agent gonflant, un dérivé d'isopentane (M= 78 g/mol) et un additif : le TCPP (ignifugeant).

Table SI 1: Exemple de calcul de formulation d'une mousse PUR destiné à l'isolation du bâtiment

Index	115				
Produit	Nature	Indice (%NCO ou IOH)	Masse (g)	Nombre de part	%pds
Daltolac R570	Polyol	570	20	100	36,4
Ongronat 2500	Isocyanate	31	31,6	158	57 ,6
DMCHA	Catalyseur	---	0,4	2	0,73
Silicone	Surfactant	---	0,4	2	0,73
Isopentane	Agent gonflant	---	4	20	3.6
TCPP	Additif	---	0,5	5	0,9
				Taux de gonflement	1,15

- ***Exemple 2 – mousse PUR***

Cas d'une mousse PUR contenant deux agents gonflants, 50% d'un dérivé d'isopentane (M =78 g/mol) et de 50% d'eau. Attention l'eau à un IOH de 6227 mg KOH/g, en plus d'être un agent gonflant, elle doit être prise en compte pour le calcul de l'Ic. Ainsi pour remplir le tableau de formulation, il faut calculer la quantité d'eau présente dans la formulation et ajuster la quantité de polyisocyanate. A cause de l'IOH élevé de l'eau, la quantité de polyisocynate contenus dans la mousse est supérieure à celle présentée dans l'exemple 1.

Table SI 2: Exemple de calcul d'une mousse PUR avec un mélange d'agents gonflants chimiques et physiques

Index	115				
Produit	Nature	Indice (%NCO ou IOH)	Masse	Nombre de part	% pds
Daltolac R570	Polyol	570	20	100	31,5
Ongronat 2500	Isocyanate	31	39,8	200	62,6
DMCHA	Catalyseur	---	0,45	2	0,7
Silicone	Surfactant	---	0,4	2	0,63
Isopentane	Agent gonflant 1	---	2,00	10	3,1
Eau	Agent gonflant 2	6227	0.47	2.35	0,74
TCPP	Additif	---	0,5	5	0,79
				Taux de gonflement	1,15

- ***Exemple 3 – mousse PIR***

Pour la formulation d'une mousse PIR il est courant d'utiliser des polyols avec des IOH plus bas que dans le cas d'une formulation de mousse PUR. Également, il y a souvent deux catalyseurs : (i) un pour catalyser la réaction polyol / polyisocyanate et (ii) un catalyseur de trimérisation du polyisocyanate

Table SI 3 : Exemple de calcul d'une mousse PUR avec un mélange d'agents gonflants chimiques et physiques

Index	320				
Produit	Nature	Indice (%NCO ou IOH)	Masse (g)	Nombre de part	%pds
Stepanpol PS 2412	Polyol	195	20	100	35,59
Ongronat 2500	Isocyanate	31	30	150	53,38
Kzero 3000	Catalyseur	---	0,6	3	1,06
Niax PM20+	Catalyseur		0,2	1	0,36
Silicone	Surfactant	---	0,4	2	0,72
Isopentane	Agent gonflant	---	4	20	7,12
TCPP	Additif	---	1	5	1,78
				Taux de gonflement	1,15

Annexe 2 : Supporting information du sous-Chapitre 2.1

Sorbitol and glycerol comparison

Sorbitol and glycerol main properties and price are presented in Table SI.4.

Table SI 4 : Main properties and cost of glycerol and sorbitol

	Glycerol	**Sorbitol**
Molecular formula	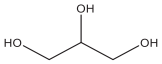	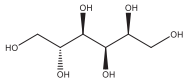
Average price per Kg (Euro)	0.7	0.8
Functionality based on hydroxyl (OH) groups	3 (2 primary and 1 secondary)	6 (2 primary and 4 secondary)
Molar mass (g/mol)	92.09	182.17
Melting point (°C)	18	97
Boiling Point (°C)	290	296
Density (kg/m^3)	1260	1489
OH-Value (mg KOH/g)	1829	1848

^{1}H-NMR spectra at the end of the first reactional step

Figure SI 1 shows the ^{1}H-NMR spectra of the reactional intermediate, at the end of the first reaction step. This intermediate structure is common to future EASAE, PASAP, BASAB, HASAH, OASAO, DASAD and DoASADo polyester polyol. Signal attribution and integration are in good agreement with the determine structure of the reactional intermediate.

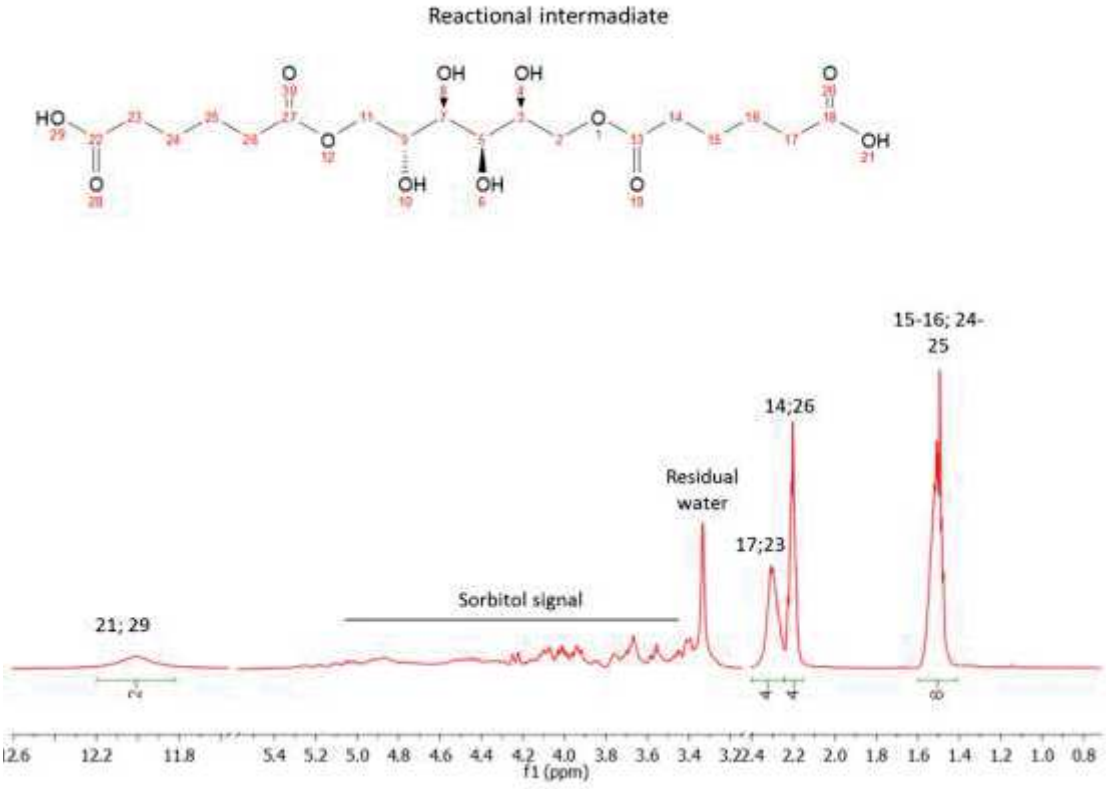

Figure SI 1: 1H-NMR of the reactional intermediate

[1]H-NMR spectra at the end of the second reactional step

Figure SI 2 to 8 shows the global [1]H-NMR spectra of the final products with characteristic peak integration used to determine the reaction global yields presented Table SI 5.

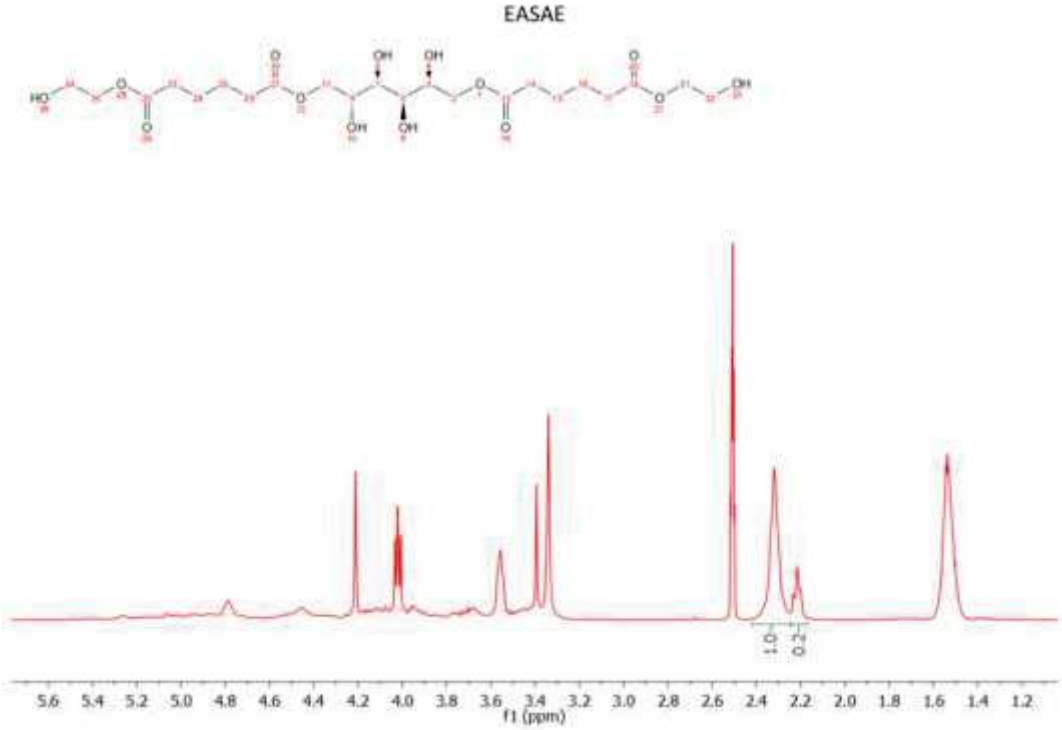

Figure SI 2: 1H-NMR spectra of EASAE

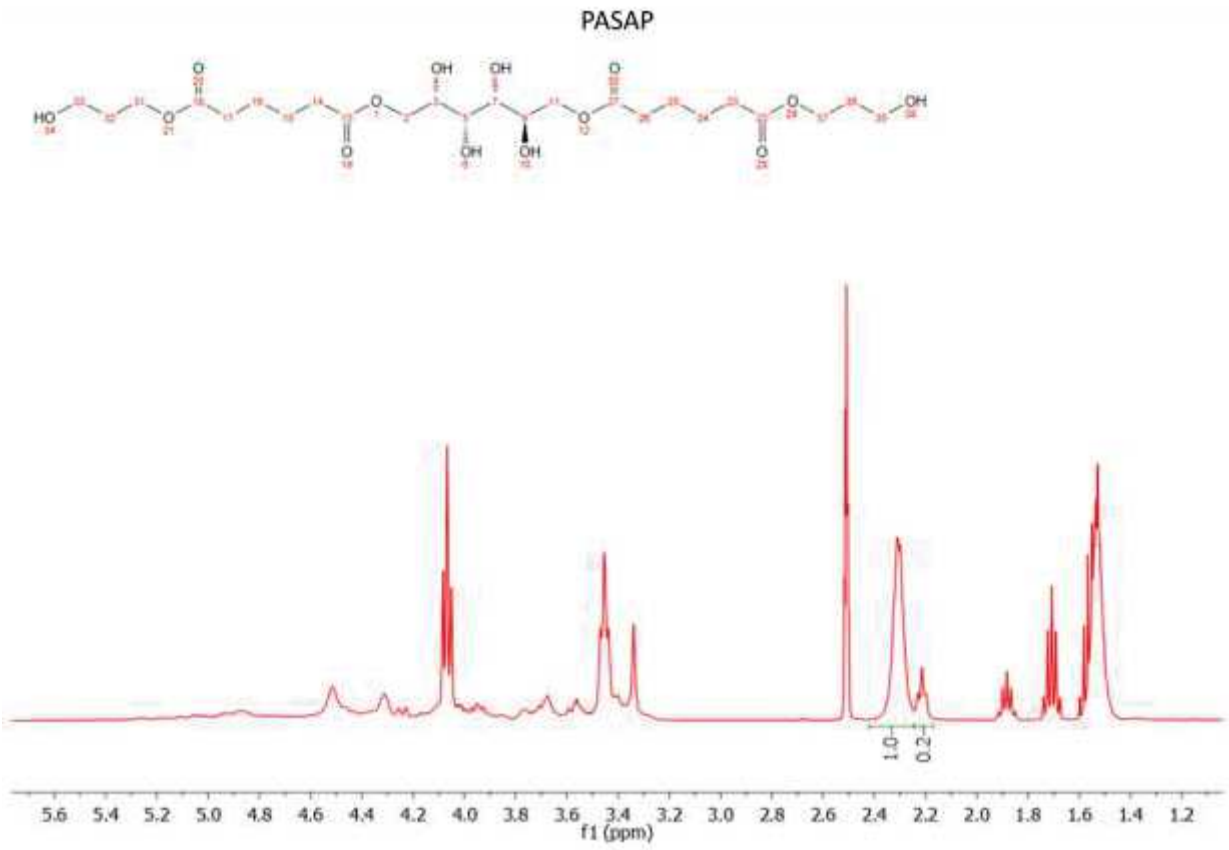

Figure SI 3: 1H-NMR spectra of PASAP

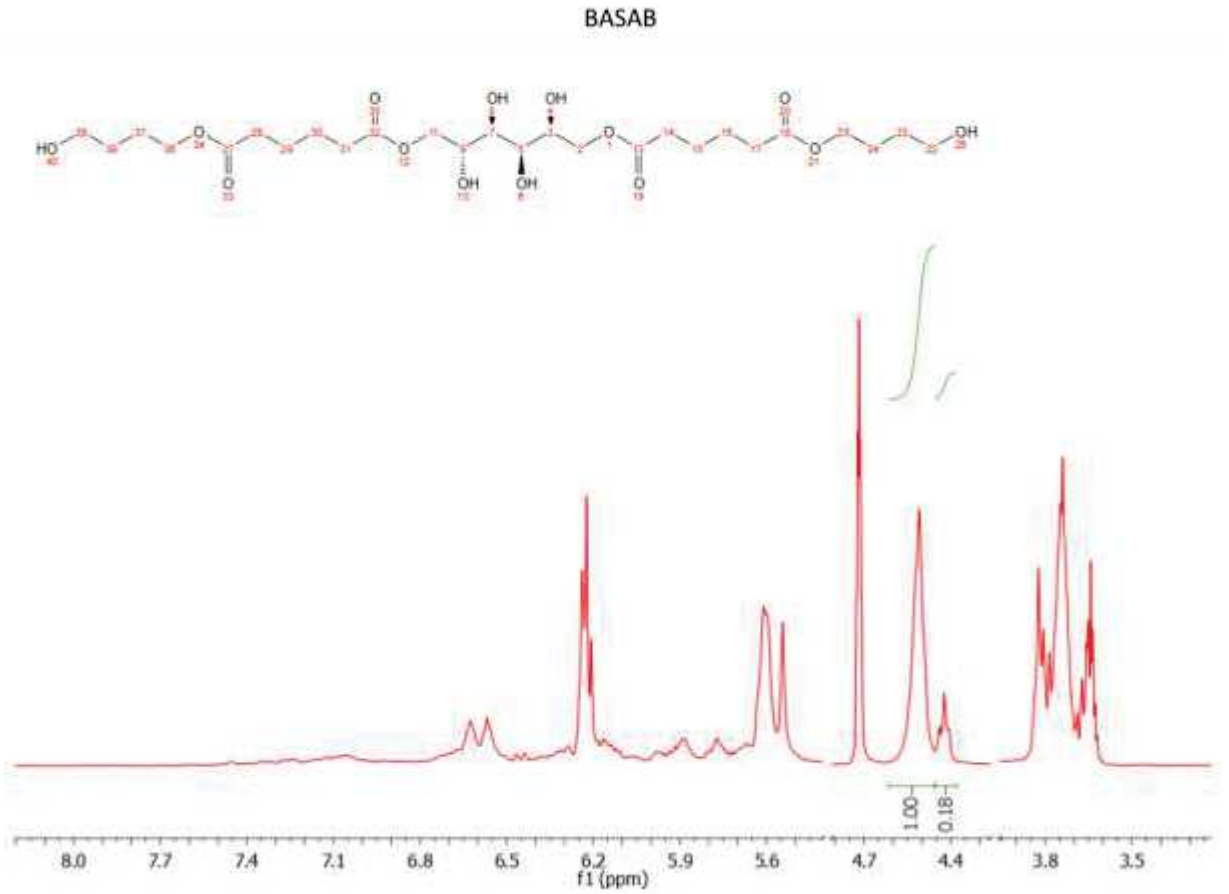

Figure SI 4: [1]H-NMR spectra of BASAB

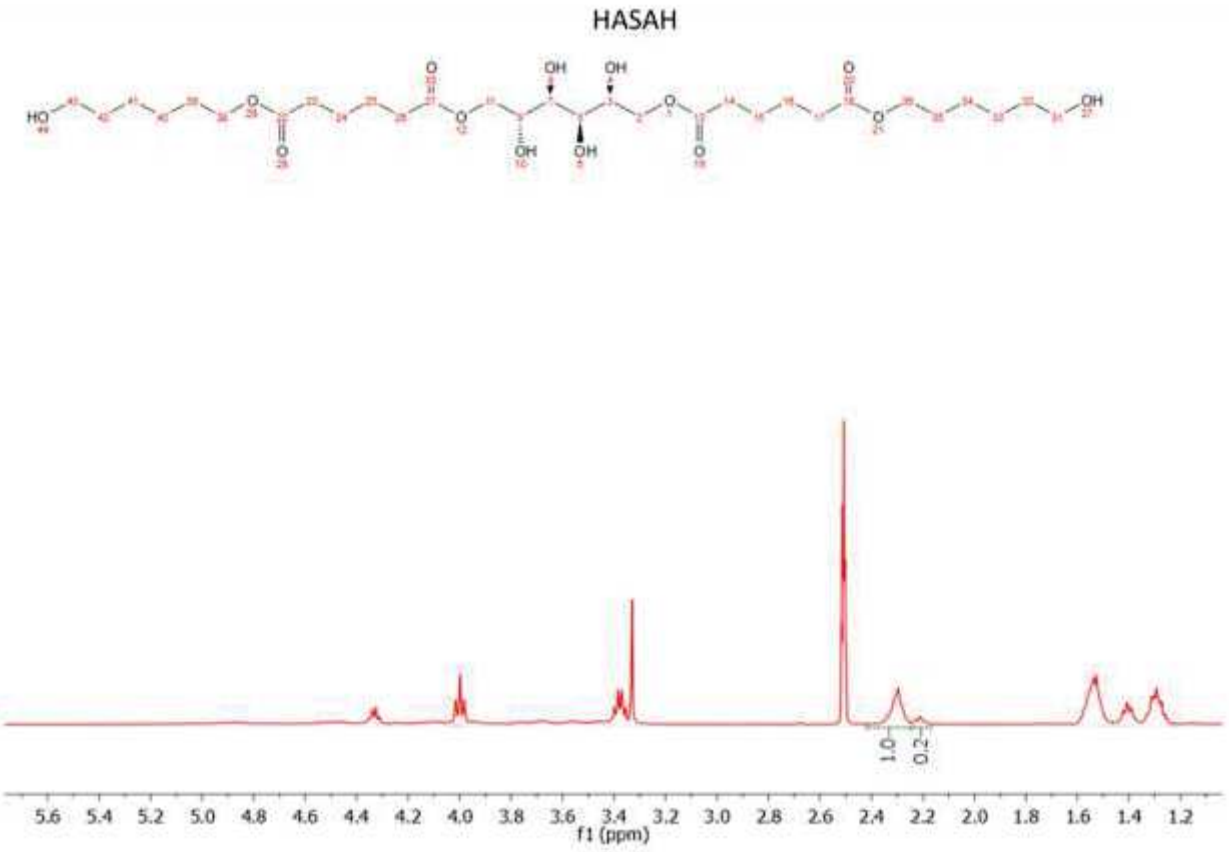

Figure SI 5: [1]H-NMR spectra of HASAH

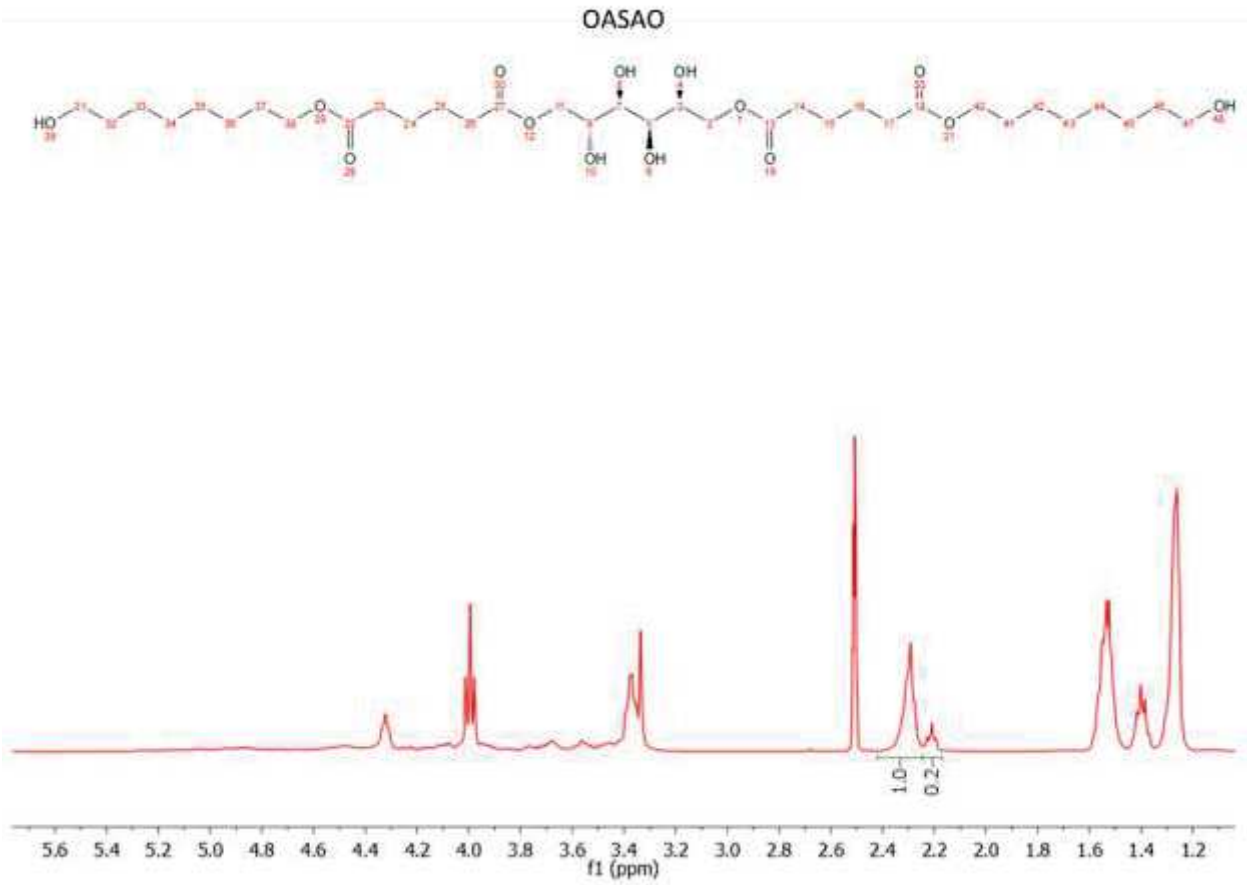

Figure SI 6: ^{1}H-NMR spectra of OASAO

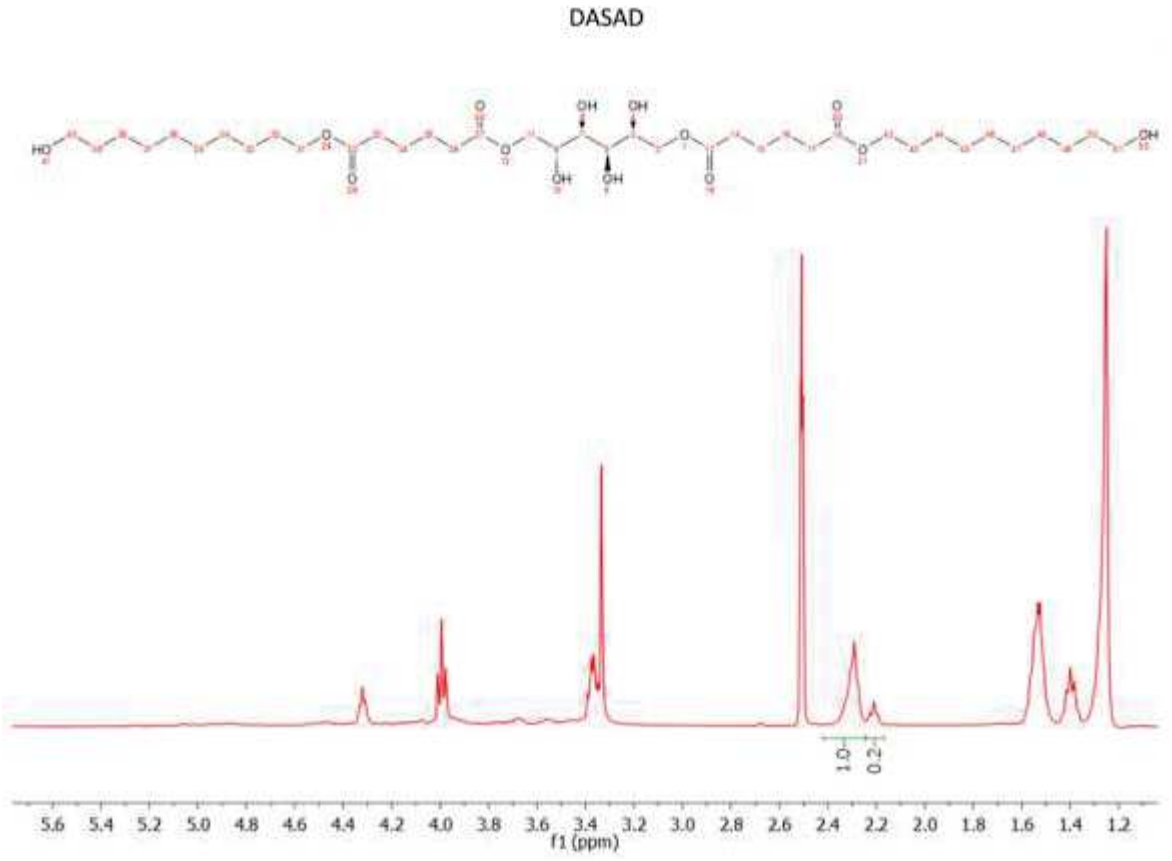

Figure SI 7: ^{1}H-NMR spectra of DASAD

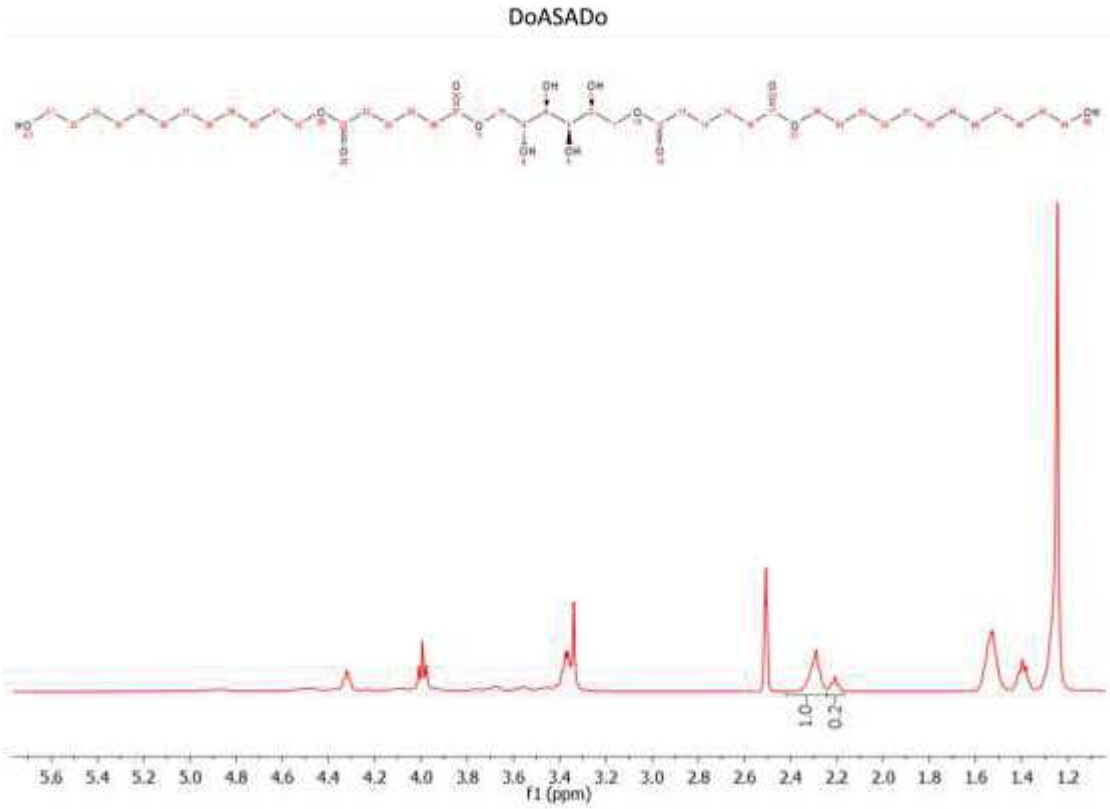

Figure SI 8: [1]H-NMR spectra of DoASADo

Table SI 5: Global yields of the polyol polyesters from 1H-NMR integration

	EASAE	PASAP	BASAB	HASAH	OASAO	DASAD	DoASADo
Yield (%)	81	85	85	86	85	84	81

[13]C-NMR spectra

Figure SI 16 to 18 shows sorbitol, adipic acid and succinic acid ^{13}C-NMR spectra with attributed signal.

Figure SI 19 shows the reactional intermediate at the end of the first reaction step ^{13}C-NMR spectra. This intermediate structure is common to future EASAE, PASAP, BASAB, HASAH, OASAO, DASAD and DoASADo polyester polyol. Signal attribution is in agreement with the molecular structure except for the sorbitol signal which is really weak and closes to the baseline noise.

Figure SI 9 to 15 shows ^{13}C-NMR spectra are strong information regarding polyesters polyols structure. Regarding the number of peak and chemical shift, these spectra are comforting the hypothesis of linear structure. All signals attributions are in goo agreement with the polyester polyol molecular structure. For all ^{13}C-NMR analysis of final polyester polyol the sorbitol signal was weak.

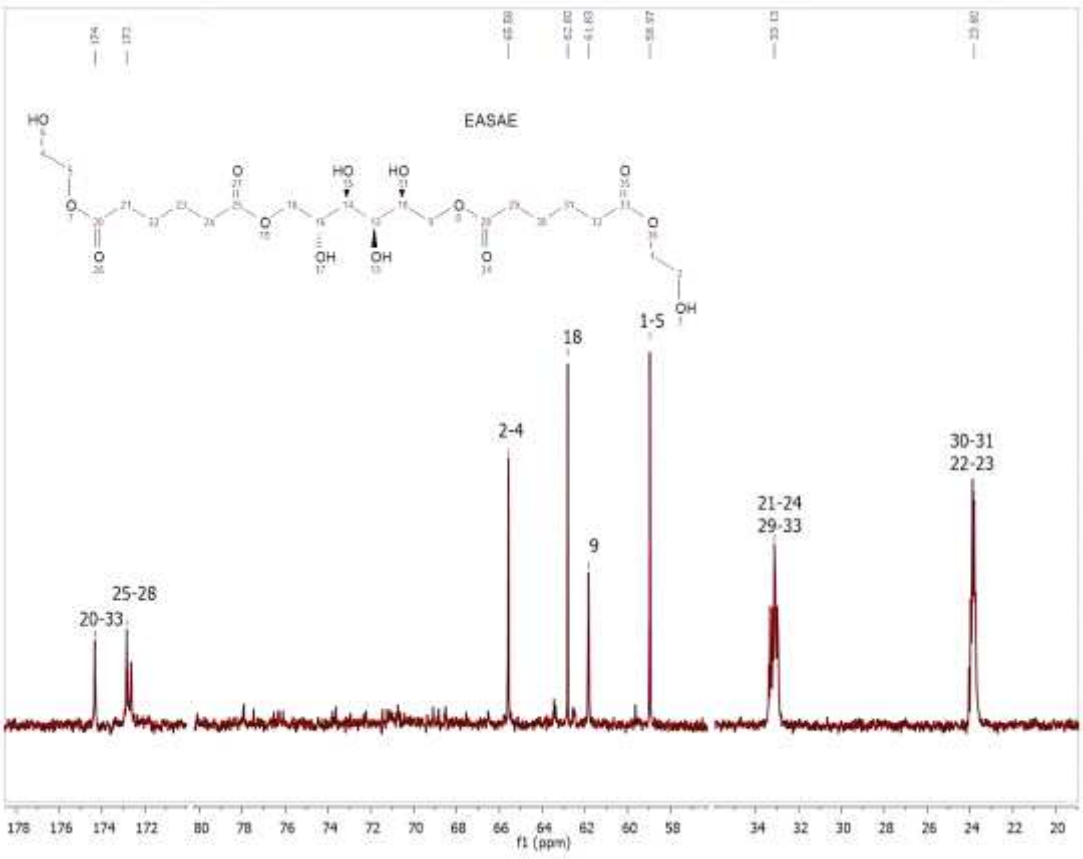

Figure SI 9: ^{13}C-NMR spectra of EASAE

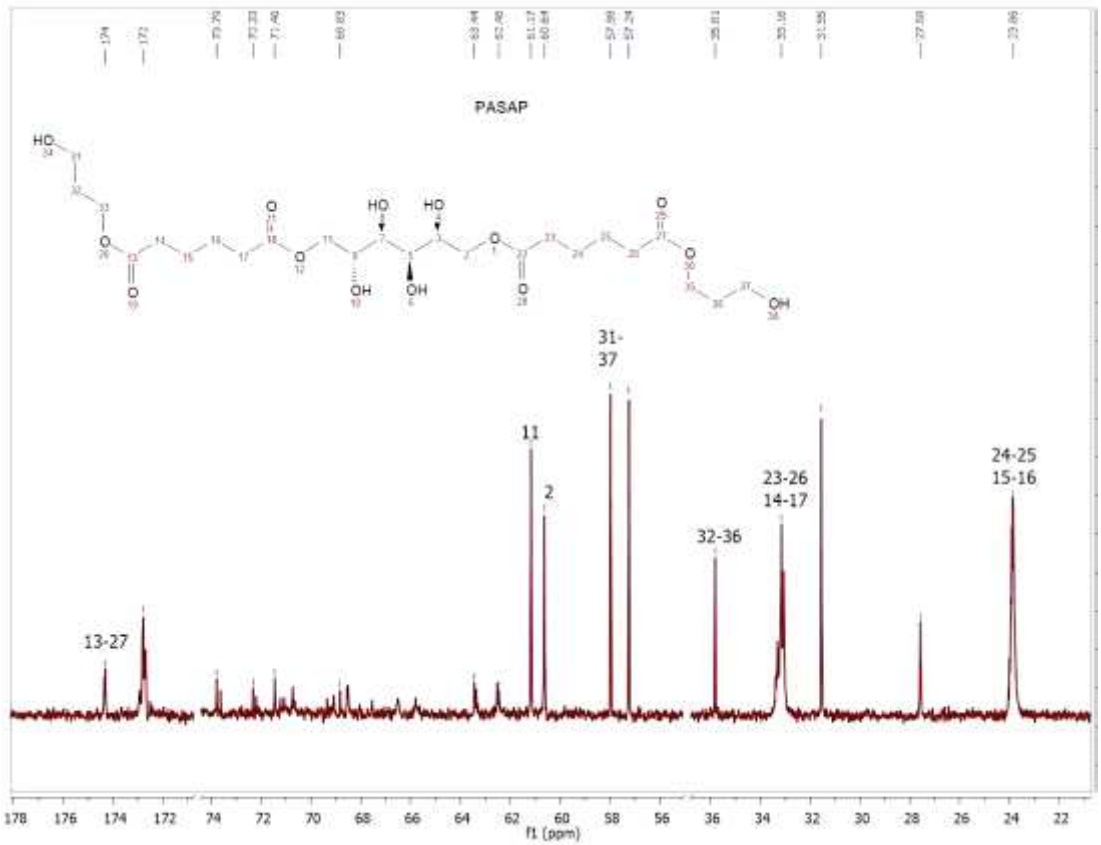

Figure SI 10: ^{13}C-NMR spectra of PASAP

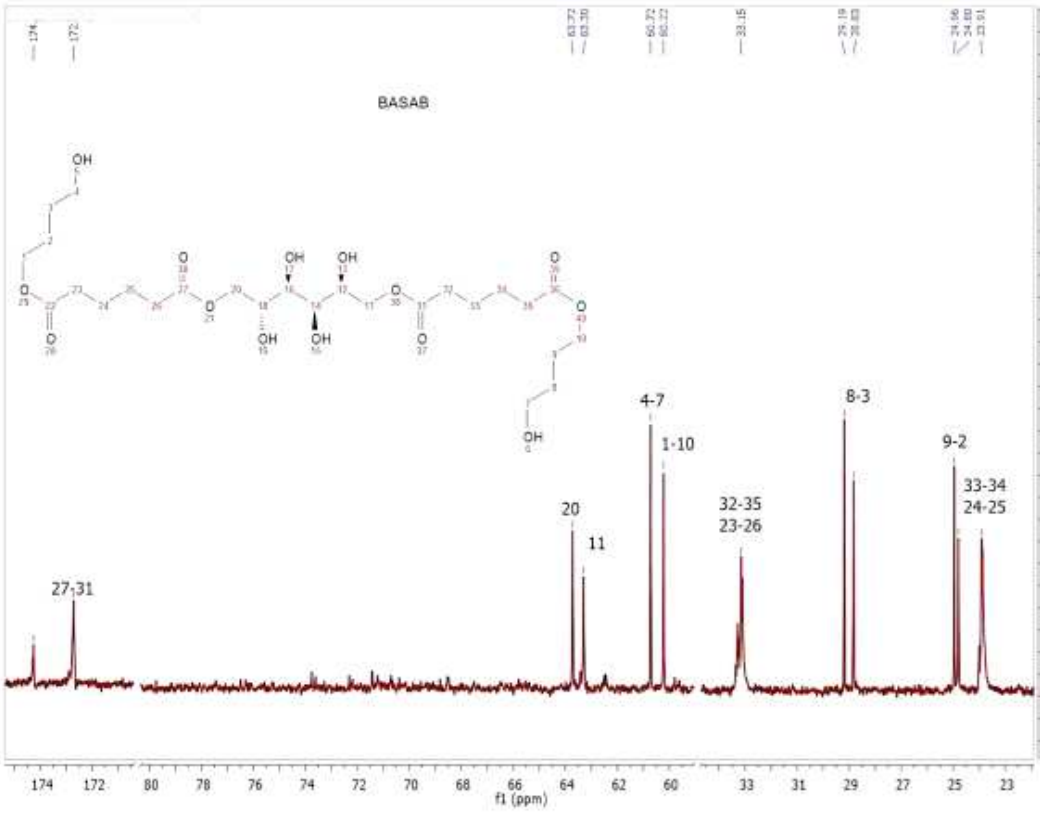

Figure SI 11: ^{13}C-NMR spectra of BASAB

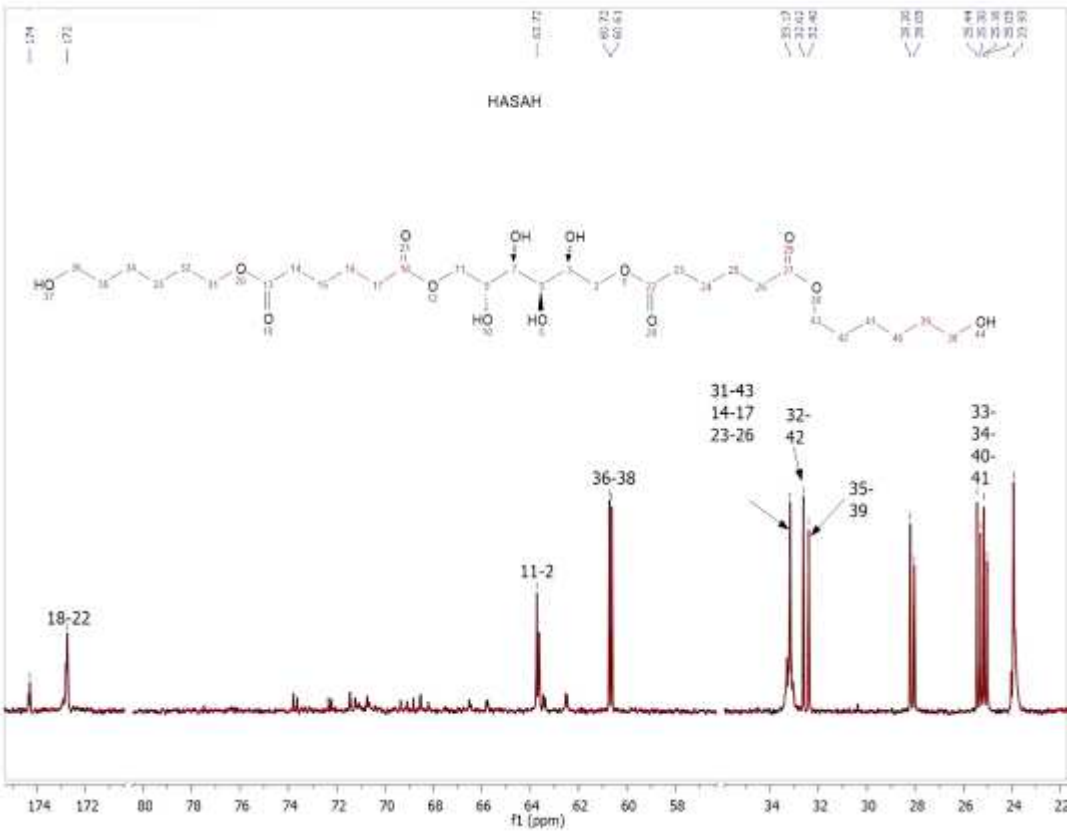

Figure SI 12: ^{13}C-NMR spectra of HASAH

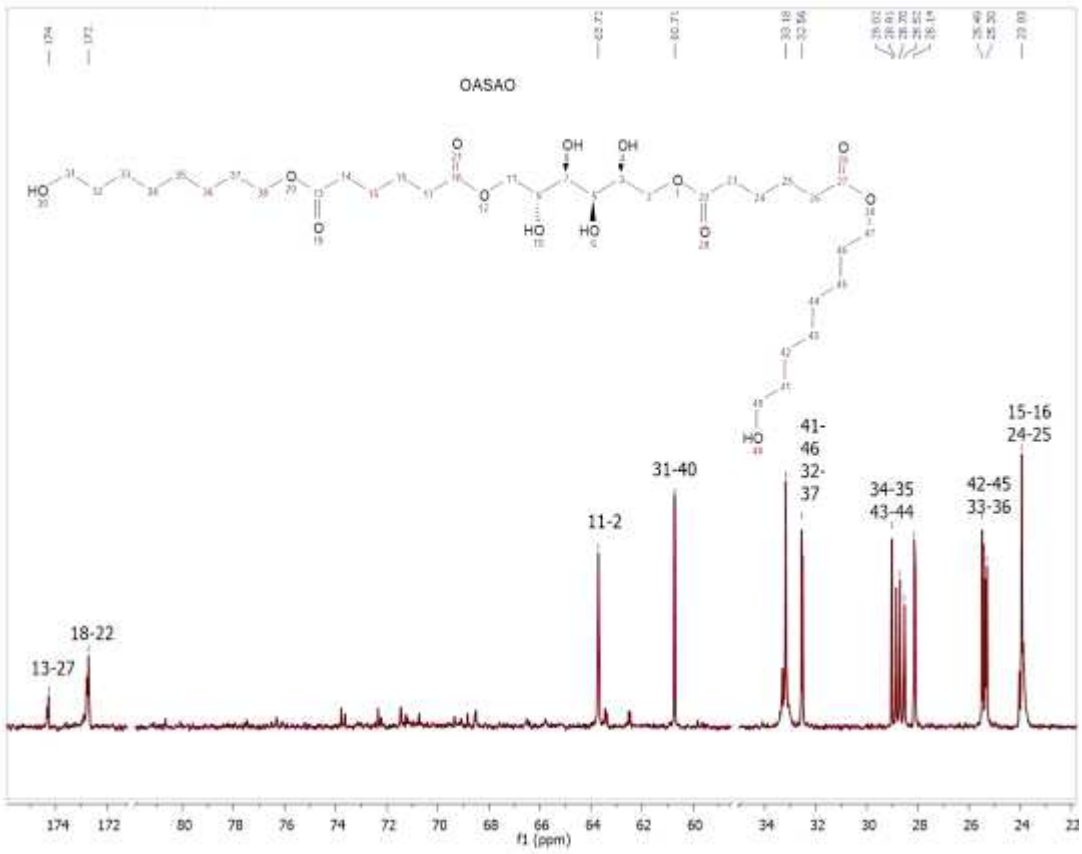

Figure SI 13: ^{13}C-NMR spectra of OASAO

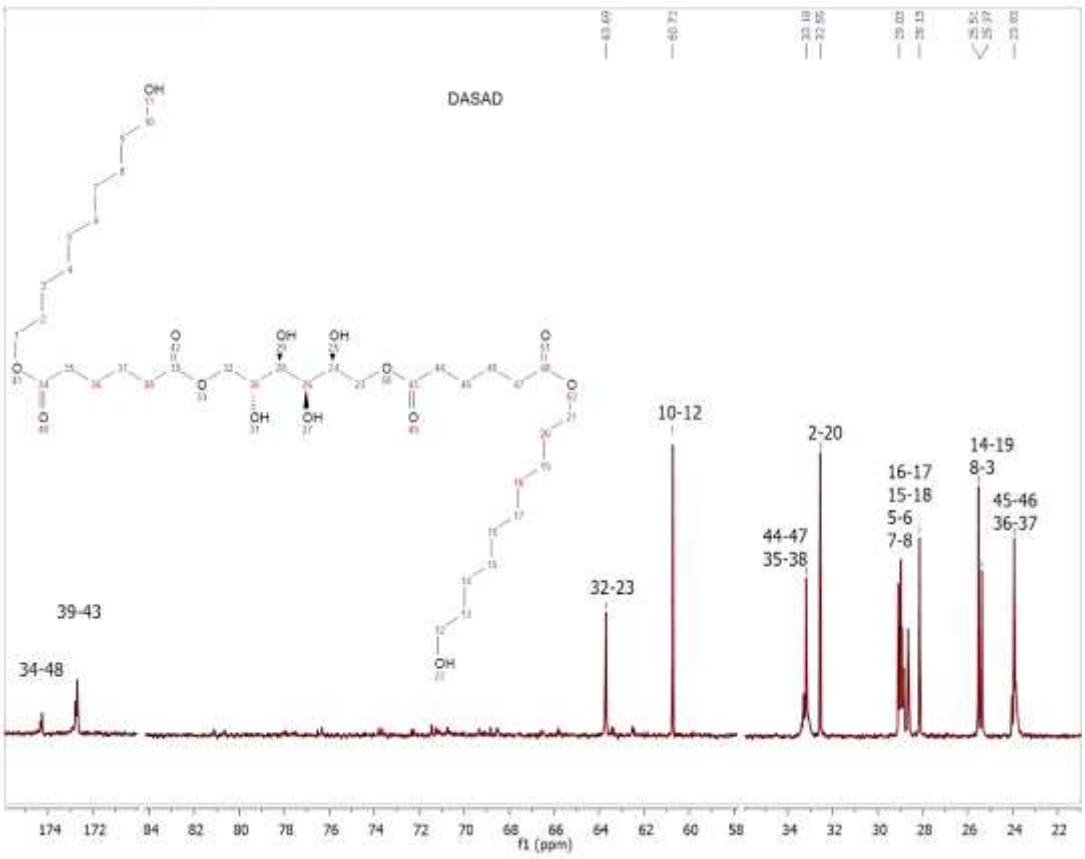

Figure SI 14: ^{13}C-NMR spectra of DASAD

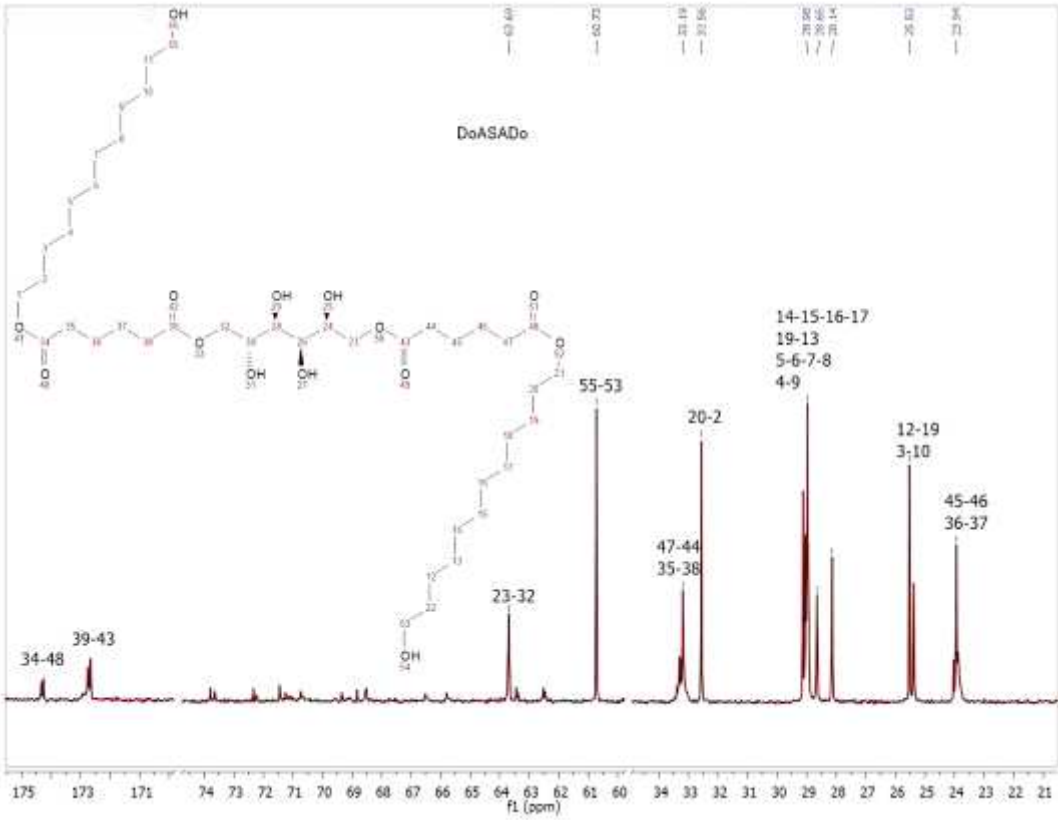

Figure SI 15: ^{13}C-NMR spectra of DoASADo

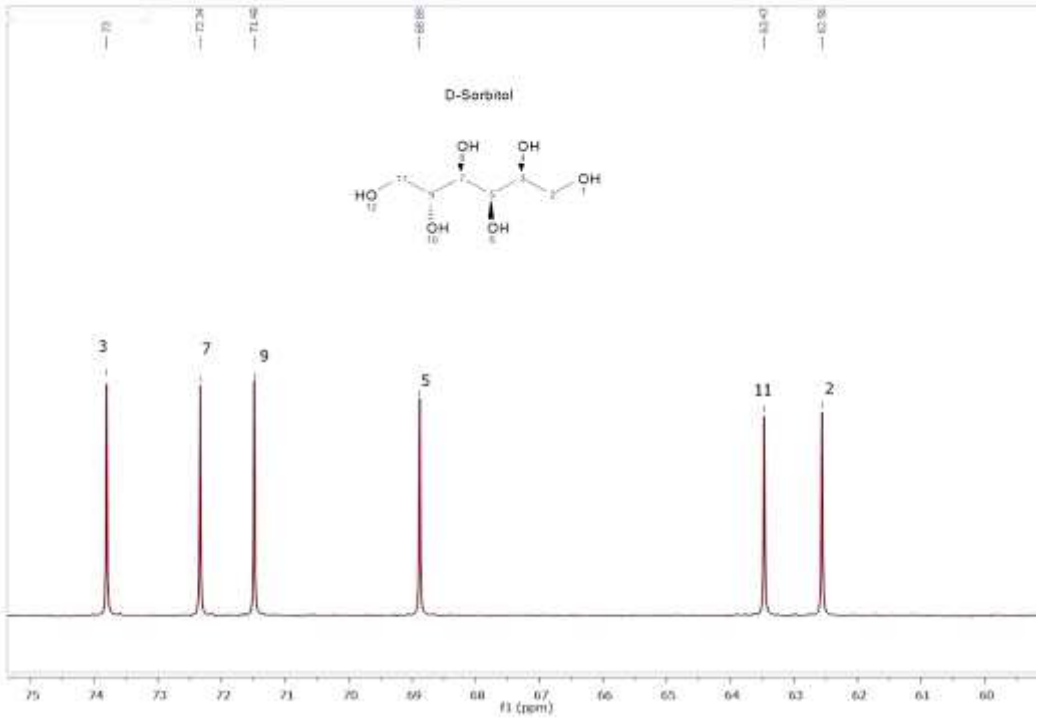

Figure SI 16: ^{13}C-NMR spectra of neat sorbitol

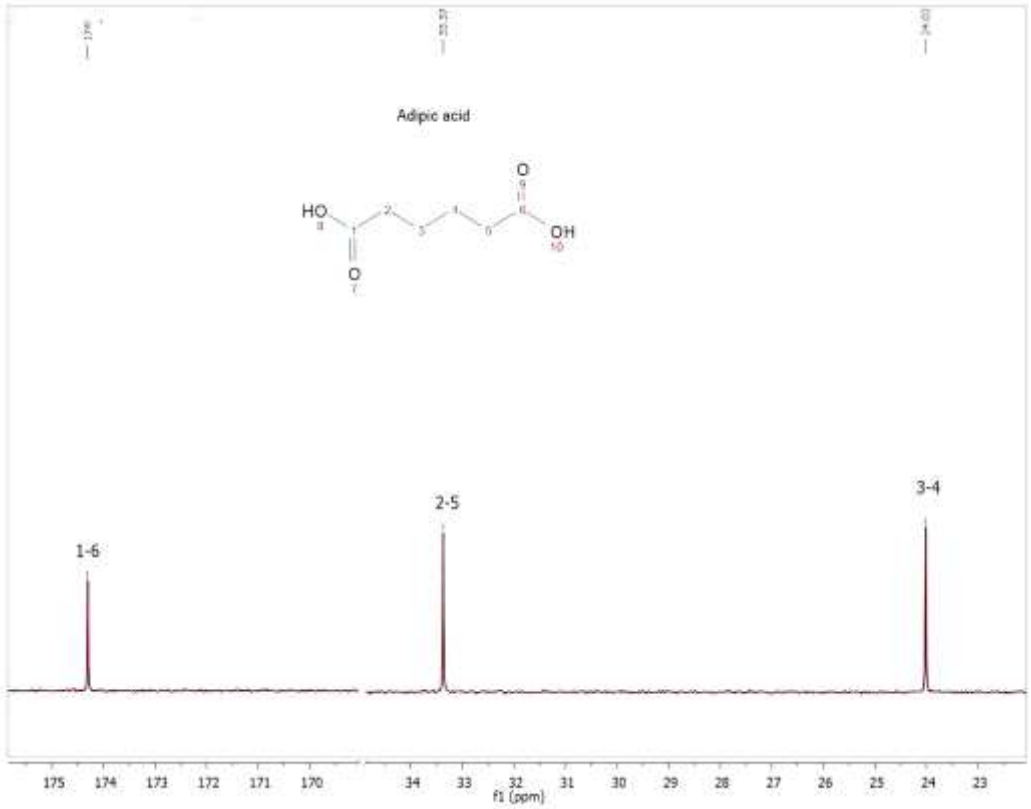

Figure SI 17: ^{13}C-NMR spectra of adipic acid

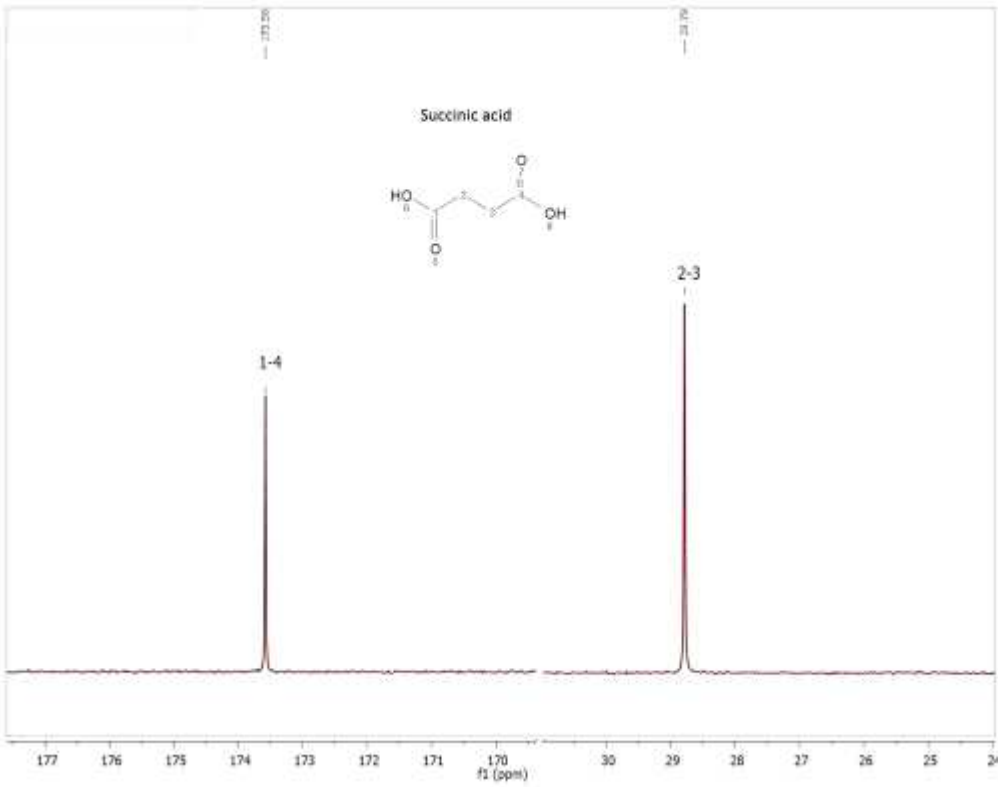

Figure SI 18: ^{13}C-NMR spectra of succinic acid

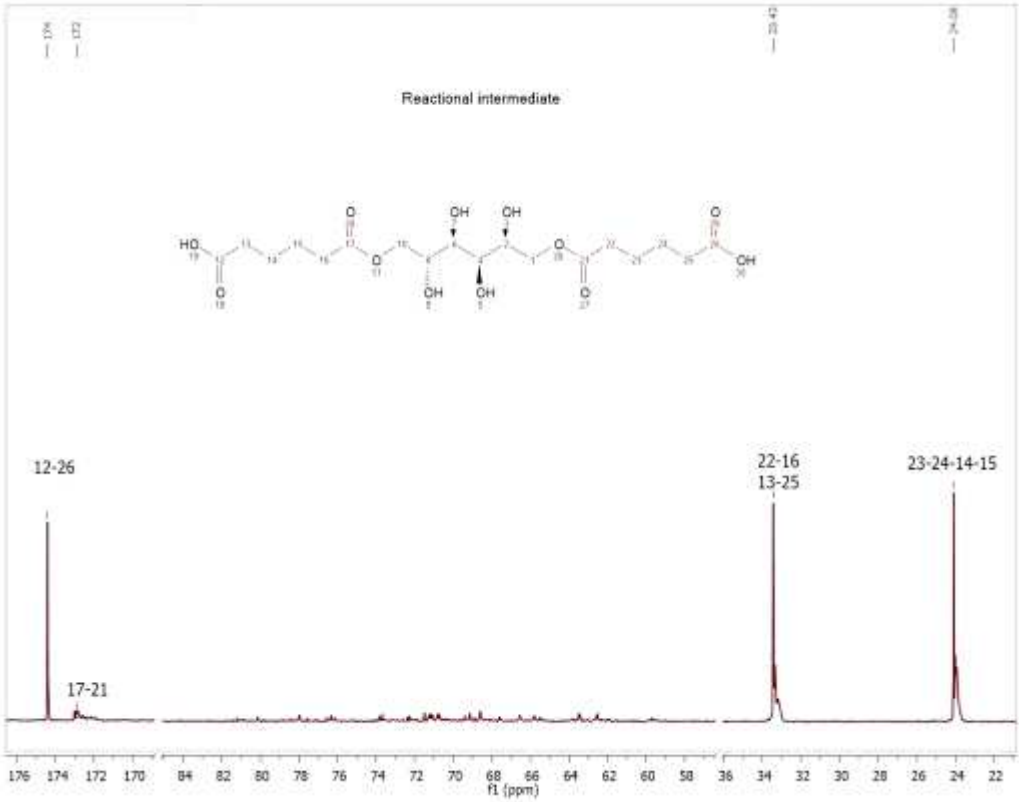

Figure SI 19: ^{13}C-NMR spectra of the reactional intermediate

^{31}P-NMR spectra

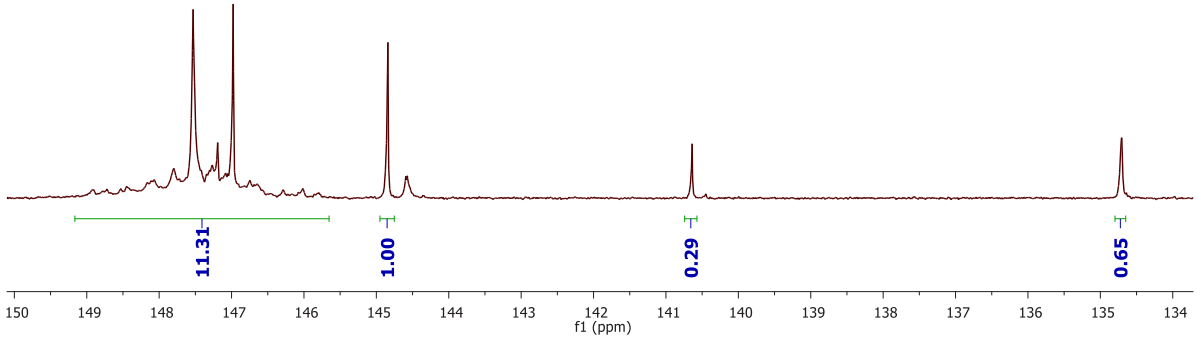

Figure SI 20 : ^{31}P-NMR spectra of EASAE

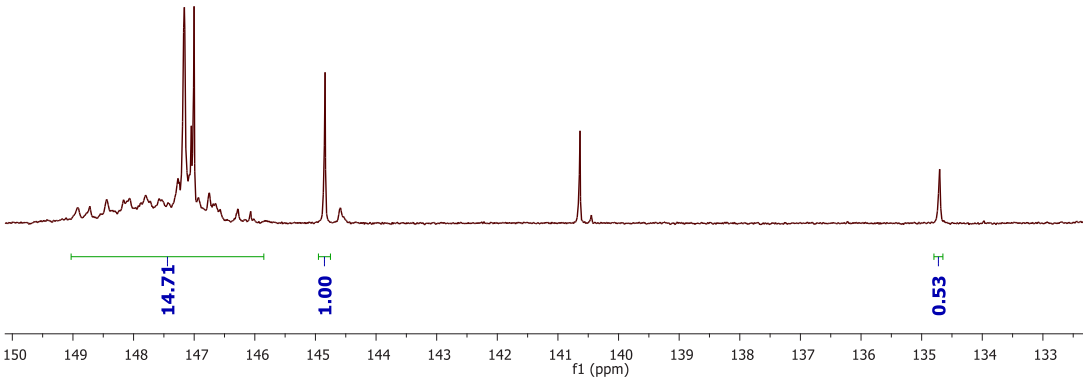

Figure SI 21: ^{31}P-NMR spectra of PASAP

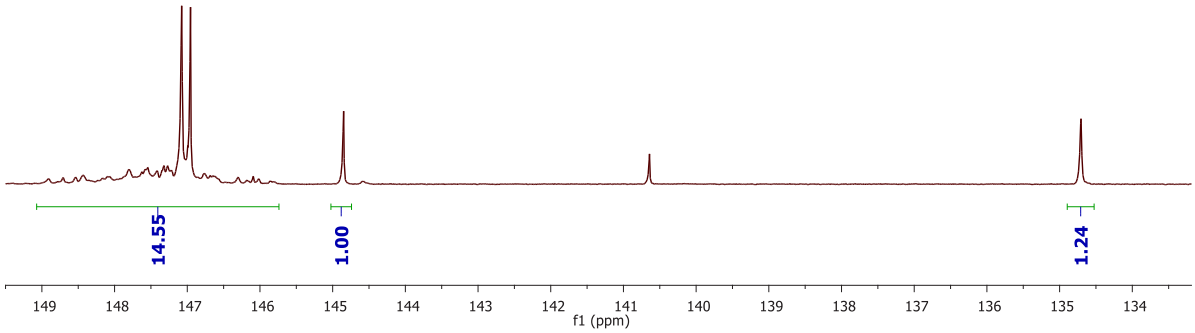

Figure SI 22: ^{31}P-NMR spectra of BASAB

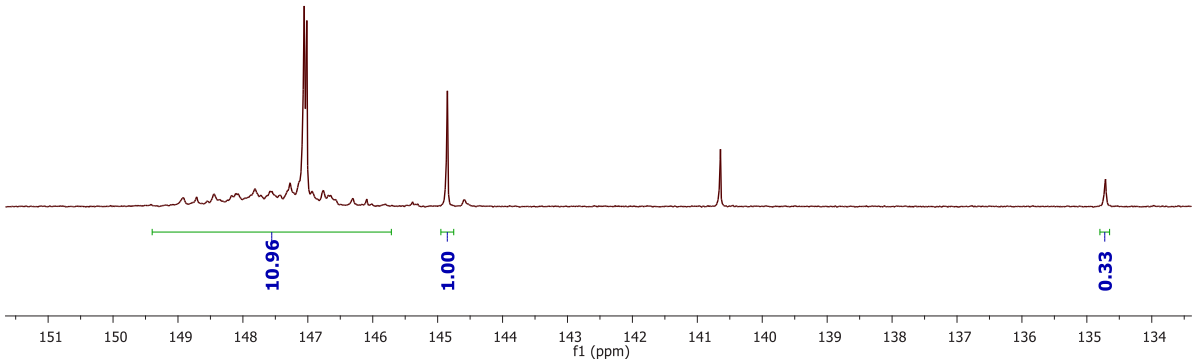

Figure SI 23: ^{31}P-NMR spectra of HASAH

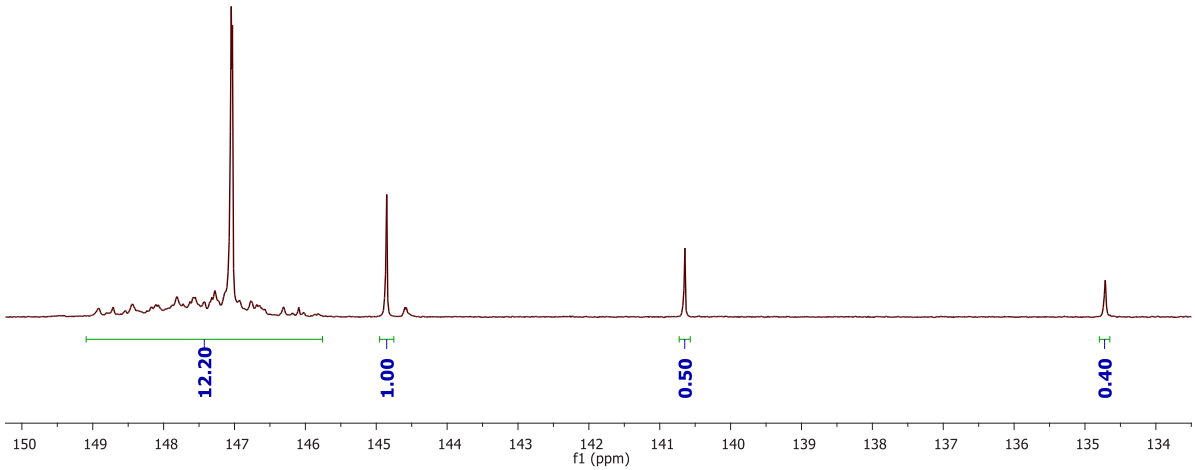

Figure SI 24: ^{31}P-NMR spectra of OASAO

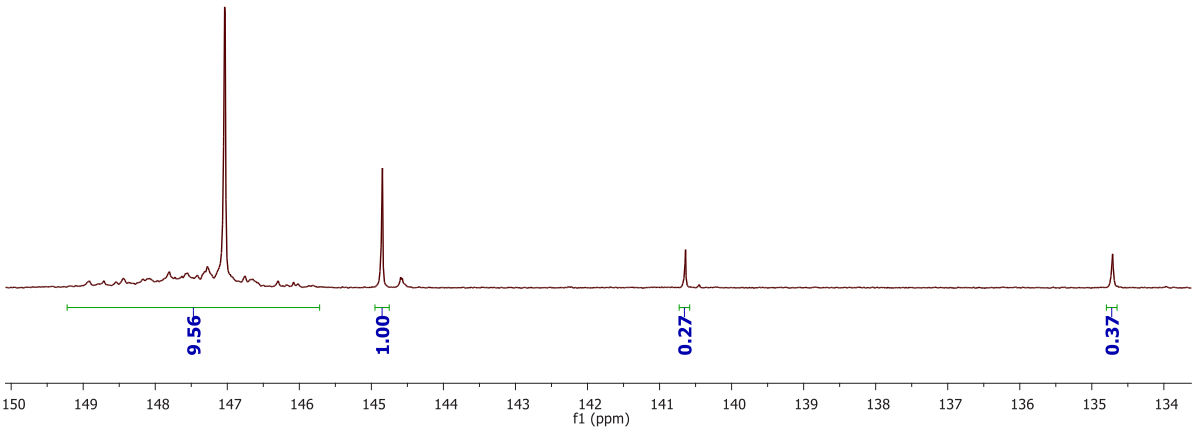

Figure SI 25: ^{31}P-NMR spectra of DASAD

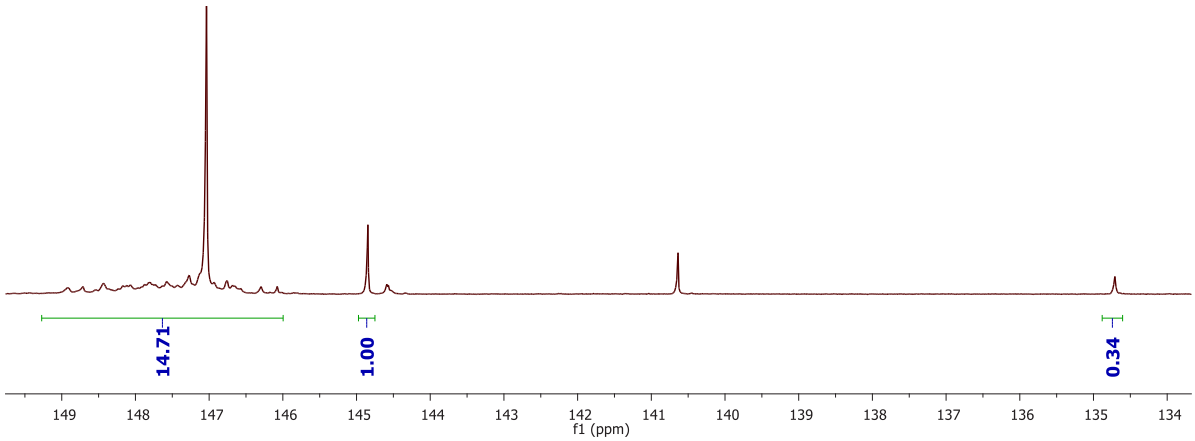

Figure SI 26: ^{31}P-NMR spectra of DoASADo

Table SI 6: Polyester polyol hydroxyl and carboxyl acid quantifications from ^{31}P-NMR integration

Polyester polyol designation	EASAE	PASAP	BASAB	HASAH	OASAO	DASAD	DoASADo
Total OH content (mmol/g)	10.37	11.21	10.23	9.03	8.24	7.84	8.7
COOH content (mmol/g)	0.6	0.4	0.88	0.33	0.40	0.22	0.2

BASAB and HASAH viscosity

Figure SI 27 shows BASAB and HASAH viscosity in function of the shear rate was measured at two different temperature i.e. 20 (solid line) and 25 °C (dash line).

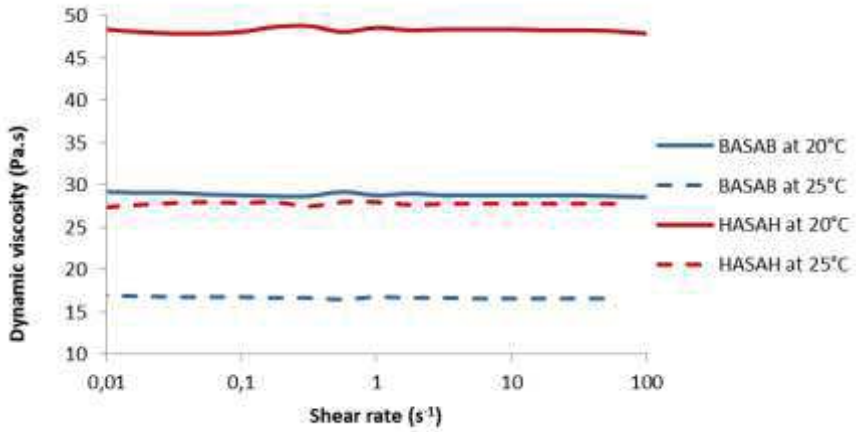

Figure SI 27: polyester polyols viscosity vs. the shear rate at 20°C and 25°C

BASAB thermal analysis

TGA and DTG of BASAB (Figure SI 28) indicates two steps degradation. First step is the evaporation of residual water and 1.4 BDO due to the global yield of 86%. Then the second degradation occurs and the weight loss derivative curve indicate a sequencing process, this is due to the different α and β scission of the different esters linkage present in the molecule.

BASAB DSC analysis (Figure SI 29) shows no thermal events from -10 to 150°C. Tg is not visible during the heating ramp due to unstable baseline however we can show it during the cooling just before baseline drops.

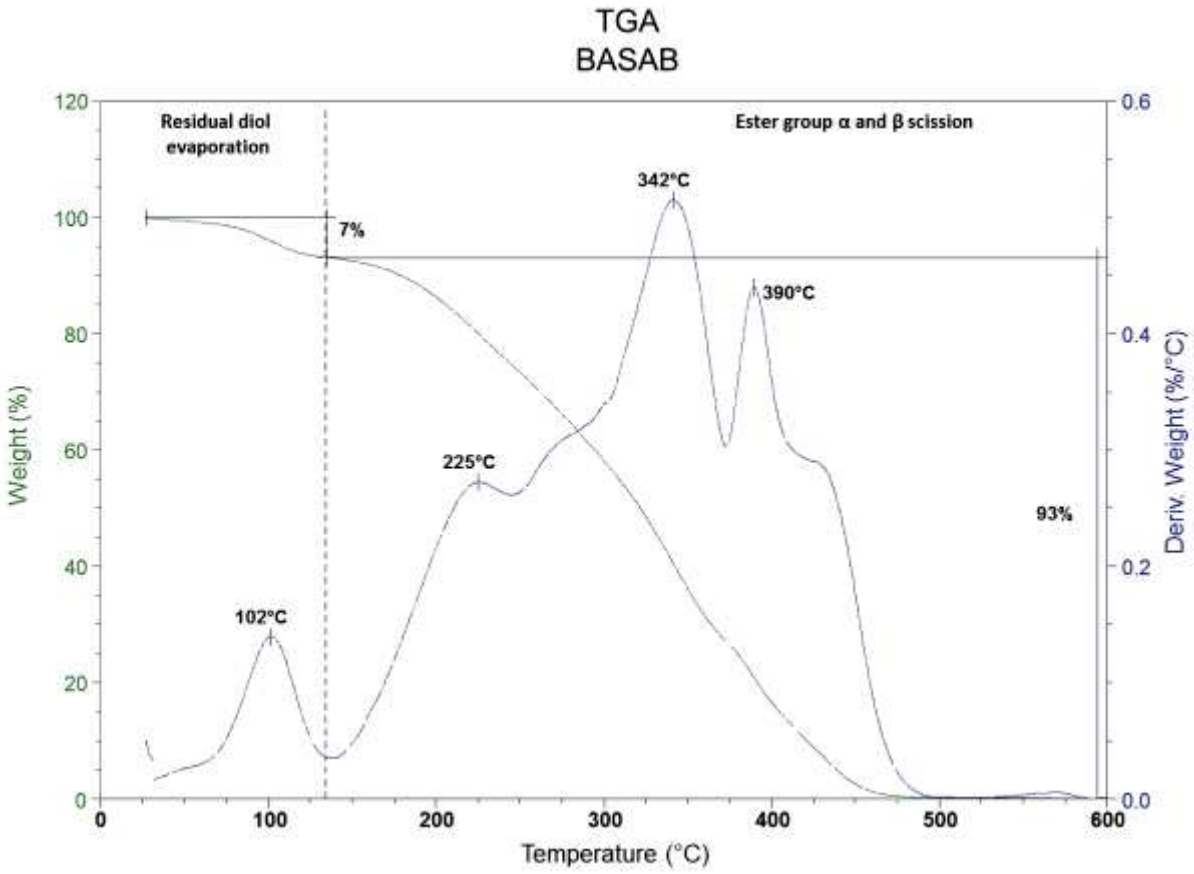

Figure SI 28: TGA and DTG of BASAB

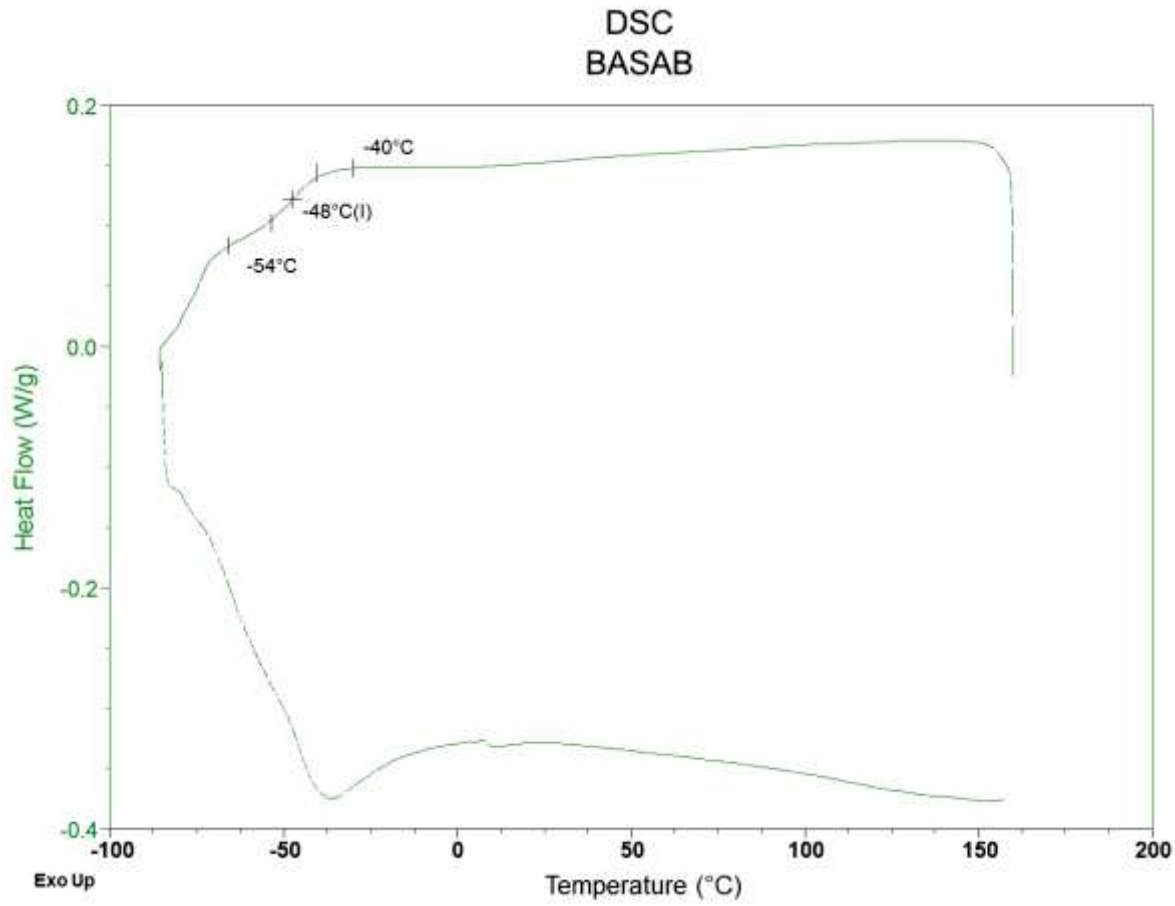

Figure SI 29: DSC of BASAB

Polyester α and β scissions mechanism

Figure SI 30: Polyester α-and β-scission mechanisms

Specific preliminary tests prior the foaming tests

To ensure a foaming process, all components of the foam must be compatible. It is mandatory that no phase separation occurs from the beginning to the end the foaming process. Before the addition of the polyisocyanate, an emulsion with all other constituent is performed. The entrapped air bubbles of the emulsion act on the cells nucleation and the foam growing process.

In a first approach, the surface tension of both BASAB and polyether-based polyols. Measurements were performed on a KRUSS DSA25 apparatus using the pending drop method. Polyols present similar surface tension of 40.0±0.8 and 39.8±2.3 for the BASAB and polyether polyol, respectively. These very close results are very promising for a good miscibility of both polyols.

Secondly, the stabilities of the emulsions of several components prior isocyanate addition were investigated. Emulsions were obtained by mixing all components together at the same stirring rate, as the one used in foams elaboration process. Three formulations containing (i) BASAB polyol, TCPP, surfactant (B84501), isopentane, (ii) polyether polyol, TCPP, surfactant (B84501), isopentane, (iii) BASAB/ polyether polyol (35/65, wt%/wt%), TCPP, surfactant (B84501), isopentane were prepared. No phase separation or notable aspect changes occur after 40h. This last value must be compared to the foaming process duration, which is less than 15 min. Stable emulsions is mandatory to ensure a good cell nucleation and a foaming growth. These emulsions proved the components miscibility to ensure a stable emulsion on agreement with the process.

Annexe 3: Supporting information de sous-Chapitre 2.2

BASAB polyol synthesis

A synthesis in two steps was performed in a 600 mL thermo-regulated reactor (Parr, model N°4568) equipped with a heating mantle, mechanical stirrer, a thermocouple, a Dean Stark apparatus and a gas inlet. The reactor was filed with one molar equivalent sorbitol and two molar equivalents of adipic acid. The mixture was heated to 150 °C for three hours under stirring. Then, the reactor was stopped and opened to add two molar equivalents of 1.4-butanediol. The reactor was relaunched and the second step was initiated to complete the reaction within 6 additional hours. The mix was purged under vacuum after 5 or 7 h during 1 or 2 min, to remove the produced water in order to increase the yield.

The extent of the reaction was determined from the residual acidic function present in the polyester polyol and the reaction global yield was 82%. It was calculated from ^{1}H-NMR according to equation SI.1 by comparing the intensity of hydroxyl protons in the alpha position (α) from an ester group and in α of an acid end-group at δ = 2.29 ppm and δ = 2.20 ppm, respectively.

$$Average\ acidic\ function = \frac{I_{2.2ppm}}{I_{2.29ppm}} \quad (SI.1)$$

Where $I_{2.2ppm}$ and $I_{2.29ppm}$ represent the integral of the corresponding signal.

BASAB structural characterization

The BASAB reactional intermediate (end of the first step) and the BASAB structures were determined by FT-IR, ^{1}H-NMR and ^{13}C-NMR. The reaction has been designed to obtain a linear intermediate such as sorbitol diadipate molecules. Then the second reactional step product, the BASAB, is a linear polyester polyol.

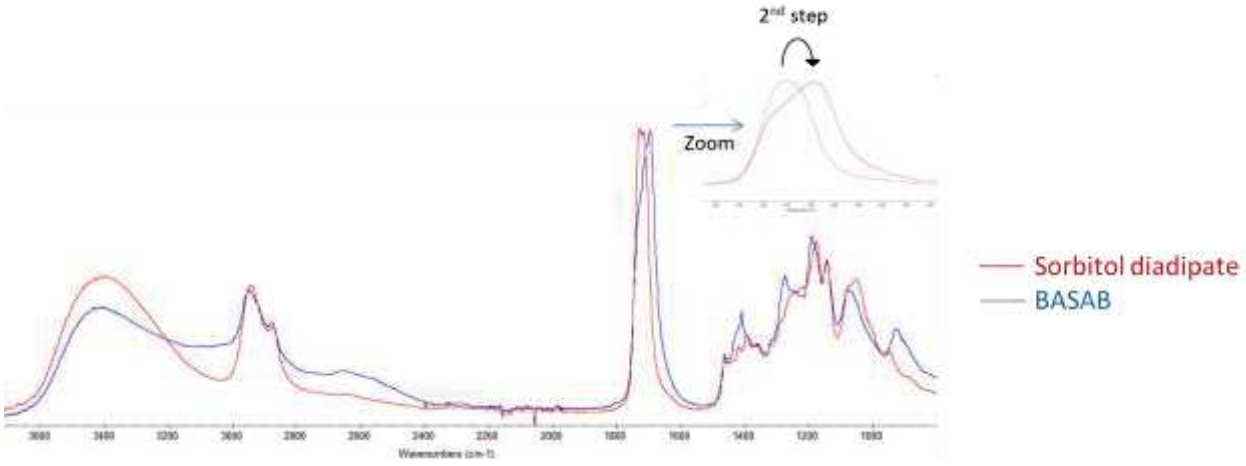

Figure SI 31: FT-IR spectra of the BASAB reactional intermediate and the BASAB polyester polyol

The FT-IR spectrum presented in Figure SI 31 of the BASAB intermediate product (red curve) obtained at the end of the first reactional step shows characteristic peak of the O-H stretching band at 3,400 cm^{-1}. The two signals at 2,948 and 2,877 cm^{-1} are related to the C-H symmetric and asymmetric stretching vibrations The strong peak at 1693 cm^{-1} is related to the C=O stretching band of the carboxylic acid. Additionally, the

C=O stretching band has a shoulder on the left side demonstrating the presence of C=O stretch from ester linkage between sorbitol and diacids. These signals are in agreement with a reactional product derived from sorbitol and adipic acid.

The FT-IR spectrum of the BASAB (blue curve) presented in Figure SI 31 is similar to the reactional intermediate FT-IR spectrum with the exception of the C=O band. The signal is now narrow and centered on 1,727 cm^{-1} corresponding to the C=O stretch of ester linkage. The FT-IR observations confirmed that the BASAB is a polyester polyol.

Figure SI 32 shows the ^{1}H-NMR spectra of the BASAB reactional intermediate, at the end of the first reaction step. Signal attribution and integration are in good agreement with the proposed structure of the reactional intermediate.

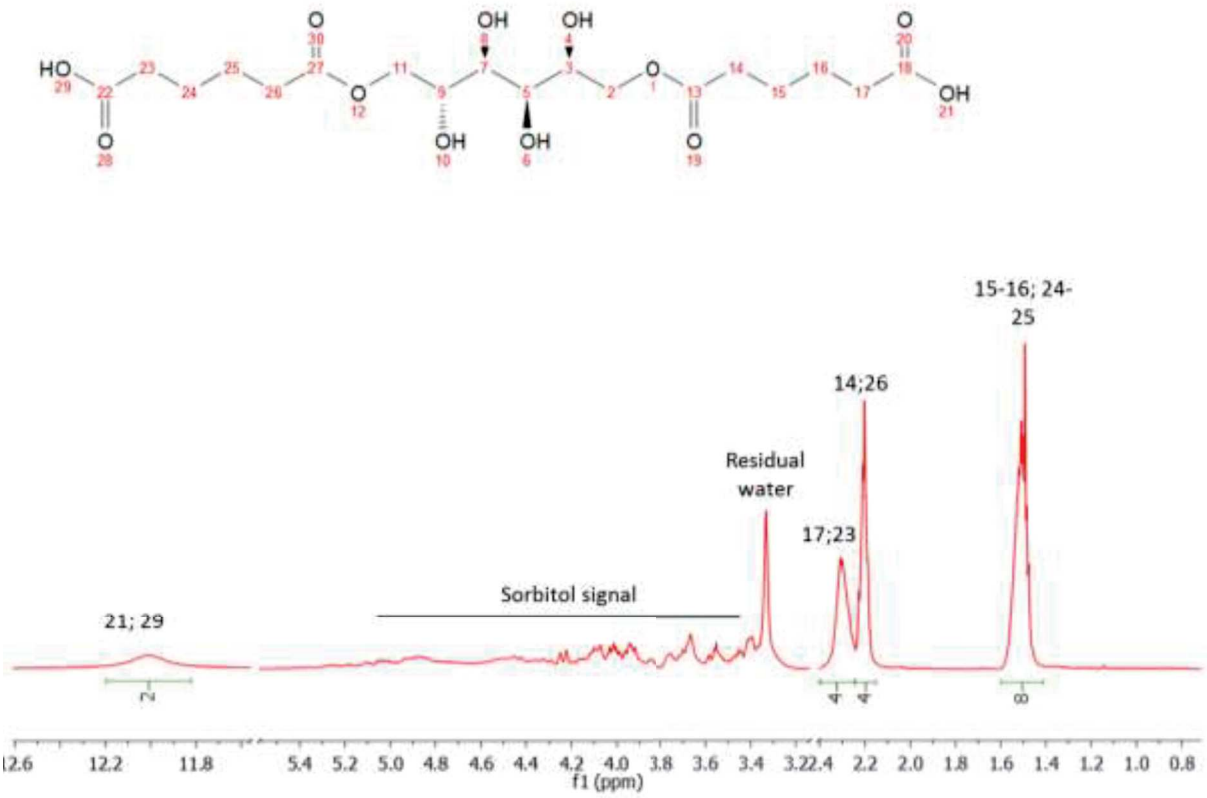

Figure SI 32: ^{1}H-NMR of the BASAB reactional intermediate

Figure SI 33 shows the ^{13}C-NMR of the BASAB reactional intermediate. Signals attribution confirmed the proposed structure. Only the sorbitol signal cannot be observed as it is really weak and closes to the baseline noise.

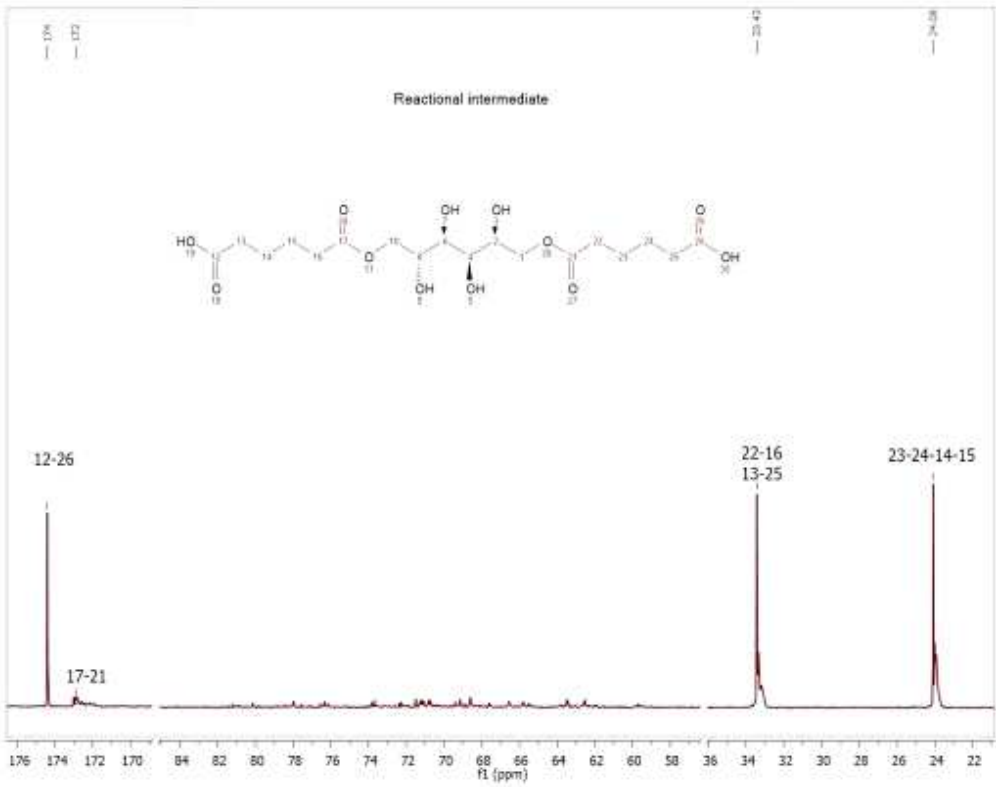

Figure SI 33 : ^{13}C-NMR spectra of the BASAB reactional intermediate

Figure SI 34 presented BASAB ^{1}H-NMR spectrum with the characteristic peak integration used to calculate the reaction extends.

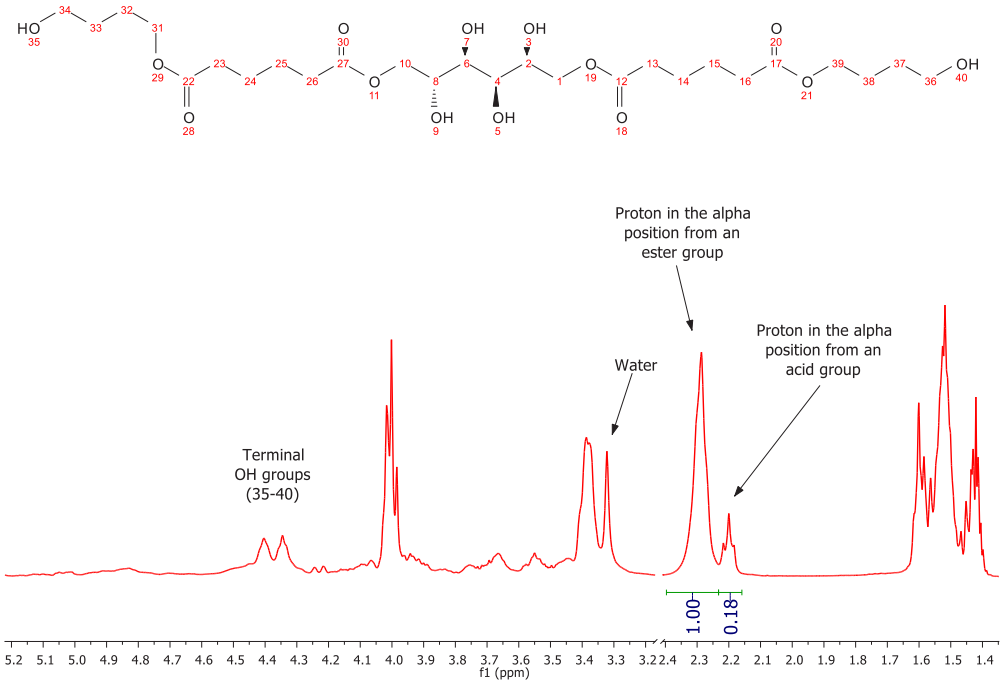

Figure SI 34: ^{1}H-NMR spectra of BASAB

Figure SI 35 shows the BASAB ^{13}C-NMR spectra. Regarding the number of peak and chemical shift, this spectrum is comforting the linear structure of the polyester polyol. All signals attributions are in good

agreement with the polyester polyol molecular structure. For ^{13}C-NMR analysis of BASAB polyester polyol the sorbitol signal was weak as previously observed on reactional intermediate ^{13}C-NMR.

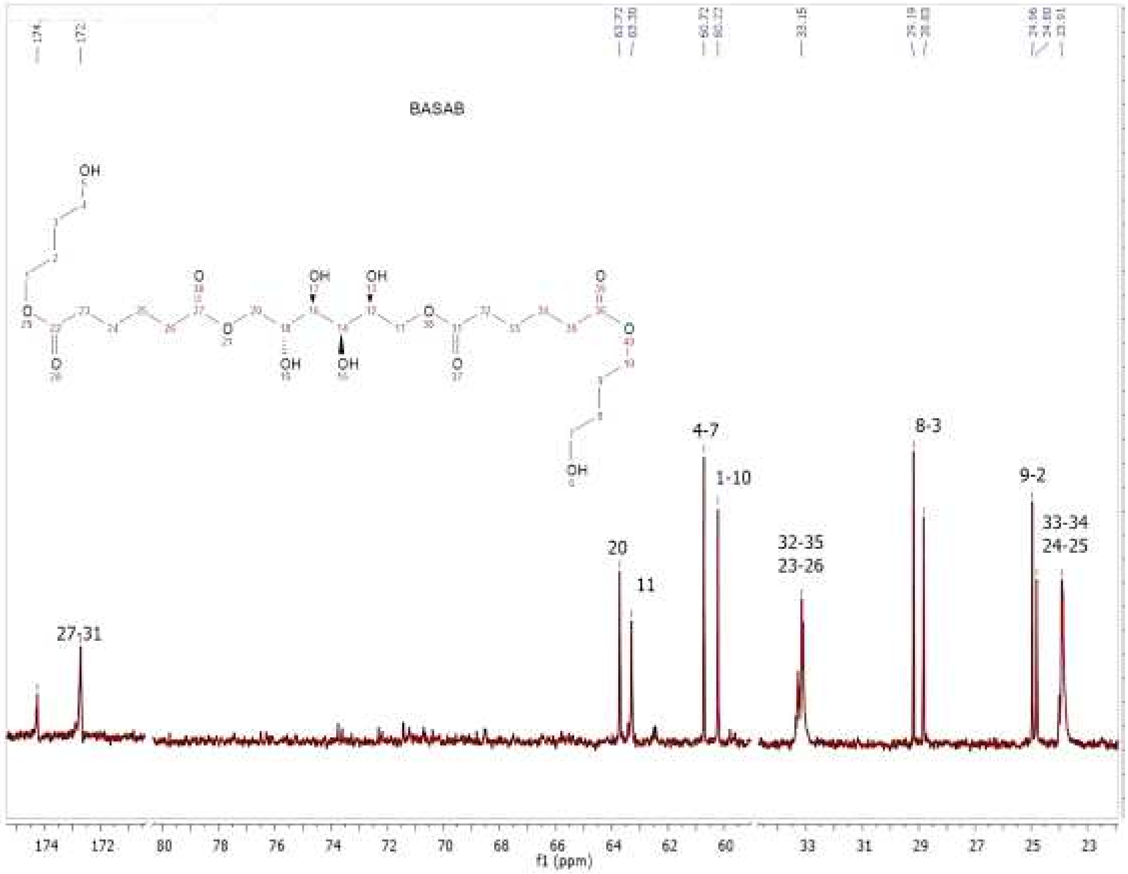

Figure SI 35: ^{13}C-NMR spectra of BASAB

Tomography images of the foams

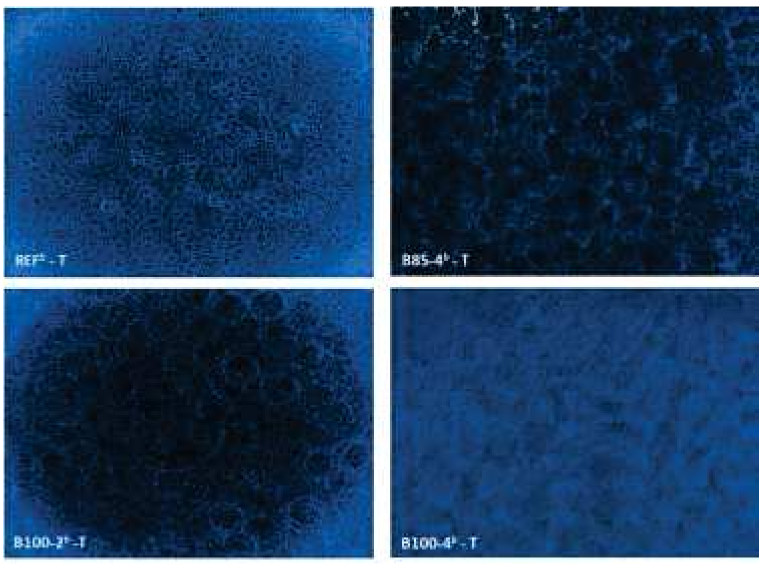

Figure SI 36: Foams tomography images in T direction of B85-4, REF, B100-4 and B100-2

Figure SI 36 gives the tomographic images of REF and biobased polyester-based foams. The cellular structure of the REF foam is composed of small grouped spherical cells, which indicates a highly structured foam with the presence of low porosity. The tomographic images of the biobased foams indicate spherical cells with an apparent diameter higher than REF. When 15 % of small polyols are added to the BASAB, the resulted foam microstructure displays a more complex structure. In the case of B85-4 foam, cells are uniformly distributed with various dimensions and a quasi polyedric shape. For B100-4 foam the porosity increases, leading to an increase of the open cells content. The tomographic image displays thus a very complex structure, with non-homogeneous shapes and sizes in agreement with SEM images.

Annexe 4: Supporting information de Chapitre 3

Hansen solubility parameters

A small quantity (around 100 mg) of polyol was poured into a 5 mL vial which was then filled up with a solvent. Vials were placed in an ultrasonic bath for 1h, and then polyols solubility was visually evaluated 3h later and confirmed after 24h. The corresponding results (soluble or insoluble) were collected. The Hansen solubility parameters and the predicted compatibility of both polyols were determined by modeling their solubility sphere with HSPiP software (HSPiP, V.5.0.06).

Table SI.1 displays the list of used solvents and their three Hansen parameters (i) dispersion parameter (δ_d), (i) polar parameter (δ_p) and (iii) hydrogen bonding parameter (δ_h). These parameters were used to determine a solubility sphere. The solubility score expresses the polyol solubility into the solvent (score of 0 or 1, Table SI-1) When the polyol is insoluble or partially soluble the resulting score is 0.

Table SI 7: detailed used solvents for solubility sphere modeling and their Hansen parameters associated with BASAB and PS 2412 solubility score

Solvent	δ_d	δ_p	δ_h	Solubility score	
				Fossil polyol	BASAB
Dimethyl Sulfoxide (DMSO)	18.4	16.4	10.2	1	1
Tetrahydrofuran (THF)	16.8	5.7	8.0	1	0
Dimethyl Formamide (DMF)	17.4	13.7	11.3	1	1
p-Xylene	17.8	1.0	3.1	0	1
Toluene	18.0	1.4	2.0	0	0
Pyridine	19.0	8.8	5.9	1	1
Chloroform	17.8	3.1	5.7	1	0
Methylene Dichloride (Dichloromethane)	17.0	7.3	7.1	1	0
Ethyl Acetate	15.8	5.3	7.2	1	0
Acetone	15.5	10.4	7.0	1	0
Ethanol	15.8	8.8	19.4	1	1
2-Propanol	15.8	6.1	16.4	0	0
Acetic Acid	14.5	8.0	13.5	1	1
Acetonitrile	15.3	18.0	6.1	1	0
1,4-Dioxane	17.5	1.8	9.0	1	0

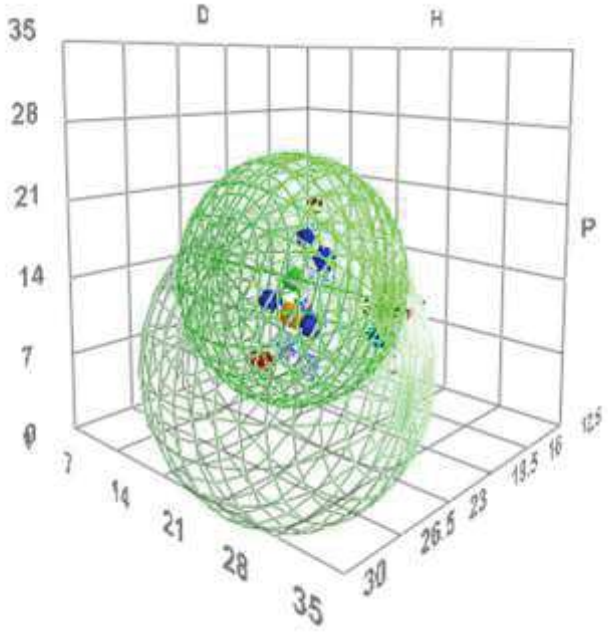

Figure SI 37 : HSPiP modeled solubility spheres of fossil-based (green wire frame sphere) and BASAB (grey wire frame sphere) polyol based on Hansen solubility parameters

Characteristic times of different foams

Figure SI 38 presents the evolution of the foam cream, gel and tack free times a function of the biobased polyester polyol content. Foams REF, PU-90/10/0-KE, PU-75/25/0-KE, PU65/35/0-KE, PU-55/45/0-KE, PU-45/55/0-KE and PU-35/65/0-KE are plotted on the Figure SI 38 corresponding to a content of biobased polyol of 0, 10, 25, 35, 45, 55, or 65% respectively.

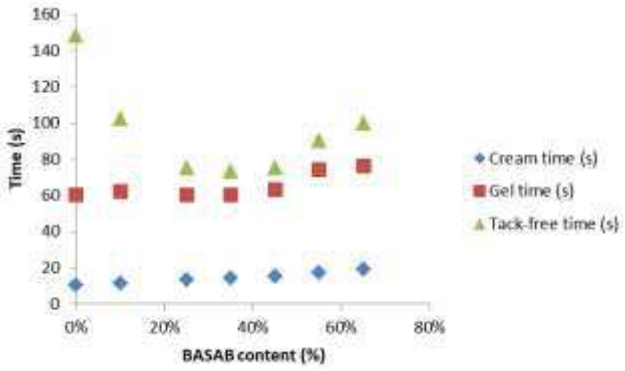

Figure SI 38: foams evolution of the cream, gel and tack free times vs. the biobased polyester polyol content

Foams morphologies and cells diameter distributions

Figure SI 39 shows SEM images of PUIR foams, in both transversal and longitudinal directions to the foam rise. In great agreement with the cell size distribution presented in Figure SI 40, SEM images clearly illustrate the cell size decrease, compared to REF for foams presenting a substitution ratio of 10 to 45 %. The opposite trend is observed for foams PU-45/55/0-KE, PU-35/65/0-KE, PU-0/85/15-KE and PU-0/85/15-KP.

Figure SI 40 presents the cells diameter size distribution in the four possible directions (maximal and minimal diameters in transverse and longitudinal directions) for formulated PUIR foams, according to a normal law. These curves were obtained by measuring a minimum average number of one hundred cells per foam in longitudinal and transversal directions, respectively. The cells diameter sizes decrease compared to REF for foams PU-90/10/0-KE to PU-55/45/0-KE with a narrower distribution. Other foams formulations presented higher cells diameters and wider distributions. These observations are in agreement with previous SEM images.

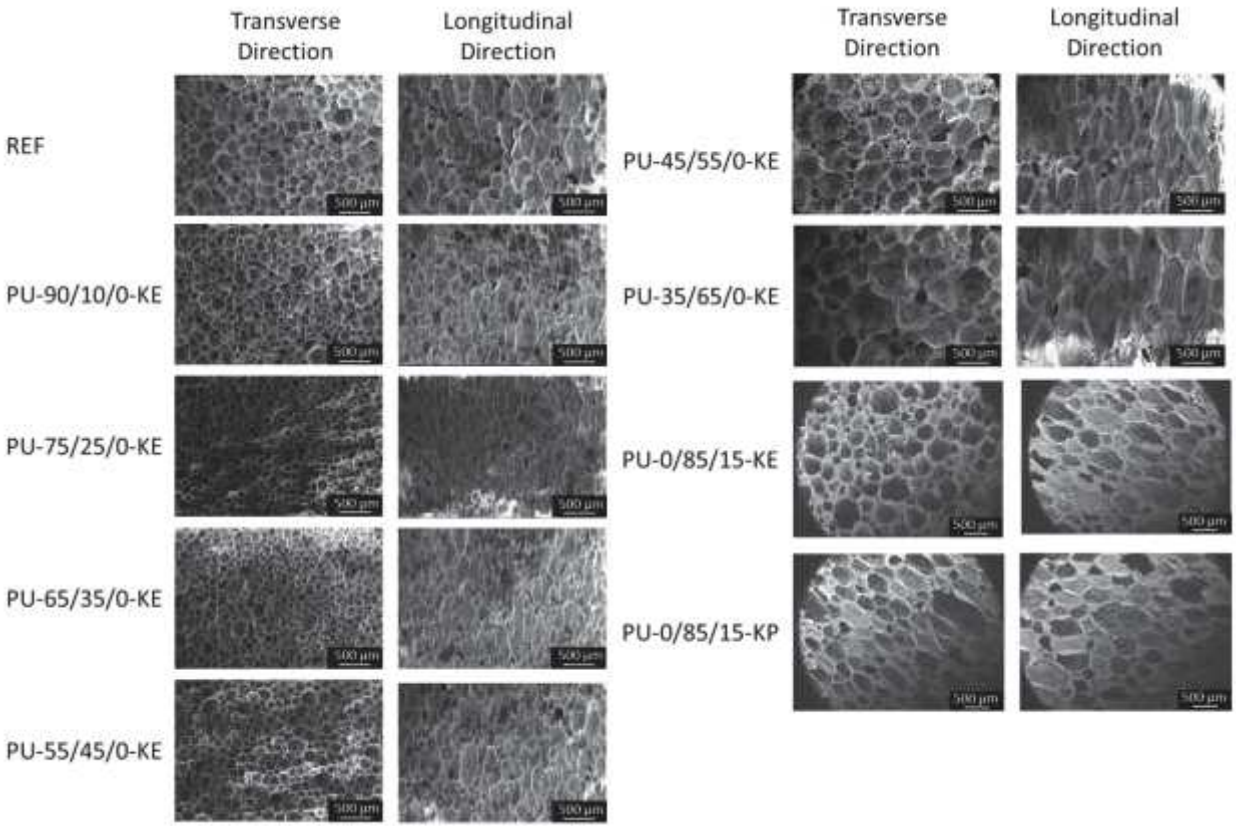

Figure SI 39: PUIR foams SEM images, magnify x40 (scales are given) of all formulations

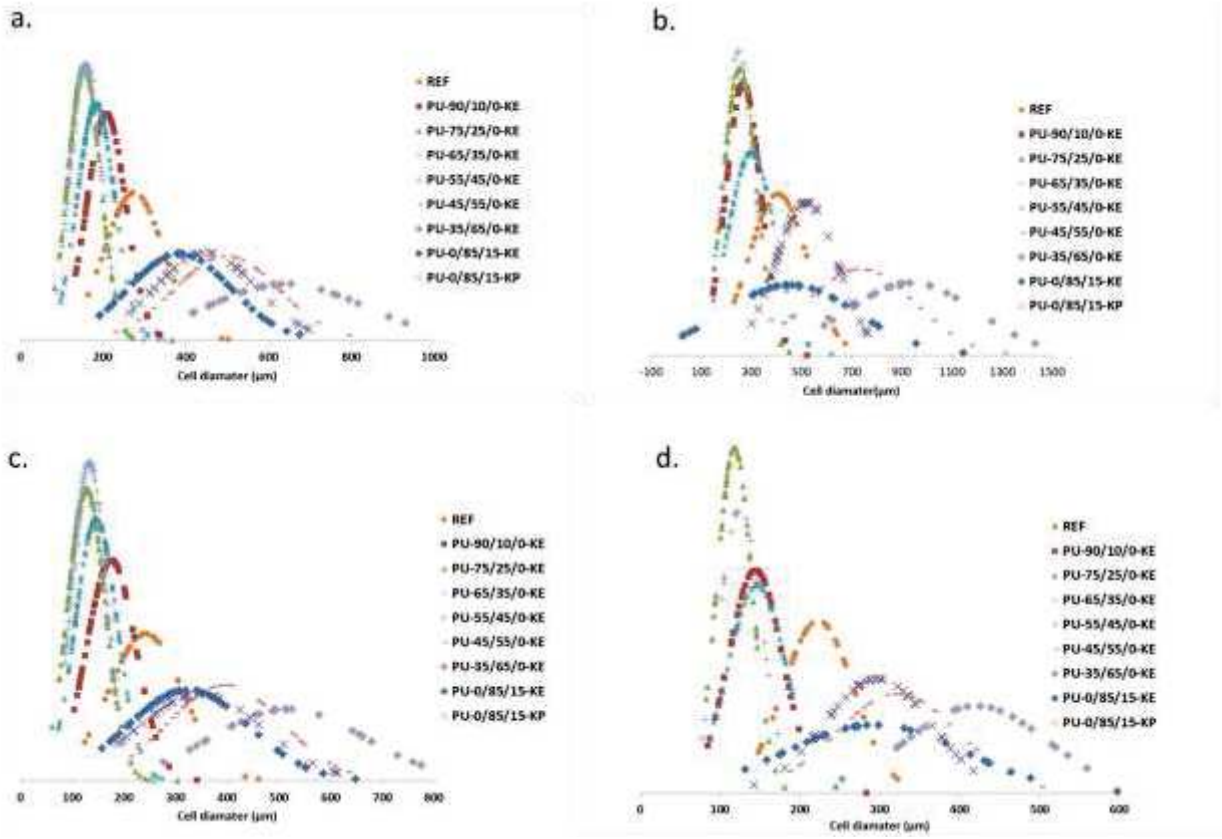

Figure SI 40: All PUIR foams cells diameters, a. minimal diameter distribution in the transversal direction, b. maximal diameter distribution in the transversal direction, c. minimal diameter distribution in the longitudinal direction, d. maximal diameter distribution in the longitudinal direction

Shore 00 hardness of foams

Table SI 8: PUIR foams Shore 00 Hardness results

	REF	PU-90/10/0-KE	PU-75/25/0-KE	PU-65/35/0-KE	PU-55/45/0-KE	PU-45/55/0-KE	PU-35/65/0-KE	PU-0/85/15-KE	PU-0/85/15-KP
Shore 00 hardness	72 ± 3	71 ± 3	71 ± 4	73 ± 2	65 ± 3	56 ± 2	43 ± 9	n.d	n.d

n.d. = not determined

Foams FTIR analysis

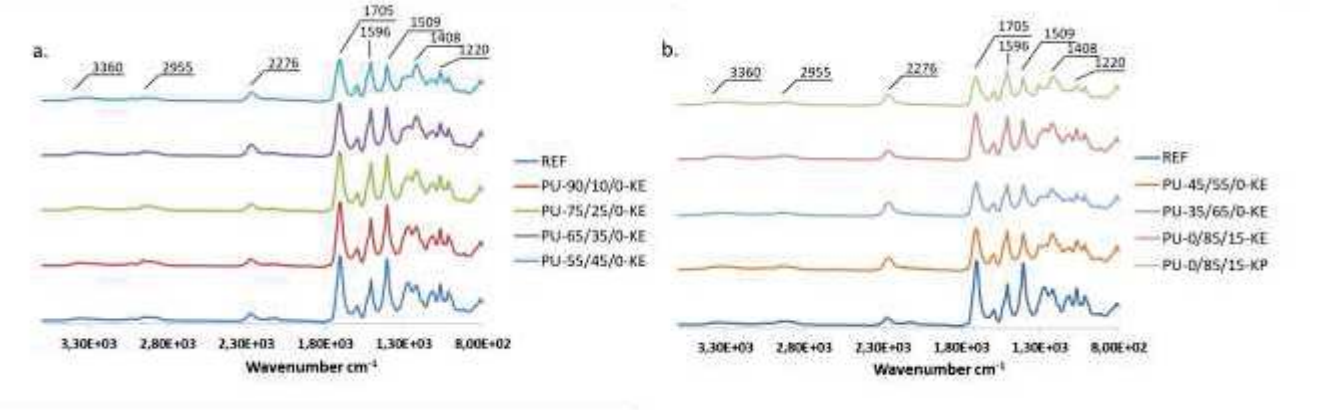

Figure SI 41: FTIR spectra of: a. REF, PU-90/10/0-KE, PU-75/25/0-KE,PU-65/35/0-KE, PU-55/45/0-KE; b. Reference, PU-45/55/0-KE,PU-65/35/0-KE, PU-0/85/15-KE , PU-0/85/15-KP foams

TGA analysis of foams

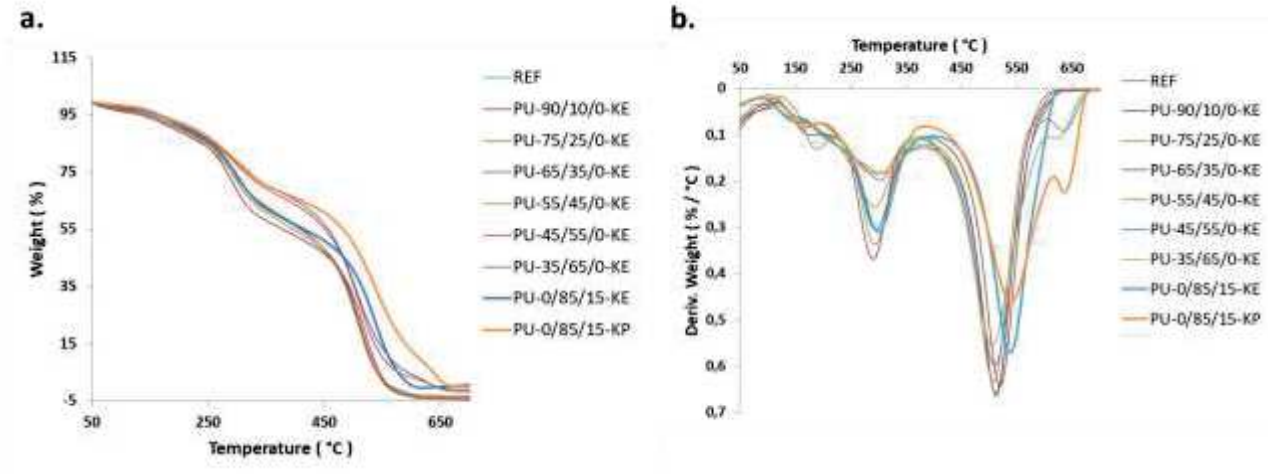

Figure SI 42: PIR foams a. TGA curves, under dry air; b. DTGA curves, under dry air

Flammability test results

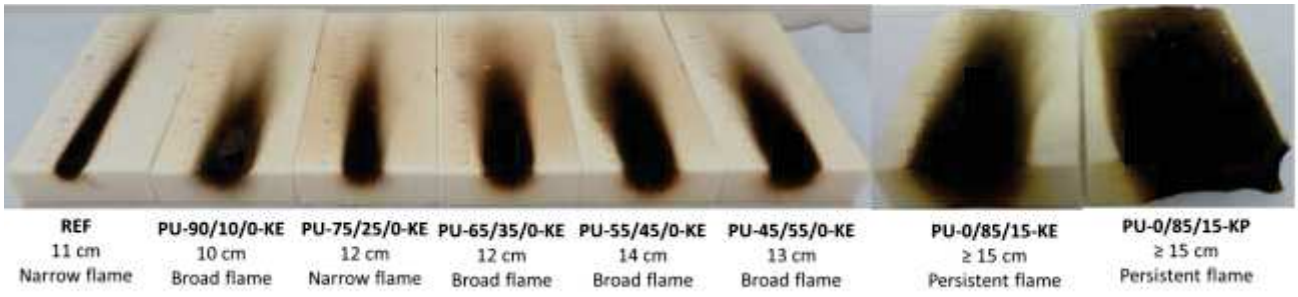

Figure SI 43: All formulated PUIR foams flammability results

Foams Young modulus evolution

By fitting the young's modulus in longitudinal and transversal directions as function of BASAB content, it was observed that Young's modulus evolution can be described by a 3D polynomial fit. (Figure SI 44). This

evolution is in agreement with the scale low established by Gibson and Ashby(Gibson et al., 1989; Gibson and Ashby, 1997) to describe the relative density as function of the ratio between the average cell walls and cell diameters. E_{longi} and E_{transv} are the longitudinal and traversal moduli respectively, and C_{polyol} the polyol concentration, those evolutions can be given by the following equations 1 and 2:

$$E_{Longi} = 0.72\,C^3{}_{polyol} - 0.026\,C^2{}_{polyol} + 2.34E-4\,C_{polyol} + 7.01 \quad (1)$$

$$E_{Transv} = 0.19\,C^3{}_{polyol} - 0.006\,C^2{}_{polyol} + 5.40E-5\,C_{polyol} + 0.23 \quad (2)$$

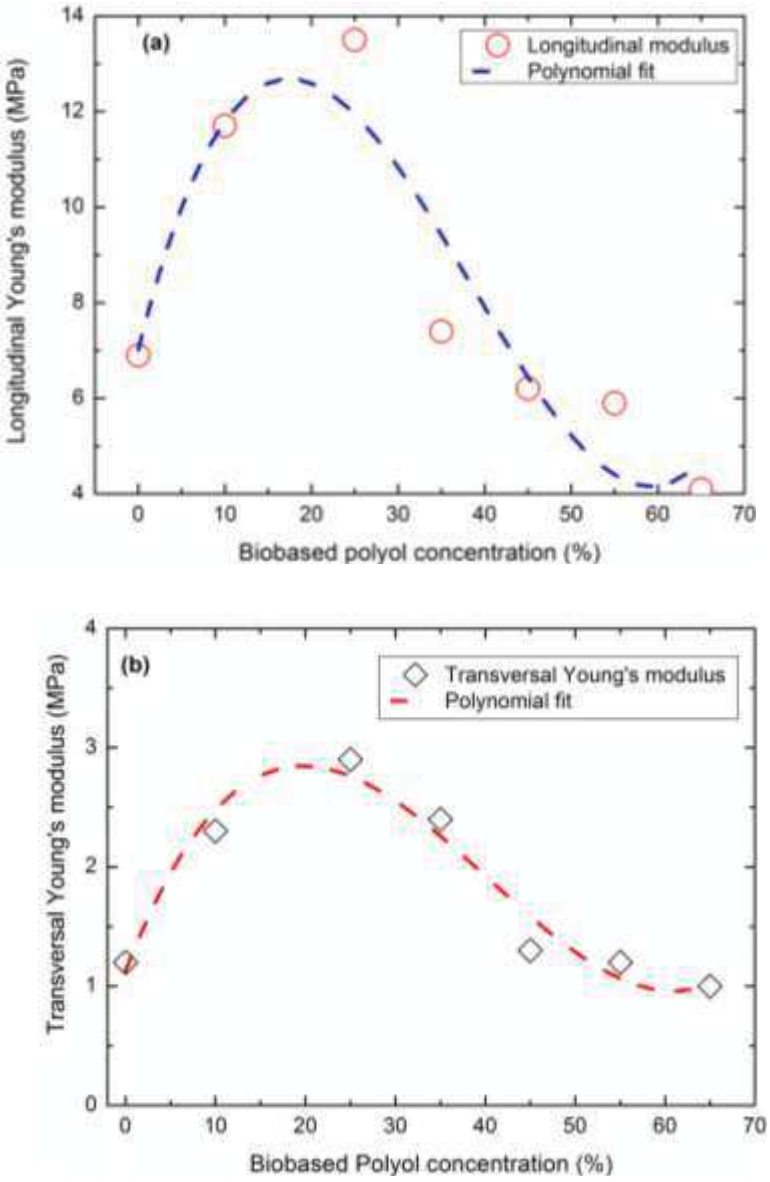

Figure SI 44: Longitudinal and transversal Young's modulus evolution as function of biobased polyol concentration

References

Gibson, L.J., Ashby, M.F., 1997. Cellular Solids: Structure and Properties, Cambridge Solid State Science Series. Cambridge University Press.

Gibson, L.J., Ashby, M.F., Zhang, J., Triantafillou, T.C., 1989. Int. J. Mech. Sci. 31, 635–663.

Annexe 5 : Supporting information de Chapitre 4

BisCC analysis

This section is dedicated to the BisCC characterization. Figure SI 45-46 present the FT-IR spectrum and DSC thermogram of the synthesized BisCC. Figure SI 47 show ^{1}H-NMR and ^{13}C-NMR spectra with the signals attribution linked with the chemical structure.

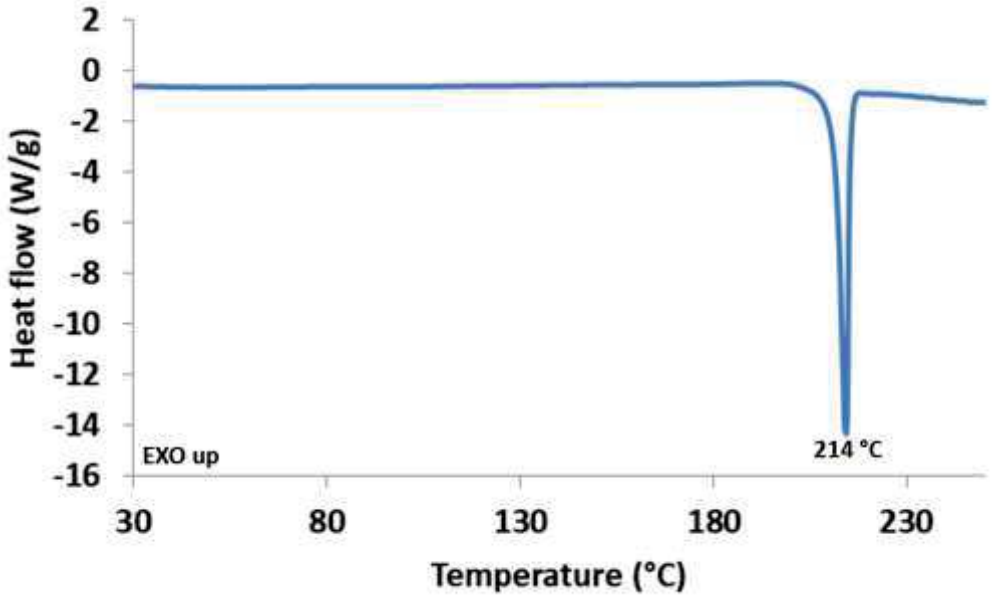

Figure SI 45: DSC analysis of the D-sorbitol-based BisCC

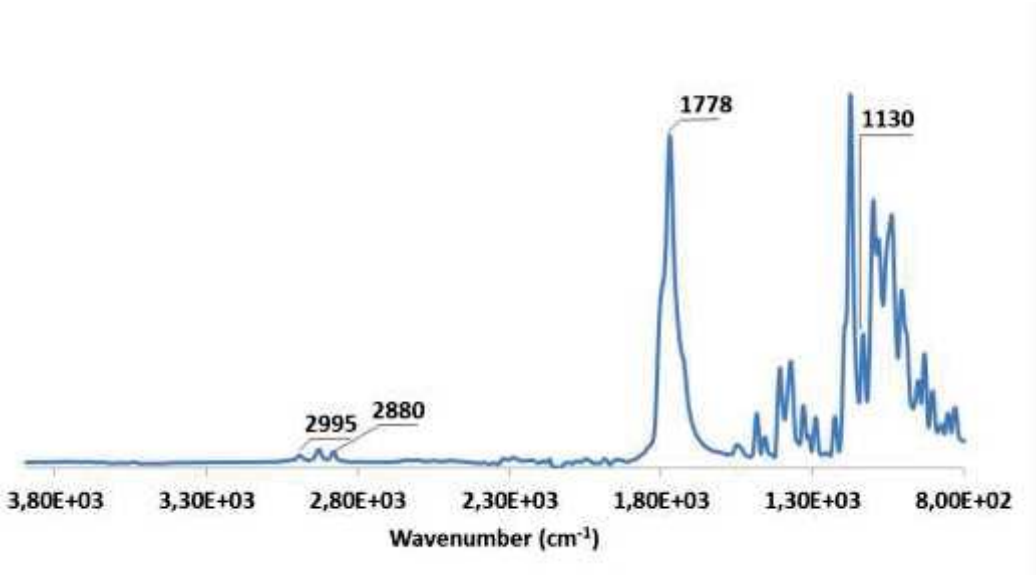

Figure SI 46: FT-IR analysis of the D-sorbitol-based BisCC

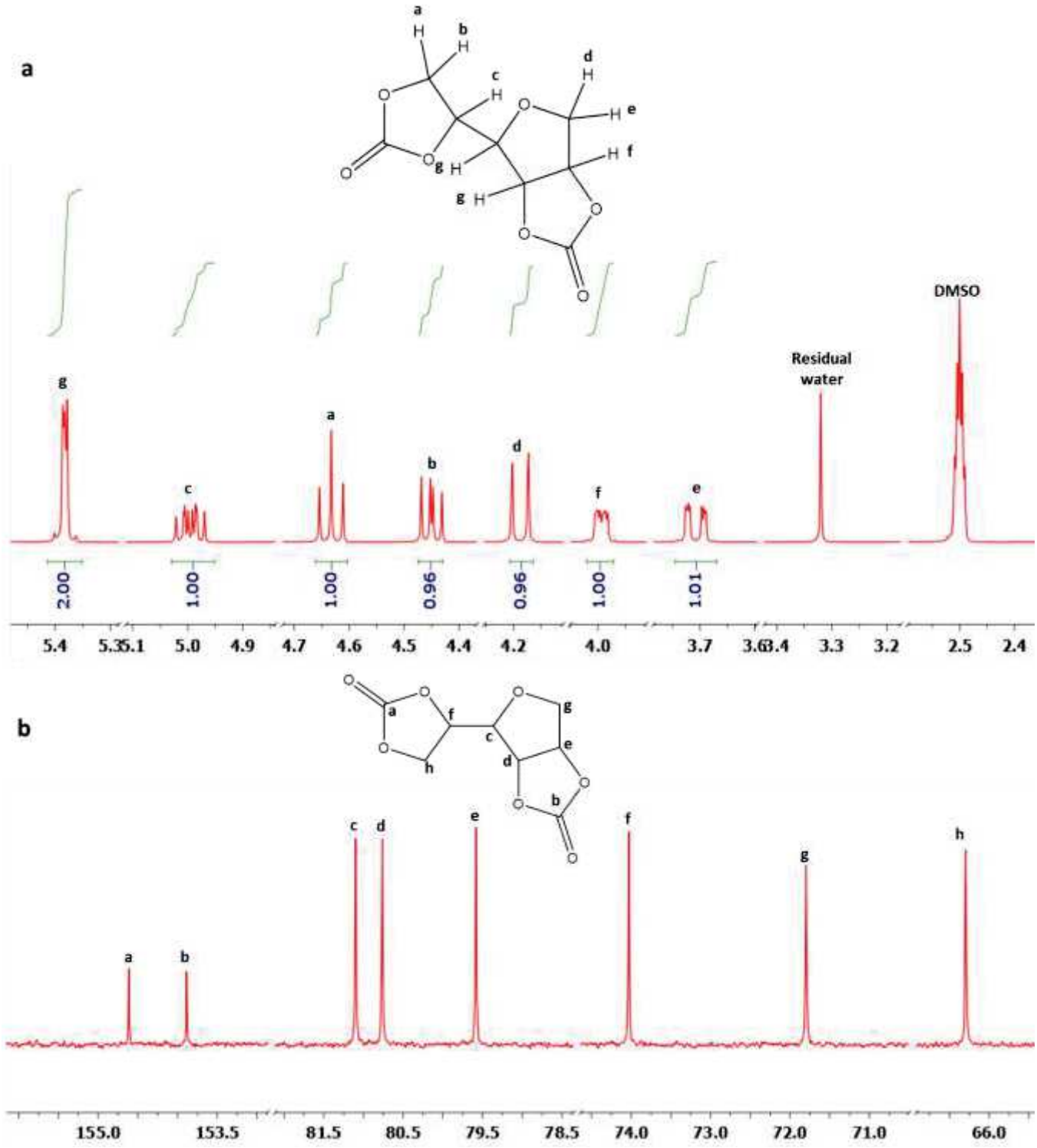

Figure SI 47 (a) ^{1}H-NMR spectrum and (b) ^{13}C-NMR spectrum of sorbitol-based BisCC

[1]H-NMR spectra

This section is dedicated to [1]H- NMR spectra of cis-1,2-cyclopentanediol, (±)-trans-1,2-cyclopentanediol and the products obtained after reaction with DMC and TBD. [1]H- NMR spectrum of the distillated product from the reaction between sorbitol and DMC (TBD catalyzed) is also available.

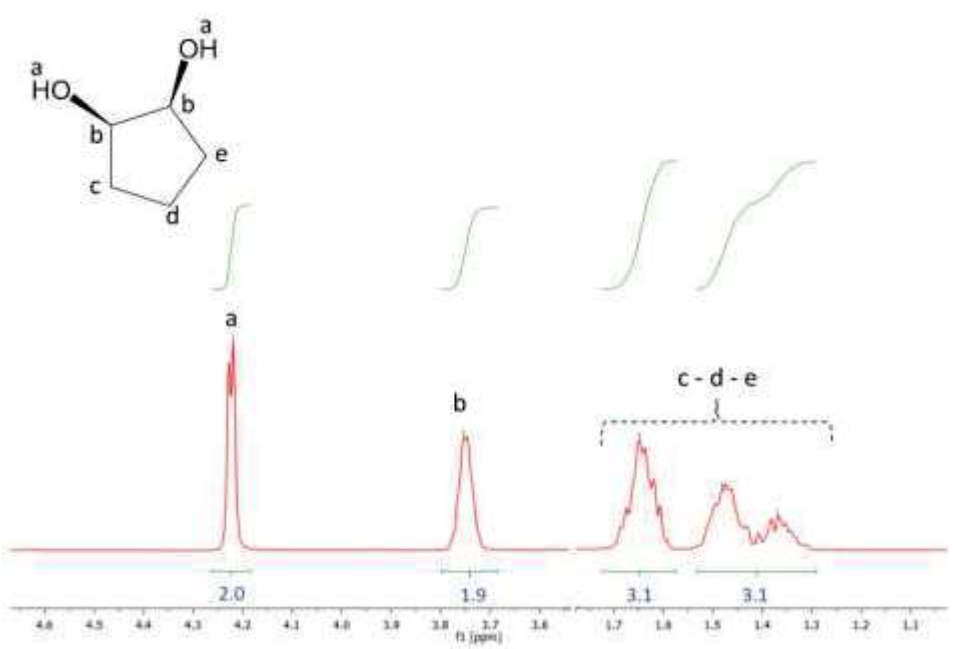

Figure SI 48: [1]H-NMR cis-1,2-cyclopentanediol before the reaction with dimethyl carbonate

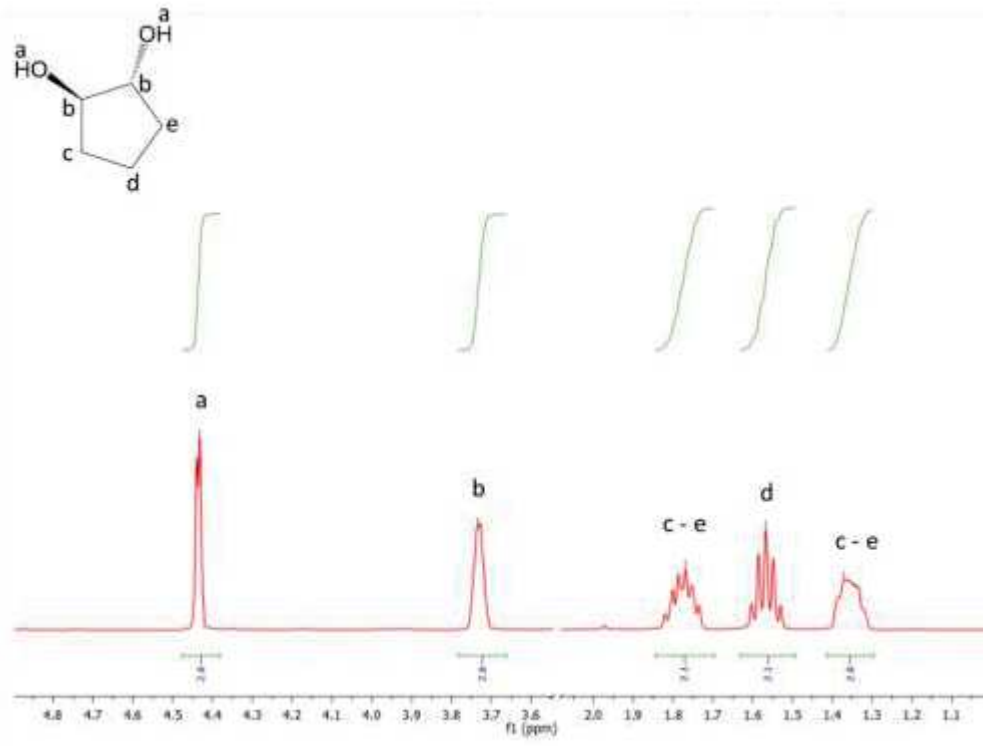

Figure SI 49: [1]H-NMR trans-1,2-cyclopentanediol before the reaction with DMC

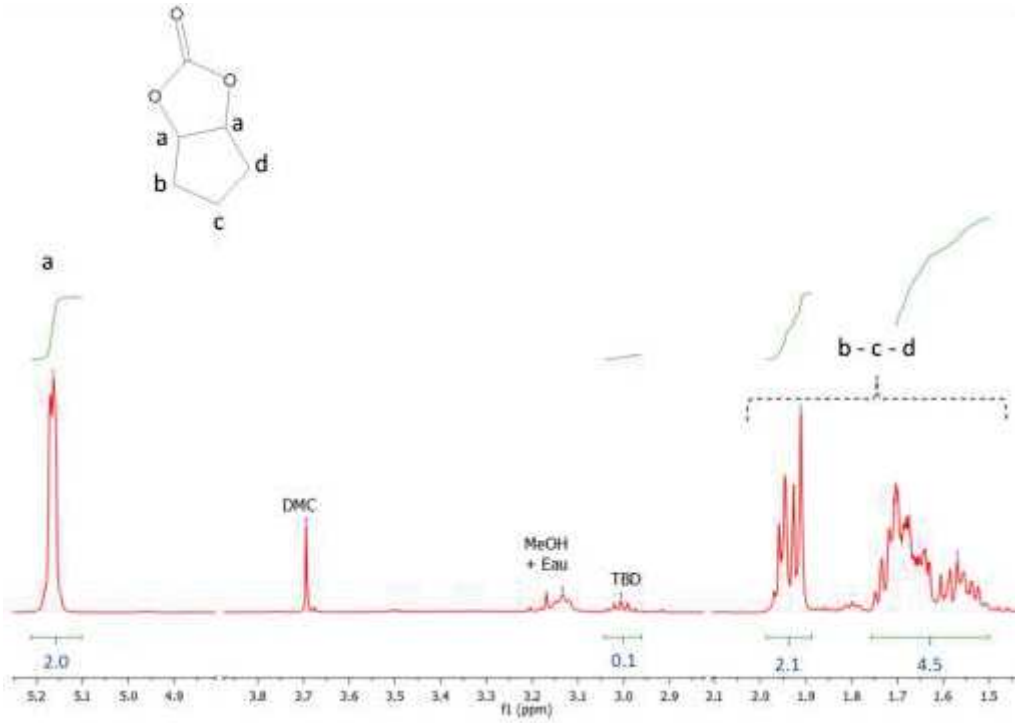

Figure SI 50: [1]H-NMR cis-1,2-cyclopentanediol after the reaction with DMC

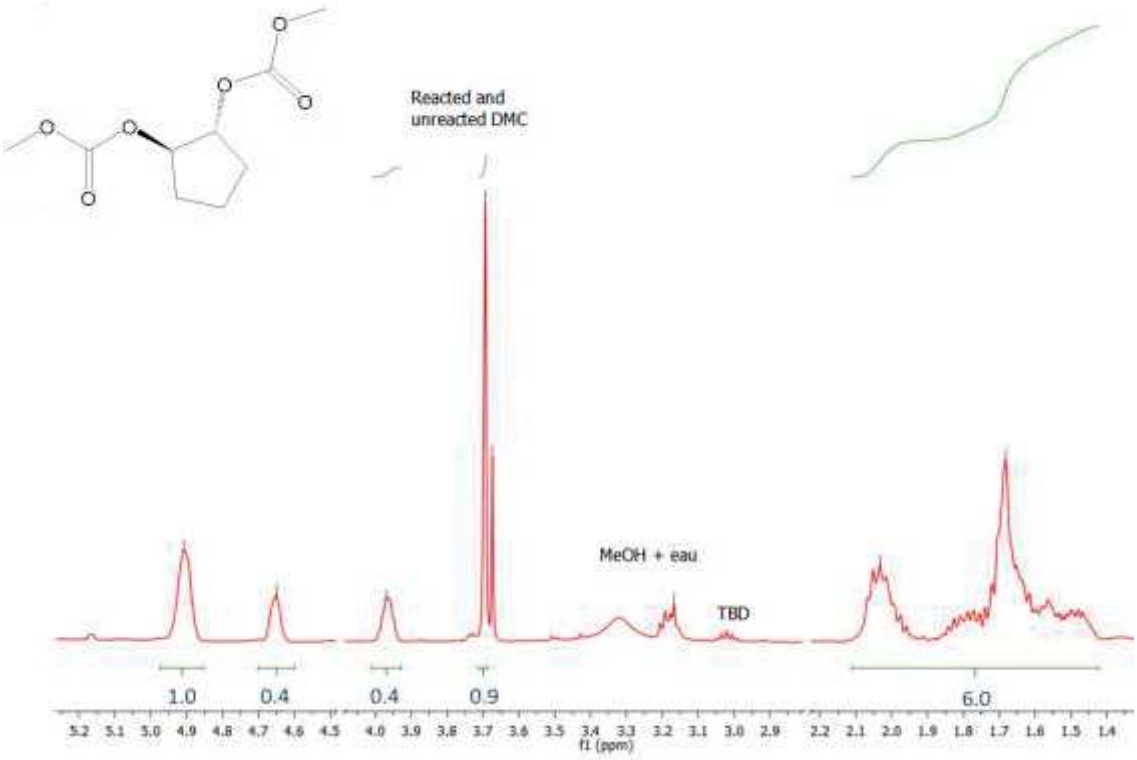

Figure SI 51: [1]H-NMR trans-1,2-cyclopentanediol after the reaction with DMC

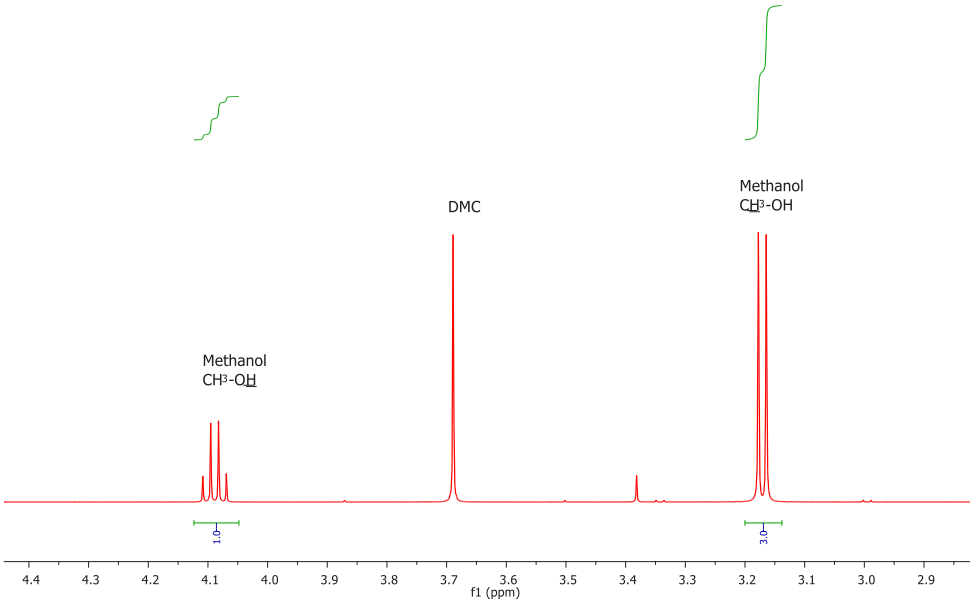

Figure SI 52: ^{1}H-NMR of distillated subsidiary products of the catalyzed reaction between D-sorbitol and DMC

Relationship betwen D-BisCC yield and the reactional device

To compensate the effect of DMC loss with the azeotrope, two different options can be developed:

(i) The first option was to increase the initial quantity of DMC. Nevertheless, 5eq. of DMC (Table 4.3, entry 13) seems to give a yield optimum (40%).

(ii) The second option was to use a reflux system to condensate the evaporated reactant or a vigreux fractionating column to break the azeotrope. Both options were studied (Table 4.3, Entry 15-16).

It appears that reflux device was not suitable as the yield is low (10% against 15% with the vigreux fractionating column). In similar condition with distillation bridge (Table 4.3, Entry 10), a yield of 22% was obtained. With the vigreux fractionating column, the number of equivalents of DMC was increased to 5, 7 and 9eq., respectively (Table 4.3, Entries 17-19). The reaction time was increased up to 48 h with 9eq. DMC. Final corresponding yields were 14, 36 and 45%, respectively. Reactions were pushed to 12 and 18 eq. of DMC and a distillation vigreux columns (Table 4.3, Entries 20-22). However, the increased of DMC yield in high amount of by-products. The recovered D-BisCC was not pure after the recovery in water. The main explanation linked to this result was that the high availability of DMC in the media promotes the synthesis of ‘’branched D-sorbitol’’ with linear carbonates instead of carbonate cyclization reactions.

Study of the potential products obtained from the reaction between BIsCC and 1,8-octanediol

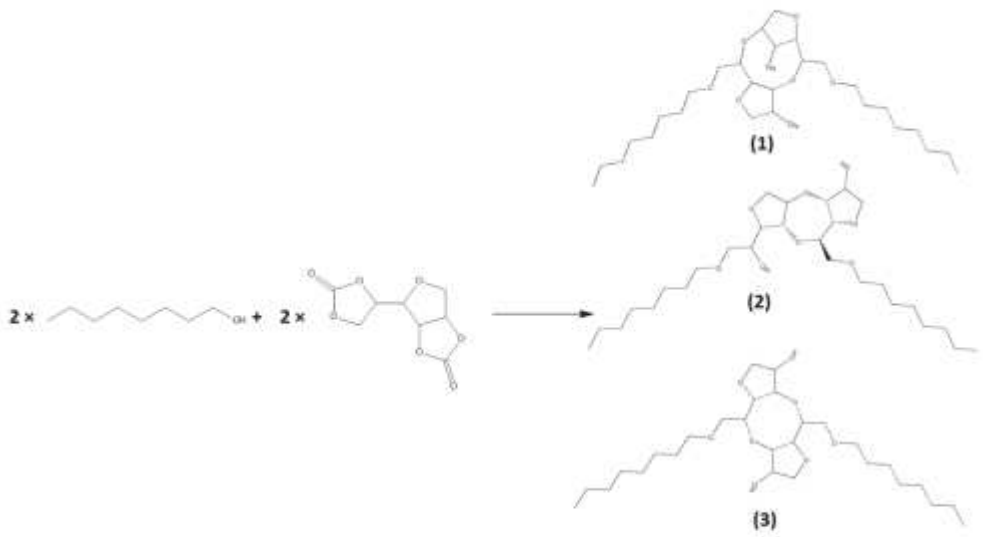

Figure SI 53: Theoretical reactional product one mole of BisCC with two moles of 1-octanol.

SEC analysis

The SEC analyses of the soluble macromolecules after an acetylation step are presented in this section.

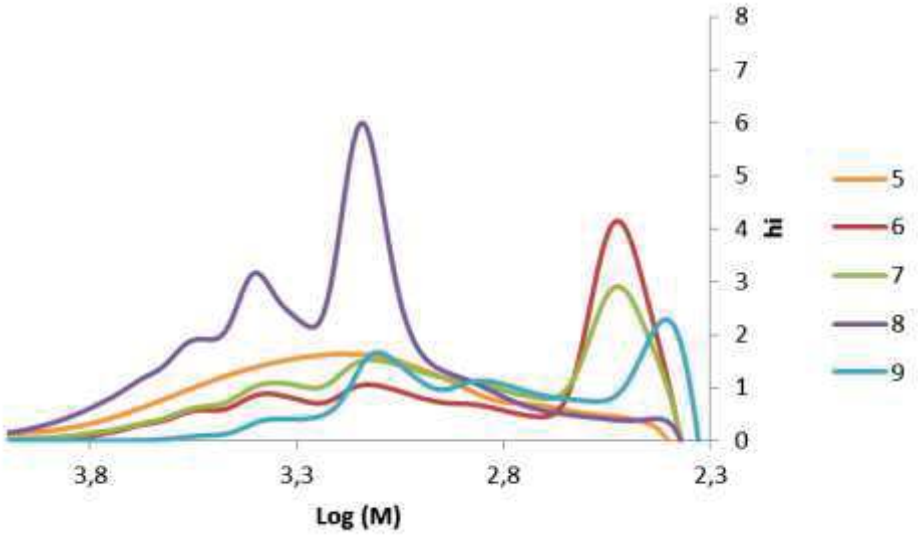

Figure SI 54: SEC curves of macromolecules products Entries 5 to 9 (Table 6)

31P-NMR of ROP products between D-sorbitol and 1,8-octanol

The targeted areas of ^{31}P-NMR spectrum were based on the signal at 132.2 ppm corresponding to environmental water, the standards signal at 144.85 ppm (cholesterol, 1 mol/L), carboxylic acid area at 134-135.5 ppm and hydroxyl area at 149-141.5 ppm. We also notice a small unexpected peak at 140.6 ppm, which comes (after several investigations) from the molecular sieves used for the solvent storage.

Figure SI 55 presents ^{31}P-NMR spectra of oligomer Entries 5 to 9 (Table 4.8) with the integration of the characteristic signals for quantification.

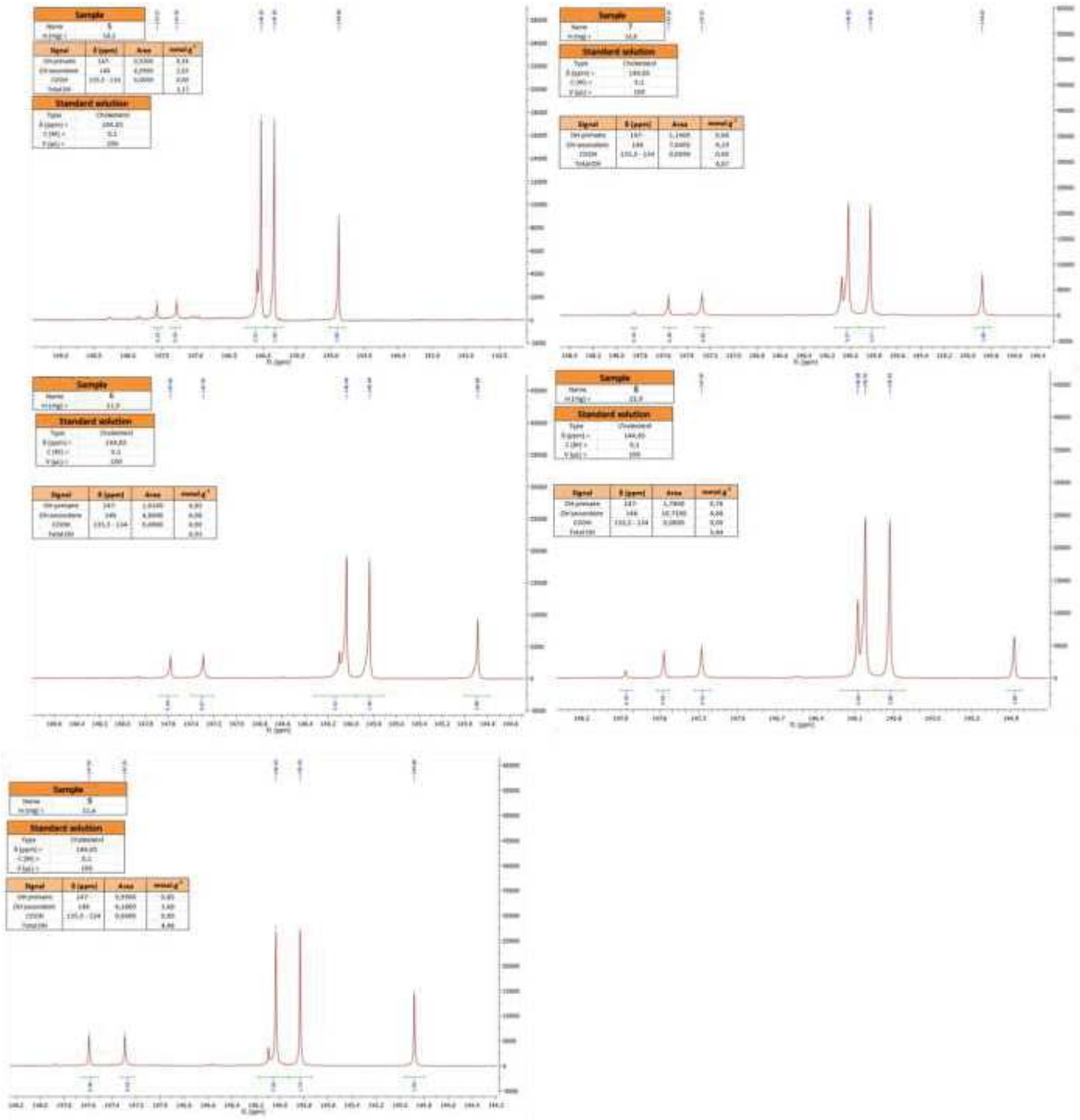

Figure SI 55: ^{31}P-NMR spectra and hydroxyl content of macromolecules 5 to 9 from Table 8

FTIR of polyether/polycarbonate synthetized from D-BisCC

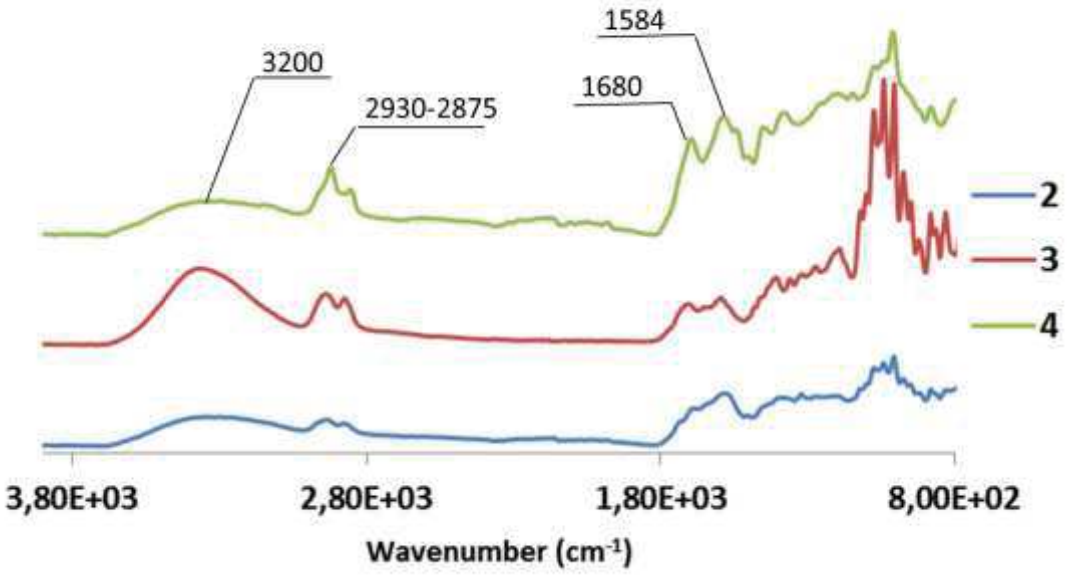

Figure SI 56: FTIR spectra of ROP products presented in Table 8, Entries 2-4

Analysis of the PHUs

This section is relative to PHUs characterizations: FTIR (Figure SI 57), SEC (Figure SI 59), ^{1}H- NMR (Figure SI 60-63), ^{13}C- NMR (Figure SI 64-67), TGA (Figure SI 68) and DSC (Figure SI 69).

- ***FTIR analyses***

FTIR analysis of the PHUs shows the absence of the C=O stretching peak at 1780 cm^{-1} from cyclic carbonate. The results of this analysis show the full conversion of the initial monomer. SEC analysis presents a large peak for all PHUs. It is a direct consequence of the different side reactions, which lead to a large Đ.

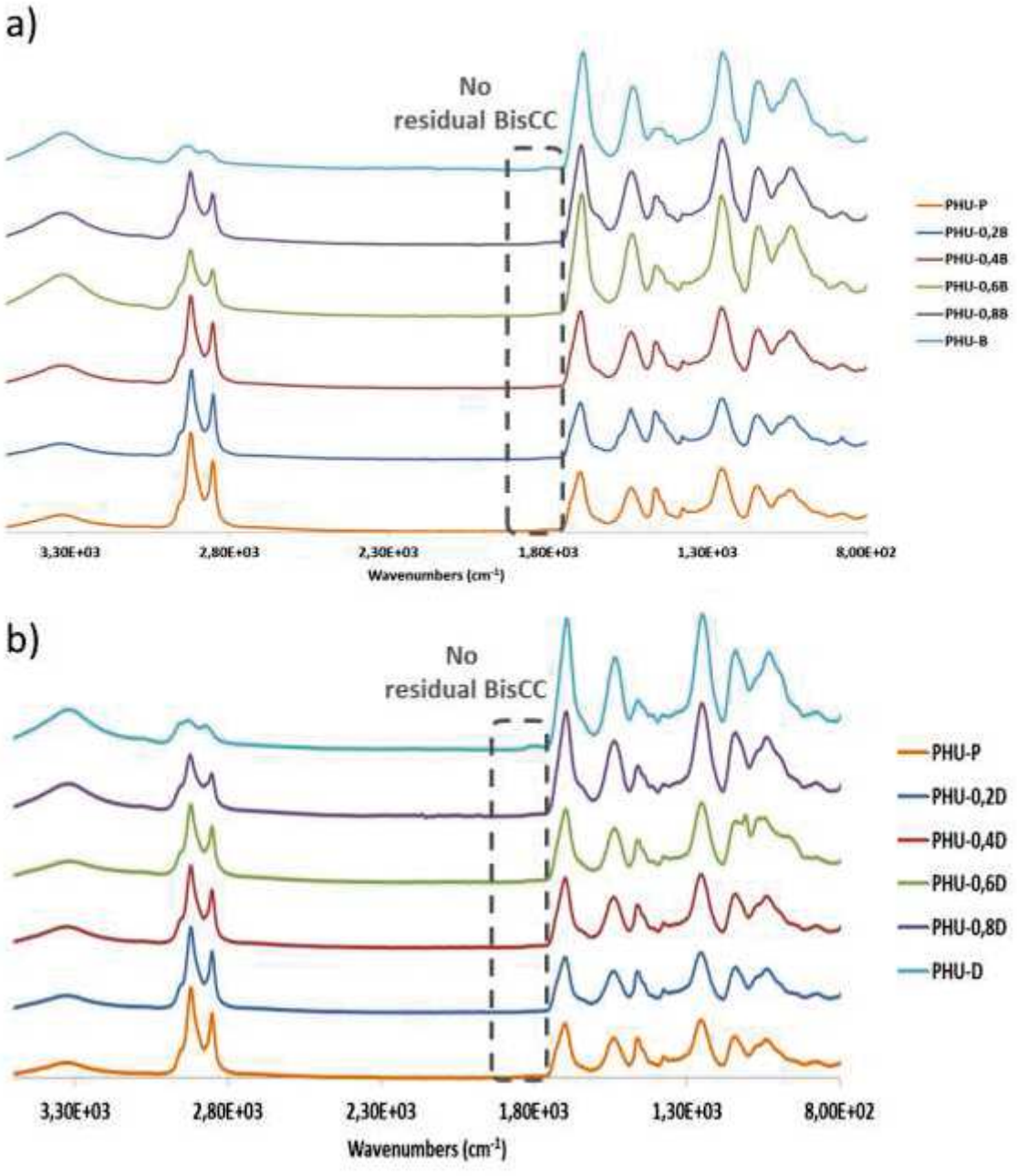

Figure SI 57: FTIR analysis of PHUs

- ***SEC analyses***

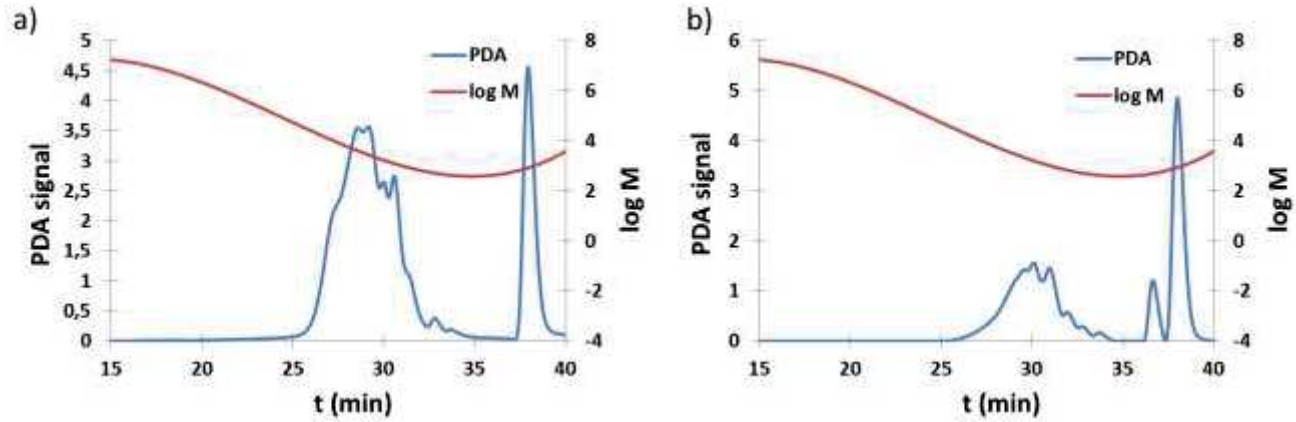

Figure SI 58 : : SEC curves a) PHU-P and b) PHU-H

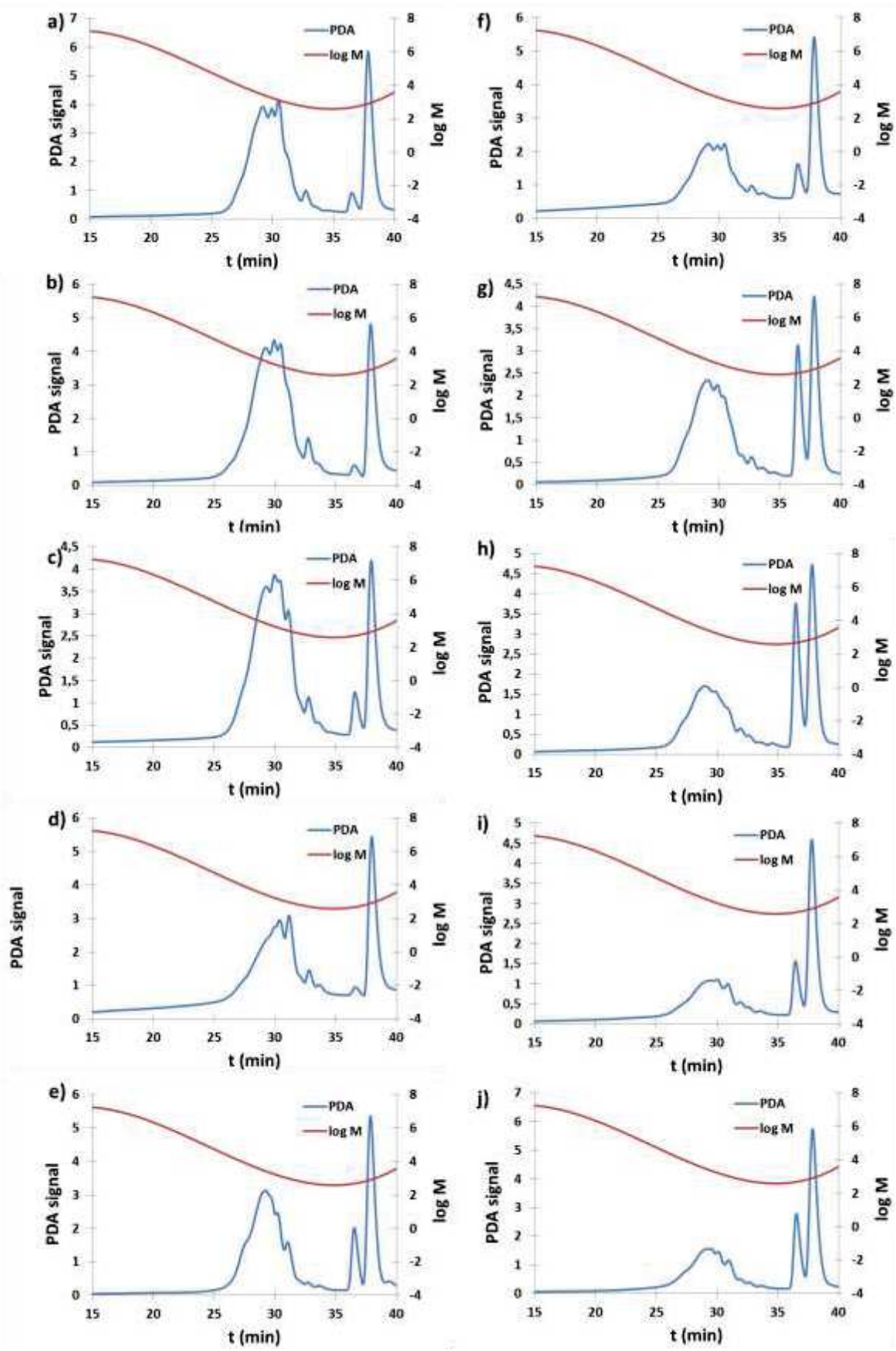

Figure SI 59: SEC curves of a) PHU-0.2B, b) PHU-0.4B, c) PHU-0.6B, d) PHU-0.8B, e) PHU-B, f) PHU-0.2D, g) PHU-0.4D, h) PHU-0.6D, i) PHU-0.8D, j) PHU-D

- ***^{1}H-NMR spectra***

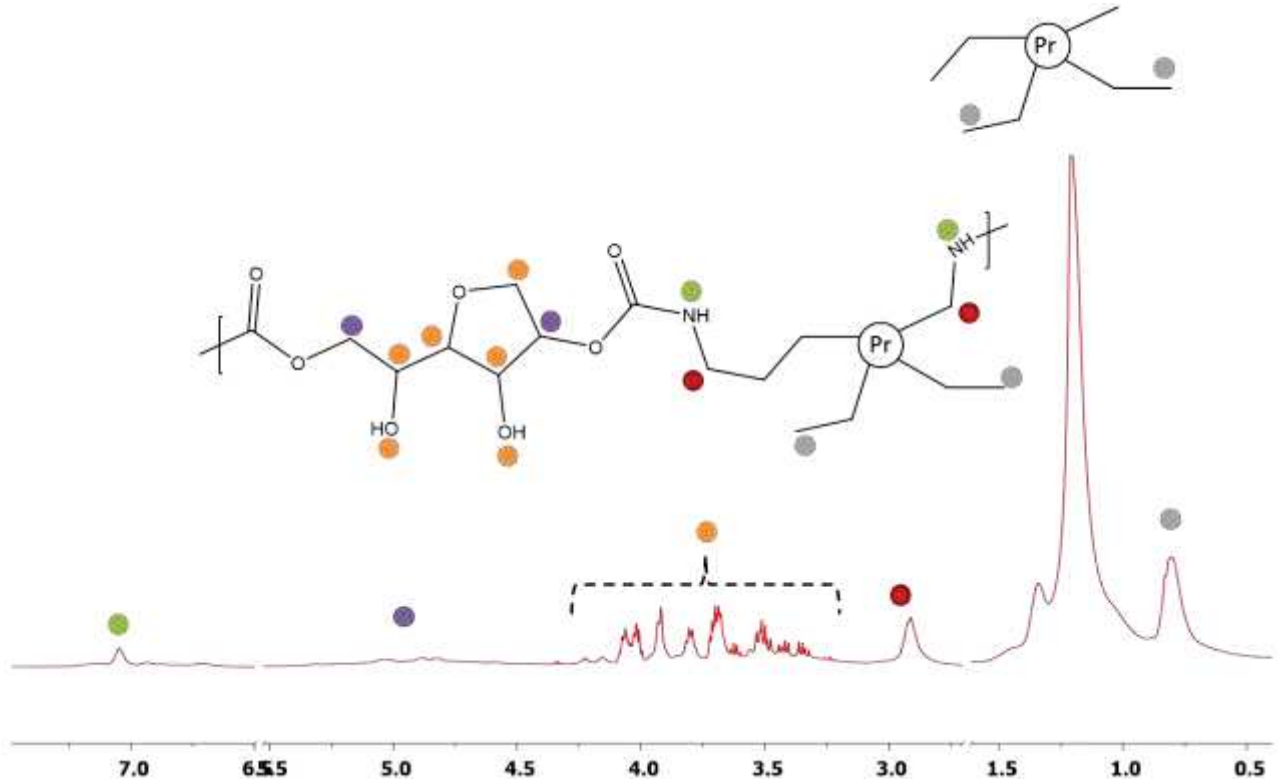

Figure SI 60:^{1}H-NMR of PHU-P sample

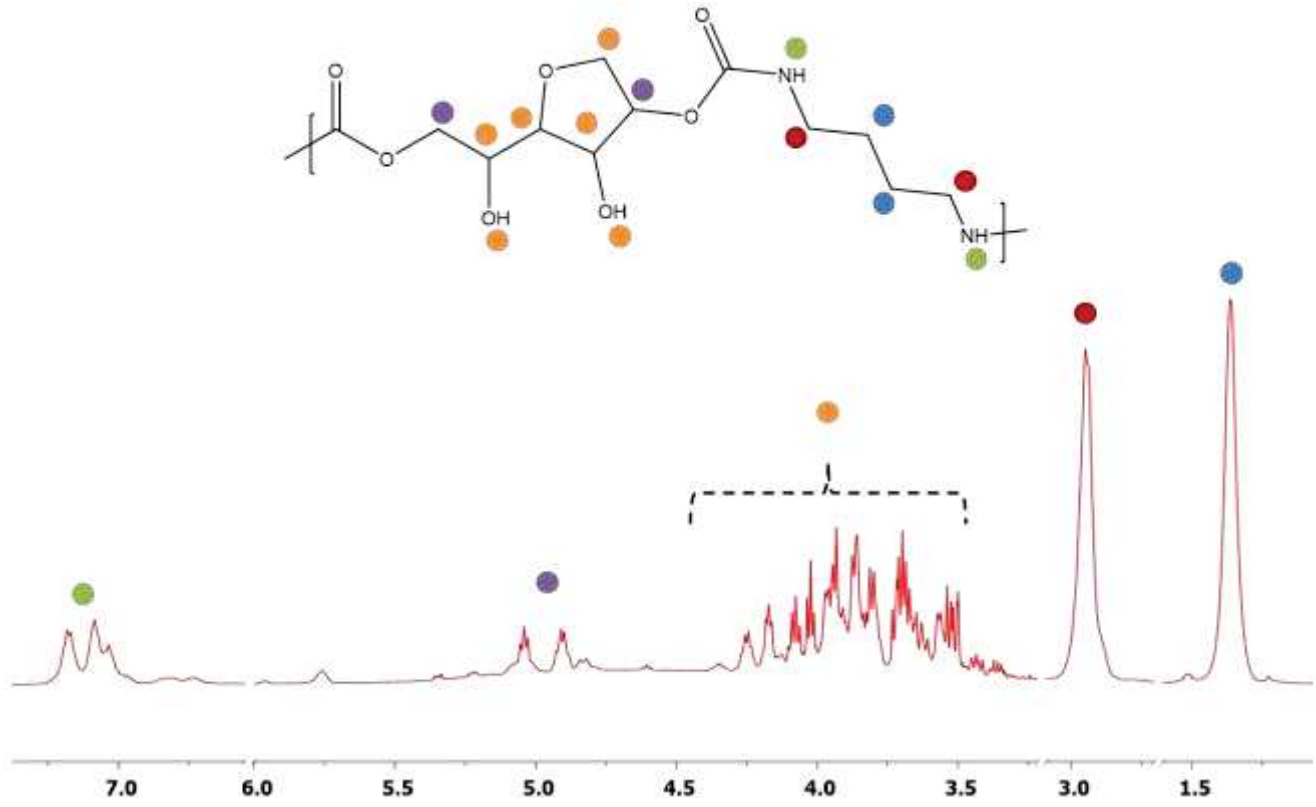

Figure SI 61: ^{1}H-NMR of PHU-B sample

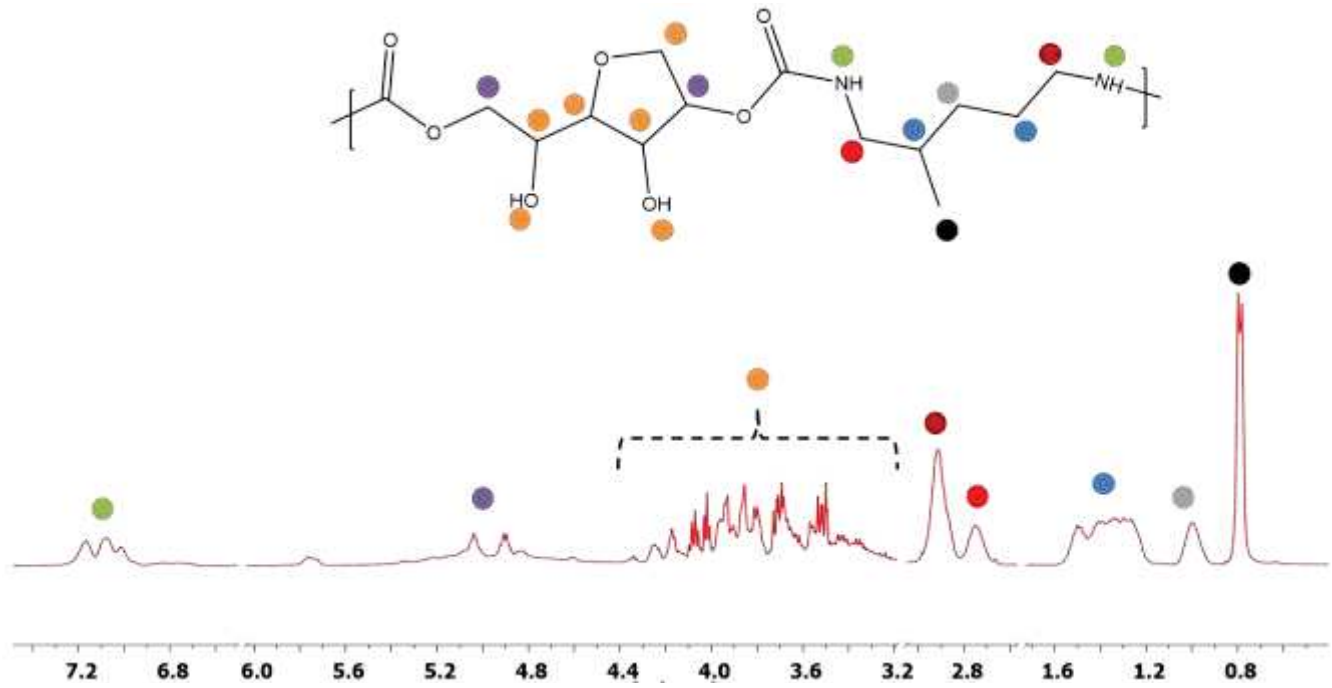

Figure SI 62: ^{1}H-NMR of PHU-D sample

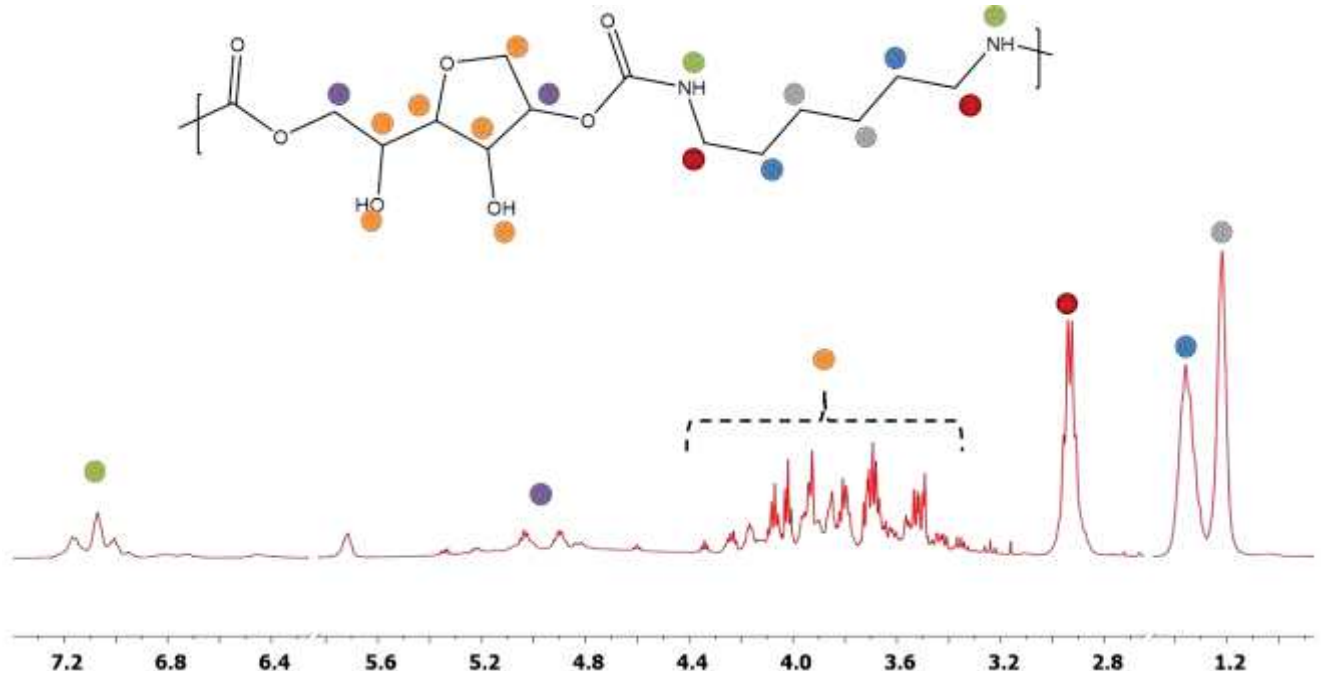

Figure SI 63: ^{1}H-NMR of PHU-H sample

- ***^{13}C-NMR spectra***

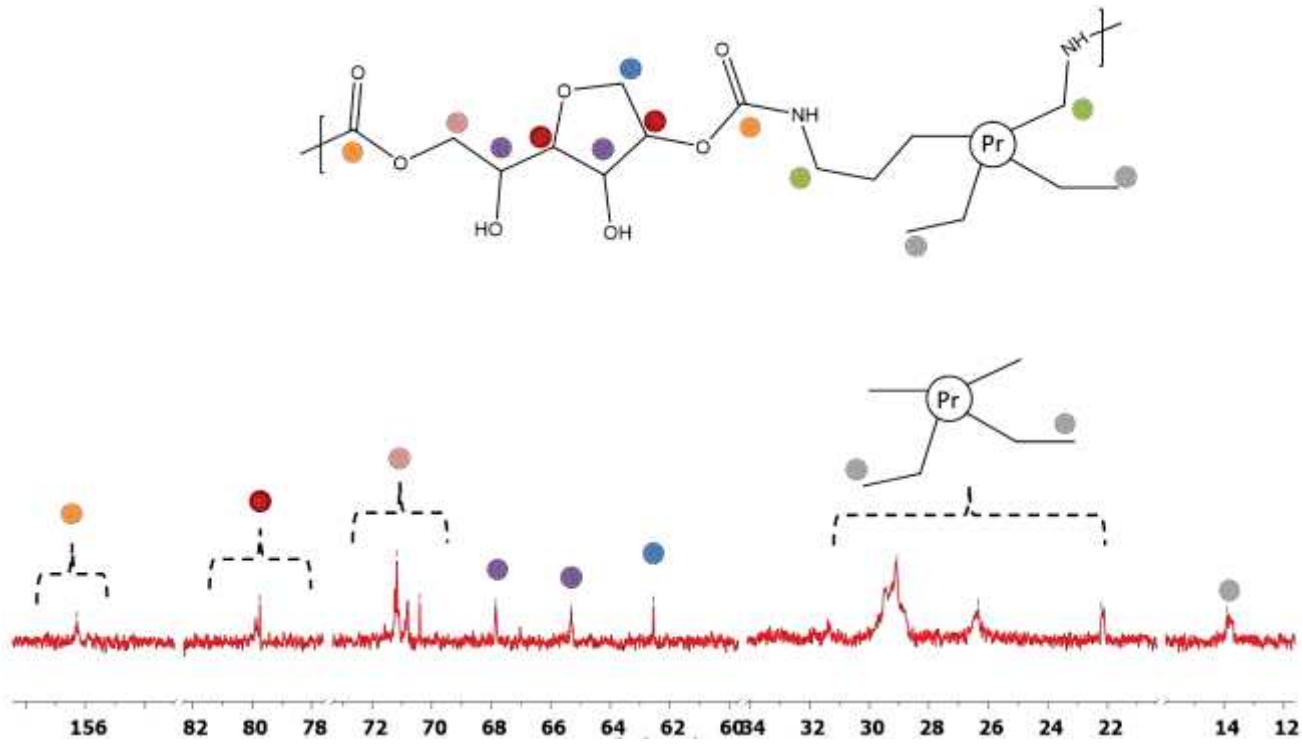

Figure SI 64: ^{13}C-NMR of PHU-P sample

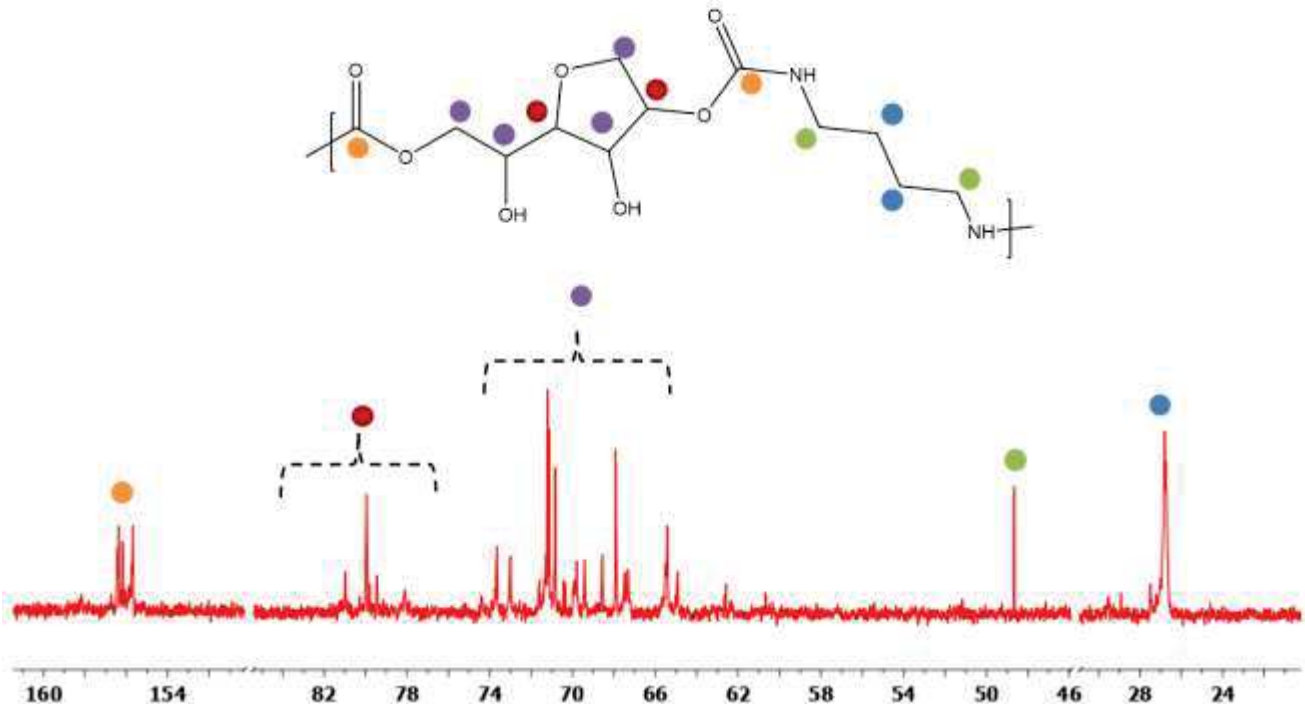

Figure SI 65: ^{13}C-NMR of PHU-B sample

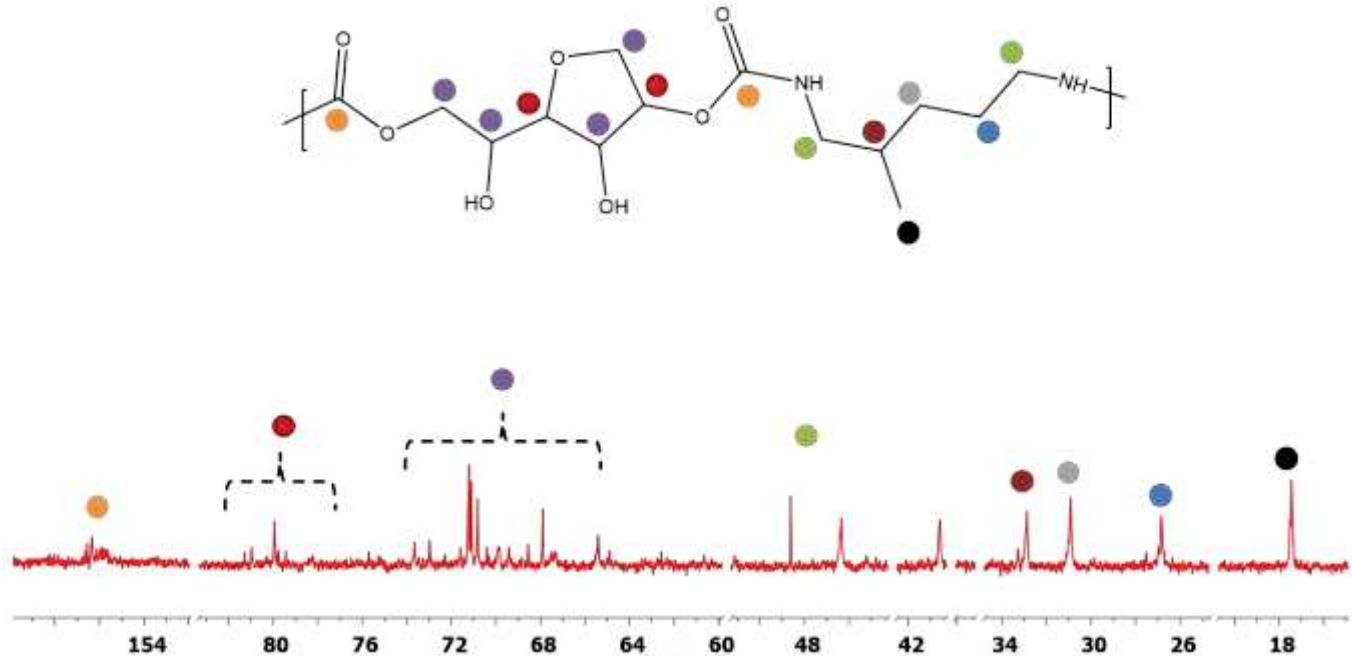

Figure SI 66: ^{13}C-NMR of PHU-D sample

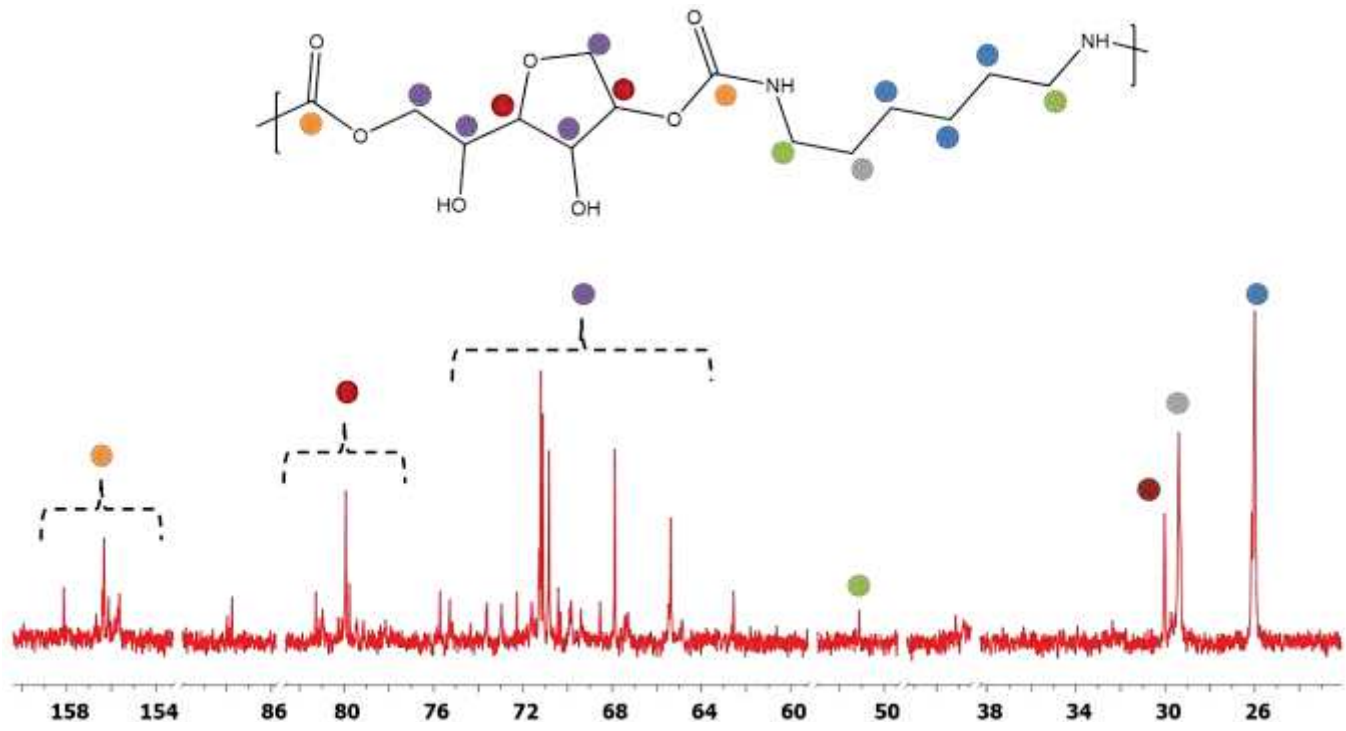

Figure SI 67: ^{13}C-NMR of PHU-H sample

- ***ATG and DSC analysis of PHUs samples***

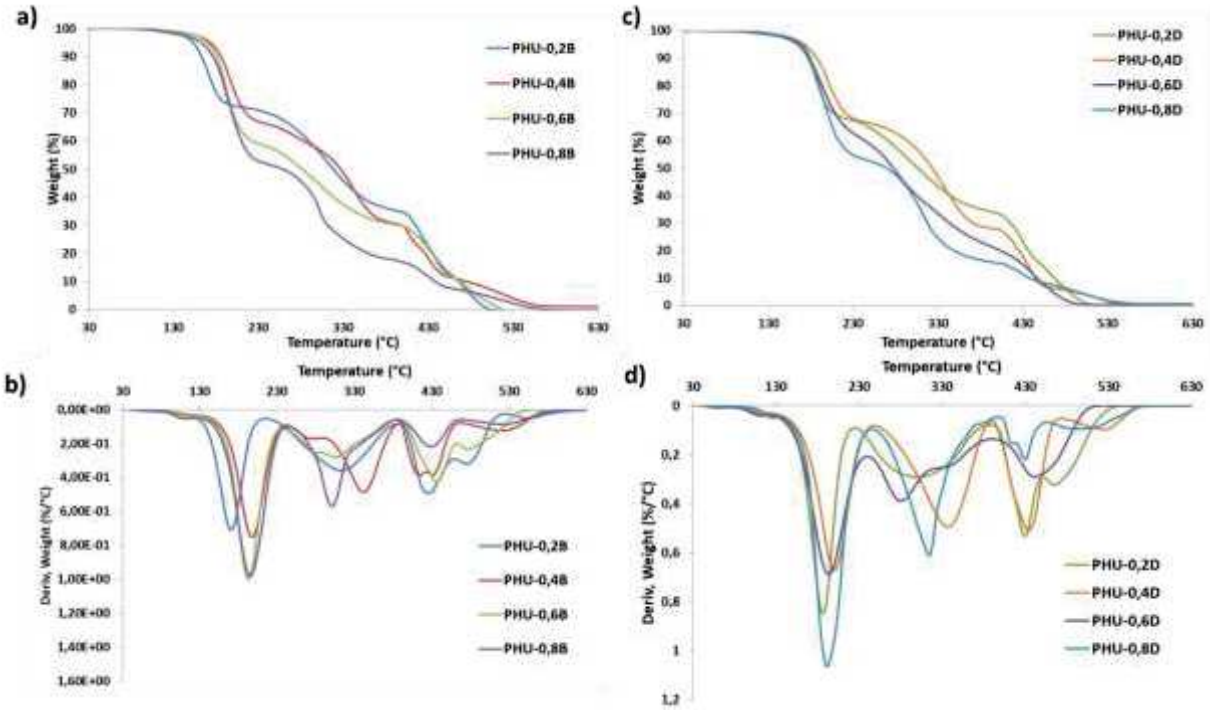

Figure SI 68: a) TGA and b) DTG curves of PHU-0.2B, PHU-0.4B, PHU-0.6B, PHU-0.8B samples; b) TGA and c) DTG curves of PHU-0.2D, PHU-0.4D, PHU-0.6D, PHU-0.8D samples

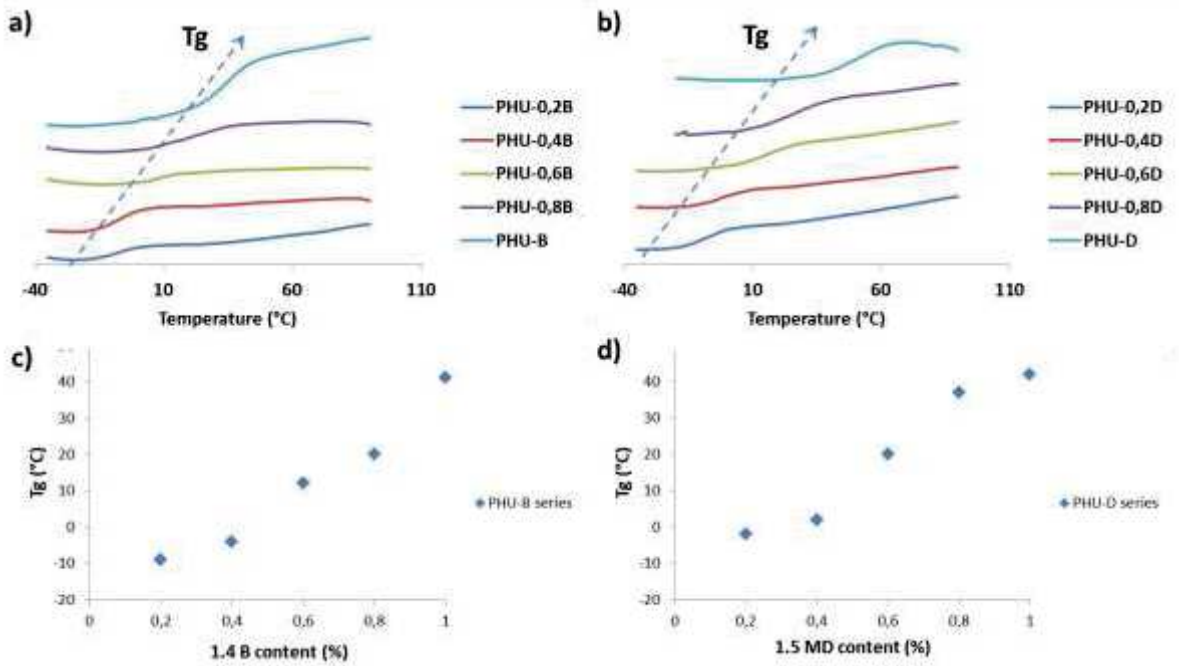

Figure SI 69: a) DSC curves of PHU-0.2B, PHU-0.4B, PHU-0.6B, PHU-0.8B, PHU-B samples and b) PHU-0.2D, PHU-0.4D, PHU-0.6D, PHU-0.8D, PHU-D samples, c) Tg evolution in function of the 1.4 B content compared to predicted Tg obtained by Fox Law, d) Tg evolution in function of the 1.5 MD content compared to predicted Tg obtained by Fox Law

DSC curves of the PHUs obtained from DDA and 1.4 B (Figure SI 69, a) or 1.5 MD (Figure SI 69, b) present a conventional increased of the Tg when the DDA content decrease. The Tg were plotted in function of the

short diamine content (wt%) in Figure SI 69, c-d and compared to the theoretical Tg determined by the Fow Law (Equation SI.1)[1].

$$\frac{1}{Tg} = \frac{W_a}{Tg_a} + \frac{W_b}{Tg_b} \quad (SI.1)$$

Where W_a and W_b are the weight fractions of components a and b, Tg_a and Tg_b are the glass transition of homopolymers a and b respectively in Kelvin, respectively. Tg is the predicted Tg of the corresponding copolymer obtained in Kelvin.

The Fox law is particularly relevant for periodic copolymer even if it is well known that the Fox law generally overestimates copolymers Tg's. It is thus normal to observe a variation between the predicted Tg (red curve) and the experimental data (blue dot). By fitting the experimental data with a linear fit, it was determined that the Tg's of PHU obtained from 1.4 B and 1.5 MD, respectively, evolved according to a first order polynomial law (Equation SI. 2-3).

$$Tg = 51.5x - 21 \qquad R^2 = 0.96 \quad (SI.2)$$

$$Tg = 87.5x - 33 \qquad R^2 = 0.99 \quad (SI.3)$$

Where x is the short diamine content in %wt.

ESI References:

[1] Fox T.G., Influence of diluent and of copolymer composition on the glass temperature of a polymer system, Bull Am Phys Soc 2, 123 (1956)

Annexe 6: Synthèse du BASAB et de mousses PUIR à l'échelle pilote

Introduction

Dans le Chapitre 2 la synthèse d'un polyol polyester à base de sorbitol, le BASAB a été développée. L'étude de ces propriétés a montré que le polyol été adapté à la formulation de mousses polyuréthanes. Les mousses développés dans ce Chapitre et les améliorations apportées dans le Chapitre 3 portant sur le développement de mousses polyisocyanurates constituent des preuves de concepts suffisantes pour envisager une production à plus grande échelle du polyol polyester et des mousses polyisocyanurates. Etant donné que le changement d'échelle a été réalisé au court du travail de doctorat, cette annexe à objectif d'exposer les grandes lignes du changement d'échelle concernant la synthèse du polyol polyester jusqu'à la production de mousses polyisocyanurates sur une ligne de production industrielle. Bien évidemment les synthèses de polyol supérieures à 300 g ne pouvant être réalisées au sein de la BioTeam, L'institut des corps gras (ITERG) de Bordeaux a été mandaté pour réaliser les synthèses.

Synthèse du polyol polyester : de 0.5 kg à 900 kg

Le changement d'échelle s'est axé autour de quatre synthèses de polyols polyesters de 0.5kg, 2 kg, 50 kg et 900 kg respectivement. Les synthèses de 0.5 à 50 kg ont présenté peu de différence avec les synthèses décrites dans le Chapitre 2.1. Le seul changement observé à partir de la synthèse de 50 kg est un allongement du temps de réaction de la seconde étape d'estérification pour atteindre un taux de conversion des fonctions acides de plus de 80%. Ainsi, la deuxième étape a duré environ 8h contre 6h pour les réactions réalisées à l'ICPEES sur 300g. Cette augmentation du temps de réaction a principalement été due à un retard de la distillation des sous-produits de réaction (l'eau). En effet les colonnes de distillation sur le réacteur pilote de 50 kg sont garnies et donc plus longues à monter en température que celle classiquement utilisée en laboratoire. Les réactions d'estérification étant basée sur un équilibre, le retard induit lors de l'élimination des sous-produits de la réaction, retarde le déplacement l'équilibre réactionnel vers les produits.

Le Table SI 9 présente les quantités de matière et de produit impliqué dans la quatrième réaction (900 kg). Ici le 1,4-butanediol a été introduit en excès pour favoriser le déplacement de l'équilibre réactionnel vers les produits, dans le but de minimiser le délai de réaction observé sur la synthèse précédente. Par rapport aux synthèses réalisées en plus petites quantités, l'ensemble des réactifs impliqués dans celle-ci sont d'un grade de pureté inférieur, un grade industriel. Ce choix avait pour objectif de diminuer le coût de la réaction et surtout d'appréhender les éventuels impacts sur le produit final.

Table SI 9 : quantité de matière nécessaire à la synthèse du BASAB à l'échelle pilote

Produit	Mn (g/mol)	Nombre d'équivalent molaire	Masse (kg)
Sorbitol	182	1,0	250
Acide adipique	146	2,0	401
1,4-butanediol	90	3,1	383
K_2CO_3	138	---	29
Total matière premières			**1063**
Total polyol polyester			**891**

Dans un réacteur de 2500 L équipé d'une pâle d'agitation centrale, d'une contre pâle raclante, d'une colonne de distillation et d'un système d'injection de gaz / vapeur d'eau, le sorbitol et l'acide adipique ont été introduits à l'état solide (poudre) puis le réacteur a été inerté sous azote. À ce stade, l'agitation du réacteur est figée, et ceux même après 4h de chauffe. Pour débloquer l'agitation, il a été nécessaire de procéder à une injection de vapeur d'eau (11 kg/h) par le bas du réacteur pendant 15 min. Le milieu réactionnel est passé à l'état fondu 4h après dégagement de l'agitation centrale, soit 8h après le lancement de la chauffe.

Une fois que le milieu fondu a atteint la température de réaction, la première étape de synthèse entre le sorbitol et l'acide adipique a été réalisée en 2h50, soit un peu plus rapidement que dans le cas des synthèses réalisées à l'échelle laboratoire présenté dans le Chapitre 2.1.

Le 1,4-butanediol préchauffé à 100°C est introduit dans le réacteur et la réaction entre le produit de la première étape de synthèse et le 1,4-butanediol a duré environ 15h. L'excès de 1,4-butanediol présent dans le réacteur a été distillé en 15 min. Enfin 2h ont été nécessaire pour refroidir le réacteur de 150 à 70 °C avant de procéder à la neutralisation de polyol par le K_2CO_3. Cette étape a duré 40h soit 38h de plus qu'à l'échelle laboratoire. L'ensemble des temps de fonte, étapes de réaction et neutralisation sont présentés sur la Figure SI 70.

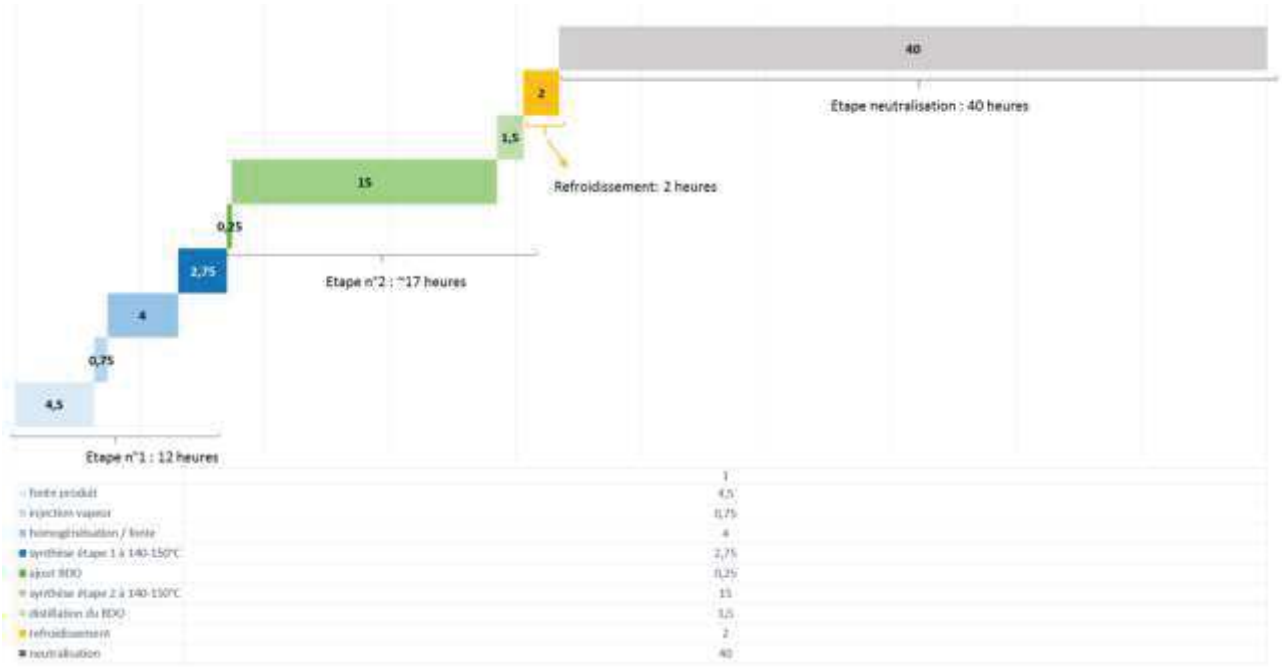

Figure SI 70: enchaînement des étapes de synthèse du BASAB à l'échelle pilote (900kg)

L'étape de neutralisation a été particulièrement lente à l'échelle pilote. L'hypothèse principale est orientée vers la granulométrie (inconnue) du K_2CO_3 utilisé dans cet essai qui était trop importante, ralentissant la dissolution du K_2CO_3 dans le polyol et donc sa neutralisation. La deuxième étape de la réaction d'estérification a également été rallongée par rapport aux temps de références présentés dans le Chapitre 2. Après filtration en sortie de réacteur un polyol jaune, visqueux similaire aux produits obtenus sur des échelles de synthèses plus petites est récupéré. Les caractéristiques du produit sont présentées dans le Table SI 10 et comparé aux propriétés du BASAB présenté dans le Chapitre 2.1.

Table SI 10 : comparaison des propriétés du BASAB produit à l'échelle du laboratoire et pilote

Produit	Echelle	Quantité (kg)	Indice d'hydroxyles (mg KOH/g)	Indice d'acidité (mg KOH/g)
BASAB	Laboratoire	0.3	478[a]	3.4
BASAB	Pilote	890	483	3.5

[a] : moyenne des résultats de titration par RMN ^{31}P et dosage

Les produits présentent des indices d'hydroxyle et d'acidité similaires. Ces deux paramètres avaient été définit comme étant les paramètres de contrôle qualité du produit. L'étape de passage à l'échelle pilote de la synthèse du polyol polyester BASAB est donc validée.

Essais industriel de moussage polyisocyanurate sur ligne de production

Sur la base des travaux présentés dans le Chapitre 3, nous nous sommes orientés vers une formulation de type polyisocyanurate contenant 25 %pds de BASAB dans 75 %pds d'un polyol polyesters pétrosourcé. L'essai industriel a été réalisé sur une ligne de moussage en continue permettant d'obtenir des panneaux de mousse polyisocyanurate recouvert sur la face inférieure et supérieure de parements étanches (Figure SI 71).

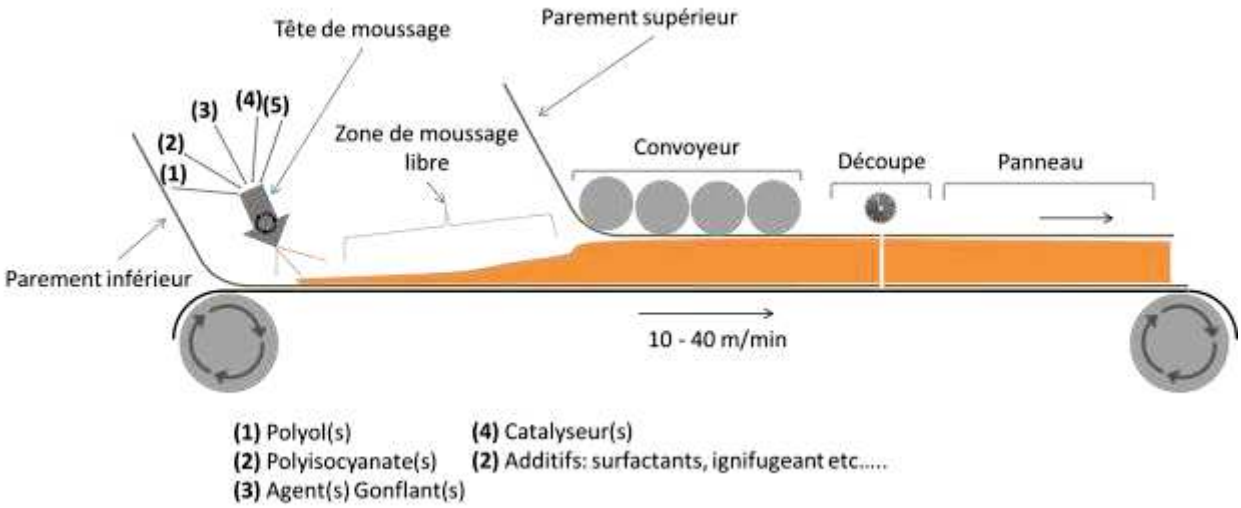

Figure SI 71: principe de fonctionnement d'une ligne de production de mousse polyuréthane

Les parements n'ont jamais été utilisés à l'échelle laboratoire pour des raisons évidentes de mise en œuvre. Ceux-ci limitent les échanges gazeux entre le gaz d'expansion emprisonné dans les cellules de la mousse avec l'air extérieur. L'objectif étant de préserver les propriétés isolantes des panneaux de mousses dans le temps. La formulation utilisé était similaire à celle présenté dans le Chapitre 3 avec les réglages machine suivant :

- Vitesse : 18 m/min
- Hauteur de conformation : 60 mm
- Largeur de panneau : 1200 mm
- Longueur de panneau : 2500 mm

Au terme de l'essai industriel environ 2500 m² de panneaux de mousse polyisocyanurate (Figure SI 72) à base de BASAB ont été obtenu. Sur l'ensemble de la production 60% des panneaux obtenus présentaient des défauts de surface. Cela est principalement dû au rapprochement des temps caractéristiques de gel et de hors poisse observés pour la mousse biosourcé (Chapitre 3) par rapport à la mousse de référence. Ainsi la mousse avait déjà fini de polymérisée lors de son arrivé dans le convoyeur, empêchant la bonne adhérence du

parement supérieur. En abaissant légèrement le taux de catalyse par rapport à la formulation de référence le système a été optimisé et les 40% de panneaux restant présentaient un meilleur aspect de surface.

Figure SI 72: exemple de panneaux de mousses PUIR issus de l'essai à l'échelle du pilote industriel

Les propriétés des panneaux de mousses polyisocyanurate obtenus lors de cet essai sont présentées dans le Table SI 11 et comparé aux propriétés d'une mousse équivalente obtenus à l'échelle du laboratoire.

Table SI 11 : comparaison des propriétés des mousses produite à l'échelle du laboratoire et pilote

Echelle	**Laboratoire**	**Pilote**
Coefficient de conductivité thermique à 10 °C (mW/mK)	22	22
Taux de cellules fermées (%)	92	94
Diamètre des cellules (µm)	155 ± 39	124 ± 24
Densité (kg/m^3)	30.5	35
Résistance 10 % de compression (kPa)	320.3	330
Dureté Shore	73	nc

Pierre FURTWENGLER

Résumé

Dans un contexte de valorisation de molécules issues de la biomasse, de nouvelles architectures moléculaires et polyols ont été développé à partir du sorbitol et divers synthons biosourcés en se basant autant que possible sur les principes de la chimie verte. A partir de réactions d'estérifications contrôlées plusieurs polyols polyesters ont été synthétisés, en l'absence de solvant. Grace à l'utilisation de diols de différentes tailles (C2 à C12) comme monomères, la viscosité et la teneur en fonctions hydroxyles des polyols finaux ont pu être adaptée jusqu'à obtention de propriétés satisfaisantes à l'élaboration de mousses polyuréthanes. Ainsi, des mousses polyuréthanes semi-flexible et des mousses polyisocyanurate rigides ont pu être formulés avec des profils cinétiques de moussage rapide (inférieur à 3 min). Les mousses polyisocyanurates rigides présentent d'excellente propriétés mécaniques et thermiques pouvant pleinement satisfaire à la l'isolation thermique de bâtiment. D'autre part, une voie de transestérification entre le sorbitol et diméthyle carbonate a été étudié afin d'élaborer une nouvelle molécule plateforme bi-fonctionnelle : un bis-cyclocarbonate. A partir de cette molécule plateforme des réactions de polymérisation par ouverture de cycles et d'aminolyses ont été mise en place pour la synthèse de diols, polyéthers réticulés, et de polyuréthanes sans isocyanate (NIPU). Les synthèses de NIPU réalisées à partir de diamines courtes ou longues (issus de dimer d'acide gras) a permis d'étudier les relations existantes entre le choix des monomères et les températures de transitions vitreuses des matériaux polymères résultant.

Mots-clés : Sorbitol, Molécules plateformes, Polyols biosourcés, Mousses polyuréthanes, Mousses polyisocyanurates, Relations polyols-profils cinétiques de moussage, Relations structures-propriétés

Abstract

In a context of renewable molecules valorization, new molecular architectures and polyols have been developed from sorbitol and various biobased building-blocks with respect to the green chemistry principles. Several polyesters polyol have been synthesized from controlled esterification reactions in bulk conditions. Thanks to the used of variable size diols (C2 to C12) monomers, polyols final viscosity and hydroxyls values were tuned until the obtaining of suitable properties for polyurethanes foams elaborations. Thus, semi-flexible polyurethane foams and rigid polyisocyanurate foams were formulated with fast foaming kinetic profiles (less than 3 min). Rigids polyisocyanurates foams exhibit excellent mechanical and thermal properties, in great agreement with building insulating application requirement. Otherwise, transesterifications reaction involving sorbitol and dimethyl carbonate were studied in order to develop a new bi-functional chemical platform, a bis-cyclocarbonate. Ring opening polymerization and aminolysis reactions were investigated from this chemical platform to the elaboration of cross-linked polyether and non-isocyanate polyurethanes (NIPU). NIPU syntheses were performed with short and long diamines in order to study the relationships between monomers choice and the resulting polymer material temperature of glass transition.

Keywords: Sorbitol, Platform molecules, Biobased polyols, Polyurethane foams, Polyisocyanurate foams, Polyols-foaming kinetic profiles relationships, Structure-properties relationships.